LUND UNIVERSITY

Impact of Drinking Water Treatment and Pipe Biofilms on Bacterial Dynamics in the Distribution System

Pullerits, Kristjan

2020

Impact of Drinking Water Treatment and Pipe Biofilms on Bacterial Dynamics in the Distribution System

KRISTJAN PULLERITS | DIVISION OF APPLIED MICROBIOLOGY | LUND UNIVERSITY

Impact of Drinking Water Treatment and Pipe Biofilms on Bacterial Dynamics in the Distribution System

Kristjan Pullerits

LUND
UNIVERSITY

DOCTORAL DISSERTATION

which, by due permission of the Faculty of Engineering,
Lund University, Sweden,
will be defended at Kemicentrum, Lecture Hall A, Lund
Friday, 4th December 2020, at 09:00.

Faculty opponent
Dr. Isabel Douterelo Soler
Department of Civil and Structural Engineering,
University of Sheffield, UK

Organization
LUND UNIVERSITY

Division of Applied Microbiology

Author:
Kristjan Pullerits

Document name
DOCTORAL DISSERTATION

Date of issue: 4th December, 2020

Sponsoring organizations: Sweden Water Research AB, Norrvatten AB, DRICKS center for drinking water research, Vatten & Miljö i Väst AB (VIVAB), Swedish Water and Wastewater Association (SVU), Swedish Civil Contingencies Agency (MSB)

Title and subtitle:
Impact of Drinking Water Treatment and Pipe Biofilms on Bacterial Dynamics in the Distribution System

Abstract
This thesis addresses drinking water quality and microbiology in full-scale drinking water distribution systems (DWDSs). It examines how UV irradiation and slow sand filters (SSFs) alter the water bacteriome, and how the biofilm in the DWDS affects the drinking water quality. In addition, the effects of installing a combined ultrafiltration and coagulation treatment stage on the pipe biofilm community in a DWDS were assessed.

PCR-based methods were assessed and developed to be able to monitor the effects of UV irradiation. The impact of UV doses of 250, 400, and 600 J/m^2, delivered to water at a full-scale drinking water treatment plant (DWTP), was investigated using 16S rRNA gene amplicon sequencing. Phylogenetic analysis, including differential abundance analysis using DESeq2, showed that *Actinobacteria* were more resistant to UV irradiation, whereas *Bacteroidetes* were sensitive to UV irradiation. Amplicon sequence variants (ASVs) resistant to UV had a greater average guanine-cytosine (GC) content than ASVs sensitive to UV irradiation: 55% ± 1.7 (n = 19) vs. 49% ± 2.5 (n = 16), respectively. UV irradiation may affect the microbial dynamics and the biostability throughout the DWDS, as the composition of a bacterial community in irradiated water stored for 6 days at 7 °C to approximate conditions in the DWDS, changed compared to the non-irradiated controls.

Full-scale SSFs were studied using flow cytometry (FCM) and cytometric histogram image comparison (CHIC) analysis. An established, well-functioning SSF removed coliforms and *Escherichia coli*, and reduced the pH and the amount of total organic carbon, even when the *schmutzdecke* of the SSFs was removed. This was in contrast to two new filters, which showed compromised performance, including breakthrough of coliforms and *E. coli*. FCM analysis showed that well-functioning SSFs changed the microbial community of the influent water to include more low nucleic acid (LNA) bacteria in the filter effluent. The SSF with a mixture of new sand plus sand from established SSFs on top exhibited better performance than a SSF with new sand, indicating that priming with sand from established SSFs may be favorable when constructing new SSFs. Monitoring the SSFs with FCM and CHIC analysis was demonstrated to be a fast, reliable and informative method of monitoring the bacterial community in water.

An ultrafiltration and coagulation step was installed at a DWTP (hereafter defined as UF start). This removed almost all the bacteria from the finished water, and reduced the total cell concentration (TCC) in the distributed water from 6.0 × 10^5 (± 2.3 × 10^5) cells/mL to 6.0 × 10^3 (± 8.3 × 10^3) cells/mL, taking seasonal variations into account. After the UF start, almost all the bacteria in the drinking water leaving the DWDS originated from the pipe biofilm, although no significant biofilm detachment was observed. The removal of cells by UF allowed the identification of the bacteria released from the mature pipe biofilm, which included *Sphingomonas*, *Nitrospira*, *Mycobacterium*, and *Hyphomicrobium*. The biofilms of excavated pipe sections were analyzed over a period of 27 months in order to study how the biofilm adapted to the new UF water quality. It was observed that the bacterial community was dominated by *Nitrosomonadaceae*, *Nitrospira*, *Hyphomicrobium* and *Sphingomonas*, confirming the previous results. DNA sequences classified as belonging to the opportunistic pathogens *Mycobacterium* and *Legionella* were also detected in the pipe biofilms. The high relative abundance of the nitrifying bacteria *Nitrosomonadaceae* and *Nitrospira*, together with the fact that the turnover of nitrogen compounds was unchanged by UF start indicated that nitrification in the DWDS was localized to the pipe biofilm. The bacterial community on the pipes changed following UF start and a stable community was reached after 18 months, while still maintaining the turnover of nitrogen compounds. The bacteria leaving the biofilm after a shorter residence time (<25 h) were high nucleic acid (HNA) bacteria, and a shift to an increased relative abundance of LNA bacteria was observed with longer residence times of up to about 170 h.

Key words: Drinking water treatment, Drinking water treatment plant, UV, Slow sand filter, Ultrafiltration, Drinking water distribution system, Biofilm, Biostability, Nitrification, Bacterial communities, flow cytometry, Next-generation sequencing, 16S rRNA gene amplicon sequencing

Classification system and/or index terms (if any)

Supplementary bibliographical information | **Language:** English

ISSN and key title | **ISBN:** 978-91-7422-764-2

Recipient's notes | **Number of pages:** 254 | Price

Security classification

Impact of Drinking Water Treatment and Pipe Biofilms on Bacterial Dynamics in the Distribution System

Kristjan Pullerits

LUND
UNIVERSITY

Cover illustration:

Drinking water treatment processes and bacterial dynamics in the drinking water distribution system; by Kristjan Pullerits

Back cover photo and illustration:

The universal brain and body lubricant; photo and illustration by Kristjan Pullerits

Division of Applied Microbiology
Department of Chemistry
Faculty of Engineering
Lund University
P.O. Box 124
SE-221 00 Lund
Sweden

ISBN 978-91-7422-764-2 (print)
ISBN 978-91-7422-765-9 (digital)

Printed in Sweden by Media-Tryck, Lund University
Lund 2020

All we have to decide is what to do with the time that is given us

— J.R.R. Tolkien, The Fellowship of the Ring

Contents

Abstract viii
Populärvetenskaplig sammanfattning x
Popular scientific summary xiii
List of publications xvi
My contributions to the studies xvii
Abbreviations xviii

1. **Introduction 1**
Objectives 3

2. **Analyzing microbes in drinking water 5**
Study design and sampling 5
Quantifying microorganisms and exploring community composition 7
Cultivation-based techniques 8
Cultivation-independent techniques 9
Cell counting 9
Flow cytometry 9
Community composition and fingerprinting 13
Molecular methods 16
PCR and qPCR 16
DNA Sequencing 17
16S rRNA gene amplicon sequencing 18
Biases and challenges in PCR and sequencing workflows 23
Analysis methods – Summary and perspectives 26

3. **Impact of treatment processes on the microbial community 31**
UV treatment 32
Using PCR to assess UV damage 33
Impact of UV irradiation on microorganisms 36

Biofiltration 38
Biofilms 39
Slow sand filtration 40
4. **Biofilms in the DWDS** **45**
Nitrification and nitrogen cycling in the DWDS 49
Impact of the DWDS biofilm 52
Biostability 54
5. **Conclusions** **55**
6. **Outlook** **57**
Acknowledgements **60**
References **62**

Abstract

This thesis addresses drinking water quality and microbiology in full-scale drinking water distribution systems (DWDSs). It examines how UV irradiation and slow sand filters (SSFs) alter the water bacteriome, and how the biofilm in the DWDS affects the drinking water quality. In addition, the effects of installing a combined ultrafiltration and coagulation treatment stage on the pipe biofilm community in a DWDS were assessed.

PCR-based methods were assessed and developed to be able to monitor the effects of UV irradiation. The impact of UV doses of 250, 400, and 600 J/m^2, delivered to water at a full-scale drinking water treatment plant (DWTP), was investigated using 16S rRNA gene amplicon sequencing. Phylogenetic analysis, including differential abundance analysis using DESeq2, showed that *Actinobacteria* were more resistant to UV irradiation, whereas *Bacteroidetes* were sensitive to UV irradiation. Amplicon sequence variants (ASVs) resistant to UV had a greater average guanine-cytosine (GC) content than ASVs sensitive to UV irradiation: 55% ± 1.7 (n = 19) vs. 49% ± 2.5 (n = 16), respectively. UV irradiation may affect the microbial dynamics and the biostability throughout the DWDS, as the composition of a bacterial community in irradiated water stored for 6 days at 7 °C to approximate conditions in the DWDS, changed compared to the non-irradiated controls.

Full-scale SSFs were studied using flow cytometry (FCM) and cytometric histogram image comparison (CHIC) analysis. An established, well-functioning SSF removed coliforms and *Escherichia coli*, and reduced the pH and the amount of total organic carbon, even when the *schmutzdecke* of the SSFs was removed. This was in contrast to two new filters, which showed compromised performance, including breakthrough of coliforms and *E. coli*. FCM analysis showed that well-functioning SSFs changed the microbial community of the influent water to include more low nucleic acid (LNA) bacteria in the filter effluent. The SSF with a mixture of new sand plus sand from established SSFs on top exhibited better performance than a SSF with new sand, indicating that priming with sand from established SSFs may be favorable when constructing new SSFs. Monitoring the SSFs with FCM and CHIC analysis was demonstrated to be a fast, reliable and informative method of monitoring the bacterial community in water.

An ultrafiltration and coagulation step was installed at a DWTP (hereafter defined as UF start). This removed almost all the bacteria from the finished water, and reduced the total cell concentration (TCC) in the distributed water from 6.0 × 10^5 (± 2.3 × 10^5) cells/mL to 6.0 × 10^3 (± 8.3 × 10^3) cells/mL, taking seasonal

variations into account. After the UF start, almost all the bacteria in the drinking water leaving the DWDS originated from the pipe biofilm, although no significant biofilm detachment was observed. The removal of cells by UF allowed the identification of the bacteria released from the mature pipe biofilm, which included *Sphingomonas*, *Nitrospira*, *Mycobacterium*, and *Hyphomicrobium*. The biofilms of excavated pipe sections were analyzed over a period of 27 months in order to study how the biofilm adapted to the new UF water quality. It was observed that the bacterial community was dominated by *Nitrosomonadaceae*, *Nitrospira*, *Hyphomicrobium* and *Sphingomonas*, confirming the previous results. DNA sequences classified as belonging to the opportunistic pathogens *Mycobacterium* and *Legionella* were also detected in the pipe biofilms. The high relative abundance of the nitrifying bacteria *Nitrosomonadaceae* and *Nitrospira*, together with the fact that the turnover of nitrogen compounds was unchanged by UF start indicated that nitrification in the DWDS was localized to the pipe biofilm. The bacterial community on the pipes changed following UF start and a stable community was reached after 18 months, while still maintaining the turnover of nitrogen compounds. The bacteria leaving the biofilm after a shorter residence time (<25 h) were high nucleic acid (HNA) bacteria, and a shift to an increased relative abundance of LNA bacteria was observed with longer residence times of up to about 170 h.

Populärvetenskaplig sammanfattning

Vatten är livsviktigt för allt liv. Rent och säkert dricksvatten ska vara fritt från kemiska föroreningar och sjukdomsframkallande mikroorganismer, så kallade patogener, men det behöver inte betyda att det ska var fritt från alla mikroorganismer. Mikroorganismer finns överallt och är väldigt allsidiga, de kan leva i allt från varma källor med temperaturer över 100 °C till väldigt sura miljöer i vår mage, vilket också betyder att det nästan är omöjligt att förhindra förekomst och växt av mikroorganismer. Även om vissa mikroorganismer är sjukdomsframkallande är de flesta mikroorganismer ofarliga för människor och kan till och med vara hälsobefrämjande och användas för att rena vatten.

Vattenverk använder vanligen råvattentäkter som ytvatten eller grundvatten som renas med hjälp av olika sorters beredningsprocesser för att leverera dricksvatten via ledningsnät till kran. Sandfilter (långsamfilter), ultraviolett (UV)-ljus eller ultrafilter (UF) är några exempel på beredningssteg som används. Mikroorganismer kan leva tillsammans på ytor i en så kallad biofilm, vilket återfinns på ytan av sandkornen i ett långsamfilter. Denna biofilm renar vattnet med hjälp av biologiska processer och bidrar till vattenreningen med hjälp av att ta bort och minska patogener, organiskt material eller kemikalier i vattnet. Med hjälp av UV bestrålas vatten där UV-ljus penetrerar celler och skadar arvsmassan vilket leder till att oönskade mikroorganismer avdödas. I ett UF finns ytterst små porer (0.020 µm – ungefär 5000 gånger mindre än ett hårstrå) som separerar mikroorganismerna (storlek kring 1 µm) från vattnet. Slutligen pumpas det rena vattnet ut till konsumenter via milslånga ledningsrör, som är betäckta av en biofilm och påverkar den slutgiltiga dricksvattenkvalitén.

Framtida utmaningar inom dricksvattenbranschen innebär en ökad förorening av råvattentäkter. Detta på grund av en ökad brunifiering vilket beror på organiskt material som spolas ner från marken till sjöar och vattendrag. Det organiska materialet i sin tur göder mikroorganismer. Även klimatförändring påverkar råvattenkvalitén med skyfall och torka som kan öka risken för patogener och varmare temperatur som ökar tillväxten av mikroorganismer. För att vi även i framtiden ska kunna producera och leverera säkert dricksvatten krävs det en ökad förståelse och kunskap om hur olika reningsprocesser påverkar den mikrobiella floran (mikrobiotan), men även hur biofilmen i ledningsnätet påverkar dricksvattenkvalitén.

För att säkerställa att dricksvattenkvalitén och säkerheten är god tas dricksvattenprover på vattenverk och ledningsnätet. De mikrobiologiska analysmetoder som används idag är ofta odlingsbaserade där t.ex. bakteriehalten

undersöks med hjälp av odlingsmedier. Nackdelen med dessa metoder är att endast en bråkdel av alla bakterier i vattnet kan odlas, samtidigt som analysen tar dagar att genomföra innan man får resultat. I detta arbete har snabbare, känsligare och mer informativa metoder används för att undersöka hur UV-ljus, långsamfilter och biofilmen i ledningsnätet påverkar mikrobiotan och dricksvattenkvalitén. DNA-baserad flödescytometri användes för att snabbare analysera antalet bakterier och dess sammansättning. Denna teknik, tillsammans med flödescytometrisk mönsteranalys visade sig vara mycket användbar för att övervaka och följa förändringen av den bakteriella floran genom långsamfilter och vattnet i ledningsnätet. Med PCR (polymerase chain reaction) teknik tillsammans med nästa generations sekvensering (NGS) kunde den genetiska informationen bestämmas för att påvisa identiteten och sammansättningen av bakterierna i vatten och biofilm.

UV aggregat i fullskala är svåra att övervaka med traditionell mikrobiologisk analys. I detta arbete undersöktes hur PCR-baserade metoder skulle kunna användas för att övervaka UV-ljus på vattenverk. Efter provtagning på Görvälnverket i Stockholm (Norrvatten) visade jag att släktskap och sammansättningen av arvsmassan påverkade om bakterier var resistenta eller känsliga för UV-ljus. Det visade sig också att sammansättningen av bakterierna förändrades dagar efter UV-bestrålningen, vilket indikerar att UV-ljus troligtvis påverkar bakteriernas återväxtpotential i ledningsnätet, dvs. vattnets biostabilitet.

Olika långsamfilter undersöktes i denna avhandling på Ringsjöverket i Stehag (Sydvatten). Välfungerande långsamfilter förändrade sammansättningen av den bakteriella floran och reducerade antalet koliforma bakterier och *Escherichia coli* som ofta förknippas med en högre risk för kontaminerat vatten. Det ytliga lagret av biomassa på långsamfilter s.k. *schmutzdecke* har ofta antagits stå för den största delen av vattenreningen. I denna avhandling visades att underhållsarbete i form av borttagning av *schmutzdecke* inte påverkade reningsförmågan för ett välfungerande långsamfilter då det bibehöll samma förmåga att avskilja organiskt material, koliforma bakterier och *E. coli* som med *schmutzdecke*. Dessutom visade den flödescytometriska analysen att välfungerade långsamfilter behöll samma förmåga att förändra vattnets bakterieflora som med *schmutzdecke*.

Eftersom vattenledningsnät ofta ligger nergrävda är det svårt att undersöka vilka mikroorganismer som lever på ytan av rören i biofilm. Under detta arbete installerades en UF-anläggning på Kvarnagården i Varberg (VIVAB) som tog bort mer eller mindre alla bakterier i det utgående vattenverksvattnet. Detta gjorde det möjligt att undersöka vilka och hur många bakterier som lämnade biofilmen i ledningsnätet under distributionen. En ledningsrörstudie utfördes också där

biofilmen i uppgrävda rörprover analyserades innan och efter UF start för att undersöka hur biofilmen påverkades av en stor förändring i reningsprocessen på vattenverket. Jag kunde visa att sammansättningen av den bakteriella floran förändrades av UF emedan biofilmen bibehöll sin övergripande funktion att omsätta kväveföreningar i vattnet. Majoriteten av bakterierna som påvisades i biofilmen var nitrifikationsbakterier men även bakterier som kan växa vid väldigt låga halter av näringsämnen. I vattenverket som undersöktes användes monokloramin för att förhindra återväxt av mikroorganismer i ledningsnätet. Monokloramin är en ostabil förening som kan reagera med naturligt organiskt material och sönderfalla till att bilda ammoniak. Nitrifikationsbakterierna kan i sin tur använda ammoniak som energikälla och omvandla det till nitrit och nitrat. Jag påvisade att omvandlingen av kväveföreningar var densamma före och efter UF start, vilket indikerade att nitrifikationen endast utförs av distributionssystemets biofilmsbakterier.

Denna avhandling har bidragit till en ökad förståelse och kunskap kring mikrobiella analysmetoder men även hur olika reningsprocesser och biofilmen i ledningsnätet påverkar dricksvattenkvalitén. Detta för att vi även i framtiden ska kunna säkra tillgången till rent och säkert dricksvatten i våra kranar.

Popular scientific summary

Water is essential for all life. Clean and safe water should be free from chemical contamination and pathogenic microorganisms, but this does not mean it should be free from all microorganisms. Microorganisms are ubiquitous and are very versatile; they can live in various environments ranging from hot springs, with temperatures over 100 °C, to very acidic habitats, like the human gut. This also means that it is almost impossible to prevent the presence and growth of microorganisms in water. Although some microorganisms are pathogenic, most are harmless to humans, and some can even be beneficial and used to purify water.

Drinking water treatment plants (DWTPs) usually use surface water and groundwater as their source. This is treated in various processes to ensure the delivery of safe drinking water through distribution systems to the tap. Slow sand filters, ultraviolet (UV) irradiation and ultrafiltration (UF) are some of the treatment processes used. Microorganisms may live together on surfaces in a so-called biofilm, which is found on the surface of the sand grains in slow sand filters. The biofilm purifies the water through biological processes by removing or reducing the numbers of pathogens, organic material or chemicals in the water. UV irradiation penetrates cells and damages the genetic material, inhibiting cell reproduction, leading to cell inactivation. UF separates microorganisms (usually with a size of 1 µm) from the water using filters with very small pores (0.020 µm, which is about 5000 times smaller than a human hair). The clean water is then pumped to consumers through pipes in a drinking water distribution system (DWDS) which are covered in biofilm which may affect the final drinking water quality.

Increased contamination of source waters will pose challenges in the delivery of clean drinking water in the future. This is due to increased "brownification" by organic matter that is washed out of the ground and into lakes and streams. This organic material serves as a source of nutrition for microorganisms. Climate change is also affecting source water quality, due to heavy rain and draught, and higher temperatures, which increase the growth of microorganisms and may increase the risks from pathogens. To be able to keep producing and delivering safe and clean drinking water in the future, there is a need for a better understanding and increased knowledge on how different treatment processes affect the microbial community (or "microbiome"), as well as on the way in which the biofilm in the DWDS affects the quality of drinking water.

To ensure good quality of drinking water, samples from the DWTP and distribution system are collected and analyzed. The microbiological analysis methods used today are usually cultivation-based where, for example, the bacterial concentration is assessed on a growth medium. The drawback of this is that only a fraction of all bacteria can be grown in this way, and it takes several days to obtain the results. In this work, faster, and more sensitive and informative methods have been used to study how UV irradiation, slow sand filters and the biofilm in the DWDS affect the microbiome and the quality of drinking water. DNA-based flow cytometry was used for rapid quantification and the determination of the composition of the bacterial community. This technique, together with flow cytometric fingerprinting (pattern analysis), was found to be very useful for monitoring and observing the changes in the bacterial community through a slow sand filter and in water in the DWDS. Genetic information was obtained with the PCR (polymerase chain reaction) technique together with next-generation sequencing (NGS), to determine the taxonomic identity and community composition of the bacteria in water and the biofilm.

Full-scale UV reactors are difficult to monitor with traditional microbiological analysis methods. In this work, PCR-based methods were studied to enable disinfection with UV irradiation at DWTPs to be monitored. By collecting and analyzing samples from *Görvälnverket* in Stockholm (Norrvatten), I showed that the evolutionary relationship and the composition of the genetic material influenced resistance and sensitivity to UV irradiation in bacteria. I also showed that the bacterial community changed days after UV irradiation, which indicates that this likely influences the microbial dynamics and biostability in the DWDS.

Several slow sand filters at *Ringsjöverket* in Stehag (Sydvatten) were investigated in this work. Well-functioning slow sand filters changed the bacterial community, and reduced the number of coliforms and *Escherichia coli*, which are associated with a greater risk of contaminated water. It has often been believed that the uppermost layer of biomass in slow sand filters, called the *schmutzdecke*, accounted for most of the water treatment. In this research, it was shown that removal of the *schmutzdecke* during maintenance did not affect the treatment capacity of a well-functioning slow sand filter, as it retained its ability to reduce organic matter and remove coliforms and *E. coli*. In addition, the flow cytometric analysis showed that well-functioning slow sand filters retained its ability to change the bacterial community in the same way as those with a *schmutzdecke*.

Pipes in the DWDS are buried underground, which makes it difficult to study the microorganisms living in pipe biofilms. In this work, installation of UF (hereafter defined as UF start) at *Kvarnagården* DWTP in Varberg (VIVAB)

removed almost all the bacteria in the finished water leaving the treatment plant. This made it possible to investigate which, and how many bacteria, originated from the biofilm in the DWDS during distribution. The biofilm of excavated pipes was studied before and after UF start, to investigate how the biofilm was affected by a change in the treatment process. I showed that the bacterial community changed, while the biofilm retained its ability to convert nitrogen compounds in the water. Most of the bacteria in the biofilm were nitrifying bacteria, but also included some that can live in very nutrient-limited conditions. The disinfectant monochloramine is used at this plant to prevent microbial regrowth in the DWDS. Monochloramine is an unstable compound and can react with natural organic matter, resulting in the formation of ammonia. Nitrifying bacteria can then use this ammonia as an energy source, and convert it into nitrite and nitrate. I showed that the turnover of nitrogen compounds was the same before and after UF start, which indicated that nitrification was localized to the pipe biofilm.

The studies presented in this thesis have contributed to a better understanding of, and increased knowledge on, microbial analysis methods, and ways in which different treatment processes and the pipe biofilm in the DWDS affect the quality of drinking water. This knowledge will be useful in ensuring the supply of clean and safe drinking water in our taps in the future.

List of publications

Paper I: **Impact of UV irradiation at full scale on bacterial communities in drinking water**

Pullerits, K., Ahlinder, J., Holmer, L., Salomonsson, E., Öhrman, C., Jacobsson, K., Dryselius, R., Forsman, M., Paul, C.J., & Rådström, P. (2020). npj Clean Water, 3(1), 1-10. https://doi.org/10.1038/s41545-020-0057-7

Paper II: **Monitoring biofilm function in new and matured full-scale slow sand filters using flow cytometric histogram image comparison (CHIC)**

Chan, S., **Pullerits, K.**, Riechelmann, J., Persson, K. M., Rådström, P., & Paul, C. J. (2018). Water Research, 138, 27-36. https://doi.org/10.1016/j.watres.2018.03.032

Paper III: **Impact of coagulation-ultrafiltration on long-term pipe biofilm dynamics in a full-scale chloraminated drinking water distribution system**

Pullerits, K., Chan, S., Ahlinder, J., Keucken, A., Rådström, P., & Paul, C. J. (2020). Environmental Science: Water Research & Technology, 6, 3044-3056. https://doi.org/10.1039/D0EW00622J

Paper IV: **Bacterial release from pipe biofilm in a full-scale drinking water distribution system**

Chan, S., **Pullerits, K.**, Keucken, A., Persson, K. M., Paul, C. J., & Rådström, P. (2019). npj Biofilms and Microbiomes, 5(1), 1-8. https://doi.org/10.1038/s41522-019-0082-9

Paper V: **Mapping dynamics of bacterial communities in a full-scale drinking water distribution system using flow cytometry**

Schleich, C., Chan, S., **Pullerits, K.**, Besmer, M. D., Paul, C. J., Rådström, P., & Keucken, A. (2019). Water, 11(10), 2137. https://doi.org/10.3390/w11102137

Other related publications by the author

Biofilmens funktion och korrelation med dricksvattnets kvalitet

Schleich, C., Chan, S., **Pullerits, K.**, Habagil, M., Lindgren, J., Paul, C. J., Keucken, A. & Rådström, P. (2020). Svenskt Vatten Utveckling (SVU) rapport (in Swedish).

My contributions to the studies

Paper I: I participated in the study design, and performed sampling and experimental work, except for the dead-end ultrafiltration. I performed the bioinformatics and data analysis together with the other authors, and I drafted the manuscript.

Paper II: I participated in the study design, and performed sampling and experimental work together with another co-author. I performed the initial data analysis, and was involved in finalizing the manuscript.

Paper III: I participated in the study design, and performed sampling and experimental work together with another co-author. I carried out the bioinformatics and data analysis, except for the SourceTracker analysis, and I drafted the manuscript.

Paper IV: I participated in the study design, and performed sampling and experimental work together with another co-author. I analyzed the flow cytometry data and participated in the interpretation of the sequencing data. I was involved in finalizing the manuscript.

Paper V: I participated in the study design, supervised a co-author in the experimental work and data analysis, assisted in the interpretation of the data, and was involved in finalizing the manuscript.

Abbreviations

AOA	Ammonia oxidizing archaea
AOB	Ammonia oxidizing bacteria
AOC	Assimilable organic carbon
ASV	Amplicon sequence variant
BAC	Biological activated carbon
BF	Biofilm
CFU	Colony forming units
CHIC	Cytometric histogram image comparison
Comammox	Complete ammonia oxidizer
Cq	Cycle of quantification
DP	Distribution point
DWDS	Drinking water distribution system
DWTP	Drinking water treatment plant
EPS	Extracellular polymeric substances
FCM	Flow cytometry
FISH	Fluorescent in situ hybridization
GAC	Granular activated carbon
GC content	Guanine-cytosine content
HNA	High nucleic acid
HPC	Heterotrophic plate count
ICC	Intact cell concentration
LNA	Low nucleic acid
NGS	Next-generation sequencing
NOB	Nitrite oxidizing bacteria
NOM	Natural organic matter
OTU	Operational taxonomic unit
PCR	Polymerase chain reaction
PI	Propidium iodide
PMA	Propidium monoazide
qPCR	Quantitative polymerase chain reaction
rRNA	Ribosomal ribonucleic acid
RSF	Rapid sand filter
RT-qPCR	Reverse transcription quantitative polymerase chain reaction
SSF	Slow sand filter
TCC	Total cell concentration
TOC	Total organic carbon
UF	Ultrafiltration
UV	Ultraviolet

Chapter 1
Introduction

Safe and clean water is essential for all life. Drinking water should be free from harmful microorganisms, i.e. pathogens, and undesirable chemicals. To achieve this, drinking water is treated in numerous ways at drinking water treatment plants (DWTPs), depending on factors such as the raw water quality and national regulations. Treatment may be physical, chemical, or biological, and include ultraviolet (UV) irradiation, ultrafiltration (UF) or slow sand filters (SSFs). UV irradiation damages the genetic material in microorganisms preventing reproduction. The small pore size of UF filters prevents most microorganisms from passing through. Microbial communities live in a slimy matrix, called a biofilm, on the surface of the sand of SSFs. This biofilm treats the water through biological processes. To prevent the growth of unwanted microorganisms in the drinking water distribution system (DWDS), some countries aim to maintain residual disinfectant in the system, whereas others reduce the available organic carbon (Zhang and Liu, 2019) to limit the growth of indicator microorganisms.

In the future, it will become more challenging to ensure safe and clean drinking water due to increased levels of contaminants in raw water sources (Delpla et al., 2009). This is partly due to the increase in natural organic matter (NOM), which has increased in raw water sources worldwide in recent decades (Eikebrokk et al., 2004; Evans et al., 2005), leading to the brownification of water. Brownification may also be the result of changes in the climate, such as an increase in air temperature, rainfall intensity and acid deposition from industrial air emissions (Ekström et al., 2011; Evans et al., 2005; Köhler et al., 2009). The increased NOM levels and changes in climate may reduce raw water quality by cyanobacterial growth (Urrutia-Cordero et al., 2016), increasing the risk of microbial contamination of the water (Delpla et al., 2009).

Safe and clean drinking water is not sterile, and total cell concentrations of 10^3 to 10^5 cells/mL have been measured (Proctor and Hammes, 2015a). As long as no pathogens are present, these large numbers of bacteria are not thought to constitute a risk to humans. Microorganisms are assessed throughout the

treatment at DWTPs, and in the bulk water in the DWDS. Conventional methods of assessing microorganisms in drinking water are usually culture-based, which can only detect a fraction of the whole community, and several days are required to obtain the results (Allen et al., 2004a). Therefore, faster, more sensitive and informative methods have been developed to analyze the microbial community in drinking water. These methods do not rely on culturing, and include methods such as the polymerase chain reaction (PCR) to analyze the DNA in a sample (Mullis, 1990) and identify the presence or quantity of specific bacteria; or flow cytometry (FCM) in which the number of cells in a sample can be counted in a matter of minutes (Hammes et al., 2008). With next-generation sequencing (NGS) it has become possible to identify the nucleic acid sequence bases in DNA relatively cheaply, and thus obtain taxonomic and functional information on the whole microbial community in environmental samples (Gilbert et al., 2014).

Most of the biomass in a DWDS is found in pipe biofilms. It has been estimated that over 95% of the biomass in DWDSs resides in the pipe biofilm or loose deposits (Flemming et al., 2002; G. Liu et al., 2014), and that the pipe biofilm may consist of up to 10^8 bacteria per cm^2 (Proctor and Hammes, 2015a). The pipe biofilm can affect drinking water quality by changing the aesthetics of the water (Fish et al., 2017), or it may harbor potential opportunistic pathogens (Wingender and Flemming, 2011). Chloramines are commonly used disinfectants, which can auto-decompose or react with NOM to form ammonia (Ricca et al., 2019; Valentine and Jafvert, 1992). The biofilm community in the pipe biofilm may use the ammonia for nitrification, which can result in further depletion of the chloramine residuals (Vikesland et al., 2001). Although the pipe biofilm can have undesirable effects on water quality, biofilms in SSFs are beneficial, and help treat the water, and similarly, the pipe biofilm may treat the water through the DWDS.

Different methodological approaches for studying the microbiome in drinking water are described in Chapter 2, while the effects of UV irradiation and SSFs on the bacteriome are explained in Chapter 3. Ways in which the pipe biofilm may affect drinking water quality are described in Chapter 4, where the effect of the installation of UF with coagulation on the bacterial community in the pipe biofilm is also discussed.

Objectives

The overall objective of the work presented in this thesis was to apply FCM, 16S rRNA gene amplicon NGS, and conventional biological and chemical analyses to investigate how treatment processes and DWDS pipe biofilm affect the bacteriome and drinking water quality. The bacteriome-transforming treatment processes examined were UV irradiation and slow sand filtration.

In the first study, 16S rRNA gene amplicon NGS, heterotrophic plate counts (HPCs), coliforms and *E. coli* counts were used to investigate how full-scale UV treatment impacted and transformed the bacterial community (Paper I). Prior to this study, PCR-based techniques to assess UV damage was developed on laboratory scale. Three different UV doses: 250, 400, and 600 J/m^2, were studied during full-scale DWTP operation. Differential abundance analysis using DESeq2 was applied to investigate which amplicon sequence variants (ASVs) were affected by UV irradiation. The biostability of the water was also investigated by storing samples for periods of time for 6 days at 7 °C.

The aim of the second study was to investigate the performance of full-scale SSFs using HPCs, coliforms and *E. coli* counts together with chemical analyses (Paper II). In addition, FCM and the cytometric fingerprinting tool, cytometric histogram image comparison (CHIC), was also investigated as a fast monitoring tool for the analysis of the bacterial community in water. The SSFs included two established well-functioning SSFs, and two newly constructed SSFs; one containing new sand plus sand from established filters on top, and the other containing only new sand. The impact of removing the uppermost layer of the biofilm, the *schmutzdecke* (from the German meaning "dirt cover"), on the performance of the SSFs was also investigated.

Papers III, IV, and V describe the long-term impact of the full-scale installation of UF combined with coagulation on the DWDS pipe biofilm, and the effects on biological and chemical water quality.

The bacterial community in the biofilm of DWDS pipes from a fully operational DWDS was investigated in Paper III. Excavated pipe sections were analyzed with 16S rRNA gene amplicon NGS over a period of two years and three months, before and after installation of UF (hereafter defined as UF start). Water samples in the DWTP, and at three distribution points (DPs) in the DWDS at different residence times, were investigated with 16S rRNA gene amplicon NGS, FCM, and conventional biological and chemical analyses, including nitrogen compounds. The bioinformatics tool SourceTracker was used to predict the

contribution of biofilm bacteria to the bulk water of the DWDS, before and after UF start.

The study described in Paper IV was designed to investigate the identity and number of bacteria leaving a full-scale DWDS pipe biofilm shortly after UF start. Water was sampled at the DWTP and at three DPs in the DWDS and analyzed with FCM and 16S rRNA gene amplicon NGS. Comparisons between the finished water from the DWTP and the DPs using DESeq2 made it possible to estimate which bacteria in the bulk water originated from the biofilm.

Finally, the seasonal impact of the pipe biofilm and biostability on the water quality of the bulk water in a full-scale DWDS was studied (Paper V). The water quality at various DPs at different residence times were assessed over at least a year, using FCM together with CHIC, and the results were correlated with chemical parameters and temperature.

Chapter 2
Analyzing microbes in drinking water

To ensure the safety and quality of drinking water in Sweden, water producers are required by law to monitor microbial water quality according to regulations issued by the National Food Agency (Livsmedelsverket, 2001). Various methods used to analyze microbes in drinking water are described below. No single method can provide all the information required, and a variety of methods, using appropriate sampling practices and replication, should be used to give a comprehensive understanding of drinking water microbiology.

Study design and sampling

The microbial ecology of drinking water can be investigated on experimental or pilot scale in the lab, or by field sampling from full-scale operational DWTPs and DWDSs. Many different laboratory setups have been used to study the effects of water treatment and biological processes such as UV irradiation (Hijnen et al., 2006), SSFs (Haig et al., 2014), DWDS biofilms with reactors (Batté et al., 2003; Murga et al., 2001) as well as model pilot- and full-scale systems (Boe-Hansen et al., 2002; Fish et al., 2015; Långmark et al., 2005), pesticide biodegradation (Hedegaard et al., 2020) and biogeochemical cycling (Mooshammer et al., 2020). Lab and model full-scale setups are more versatile than full-scale systems. It is easier to obtain samples and to challenge the system by changing operational parameters such as water chemistry, hydraulics and temperature. It is also possible to spike the water with pathogenic microorganisms to test the reduction capacities of various treatments. Full-scale studies are important when applying and relating the knowledge gained from lab studies. However, since it is known that lab-grown organisms are less tolerant to stress than bacteria that originate from the environment (Hijnen et al., 2006), results based on lab-scale spiking experiments

are difficult to interpret and apply to full-scale treatment for the reduction of pathogens. Although model full-scale systems are useful for initial biofilm formation studies, it is difficult to study the effects of a mature biofilm in a full-scale DWDS pipe or SSF on water quality, or the effects of changes in treatment, since it can take years for a biofilm to mature (Martiny et al., 2003). Furthermore, seasonal variations have been observed in the microbial community in both bulk water and biofilms in full-scale studies (Douterelo et al., 2016; Kelly et al., 2014; Pinto et al., 2014). Full-scale studies are thus of the utmost importance to understand the microbial ecology of the water in DWTPs and DWDSs.

It is important to analyze replicate samples to ensure the reliability of the results and to allow robust statistical analysis, however, this is often neglected in practice (Prosser, 2010). Collecting replicate samples in full-scale drinking water systems can be challenging due to reasons such as the volume of water needed, distance to different parts of a DWDS and the laboratory, difficulties of processing samples (e.g. filtering water) on-site and storage of samples over a longer time period. Depending on the research question, the characteristics of the sampling environment (e.g. biomass, diversity and stability of water quality), and analysis method, the researcher must decide at what level of replicate samples are needed such as replicate water samples, technical replication, or to repeat the experiment or field sampling, itself (Bautista-de los Santos et al., 2016a).

When sampling bulk water, it is important to consider the type of sampling container to be used, storage during transport, and how to avoid contamination (Douterelo et al., 2014). The number of microorganisms increases in stagnant water due to disinfectant decay and microbial regrowth (Lautenschlager et al., 2010). In the present work, full-scale systems were investigated, and samples were obtained from sampling taps which were always flame sterilized and flushed for at least 10–15 min, or until the temperature of the water was constant, to avoid sampling stagnant water in the pipe system. Sampling without flushing distribution systems in buildings has been hypothesized to increase the probability of detecting higher numbers of opportunistic pathogens due to stagnation (H. Wang et al., 2017). This has been observed by Ley et al. (2020), where lower flows and reduced water usage were correlated with higher levels of opportunistic pathogens in a residential building. Sampling bottles containing sodium thiosulfate to neutralize monochloramine are commonly used when appropriate (H. Wang et al., 2017). Water samples are relatively easy to collect in full-scale compared to pipe biofilm, due to problems of accessibility. However, most of the bacterial community in a DWDS (>95%) is found in the biofilm on the pipes (Flemming, 2002; G. Liu et al., 2014). When the bacterial concentration in the

bulk water is high, it can be difficult to estimate the contribution of bacteria to the bulk water from the biofilm (Paper III, before UF start). In contrast, when the bacterial concentration in the bulk water of the DWDS is very low, sampling water at different residence times can be used as a proxy to study which bacteria are present in the biofilm and may leave it (Papers III & IV). It may be necessary to concentrate the bacterial population in the water, depending on the type of downstream analysis, and according to the literature, sample volumes usually range from 1–100 L, although volumes of 2000 L have also been used (Y. Wang et al., 2017). In the present work, the bacterial cells in the water were concentrated by filtration of a 1–5 L water sample through 0.22 µm filters, or by using the eluate from dead-end UF (Smith and Hill, 2009) of a 60 L sample.

Various methods have been used to sample biofilm in DWDSs. Biofilms have been sampled from water meters (Lührig et al., 2015), coupons recovered from pilot- and full-scale systems (Deines et al., 2010; Douterelo et al., 2013; Fish et al., 2015), and excavated DWDS pipes during maintenance or for research purposes (Cruz et al., 2020; G. Liu et al., 2014; Liu et al., 2020; Ren et al., 2015; Waak et al., 2019a, 2018). Biofilm samples can be obtained by various methods, for example, by swabbing with cotton swabs (Lührig et al., 2015), brushing (Neu et al., 2019, 2018; Ren et al., 2015), cell scraping (Kelly et al., 2014; Långmark et al., 2005), or using glass beads (Wingender and Flemming, 2004). Due to variations in the biofilm community over the 360° pipe surface (Liu et al., 2020), and due to biofilm heterogeneity, it has been suggested that the area of biofilm sampled should be as large as possible, to increase the probability of obtaining representative biofilm communities (Neu et al., 2019). In the present studies, pipe biofilm was sampled from excavated full-scale DWDS pipe sections, both by swabbing with cotton swabs (360°), and scraping a large area with a custom-made metal scraper (Fig. S2 in Paper III) along the bottom half of the pipe.

Quantifying microorganisms and exploring community composition

The methods used are described below, with emphasis on the cultivation-based assessment of bacteria, flow cytometry, PCR and DNA sequencing methodologies. For a broader perspective on the methodologies used to study drinking water microbiomes, the reader is referred to recent review articles (Douterelo et al., 2014; H. Wang et al., 2017; Zhang and Liu, 2019).

Cultivation-based techniques

In 1881, Robert Koch published the gelatin plate method (Koch, 1881). This allowed pure cultures of bacteria to be grown, isolated and quantified. Gelatin was later replaced by agar and, for drinking water monitoring, the nutrient composition was changed to allow detection of a larger fraction of the bacteria (Reasoner, 1990). The term heterotrophic plate counts (HPCs), used in the analysis of drinking water, refers to the plate-based methods that are used to enumerate the microorganisms that use organic carbon for growth (Bartram et al., 2003). There are several types of HPC methods, using various nutrient compositions, incubation temperatures (20–37 °C), and times (one to several days) (Allen et al., 2004b). HPC tests have been used historically and are still used as indicators for water quality (Bartram et al., 2003). While HPC methods aim to detect a large fraction of the microorganisms in a sample, culture-based techniques are also used to detect indicator microorganisms such as coliforms. Coliforms are a group of bacteria that includes *Escherichia coli*, which are found in the environment, as well as in the feces of humans and animals, and are used as an indicator of water quality and risk (Boubetra et al., 2011; Livsmedelsverket, 2017). Coliforms and *E. coli* can be detected using membrane filtration followed by cultivation on a selective medium; or, using multiple tubes containing liquid medium, inoculated with a dilution series of water sample to detect growth, followed by the most probable number technique to estimate the average number of bacteria in a sample (Sutton, 2010). Colorimetric tests such as Colilert (IDEXX Laboratories) are enzymatic assays that rely on enzyme substrates in a liquid medium that produce different color changes based on β-galactosidase and β-glucuronidase activity to detect coliforms and *E. coli*, respectively (George et al., 2000).

The advantage of culture-based techniques such as HPC is that a positive result shows the viability of the cells that form colonies. HPC methods are commonly used by water utilities to measure microorganisms due to their high degree of standardization, low cost, the simplicity of conducting the analysis, and clear guidelines from authorities (Bartram et al., 2003; Douterelo et al., 2014; Livsmedelsverket, 2001). The community composition of the water can be estimated by visually inspecting the size, shape, elevation, margin, and color of the colony. However, it is known that most of the microorganisms found in water cannot be cultured on the nutrient combinations used in standard HPCs, and it has been estimated that only 0.001 to 8.3% is detected (Bartram et al., 2003; Burtscher et al., 2009; Hammes et al., 2008). Furthermore, some cells may exist in a viable but non-culturable (VBNC) state due to starvation or other kinds of stress

(Bogosian and Bourneuf, 2001), and may also not be cultivated by HPC methods. A significant difference has been found between the number of culturable bacteria and the number of bacteria observed and counted with microscopy in the environment, and has been called "the great plate count anomaly" (Staley and Konopka, 1985). The colonies originating from HPCs are mostly copiotrophic (i.e., they grow in environments rich in nutrients), whereas the majority of the microorganisms found in drinking water are oligotrophic (i.e., they grow in environments low in nutrients), and cannot therefore be detected by HPC methods (Burtscher et al., 2009). The disadvantages of HPC methods have initiated the development and application of other techniques that are cultivation-independent, with the potential for better detection, quantification and compositional understanding of microorganisms in drinking water.

Cultivation-independent techniques

Various cultivation-independent techniques have been developed to overcome the limitations of cultivation-based techniques, in order to detect, quantify and explore the composition of microorganisms in drinking water.

Cell counting

Cells can be quantified using microscopy, which can be combined with fluorescent dyes to measure, e.g., total bacteria, viable bacteria or respiration using epifluorescence microscopy (Douterelo et al., 2014; Hobbie et al., 1977). Fluorescent *in situ* hybridization (FISH) uses fluorescently labelled oligonucleotide probes that bind to microbial DNA/RNA, and it is used to detect specific organisms (Wagner et al., 1994), such as pathogens in water (Moreno et al., 2003), or nitrifiers in biofilms (Lukumbuzya et al., 2020). The advantage of these methods compared to cultivation-based techniques is that they detect all or specific bacteria. However, since cell counting by microscopy is labor-intensive and requires operator expertise, it is not feasible for routine microbial monitoring at DWTPs and in DWDSs, and is mainly used for research purposes (Van Nevel et al., 2017).

Flow cytometry

Flow cytometry (FCM) makes use of the fluorescent dyes and probes used in epifluorescence microscopy and FISH, but the throughput and analysis time are improved. Since FCM provides substantially more information than cultivation-based techniques, is accurate and reproducible, fast (minutes to hours), and can be automated (Besmer et al., 2014; Hammes et al., 2012), it is a suitable

technique for monitoring drinking water microbiology (Hammes et al., 2008; Van Nevel et al., 2017). FCM was used in the present work to monitor SSF performance (Paper II) and biostability in the DWDS (Papers III, IV, & V). The possibility of automation reduces the amount of labor and expertise required, making this approach more suitable for integration in routine monitoring practices at DWTPs and in DWDSs.

FCM determines the number of individual cells and particles in a suspension by focusing them and passing them individually through a light source, usually a laser (Fig. 1). The scattered light and fluorescence are detected as the cells or particles pass through the laser beam (Muirheadi et al., 1985). For larger cells, such as mammalian cells, forward and side scatter are often used to measure cell size and granularity (Muirheadi et al., 1985). Some cells and particles may be autofluorescent, while others can be made to fluoresce by staining with fluorescent dyes or probes. Some dyes can serve the same purpose, for example, nucleic acids can be stained to distinguish cells from abiotic particles and instrumental noise (Wang et al., 2010). The dyes SYBR Green I, SYBR Green II and SYTO9 have been used to count cells in water (Hammes et al., 2008; Lebaron et al., 1998).

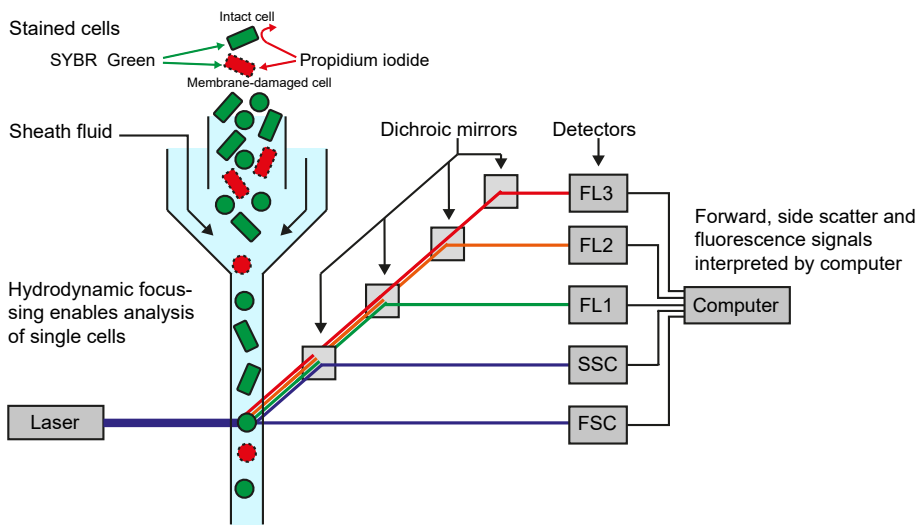

Figure 1. Schematic of the flow cytometer instrument. Cells are individually passed through a laser, and the scattered light and fluorescence are detected. In the example shown here, SYBR Green I and propidium iodide are used for cell staining. SYBR Green I stains the nucleic acid of both intact and membrane-damaged cells, whereas propidium iodide is a larger molecule and can only stain the nucleic acid of membrane-damaged cells. Abbreviations: FL, fluorescence; SSC, side scatter; FSC, forward scatter.

The dye SYBR Green I is commonly used to stain cells in drinking water to measure the total cell concentration (TCC) (Prest et al., 2013). This has been shown to be accurate (<3% relative standard deviation on measurements) and reproducible (<7% variability between laboratories) (Van Nevel et al., 2017). Combinations of dyes with FCM make it possible to measure several parameters at the same time. Viability staining of, for example, bacterial cell membrane integrity using propidium iodide (PI) has been suggested as a proxy for viable cells (Berney et al., 2007; Gatza et al., 2013). PI is a large molecule that only binds to nucleic acids of membrane-damaged cells, and not cells with intact membranes (Gatza et al., 2013). PI in combination with SYBR Green I (SYBR Green+ PI) thus discriminates between cells with intact and damaged membranes, and enables quantification of the intact cell concentration (ICC). SYBR Green + PI staining is widely used in drinking water studies, for example, to assess the effects of different types of treatment at DWTPs (Hammes et al., 2008; Ramseier et al., 2011), and the bacterial community dynamics in DWDSs (El-Chakhtoura et al., 2015; Prest et al., 2016b, 2014). It was used in the present work as a fast method of monitoring SSF performance (Paper II), to monitor the biostability in a DWDS, and to screen for samples suitable for more detailed analysis (Papers III, IV & V).

It is important to note that it is not currently possible to use FCM-ICC measurements to assess changes in cell viability due to DNA damage caused, for example, by UV irradiation, as the cell is still intact. Since PI only discriminates between intact and membrane-damaged cells, UV damage will not be detected with this stain combination (Paper I) (Van Nevel et al., 2017). Since UV irradiation is used at many DWTPs as one of the last treatment steps, the use of FCM-ICC to monitor the disinfection of finished water at a DWTP using UV irradiation will not show the real disinfection efficiency. This would require additional sample handling, for example, inducing membrane damage through heat treatment, sonication or incubation, and then inferring the ICC. However, it would be necessary to develop and test a standardized protocol, bearing in mind that elevated temperature during incubation may lead to microbial regrowth. The dye 5-cyano-2,3-ditolyl tetrazolium chloride (CTC) is used to determine the respiratory activity of bacteria (Kobayashi et al., 2012). CTC-FCM has been used to assess VBNC bacteria induced by UV irradiation (Guo et al., 2019), however, it was concluded that it may not reflect the overall activity of bacteria but instead the essential viability to keep cells alive. Different types of dyes targeting, for example, Gram-positive or Gram-negative bacteria (Holm and Jespersen, 2003) or glucose uptake (Bosshard et al., 2009) can also be used in FCM.

In the analysis of drinking water samples with FCM using SYBR Green + PI staining, the fluorescence signal from a sample is visualized as a two-dimensional (2D) histogram showing the intensity of the red and green fluorescence of all the cells and particles (Fig. 2). Bacterial cells are selected and measured by "gating" their higher intensity in green fluorescence, to remove background noise from sources such as free DNA and organic/inorganic particles (Prest et al., 2013). TCC is measured by only staining with SYBR Green I, whereas ICC involves SYBR Green + PI staining. The membrane-damaged cells will show a higher intensity of red fluorescence due to the increased uptake of PI, and thus the intact cells can be counted (Fig. 2).

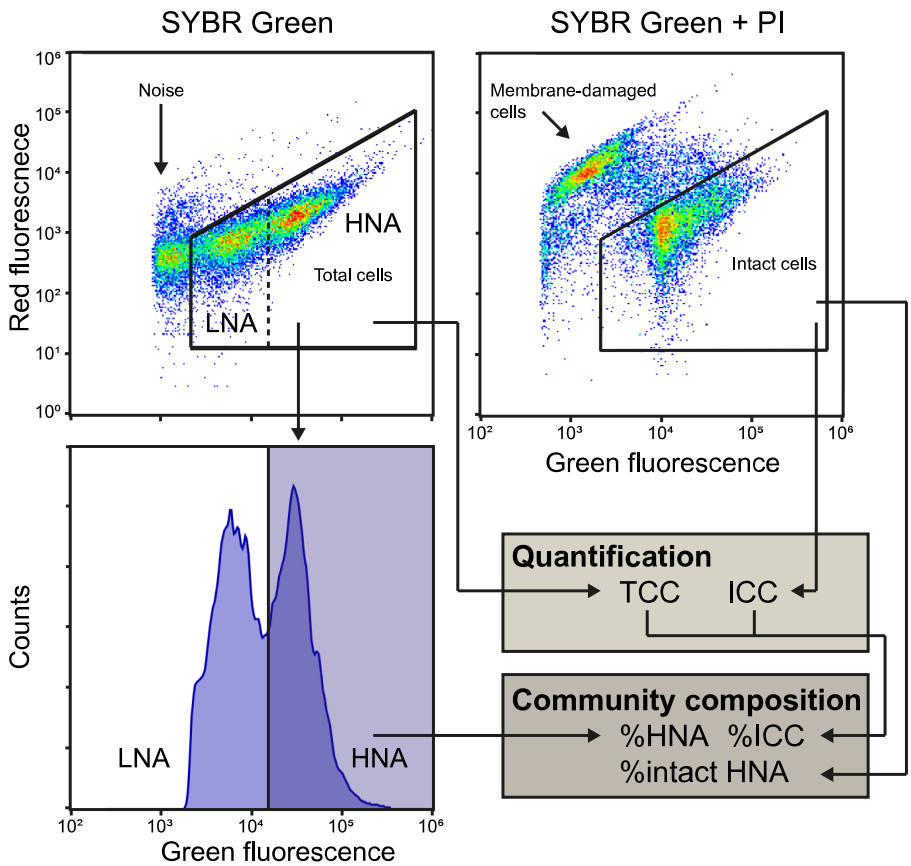

Figure 2. Overview of two different FCM staining protocols: SYBR Green I, and SYBR Green I + PI and their combined data output. The upper panels show the 2D histograms of red fluorescence intensity against green fluorescence intensity and the bottom left panel shows the gated fraction in a histogram of the number of counts against the green fluorescence intensity, called the "fingerprint". Abbreviations: TCC, total cell concentration; ICC, intact cell concentration; LNA, low nucleic acid; HNA, high nucleic acid.

The FCM method has a lower quantification limit of ~100–200 cells/mL (Hammes et al., 2008; Hammes and Egli, 2010), and a delay prior to measurements can affect the results due to changes in cell physiology, oversaturation into or leakage of dye out of cells, or stain degradation (Nevel et al., 2013; Suzuki et al., 1997). A total measurement time of less than 80 minutes has been suggested for reproducible results (Nevel et al., 2013). Excessive amounts of organic material such as humic acids can bind to dyes such as SYBR Green I and quench the fluorescence signal (Sidstedt et al., 2015), and in FCM this can lead to incomplete staining of cells from background sources such as raw water or wastewater, which often contain humic acids (Rodrigues et al., 2009). This can be overcome by diluting the samples or using more dye to fully saturate the cells. This may not be a problem when analyzing samples of drinking water, where the organic matter content is low. Only liquid samples can be analyzed directly with FCM. The enumeration of cells in biofilms, for example, requires additional handling, such as the extraction of cells from the biofilm into a liquid. Various methods have been proposed for this (Elhadidy et al., 2017; Frossard et al., 2016; Neu et al., 2019, 2018; Vignola et al., 2018). However, samples with high organic matter content pose a challenge to cell extraction, leading to false positive results, possibly due to viral particles and extracellular DNA adhering to bacterial-sized mineral or organic particles (Frossard et al., 2016). Thus, protocol optimization and testing are required to confirm the reproducibility of each method (Vignola et al., 2018).

Community composition and fingerprinting

Not only does FCM with dyes quantify TCC and ICC, it also provides information on the microbial community composition in terms of the percentage of intact cells in a sample, and the accumulated, and distribution of, fluorescence intensity of all individual cells; commonly called the "fingerprint" (Prest et al., 2013). Clusters of bacteria can be seen based on their green fluorescence intensity when staining with SYBR Green I (Fig. 2) (Prest et al., 2013). These clusters of bacteria are sometimes referred to as low nucleic acid (LNA) and high nucleic acid (HNA) bacteria. Separation between LNA and HNA bacteria in drinking water is based on previous studies (Fig. 2 and Prest et al. (2013)).

In early studies on the LNA/HNA clusters, the HNA bacteria were considered to be the active part of the community (Lebaron et al., 2001; Servais et al., 2003). However, this was later disputed as metabolically active LNA bacteria were observed in seawater and freshwater (Longnecker et al., 2005; Nishimura et al., 2005). Wang et al. (2009) showed that LNA bacteria were small and could pass through 0.45 µm filters, which could be used to roughly divide the LNA and HNA fractions. They were also able to isolate and cultivate the fraction of LNA

bacteria, confirming LNA activity; and the LNA bacteria maintained their size and LNA characteristics during growth. Due to their small size, the LNA fraction has been referred to as "ultramicrobacteria", "ultra-small bacteria" or "nanobacteria" (J. Liu et al., 2018). Phylogenetic differences have been reported between the LNA and HNA fractions (Proctor et al., 2018; Vila-Costa et al., 2012), while others found no differences (Rubbens et al., 2019). Using cell sorting, Vila-Costa et al. (2012) showed phylogenetic differences between the LNA and HNA fractions in marine water. Proctor et al. (2018) utilized the small size of LNA bacteria by filtering different types of freshwater through 0.45 µm filters, and demonstrated phylum-level differences in LNA and HNA bacteria. Rubbens et al. (2019) found no phylogenetic differences between HNA and LNA bacteria in different types of lakes. However, they observed correlations of a higher heterotrophic production, inferred by the protein synthesis rate measured with the incorporation of radiolabeled leucine, with HNA absolute cell abundances, indicating that LNA and HNA bacteria may have different functionalities. The differences in LNA and HNA bacteria are still the subject of debate, and may remain unresolved since more than two fractions of bacteria are often seen in aquatic samples (Amalfitano et al., 2018; Vila-Costa et al., 2012; Paper II), and taxa may be linked to specific subfractions based on the FCM fingerprint (Rubbens et al., 2019). Growth and division of bacteria lead to replication of DNA, which may also affect the interpretation of what is represented by bacteria identified as being LNA or HNA. Nevertheless, classifying the bacterial population as LNA or HNA bacteria is still valuable, and has been widely used to detect contamination of drinking water (Prest et al., 2013) and to monitor aquatic systems (Besmer et al., 2014). In this work, it was found that a higher proportion of LNA bacteria in the effluent from SSFs was associated with well-functioning treatment, defined as the removal of coliforms and TOC, and a consistent community fingerprint of the effluent water (Paper II). Observations also revealed that biofilm bacteria entering the water in close proximity to the DWTP (residence time < 25 h) generally existed as HNA bacteria (Papers III & IV), whereas a longer residence time was correlated with an increased proportion of LNA bacteria (Paper V), perhaps indicating a different pipe biofilm community at distances further from the DWTP. A better understanding of what lies behind the assigned identity of LNA and HNA bacteria could facilitate the use of other types of dyes in combination with SYBR Green I to investigate, for example, the LNA and HNA clusters within active cells, Gram-positive and Gram-negative bacteria, or membrane intact cells. Cell sorting in combination with other techniques to observe phylogenetic and physiological traits of LNA and HNA bacteria or other subfractions of bacteria could also be of interest,

however, due to the low cell concentrations in drinking water and limitations in the throughput of a cell sorter, this could be challenging.

Other, more sophisticated, fingerprinting tools have been developed to utilize the characteristics of each individual cell obtained from FCM. Cells with similar characteristics will appear in clusters, as shown in the histograms in Figure 2 (i.e., the cytometric fingerprint). The cytometric fingerprint represents the community structure in a sample at the point of measurement (Koch et al., 2014). Some cytometric fingerprints are easily distinguishable by the naked eye (see Fig. 4 in Paper II), but this becomes increasingly difficult with many samples. It is also more difficult to quantify changes in the cytometric fingerprint, as this requires it to be transferred to a dissimilarity matrix, which can be evaluated and explored in microbial community analyses (Koch et al., 2014). Various types of cytometric fingerprinting tools have been developed, using different analysis principles and procedures. Examples of these are CHIC (Koch et al., 2013a), Cytometric Barcoding (CyBar) (Koch et al., 2013b), Dalmatian plot (Bombach et al., 2011), FlowFP (Rogers and Holyst, 2009), and PhenoFlow (Props et al., 2016b). Koch et al. (2014) evaluated CHIC, CyBar, Dalmatian plot, and FlowFP. Cytometric fingerprinting has been used to analyze aquatic samples (Props et al., 2018), and for drinking water monitoring (Favere et al., 2020). Cytometric fingerprinting was used in the present work for the efficient comparison of SSF influent and effluent community composition (Paper II), and to find correlations between community composition in a DWDS and parameters such as residence time (Paper V). Correlations have been reported between cytometric fingerprints and taxonomic bacterial diversity measured using 16S rRNA gene amplicon sequencing (Chan, 2018; Props et al., 2018, 2016b), further demonstrating the usefulness of cytometric fingerprinting. It should be noted that robust cytometric fingerprinting requires raw data from the same flow cytometer platform, using identical detectors, protocols (Props et al., 2018), and instrumental setup, quality control using fluorescent beads between measuring days (Koch et al., 2013a), and complete saturation of the cells with dye.

The cytometric fingerprinting tool CHIC was used in the present work (Koch et al., 2013a) together with the flowCHIC package (Schumann et al., 2020) in R programming language and software environment (R Core Team, 2020). The workflow starts by selecting bacteria through identical gating of 2D histograms of red fluorescence intensity against green fluorescence intensity for all samples which are converted to grayscale images. The user decides the number of bins, i.e., the resolution to which the 2D histogram is converted. The default number of bins is 128 (Koch et al., 2013a), but should be chosen based on the number of cells analyzed. Lower resolution may be more suitable for samples with few cells

due to variation in the data, and to reduce the effect of outliers on the outcome. For this reason, 64 bins was chosen in the studies described in Papers II and V. Pairwise comparisons of the cytometric images from all the samples are performed in three steps. First, an exclusive or (XOR) function is used to compute the pixel-by-pixel differences between the images and to create a new image with a gradient from white to black, where white pixels indicate large differences and black pixels identical values. All pixels do not include signals; thus, a second algorithm is used to create an overlap image based on the informative pixels. Finally, the average gray value is calculated based on the XOR image and overlapping image, which is a measure of the dissimilarity between two samples. This analysis is repeated for all the pairs of samples, and the results are visualized in a non-metric multidimensional scaling (nMDS) plot, showing the differences between the communities (Fig. 5 in Paper II & Fig. 4 in Paper V). Additional tools can be applied to fit other recorded parameters to the nMDS plot using the Vegan package (Oksanen et al., 2019). CHIC has also been used to assess the biostability in a DWDS (Farhat et al., 2020).

Molecular methods

Molecular methods usually involve handling DNA, RNA, proteins, or lipids. DNA analysis techniques were used to quantify gene content and investigate the composition of different taxa in samples. In these methods, the DNA in the cells is first extracted by mechanical and/or chemical or enzymatic lysis of the cells (Pollock et al., 2018), followed by downstream analysis.

PCR and qPCR

The polymerase chain reaction (PCR) was invented in 1987, and is used to amplify specific nucleic acid sequences (Mullis, 1990). It has been used for many different applications, including the detection of fecal indicators and pathogenic bacteria based on the target gene copies in food (Malorny et al., 2003). The analysis time is shorter than in cultivation-based methods (hours rather than days), but more time consuming than flow cytometry (minutes to hours). The technique relies on thermal cycling during which primers bind to the target DNA region and a heat-stable DNA polymerase elongates the DNA strand in multiple cycling steps in a solution containing water, deoxyribonucleotide triphosphates (dNTPs), divalent ions and a pH buffer (Mullis and Faloona, 1987). Amplicons can be visualized using gel electrophoresis, in which DNA fragments are separated based on their length. Bacteria can be quantified with quantitative PCR (qPCR), which uses oligonucleotide probes complementary to the target region, or fluorescent dyes, by measuring the fluorescence during amplification (Bustin et

al., 2009). qPCR has been applied to drinking water samples to detect possible opportunistic pathogenic bacteria such as *Legionella* and *Mycobacterium* species (Donohue et al., 2019). The total amount of bacteria in a sample can be quantified by amplification of the 16S rRNA genes (see below) using qPCR (Nadkarni et al., 2002). RNA can be used to infer the number of active organisms, and is quantified by reverse transcription qPCR (RT-qPCR), where the RNA is first transcribed to complementary DNA which is then quantified using qPCR. RNA viruses can be detected using RT-qPCR, for example, the detection of the SARS-Coronavirus-2 in sewage (Medema et al., 2020).

Many other molecular methods are based on PCR, such as 16S rRNA gene amplicon sequencing, denaturing gradient gel electrophoresis, and terminal restriction fragment length polymorphism. The advantage of PCR-based methods is that they can be used to analyze specific bacteria of interest and non-culturable bacteria. However, since the PCR amplifies all the DNA present in a sample, it cannot be used to discriminate between living and dead cells. The DNA-binding dye propidium monoazide (PMA), which only penetrates membrane-damaged cells (similarly to PI) and makes DNA insoluble, has been used to detect viable cells using qPCR (Elizaquível et al., 2014; Nocker et al., 2006). However, PMA is not widely used in combination with PCR, possibly due to a lack of protocol optimization and standardization.

DNA Sequencing

DNA sequencing is used to identify the sequence of nucleotide bases in DNA. One of the first established sequencing techniques was Sanger sequencing (Sanger et al., 1977b), which was used to sequence the first complete genome of bacteriophage ϕX174 (5 386 bp) in 1977 (Sanger et al., 1977a), and years later, the human genome (2.91 billion bp) (Craig Venter et al., 2001). As Sanger sequencing of many samples is costly and time consuming, next-generation sequencing (NGS) technologies were developed, allowing millions to billions of DNA nucleotides to be sequenced in parallel, reducing both cost and time (Metzker, 2010). NGS technologies are often called “second-generation sequencing”, “massively parallel sequencing” or “high-throughput sequencing”. The emergence of cheap DNA sequencing has revolutionized DNA analysis, facilitating screening for pathogens and the detection of resistance to antimicrobial agents at a lower cost and in a shorter time than previous technologies (Pallen et al., 2010). Many NGS methods are available (Goodwin et al., 2016), but the Illumina technique currently dominates (Mohamed and Syed, 2013).

The Illumina MiSeq technique was used in the present work for amplicon sequencing. Illumina uses sequencing by synthesis, whereby DNA is sequenced when each nucleotide is incorporated by DNA polymerization, in combination with reversibly terminated nucleotides. Amplicons including adapters at both ends are denatured, and single strands of amplicons are bound to a flow cell surface by complementary binding to adapters. PCR amplification is performed to generate clusters of identical fragments that are sequenced in both forward and reverse directions. Sequencing is performed by the addition of uniquely fluorophore-labelled terminally blocked nucleotides, and every time a nucleotide is added to the strand, fluorescence imaging is performed. The fluorophores are removed and nucleotide termination is regenerated, followed by the incorporation of new nucleotides; the steps are repeated until the DNA strand is sequenced. Sequencing runtime depends on the version of the instrument and the cassette used. The runtime of the Illumina MiSeq v3 is about 21–56 h (Goodwin et al., 2016). This technique can be used to sequence fragments of 250–300 bp, but since it sequences DNA fragments in both directions, called paired-end sequencing, it is possible to merge the fragments together by overlapping regions using bioinformatics. Thus, ~500 bp fragments can be sequenced in practice due to a required sequence overlap (Fadrosh et al., 2014) and removal of low-base-quality regions of sequences due to higher error rate as more bases are incorporated in the sequencing, especially in the second read (Tan et al., 2019). The field of DNA sequencing is developing rapidly, and "third-generation sequencing" techniques are now available, which enable sequencing without the need for PCR amplification and which provide increased read length. Some techniques have read lengths of 10 000 to 200 000 bp (Goodwin et al., 2016).

Microbiome research utilizing sequencing is usually based on amplicon sequencing of marker genes to obtain taxonomic information, such as the 16S rRNA gene (bacteria), the 18S rRNA gene (eukaryota) or the ITS region (fungi); or shotgun metagenomics, in which the genomes of the organisms are first fragmented into smaller pieces and the fragments then sequenced. These reads can be taxonomically classified directly or, due to the redundancy of overlap between fragments, it is possible to align and merge fragments to assemble longer contiguous sequences (contigs) and to reconstruct metagenome-assembled genomes (MAGs) (Bowers et al., 2017; Breitwieser et al., 2017; Tyson et al., 2004).

16S rRNA gene amplicon sequencing

16S ribosomal RNA (rRNA) is part of the small subunit of the prokaryotic ribosome and, through evolution, the gene has been conserved with variable

regions in different groups of prokaryotes. Comparison of the 16 rRNA gene of different organisms makes it possible to resolve evolutionary relationships and visualize phylogenetic trees by quantifying sequence divergence (Hugenholtz, 2002). This revolutionized microbial taxonomy in the 1970s by the division of cellular organisms into bacteria, archaea, and eukaryota (Woese, 1987).

16S rRNA gene amplicon sequencing provides knowledge on the composition of a community in a sample, and the identity and phylogeny of taxa. The 16S rRNA gene is ~1500 bp long, and consists of nine hypervariable regions flanked by conserved regions (Fig. 3) (Johnson et al., 2019). The hypervariable regions have been widely used to specify bacterial taxa as large databases include 16S rRNA taxonomic identification (Edgar, 2018). Using PCR with primers binding to the conserved regions of the 16S rRNA gene, amplifying a hypervariable region together with subsequent DNA sequencing of the amplicons, has made it possible to identify and explore the bacterial diversity in many microbiomes, including those of environmental origin (Gilbert et al., 2014), or locations in the human body (Huttenhower et al., 2012). In the present work, PCR amplification of the 464 bp V3-V4 region was used (Klindworth et al., 2013). This region has been suggested for use in studies on the drinking water bacteriome (Brandt and Albertsen, 2018) as it has a good trade-off in variability between taxa within the hypervariable regions (high values on the y axis in Fig. 3) and low variability in the conserved regions for primer design (low values on the y axis in Fig. 3).

The workflow of 16S rRNA gene amplicon sequencing is illustrated in Fig. 4. Each sample is amplified with either unique fusion primers containing the adapters required for sequencing and identification nucleotides (index sequences),

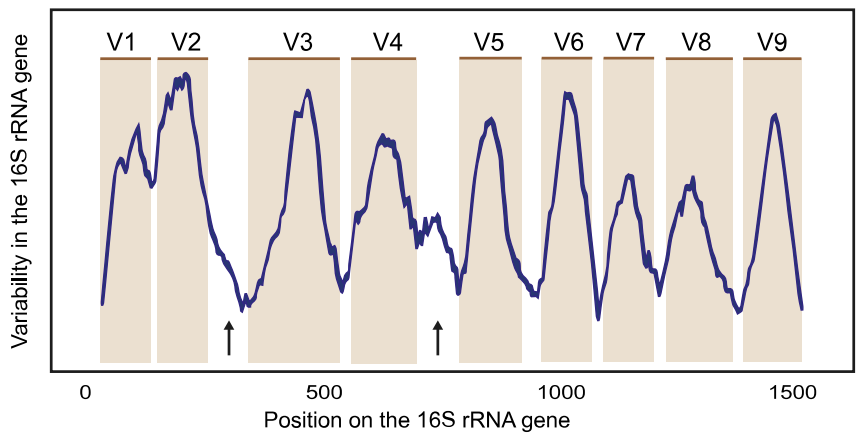

Figure 3. The 16S rRNA gene and its variable regions (V1-V9). A lower value on the y axis indicates greater similarity between bacteria. The shaded brown areas indicate the nine variable regions. The conserved regions are located between the variable regions (white background). The primer positions used in this work were the conserved regions before V3 and after V4, indicated by the two arrows. Adapted from (Johnson et al., 2019).

or they are added after PCR using adaptor ligation (D'Amore et al., 2016). The amplicons are DNA sequenced and further analyzed bioinformatically.

Many different bioinformatics pipelines and tools are available (e.g., QIIME2 (Bolyen et al., 2019), MOTHUR (Schloss, 2020) and USEARCH (Edgar, 2010)) and are being continuously developed and updated. In this work, QIIME (Caporaso et al., 2010) and QIIME2 (Bolyen et al., 2019) were used as they have been extensively applied for the assessment of environmental microbiomes (Gilbert et al., 2014). Reads for each sample are organized based on the index sequences, in a process called demultiplexing (Renaud et al., 2015), followed by sequence quality control by investigating the quality of base calls. Based on these results, sequences are trimmed and/or truncated. In the present work, truncation was used at sequence positions 250 and 250, in forward and reverse reads, in one study (Paper I), and truncation at sequence positions 280 and 215 was used in the other (Paper III), both based on visual examination of the quality of base calls. The DADA2 pipeline (Callahan et al., 2016) removes low-quality regions of sequences, filters chimeric sequences (described below), and produces a *Feature Table* (amplicon sequence variant (ASV) table) and *Feature Data* (ASV data). The ASV table consists of counts of each ASV, and the ASV data include information on each ASV nucleotide sequence. Traditionally, clusters of reads that were very similar (usually using a threshold of >97%) were grouped into operational taxonomic units (OTUs), and OTUs were considered as a "species" in taxonomic profiling (Callahan et al., 2017) (used in Paper IV). However, recent developments in bioinformatics and DNA sequencing have contributed to an ASV-based approach (used in Papers I & III), in which the exact sequence is considered a species, which is equivalent to 100% OTUs and also called exact sequence variants (ESVs) or zero-radius OTUs (zOTUs). Instead of being clustered into OTUs, ASVs are denoised, and thus have higher quality due to better quality control, and they therefore have better sensitivity and specificity than OTUs (Callahan et al., 2017). ASVs are also easier to compare between studies since the exact sequences are consistent (Callahan et al., 2017), whereas OTUs are specific to each data set and study. However, a study comparing the two methods showed similar ecological outcomes (Glassman and Martiny, 2018), suggesting that studies using OTUs are still of relevance. Phylogenetic trees are inferred based on the nucleotide sequence information from each ASV (Price et al., 2009). Taxonomic assignment of the ASV sequences is achieved by comparison with a reference database, such as Greengenes (Desantis et al., 2006), SILVA (Quast et al., 2013), RDP (Wang et al., 2007), or an environment-specific database, such as MiDAS for activated sludge (McIlroy et al., 2015). Depending on the quality of reference sequence annotations and marker gene heterogeneity,

ASVs can be, at most, classified to genus or species level using the 16S rRNA gene (Breitwieser et al., 2017), together with the widely used short-read strategy, as in the present work. Due to the limited resolution, pathogen detection using the 16S rRNA gene is not always sufficient, and more specific target genes are required in pathogen identification (Clarridge, 2004). The outcome of the bioinformatics pipeline consists of: 1) an ASV table containing reads of ASVs in each sample, 2) sequence information on each ASV, and 3) a phylogenetic tree, all of which can be used in downstream data analysis.

The output from the sequencing pipeline can be imported and further analyzed using various tools. In the present work, R programming language and software environment (R Core Team, 2020) was used, which has specific packages for the analysis of e.g. microbiome data (phyloseq, (McMurdie and Holmes, 2013)), data visualization (ggplot, (Wickham, 2016)), and data wrangling and manipulation (tidyverse (Wickham, 2017)). Since R is freely available, is versatile with many

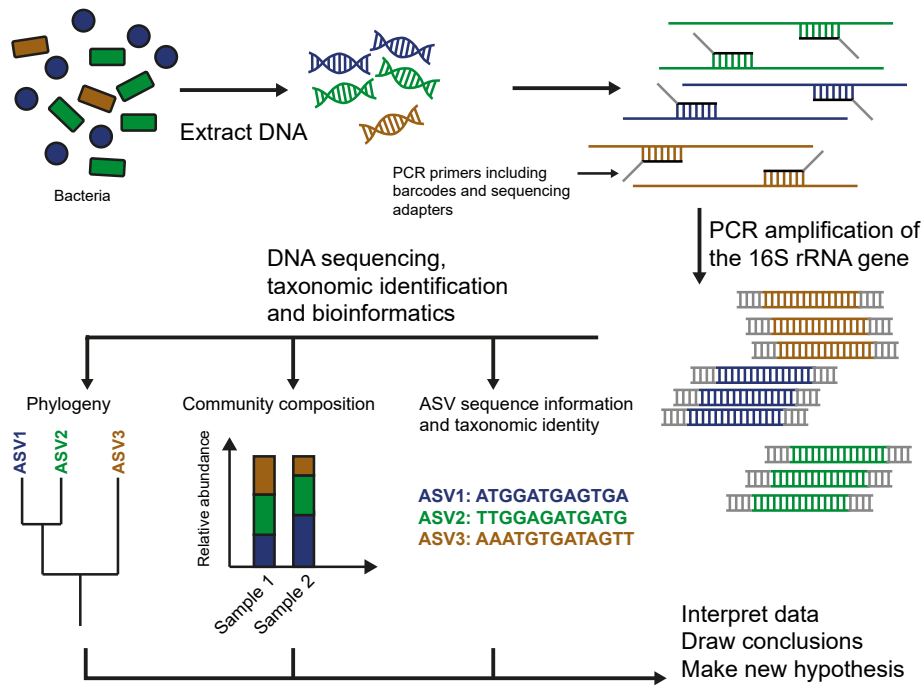

Figure 4. The 16S rRNA gene amplicon sequencing workflow. The DNA in bacteria is extracted, followed by PCR amplification of the 16S rRNA gene. In this example, fusion primers are used to amplify the 16S rRNA region. The amplicons are sequenced and the reads obtained are demultiplexed and quality checked, followed by taxonomic identification. The colors (blue, green, and brown) in this schematic represent different taxa of bacteria. The outcome of the 16S rRNA gene amplicon sequencing workflow is the amplicon sequence variant (ASV) sequence information and taxonomic identity, community composition, and phylogeny.

packages, and numerous online guides, tutorials, and forums are available, it is a useful tool for data analysis and visualization.

To avoid the analysis of low-quality reads and spurious sequences, singletons and low-abundant ASVs are removed (Bokulich et al., 2013). Since the total read count in a DNA sequencing run is of fixed size and it is difficult to load the sequencing run with exactly the same amounts of DNA for different samples, ASV reads are usually converted into relative abundance, normalized counts, or are rarefied (Gloor et al., 2017). Rarefaction has traditionally been used, but since this may result in loss of information and precision (McMurdie and Holmes, 2014), transformation to relative abundance of ASVs within samples was used in this work (Papers I & III).

Diversity analysis is typically performed in two ways: alpha diversity, measuring species diversity within a sample; and beta diversity, measuring species diversity between samples. Alpha diversity is often expressed as the number of species in a sample (observed ASVs) and how the species are distributed relative to each other (Shannon index and evenness). A high Shannon index or evenness value indicates that all the species have the same frequency in the sample. Differences in highly abundant taxa may affect alpha diversity measures drastically, for example, the *Pelagibacteraceae* family decreased in relative abundance after exposure to UV irradiation, which drastically affected the Shannon index and evenness value (Paper I). Beta diversity frequently involves quantification of the dissimilarity in composition between samples, and is often performed with a distance or dissimilarity matrix such as the Bray-Curtis. This allows plotting ordination analyses to visualize sample similarities (see, for example, Fig. 1 in Paper I & Fig. S7 in Paper III) and testing for statistical sample groupings. Barplots and heatmaps are often used to visualize taxa compositions and are valuable in obtaining an overview of the data, and when the taxa compositions are vastly different between samples. Plotting specific taxonomic levels or ASVs in panels may provide a more detailed understanding of the microbial composition, such as changes in microbial composition as a result of treatment (Fig. 2 in Paper I) or changes in dynamics over time (Fig. 6 in Paper III).

Bioinformatics tools called differential abundance methods can be used to detect relations in the abundances of bacterial taxa between sample groups, to determine whether the proportions are significantly different (McMurdie and Holmes, 2014). Some tools, such as DESeq2 (Love et al., 2014), originated from RNA-sequencing counts for the estimation of significant changes in the expression of different genes. This tool has been applied to microbial sequencing data to identify differences in taxa abundance between sick and healthy patients (Halfvarson

et al., 2017), and differences in the gut microbiome in mice given different types of drinking water (Dias et al., 2018). It has also been suggested that the model in the method is suitable for small studies, when the number of samples and replicates is low (Love et al., 2014), which is often the case in 16S rRNA gene amplicon sequencing studies. The differential abundance tool DESeq2 was used in this work to infer fold changes between UV-treated and non-treated samples (Paper I), and to compare finished water with DWDS samples to identify which bacteria were leaving the biofilm (Paper IV). These bacteria were later confirmed to be present in the biofilm by excavating pipes and analyzing the bacterial community in the pipe biofilm (Paper III).

Microbial source tracking was developed at the end of the 20th century to determine the source of fecal contamination in environmental waters. Early source tracking was performed using indicator bacteria to identify the source of contamination (Harwood et al., 2014). Advancements have since been made, and bioinformatics tools have been developed to identify the source of contamination. SourceTracker (Knights et al., 2011) is a tool that uses Bayesian modelling to estimate the proportion of contaminants or taxa in a community originating from possible source contaminants using 16S rRNA gene amplicon sequencing datasets. The tool has been used to assess fecal contamination in coastal (Henry et al., 2016) and other source waters (Hägglund et al., 2018), and to identify the origin of bacteria in tap water (G. Liu et al., 2018). SourceTracker was used in the present work to estimate the contribution of biofilm bacteria to the bulk water in a DWDS (Paper III).

Biases and challenges in PCR and sequencing workflows

Several steps are involved in PCR and sequencing workflows. These include sampling, sample preparation, DNA extraction, PCR steps, DNA sequencing, and the application of bioinformatics pipelines and tools. Virtually all these steps can lead to the introduction of bias in the final results, and thus influence the conclusions drawn (D'Amore et al., 2016; Gohl et al., 2016; Goodrich et al., 2014; D. Kim et al., 2017; Pollock et al., 2018).

Some cells, such as endospores and Gram-positive bacteria, may be more difficult to lyse than others, which can affect DNA extraction efficiency (Hwang et al., 2012; Pollock et al., 2018). The use of bead-beating has been suggested to overcome this, to yield more DNA, higher bacterial diversity, and more effective extraction of DNA from cells with strong cell walls (Guo and Zhang, 2013; Henderson et al., 2013). Many commercial kits are available for DNA extraction, for example, the FastDNA Spin Kit for Soil (MP Biomedicals), the Power Biofilm Isolation Kit (MoBio Laboratories), and the DNAeasy Kit (Qiagen). Traditional

phenol-chloroform extraction has also been used (Pinto et al., 2012). The FastDNA Spin Kit for Soil, which uses bead-beating, has been suggested as the method of choice for analyzing DWDS samples (Hwang et al., 2012), and was used for DNA extraction in the present work. It gives reproducible results (Lührig, 2016) and has been widely used to extract DNA from water samples and biofilms (Fowler et al., 2018; Han et al., 2020; Ling et al., 2016; Liu et al., 2020; Lührig et al., 2015; Waak et al., 2019a). Depending on the type of sample, DNA extraction efficiency can be affected by inhibitors such as debris or organic matter, which can also effect further downstream processes such as the PCR (Hedman and Rådström, 2013; Pollock et al., 2018; Sidstedt et al., 2020). DNA extraction kits, and the reagents used, may also contain contaminating microbial DNA (Salter et al., 2014). DNA extraction and the analysis of low-biomass samples using 16S rRNA gene amplicon sequencing can therefore be difficult, as contaminating 16S rRNA gene sequences may account for a large fraction of the sequences, leading to erroneous results (Eisenhofer et al., 2019). Including negative controls, such as empty DNA extractions, the addition of "blank" filter papers or swabs used in the study, or positive controls such as mock communities with known mixtures of free DNA, throughout the whole analysis, has been suggested as good practice (D. Kim et al., 2017).

The choice of PCR primer in 16S rRNA gene amplicon sequencing studies can affect the observed community composition. Primers can cause under-representation of taxa due to lack of sensitivity or mismatches to some taxa (Baker et al., 2003). The choice of primer set affects the taxonomic classification due to the sequences in reference databases, and the amplicon length, which has been restricted by sequencing techniques (Yang et al., 2016). Many different universal 16S rRNA gene primers have been used in drinking water studies targeting various regions: V1-V3 (Lührig et al., 2015), V3 (Waak et al., 2019a), V3-V4 (Brandt and Albertsen, 2018), V4 (Potgieter et al., 2018), V4-V5 (Ling et al., 2018), and V5-V6 (Roeselers et al., 2015), but no single primer pair can capture the whole microbial community composition (D'Amore et al., 2016; Johnson et al., 2019; Klindworth et al., 2013; Shakya et al., 2013). New sequencing techniques have been developed, permitting the sequencing of longer fragments, and sequencing of the full 16 rRNA gene is now possible, and species, and even strains, of some organisms can be discriminated and identified (Callahan et al., 2019; Johnson et al., 2019). Reverse transcription of rRNA molecules with long-read sequencing to avoid primer bias has also been used to find novel taxa, contributing to more complete rRNA databases (Karst et al., 2018).

The outcome of the PCR may be affected by, for example, the presence of PCR inhibitors, the choice of DNA polymerase, and/or the conditions during PCR

(Pollock et al., 2018; Sidstedt et al., 2020). Compounds such as humic acids, widely present in water (Rodrigues et al., 2009), may inhibit the PCR by reducing the DNA polymerase activity (Sidstedt et al., 2015). This problem can be overcome by using efficient DNA extraction that removes inhibitors, or by using robust DNA polymerases and buffer systems. Some DNA polymerases are more tolerant to inhibitors (Sidstedt et al., 2015), and the use of facilitators such as bovine serum albumin (BSA), in PCR can prevent inhibitors from interacting with the DNA polymerase, which may enhance amplification efficiency in samples containing inhibitors (Farell and Alexandre, 2012; Hedman et al., 2013). DNA polymerases can incorporate false nucleotides in both the initial PCR and the PCR required in the sequencing process (see above), leading to false discoveries of the identity of microorganisms and community composition. To solve this problem, high-fidelity DNA polymerases with low misincorporation rates and proofreading activity can be used (Lahr and Katz, 2009). However, high-fidelity polymerases with low processivity, in combination with the large number of amplicons in the later PCR cycles, can increase the formation of chimeras and influence the final result (Pollock et al., 2018). Chimeras are artifact sequences, and the majority are thought to form due to incomplete extension in the PCR. The sequence formed acts as a primer in a different, but similar, sequence in the subsequent cycles to form chimeric sequences (Smyth et al., 2010). Since the risk of chimera formation is higher in the later PCR cycles, reducing the number of PCR cycles can decrease their formation (Sze and Schloss, 2019). Chimeras can also be removed using various bioinformatics tools (Callahan et al., 2016; Edgar et al., 2011). Bearing in mind the above factors, it is important to optimize the PCR reagents and conditions, as well as to use the same protocols for all samples to allow robust comparisons.

The choice and use of bioinformatics pipeline also affects the outcome (Kaszubinski et al., 2020). A comparison of six bioinformatics pipelines showed that older pipelines such as QIIME-uclust produced many spurious OTUs, affecting alpha diversity measures (Prodan et al., 2020). This was also seen in the present work, where the same types of water from the same treatment plant appeared to have fewer observed taxa (ASVs/OTUs) when analyzed using QIIME2 (Paper III) than with QIIME (Paper IV). The taxonomic classification of sequences depends strongly on the database used, and inconsistencies have been reported between databases, as well as many annotation errors (Edgar, 2018). Thus, while the conclusions drawn from studies using the same pipeline are of value and appropriate, it may be difficult to compare the results of studies in which different bioinformatics pipelines have been used. Other bioinformatics tools, such as differential abundance methods, can be used to estimate fold

changes between samples (Love et al., 2014), although the reliability of these tools has been questioned due to the number of false discoveries by several of these methods (Hawinkel et al., 2019; Thorsen et al., 2016). Since the field of bioinformatics is still developing rapidly, new and better methods can be expected allowing researchers to perform comprehensive analyses of the microbiome.

Analysis methods – Summary and perspectives

All analysis methods have advantages and disadvantages, and it is important to be aware of their limitations. A short summary of some of the methods used in this work, together with their strengths and weaknesses is given in Table 1. Although they have several disadvantages, cultivation-based methods such as HPC have the advantage of identifying cell viability (on a specific type of medium), while the results of molecular methods, such as FCM and 16S rRNA gene amplicon sequencing, can be more difficult to interpret. However, the development of molecular methods has greatly improved our understanding of drinking water microbiology through advances in quantification, community composition, and the identification of microbes.

Advances in 16S rRNA gene amplicon sequencing have made it possible to identify bacteria in a sample to genus level, relatively cheaply (Franzosa et al., 2015). Next-generation sequencing data, for example, 16S rRNA gene amplicon

Table 1. Summary of the strengths and weaknesses of some of the analysis methods used in this work.

Method	Quantification	Composition	Analysis time	Advantages	Disadvantages
HPC	Yes	Yes/No*	Days	- "Real" viability	- Not all bacteria can grow - Coarse compositional data
FCM	Yes	Yes	Minutes to hours	- All bacteria are analyzed - Gives information on the concentration of intact bacteria	- No taxonomic identification
16S rRNA gene amplicon sequencing	No	Yes	Days to months	- All bacteria are analyzed - Taxonomic identification	- No quantification - Biased by DNA extraction, PCR, etc.

*Although HPC provides information on the composition based on colony size, shape, elevation, margin, and color, this may be subjective.

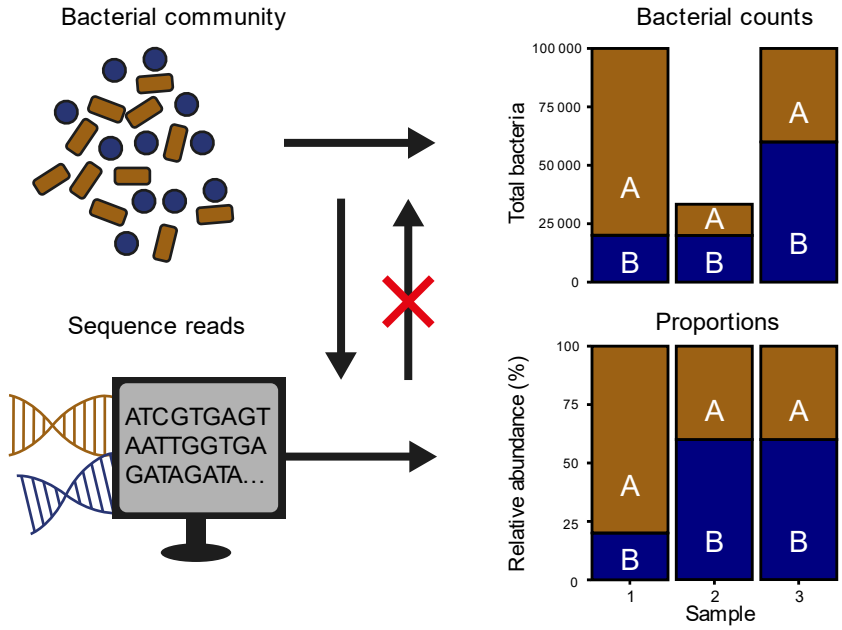

Figure 5. NGS data describe the microbial community in terms of proportions. Sequencing of the nucleic acids present in the bacterial community using 16S rRNA gene amplicon sequencing, for example, does not describe the absolute abundances of the community. Adapted from (Gloor et al., 2017).

sequencing data, is compositional (Gloor et al., 2017; Widder et al., 2016). This can cause difficulties when interpreting differences between samples (Fig. 5). As an example, consider the case where Sample 1 and Sample 2 have both different total bacterial counts and proportions of Bacteria A and B, but the same number of Bacteria B. Sample 3 has a different number of total bacteria than Sample 2, but the same proportions of the two bacteria in the community. Using 16S rRNA gene sequencing would provide only compositional data, and the conclusion would be that the proportions of Bacteria A and B in Samples 2 and 3 are similar, which is true, but no information would be obtained on the total numbers of each bacterium, although these are different in Samples 2 and 3, while Samples 1 and 2 contain the same number of Bacteria B. Efforts have been made to find standard methods for the analysis and comparison of compositional data, but no consensus has yet been reached (Quinn et al., 2017). The use of compositional identity data (i.e. from 16S rRNA gene amplicon sequencing) together with quantification methods may provide a more comprehensive picture of the microbiota, and reveal discrepancies that would not have been detected when using only a compositional method (Props et al., 2016a). Microbes can be quantified with, for example, FCM (Papers II, III, IV, & V) and qPCR. However, it can be difficult to quantify microbes in some samples, such as

biofilms, with FCM, due to the need for cell extraction from the samples. It can also be difficult to analyze the total bacterial counts in biofilm using qPCR due to difficulties in normalizing the samples before DNA extraction. Clumps and other particles in the biofilm may affect the weight or volume added, affecting the yield of extracted DNA and the outcome of bacterial gene counts.

Routine microbial drinking water analysis is usually performed using cultivation-based methods, which take several days, and there is thus a need for faster and more reliable monitoring methods. Bacterial cell counting using FCM is a faster method, which has been argued to provide more representative and relevant information on microbiological water quality than HPCs (Van Nevel et al., 2017). In addition, FCM allows for cytometric fingerprinting methods, which provide information on the microbial community (Chan, 2018; Props et al., 2016b, Papers II & V), and this, together with the possibility of automation (Besmer et al., 2014), makes FCM a valuable tool for the monitoring of microbial community dynamics. FCM monitoring can be used as an initial screening tool (Fig. 6) and, when needed, further, more costly or time-consuming analyses, such as bacterial community profiling with 16S rRNA gene amplicon sequencing, qPCR targeting specific bacteria, or metagenomics screening for genes or microbiome community profiling, can be used. As a result of rapid technological developments and improvements in portable devices for DNA sequencing (Krehenwinkel et al., 2019), 16S rRNA gene amplicon sequencing, or other even more advanced techniques, will probably be introduced for rapid monitoring of microbial water quality in the near future.

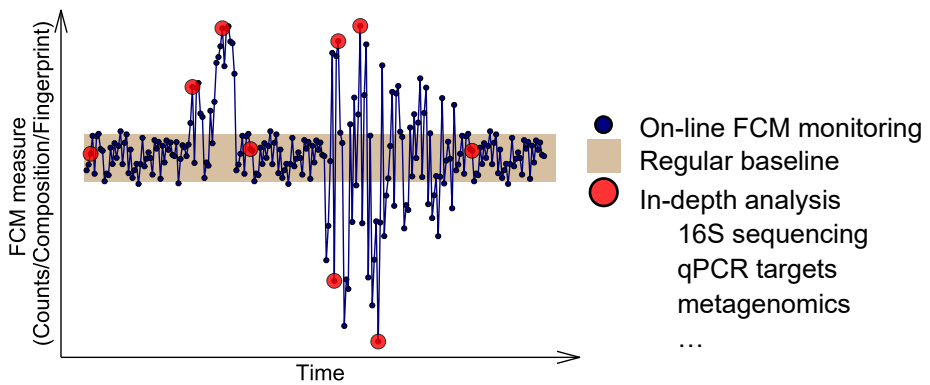

Figure 6. Strategy for fast monitoring of microbial community dynamics using FCM as a fast monitoring tool, and complementing the FCM data with more detailed analyses to obtain a more comprehensive understanding of the microbial community. More detailed analysis could include analysis of the microbial taxonomy or the measurement of specific bacteria or gene content with 16S rRNA gene amplicon sequencing, qPCR, or metagenomics. Adapted from (Props et al., 2016b).

Using marker genes, such as the 16S rRNA gene, provides a profile of the microbial community in samples, and it is possible, based on the taxonomy classification, to infer the hypothetical microbial functions from literature. If information on the microbial community profile can be combined with chemical data, it may be easier to identify the functions of the community, and the results less speculative. For example, high relative abundances of *Nitrosomonadaceae* (ammonia oxidizers) were observed with increased concentrations of ammonia, and *Nitrospira* (nitrite oxidizers) were detected in high relative abundances in combination with higher concentrations of nitrite (Paper III). Bioinformatics tools predicting the microbial community function based on marker genes have been developed during recent years, for example, PICRUSt (Douglas et al., 2020; Langille et al., 2013) and Tax4Fun (Aßhauer et al., 2015; Wemheuer et al., 2020). While these tools are valuable, their predictive ability relies on the genomes present in public databases, which may not always be updated or sufficiently comprehensive for the analysis of environmental samples such as drinking water. Assessment of microbial functions using shotgun metagenomics gives a better picture of the genes and functional profile of the community, but it is also more expensive than 16S rRNA gene amplicon sequencing (Ortiz-Estrada et al., 2019). While marker gene sequencing and metagenomics identify which DNA is present, they do not provide any information on the activity of the microorganisms. Microbial activity in drinking water can be inferred by measuring, for example, ATP, or the availability of carbon like assimilable organic carbon (AOC), or using enzymatic assay tests. ATP can be measured with a bioluminescence assay (Helm-Hansen and Booth, 1966; Van Der Kooij et al., 2003), but this is limited by a lack of standardization and instrumental noise from compounds in the water (Hammes et al., 2010). AOC is a fraction of the dissolved organic carbon, (DOC) and is measured by the growth of *Pseudomonas fluorescens* P-17 and *Spirillum* sp. strain NOX, which takes 5–7 days (Van der Kooij, 1992; Van Der Kooij et al., 1982a). Enzymatic activity tests quantify the abundance of enzymes catalyzing the degradation of substrates. Protocols for measuring microbial activity using FCM have also recently been suggested (Elhadidy et al., 2016; Farhat et al., 2018). A better understanding of the activity and the functions within a microbial community could be gained using RNA with, for example, reverse transcriptase PCR or metatranscriptomics, together with metaproteomics or metabolomics to assess proteins or metabolites, respectively.

Developments in molecular biology and DNA sequencing, allowing the sequencing of longer nucleotide fragments, and advances in bioinformatics are improving our knowledge on uncultured microbes in environmental samples. As

a result of these advancements, about 40 000 novel prokaryotic species are being discovered every year (Yarza et al., 2014). While these "omics" technologies, i.e., metagenomics, metatranscriptomics, metaproteomics, and metabolomics, are of great value to infer the physiological and ecological functions of the species in a community, the cultivation of microorganisms is a reliable way of validating hypotheses based on omics data (Cross et al., 2019; Gutleben et al., 2018). Pure cultures are useful in understanding microbial physiology and in curating and improving database annotation (Gutleben et al., 2018; Nichols, 2007). The knowledge gained from multi-omics has recently been used for medium development, screening techniques, and selective enrichment to isolate cultures and to further advance our understanding of the microbes present (Gutleben et al., 2018). Other methods such as single-cell targeted isolation may also help to isolate specific uncultured microorganisms of interest (Thrash, 2020). Simple measures, such as autoclaving agar and phosphate buffer separately, have been shown to increase colony counts and allowed growth of yet uncultured microbes (Tanaka et al., 2014). While the "omics era" has, and will continue to reshape our understanding of microorganisms, we may see a "cultivation renaissance" (Tamaki, 2019) in which omics technologies are combined with cultivation in microbial ecology studies.

Chapter 3
Impact of treatment processes on the microbial community

The use of drinking water treatment processes was documented 6000 years ago in Greek and Sanskrit texts describing the use of charcoal filters, exposure to sunlight, boiling, and straining to improve water quality (WHO, 2003). About 2000 years later, the Egyptians used coagulation to reduce the turbidity of water. In modern times, drinking water is usually treated at centralized or municipal DWTPs by various processes before the finished water is distributed to consumers. Treatment consists of physical, chemical, and biological treatment steps, and usually depends on the raw water quality, which varies between regions and countries (Zhang and Liu, 2019), but the cost and the general state of society also affect the kind of treatment used. The water used for drinking water is typically groundwater or surface water, but desalination can also be applied to sea water. In Sweden, about half of the drinking water distributed to consumers originates from surface water (approx. 170 DWTPs) and the other half from groundwater (~1500 DWTPs) (Svenskt Vatten, 2017). Physical or chemical processes such as coagulation, sedimentation, UV irradiation, and filtration can be used to remove or disinfect undesirable microorganisms or chemicals. Filtration processes such as UF combined with coagulation remove most microorganisms, and reduce most fractions of NOM in the finished water leaving the DWTP (Papers III, IV, & V). Other forms of treatment utilize microorganisms to treat the water, for example, slow sand filtration, biologically activated carbon (BAC), and infiltration. Residual disinfectants such as monochloramine or chlorine are used in many countries, including Sweden, to prevent the growth of undesirable microorganisms in the DWDS, whereas other countries such as the Netherlands, Switzerland, Austria, and Germany reduce the available carbon instead (Zhang and Liu, 2019) to prevent the regrowth of indicator microorganisms in the DWDS. The type of source water, its treatment, and the use of residual disinfectants will affect the drinking water microbiome (Dai et al., 2020; Proctor and Hammes, 2015b; Zhang and Liu, 2019). The

effects of UV irradiation, slow sand filtration, and ultrafiltration with coagulation on the drinking water bacteriome were investigated in the work described in this thesis.

UV treatment

UV irradiation is used to prevent microbial reproduction by causing damage to the nucleic acids in cells (Kowalski, 2009), and has been used to treat various kinds of foods and air (Koutchma, 2008; Reed, 2010). It was first used to treat drinking water at a treatment plant in Marseille, France, in 1910 (Hijnen et al., 2006). UV disinfection of drinking water has become increasingly popular as it is effective against the pathogens *Giardia* and *Cryptosporidium* and also due to concerns of disinfection by product (DPB) formation associated with chlorination (Hijnen et al., 2006). The UV doses used in drinking water treatment are not considered to produce any harmful DBPs (Ao et al., 2020; Hull et al., 2019a; Reckhow et al., 2010).

The wavelength of UV light is about 100–400 nm, and is divided into UVA (315–400 nm), UVB (280–315 nm), UVC (200–280 nm) and vacuum UV (100–200 nm) (Dai et al., 2012). The disinfection mechanism of UV irradiation is primarily by damage to both pyrimidines (thymine, cytosine, and uracil) and purines (adenine and guanine) in DNA, which absorb UV wavelengths of 200–300 nm; the absorption maxima of DNA being around 260–265 nm (Jungfer et al., 2007; USEPA, 2006). The absorption of UV light induces DNA damage, for example, the formation of cyclobutane pyrimidine dimers and 6-4 photoproducts. Pyrimidine dimers are the most reactive, absorbing about ten times more UV light than purines (Kowalski, 2009), and TT and TC sequences are the most photoreactive sequences (Douki and Cadet, 2001; Ravanat et al., 2001). The mutagenic DNA damage caused by UV light results in blockage of DNA replication in microorganisms, thus resulting in cell inactivation (Süß et al., 2009; Wellinger and Thoma, 1996).

Low pressure and medium pressure mercury-based UV lamps, emitting light at 253.7 nm and 200–300 nm, respectively, are mostly used at full-scale water treatment plants (Eischeid et al., 2009). Emerging techniques such as UV-LEDs, which can be manufactured to emit light at specific wavelengths, are also available, although these are mostly used in point-of-use devices (Song et al., 2016). The effect of low pressure UV irradiation was investigated in the present work.

The UV dose is a combination of UV intensity (W/m^2) and exposure time (s). If the UV intensity is constant during the exposure time, the dose is defined as the product of the intensity and the exposure time (USEPA, 2006). The units most often used for the dose are J/m^2 or mJ/cm^2; a dose of 400 J/m^2 or 40 mJ/cm^2 is a commonly used UV dose at DWTPs. German and Austrian standards specify that UV reactors should deliver a minimum dose of 400 J/m^2 with specific rules for testing and determination of the dose at specific flow rates and UV transmission (Eriksson, 2009). Full-scale UV treatment usually takes place in continuous-flow UV reactors. The speed at which microorganisms move through the reactor and their distance from the UV lamps will lead to variations in the UV dose they receive (USEPA, 2006), making it difficult to calculate the UV dose delivery in such reactors. This is currently calculated using biodosimetry tests by spiking the water with a known amount of a specific organism (commonly used organisms are *Bacillus subtilis* endospores and MS2 phages) (Leuker, 1999; Nocker et al., 2018). The kill rate is compared with dose-response values obtained under laboratory conditions, allowing the UV dose of the full-scale reactor to be calculated at a specific UV transmission and flow rate. It should be noted that suspended particles and organic matter can absorb and scatter UV light, thus affecting the disinfection efficiency (Christensen and Linden, 2003; Farrell et al., 2018).

Since all the microorganisms in drinking water cannot be cultivated using current methods, validation of full-scale UV disinfection efficiency is difficult. In addition, UV exposure can cause some bacteria to enter a VBNC state (Ben Said et al., 2010; Guo et al., 2019). In the present work, PCR-based 16S rRNA gene amplicon sequencing was used to study the UV-induced DNA damage in bacteria at a full-scale DWTP (Paper I).

Using PCR to assess UV damage

PCR amplification, or the lack thereof, could be used as a proxy for DNA damage, to assess the effectiveness of UV disinfection as an alternative method of analysis to cultivation, since the DNA polymerase is blocked by pyrimidine dimers (Wellinger and Thoma, 1996) and primers may not bind due to template strand blockage (Fig. 7). The suitability of PCR for the assessment of the effects of UV irradiation was tested by exposing 6 µL DNA samples at different concentrations to LP UV at 253.7 nm for different times, followed by amplification of the V3-V4 region, 466 bp (Nadkarni et al., 2002) of the 16S rRNA gene (Fig. 8). Extending the exposure time reduced the number of amplifiable target templates (Fig. 8A,B), and a linear relation was found on a log-

log scale (Fig. 8C). PCR or qPCR assessment of UV damage has also been used in other studies, showing bacterial or viral inactivation (Nocker et al., 2018; Rockey et al., 2020; Süß et al., 2009; Yang et al., 2020) and antibiotic resistance gene disruption (Mckinney and Pruden, 2012). It should be noted that a target with a longer fragment length could increase the resolution, due to the possibility that the DNA polymerase is blocked by a pyrimidine dimer (Ho et al., 2016). This was shown by Süß et al. (2009), where three different primer pairs were tested with qPCR (100 bp, 500 bp, and 900 bp), and the longest fragment showed the greatest increase in cycle of quantification (Cq) after UV irradiation, compared to before UV exposure.

A target 16S rRNA gene region of V3-V4 was used in the present work to assess the effect of UV irradiation on the bacterial community (Paper I). This approach has been used to study how the bacterial community is affected by UV irradiation in drinking water (V3-V4) (Nocker et al., 2018), marine water (V3-V4) (Laroche et al., 2018), and wastewater (V1-V3) (Kauser et al., 2019). This method is based on the assumption that a UV-damaged 16S rRNA gene is equivalent to an inactivated bacterium. Since the DNA of some bacteria will be damaged by UV irradiation, the number of amplifiable target templates of these bacteria will decrease, whereas the number of amplifiable target templates of the resistant bacteria will remain the same. After PCR amplification and sequencing of the 16S rRNA gene, the composition of the bacterial community of the UV irradiated samples will change and can be compared to non-irradiated controls. The relative abundance of bacteria sensitive to UV will decrease, while those that are resistant will increase (Fig. 2 in Paper I). The emergence of DNA sequencing techniques

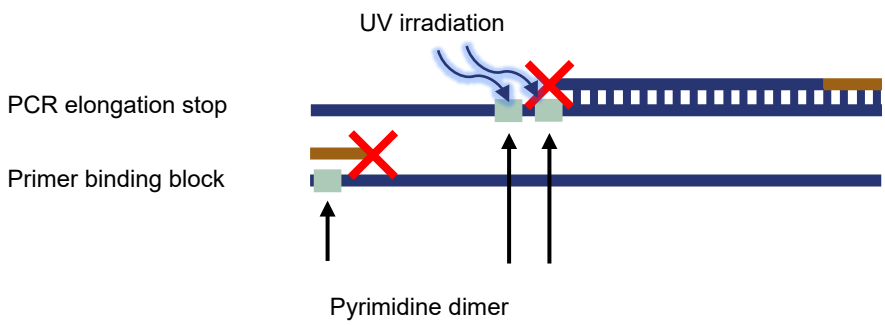

Figure 7. UV irradiation causes the formation of pyrimidine dimers in the DNA strand and inhibits the PCR either by stopping elongation or blocking the primer annealing. The brown color indicates the location of the primer oligonucleotides.

where longer fragment lengths allow sequencing of the full 16S rRNA gene could be of interest in future UV irradiation studies due to increased resolution in the PCR step amplifying a longer fragment. It would have been possible to amplify the full 16S rRNA gene fragment in the present study, using the same sequencing instrument (Illumina MiSeq). However, only the forward read fragment could then be used in further bioinformatics processing, since merging of paired end reads would not be possible due to limitations in the sequencing length of the instrument. Using the full 16S rRNA gene fragment for amplification and only the forward read would have resulted in a trade-off between resolution, due to the increased possibility of blocking DNA elongation in the PCR step, and the identification resolution, since only a shorter fragment would have been available for the taxonomic classification of reads.

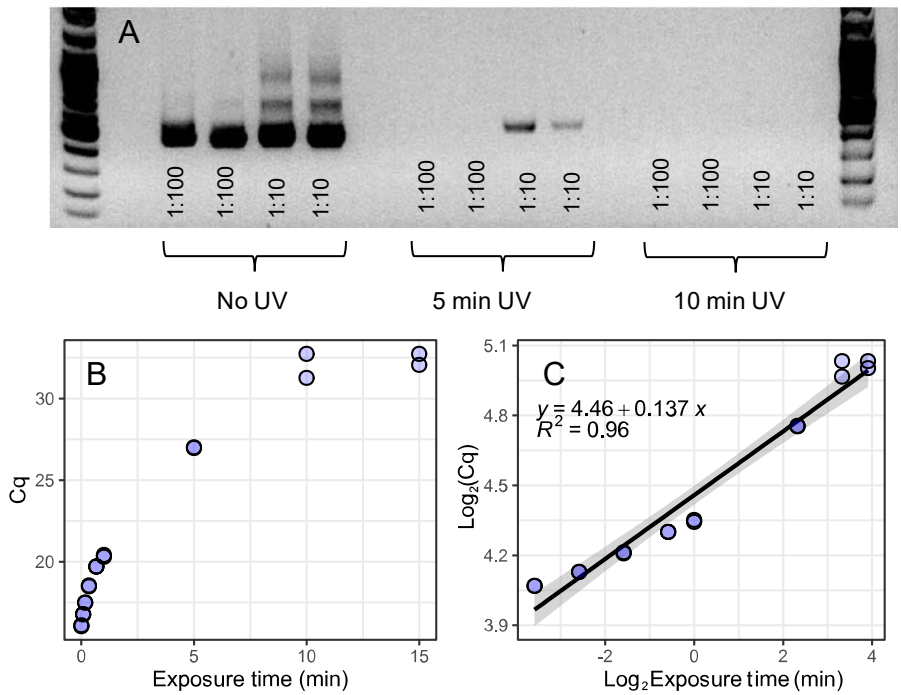

Figure 8. The effect of UV exposure on the number of amplifiable target templates in the PCR. Samples consisting of 6 µL aliquots of DNA extracted from 1 L tap water in PCR tubes (25 µL) without lid were exposed to UV irradiation for different times using a portable UV-C lamp (Sankyo Denki), in two different experiments: (A) and (B+C). (A) Two different concentrations of DNA were exposed to UV irradiation for 5 min and 10 min, amplified by PCR and visualized with gel electrophoresis. (B) DNA exposed for several times (n = 2 for each time) and quantified using qPCR. The cycle of quantification (Cq) could not be determined after exposure for 20 min (Cq > 35). (C) Data from the experiment in (B) plotting Cq against exposure time on a log-log scale. The linear regression is shown (black line) with the gray transparent area showing the 95% confidence interval. Data from the non-irradiated samples (0 minutes) were removed to be able to plot the logarithm of the values. The experiments in (A) and (B + C) were performed with different starting materials.

There is a need to monitor the UV disinfection efficiency in full-scale DWTPs (Hijnen et al., 2006), and PCR has been suggested for this purpose (Nizri et al., 2017). Analysis of the bacterial community using 16S rRNA gene amplicon sequencing, and qPCR to target bacteria naturally present in the water, for example, the *Pelagibacteraceae* or *Chitinophagaceae* families (Paper I), would provide a means of on-site verification of the UV disinfection efficiency.

Impact of UV irradiation on microorganisms

Most studies of microbial pathogen inactivation by UV irradiation are performed on lab-scale, since it is not defensible to spike UV reactors at full-scale DWTPs with known pathogens due to risk of infection. A literature review consisting of mostly lab-scale studies showed that UV irradiation is generally effective against all pathogens in drinking water (Hijnen et al., 2006), and a list of the microorganisms tested and their reductions when exposed to UV irradiation has been published and is continuously updated (Malayeri et al., 2016). Some microorganisms are sensitive to UV irradiation, and only low doses are required for their inactivation: a 4-$\log_{10}$ of *Escherichia coli* O78:K80:H12 requires a dose of 81 J/m^2 (Sommer et al., 2000). Other organisms are more resistant, and the same log reduction of *Mycobacterium avium* 33B and Adenovirus requires doses of 128 J/m^2 and 160 J/m^2, respectively (Gerba et al., 2002; Hayes et al., 2008). Different log reductions have also been observed within the same species exposed to the same dose (Malayeri et al., 2016; Sommer et al., 2000). Bucheli-Witschel et al. (2010) showed that the growth rate of the same organism had an effect on the UV resistance; stationary-phase or very slow-growing cells being most UV resistant. Observed differences in inactivation may also be due to the method of analysis used. No further increase in inactivation at higher UV doses is often seen in UV irradiation studies (called tailing), which may be due to the experimental setup, the aggregation of microorganisms or resistant subpopulations (Hijnen et al., 2006). Tailing occurs in PCR-based studies when there are many damage sites in the same fragment, and thus the log reduction cannot increase (Beck et al., 2014). It is, however, important to note that environmental bacteria have been observed to have higher UV resistance than laboratory-cultivated organisms (Hijnen et al., 2006).

Microbial characteristics and mechanisms can protect organisms from damage by UV exposure (Kowalski, 2009). UV light can be scattered by the cell membrane, and studies have shown that Gram-positive bacteria are more UV-resistant than Gram-negative ones (D. K. Kim et al., 2017; McKinney and Pruden, 2012). This was also observed to some extent in the present work (Paper I). This may be due

to the thicker peptidoglycan layers in Gram-positive bacteria, scattering the UV light and protecting the DNA from damage. The constituents within microbial cells, for example, proteins, can absorb UV light and prevent the photons from reaching the DNA (Kowalski, 2009): bacterial spores, which are highly resistant to UV damage, have acid-soluble spore proteins, and spore coating layers which contribute to UV resistance (Mason and Setlow, 1986; Moeller et al., 2009; Riesenman and Nicholson, 2000). However, degradation of proteins and other types of damage, such as protein-DNA crosslinks, may also cause cell death (Kowalski, 2009; Moss et al., 1997). The composition and size of the genome may contribute to UV resistance; a higher guanine-cytosine (GC) content in microorganisms has been suggested to contribute to UV resistance (Paper I, Warnecke et al. (2005)). Smaller genome size has also been hypothesized to play a role in reducing the susceptibility to UV, due to fewer possible pyrimidine dimer targets (McKinney and Pruden, 2012).

Throughout evolution, microorganisms have evolved to survive DNA damage by the development of DNA repair mechanisms (Sinha and Häder, 2002). This is achieved either by photoreactivation or dark-repair systems. Photoreactivation uses light and the enzyme photolyase to repair DNA damage (Sinha and Häder, 2002), however, drinking water is almost always contained in a dark environment and thus, dark repair would be the more likely mechanism of DNA repair in this context. Bacteria possess various dark-repair mechanisms that are regulated by the expression of the *recA* gene, which is part of the SOS response in bacteria (Jungfer et al., 2007). However, dark repair was not observed in some studies: for example, in *Giardia* at UV doses usually used in drinking water (160 and 400 J/m^2) (Linden et al., 2002), and when *E. coli* was exposed to UV irradiation (Oguma et al., 2001). In contrast, Oguma et al. (2001) also showed that *Cryptosporidium parvum* was able to repair UV damage, but lost its infectivity. Others have observed dark repair after UV exposure in culture-based tests (Li et al., 2017), and *recA* gene induction has been observed at UV doses of 100–600 J/m^2 (Jungfer et al., 2007). Thus, it cannot be ruled out that bacteria can repair the damage resulting from UV treatment, to some extent, and that this ability probably differs between the microorganisms present in the drinking water microbiome (Paper I).

Microorganisms can use AOC as a substrate for growth, and this can affect the biostability of the water (Van Der Kooij et al., 1982b). "Biostability" is the concept of maintaining the microbial quality of the water from the finished water, at the DWTP, through the DWDS, to the consumer (see "Biostability", Chapter 4) (Prest et al., 2016a). The effect of UV irradiation on AOC is still the subject of debate. It has been reported in some studies that UV exposure increases bioavailable organic carbon and AOC concentrations in water (Chen et al., 2020;

Sulzberger and Durisch-Kaiser, 2009), while in others a decrease or no change was found (Choi and Choi, 2010; Ijpelaar et al., 2005; Lehtola et al., 2003; Shaw et al., 2000). These differences may be due to the composition of organics and the UV dose used in the studies (Thayanukul et al., 2013). However, dead cells resulting from UV irradiation will contribute to the carbon and nutrient source for UV-resistant microorganisms (Bohrerova et al., 2015). This has been called necrotrophic growth (Temmerman et al., 2006), and has been observed in natural communities (bottled drinking water) spiked with dead cells (Chatzigiannidou et al., 2018). A comparison between the effects of UV irradiation and chlorination on microbial growth on different pipe materials revealed an increase in the metabolic activity and less biostable water when the biofilm bacteria had been exposed to UV irradiation (Schwartz et al., 2003). The community shift in the UV-irradiated and stored samples described in Paper I (Fig. 1) indicates less biostability than in the non-irradiated samples, and may be due to the necrotrophic growth of UV survivors or DNA repair. Based on the above observations, it can be concluded that UV irradiation not only affects the microbial community immediately after treatment, but probably also influences the microbial dynamics in the DWDS.

Biofiltration

Biofiltration can be carried out in drinking water treatment using slow sand filters (SSFs), rapid sand filters (RSFs) and biologically active or granulated activated carbon (BAC/GAC) filters (Proctor and Hammes, 2015a). The differences between these filters are the material used (fine/coarse sand or granulated activated carbon) and the rate of flow of water though the filter. SSFs have a residence time of 3–12 h (Haig et al., 2011), whereas RSFs and BAC/GAC filters have much shorter residence times ranging from 5 to 15 min (Hammes et al., 2008; Lee et al., 2014). Water percolates through the filters and, depending on the size and properties of the filter material, larger particles, organic matter, and microorganisms will be removed or adsorbed from the water (Huisman and Wood, 1974; Verma et al., 2017). The surface of the filter medium in biofilters is colonized by microbial communities (biofilms) that contribute to water treatment through biological processes by removing or immobilizing pathogens, organic matter, or chemicals (Haig et al., 2011). GACs are commonly used to remove natural or synthetic organic compounds and taste and odor compounds from the water by adsorption, due to the porosity of the material (Servais et al., 1994; Urfer et al., 1997; Velten et al., 2011). However, with time, biofilms will form on

the surface of the activated carbon and the GAC will eventually develop into a BAC filter (dos Santos and Daniel, 2019; Velten et al., 2011). Since biological processes generally take longer, the retention time of RSFs and BAC/GACs may be too short to efficiently contribute to the water treatment. For example, increased microbial polysaccharide degradation has been observed in SSFs compared to GACs/BACs/RSFs (Lautenschlager et al., 2014), and the nitrification process in RSFs may not be sufficiently rapid (Albers et al., 2018), requiring specific actions for optimization (Wagner et al., 2019). The contribution of biological activity probably follows a gradient and is dependent on several variables, such as the residence time in the filter and the temperature, or the nutrients present in the water.

Biofilms

Biofilms are often described as a slimy matrix (Willey et al., 2011), and can be defined as "aggregate(s) of microorganisms in which cells that are frequently embedded within a self-produced matrix of extracellular polymeric substance (EPS) adhere to each other and/or to a surface" (Vert et al., 2012). The biofilm matrix consists mostly of water (over 97%) whereas the EPS accounts for over 90% of the dry mass in a biofilm, and is composed of polysaccharides, proteins, lipids, and extracellular DNA (Flemming and Wingender, 2010). The first biofilm studied is thought to have been the biofilm community of dental plaque, by Antony van Leeuwenhoek in the 17th century (Willey et al., 2011). It has been estimated that 40–80% of all cells on Earth live in biofilms (Flemming and Wuertz, 2019). Due to the ubiquity of biofilms, drivers for biofilm formation have been hypothesized to include: protection from harmful agents; the ability to colonize nutrient-rich areas; cooperation within the biofilm; and the fact that the default mode for microbial growth is in biofilms and not as planktonic cultures (Jefferson, 2004). Nutrient gradients within biofilms create different habitats for species, and also possibilities for communication and cooperation through quorum sensing. Examples include nitrification, where ammonia oxidizers supply nitrite to nitrite oxidizers (Paper III), and competition by nutrient depletion or the production of antibiotics (Flemming et al., 2016). The development of a biofilm can be described in five different stages (Fig. 9 and Stoodley et al., 2002). First, cells attach to and detach from a surface, which then triggers the second stage of irreversible attachment of cells by the production of EPS. The third and fourth stages are early development and maturation of the biofilm architecture. In the fifth and final stage, cells and microcolonies may be dispersed from the biofilm by random detachment or motility-driven detachment of cells to find

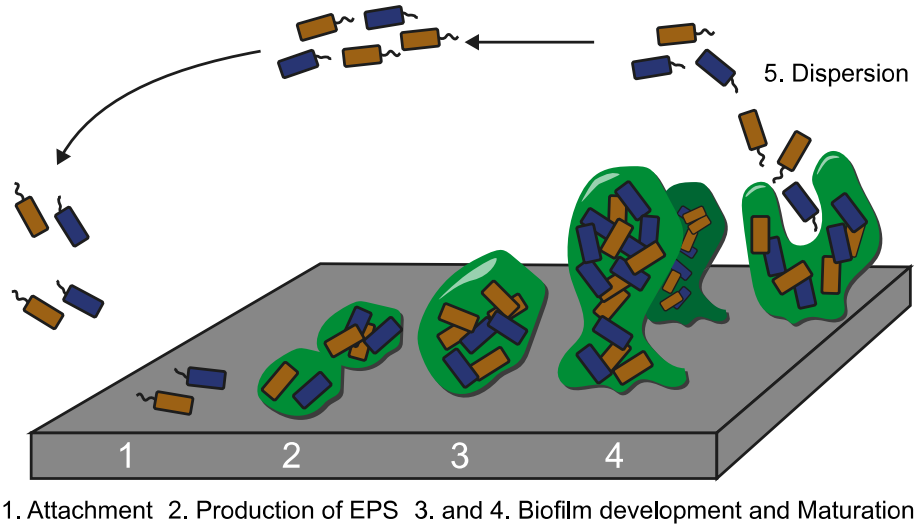

Figure 9. The five stages in the development of a biofilm. Stage 1: Initial attachment/detachment of cells. Stage 2: Irreversible attachment and production of EPS. Stages 3 and 4: Early development and Maturation of the biofilm. Stage 5: Dispersion of cells from the biofilm. Adapted from (Stoodley et al., 2002).

other environments for growth. The structure of the biofilm will differ depending on environmental factors and the type of organisms. For example, shear stress caused by the flow of fluid may affect the density and strength of the biofilm (Stoodley et al., 2002). The type of EPS may also affect the development of biofilms by different bacteria. For example, Izano et al. (2008) showed that the polysaccharide poly-N-acetylglucosamine and extracellular DNA had completely different roles in the structure of biofilms formed by S*taphylococcus aureus* and *Staphylococcus epidermidis,* where extracellular DNA contributed to biofilm integrity in *S. aureus* and poly-N-acetylglucosamine in *S. epidermidis* (Izano et al., 2008).

Slow sand filtration

The use of SSFs dates back over 200 years, when a SSF was built and used to purify water at a bleachery in Scotland, and the excess treated water was sold to the public (Huisman and Wood, 1974). The technique was implemented in the first public water supply in London in 1829, and SSFs were later installed in other European cities, for example, Paris and Amsterdam (Haig et al., 2011). At that time, the biological activity and removal of pathogens by SSFs was unknown, and the treatment was regarded as mechanical filtration to decrease turbidity and suspended solids in of the water (Huisman and Wood, 1974). The capability of SSFs to remove waterborne pathogens from water was first observed in 1892,

when the source water for two German cities, Hamburg and Altona, was infected by cholera. The water in Altona was treated with SSFs, and its inhabitants did not suffer as badly as those in Hamburg, where the mortality rate due to cholera was high (Ashbolt, 2004; Huisman and Wood, 1974).

The SSFs used for water treatment today are usually large basins containing a layer of gravel in the bottom, followed by fine-grained sand, to a height of 0.6–1.2 m (Fig. 10). Water is pumped in above the sand to fill the basin to a depth of 1–1.5 m, which then continuously percolates through the sand by gravity (Huisman and Wood, 1974). SSFs can be covered to prevent wind-borne or wild-

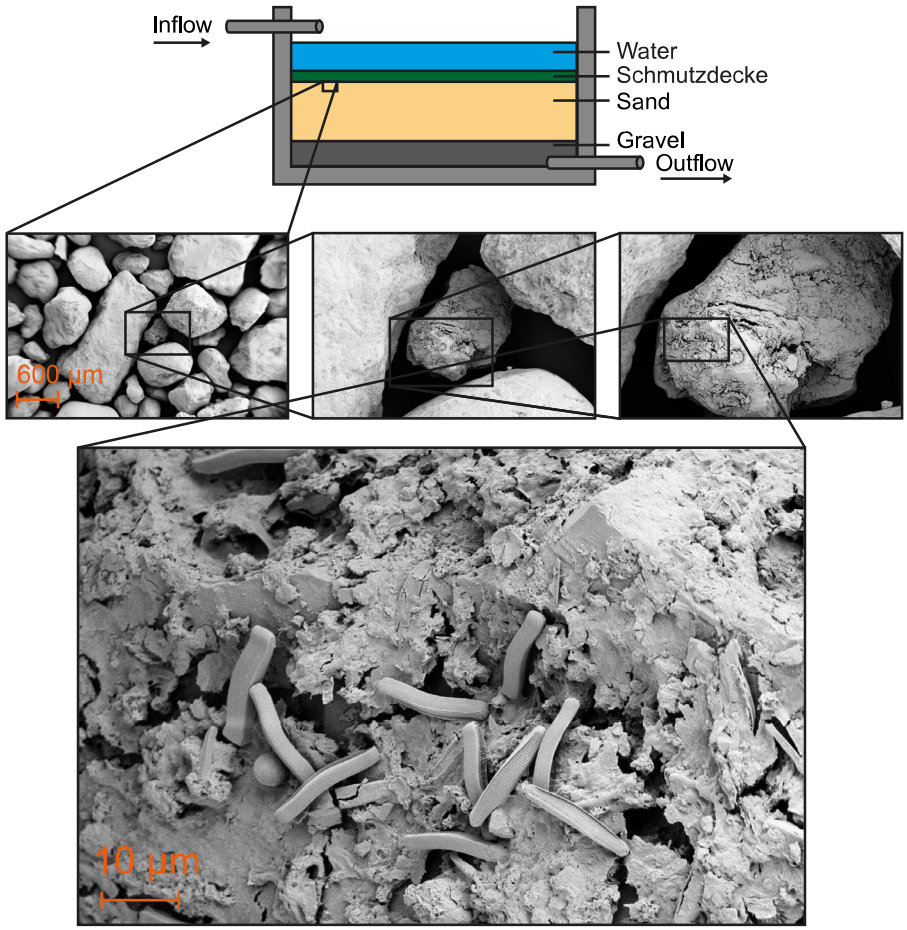

Figure 10. Above: Schematic illustration of the components of a slow sand filter. Below: scanning electron microscope images of sand grains at increasing magnification. (Images provided by Sarunas Petronis.)

life contamination and sunlight exposure, which can promote the growth of algae. The technical advantages of SSFs include its simple design and construction, and no need for chemicals or electricity for operation (Haig, 2014; White et al., 2012). However, SSFs cover large areas and are difficult to install when the available land area is limited.

SSFs efficiently remove pathogens and contaminants such as *E. coli, Clostridium spp.,* viral pathogens and toxins from the water (Bourne et al., 2006; Elliott et al., 2008; Hijnen et al., 2004) by biological activity, but also via straining and adsorption (Hijnen et al., 2004). Studies using lab-scale SSFs have shown that protozoan grazing was responsible for most of the removal of *E. coli* when used to spike the water, but other mechanisms were also involved, such as reactive oxygen species produced by algae, fungal-algae mutualistic interactions, and viral killing (Haig et al., 2015b). The ability of SSFs to remove pathogens from the water may not be their only function. SSFs are commonly used in the final treatment steps, and the water leaving them can thus shape the microbial community in the DWDS (Pinto et al., 2012; Proctor and Hammes, 2015b). In this work, it was shown that treatment with a well-functioning established SSF removed *E. coli* and coliforms, and reduced both the TOC and pH (Paper II). However, although the SSF did not decrease the total cell concentrations to a large extent, it increased the proportion of LNA bacteria in the microbial community. The shift to more LNA bacteria by SSFs has also been observed in other studies (Lautenschlager et al., 2014; Vital et al., 2012). Thus, SSFs may play an important function in shaping and controlling the microbial community and biostability in DWDSs (Chan, 2018). Well-functioning SSFs reduce the amount of biodegradable organic carbon (Lautenschlager et al., 2014; Wakelin et al., 2011) by metabolic activity (Taylor Eighmy et al., 1992), which could otherwise have led to microbial growth of indicator bacteria in the DWDS (Prévost et al., 1998).

Particles and organic matter accumulate on top of the SSFs, where a biofilm layer is formed (Fig. 10). This is called the *schmutzdecke*, and consists of a wide variety of bacteria, eukaryotes, and archaea (Wakelin et al., 2011; Wotton, 2002). The flow of water through a SSF decreases over time due to the accumulation of biomass in the *schmutzdecke*. A few centimeters of the top layer of the sand including the *schmutzdecke* is usually removed to increase the water flow, and in Sweden this process (scraping) is performed 2 to 3 times per year. The *schmutzdecke* has been regarded as being a major contributor in water treatment (Pfannes et al., 2015; Tyagi et al., 2009), however, removal of this layer from an established SSF had no effect on the function of the SSF in terms of the removal of *E. coli* and coliforms, decreasing the TOC and pH (Paper II). The community fingerprint of the effluent water was also stable. When the surface of SSFs without

any established biofilm was scraped, breakthrough of coliforms and *E. coli* was observed. This suggests that the function of SSFs may be within the deeper layers of sand, which requires time to develop, and not only the *schmutzdecke*. The performance of newly constructed SSFs has been shown to improve over time (Chan, 2018; Haig et al., 2015a). The community composition of a start-up SSF with new sand plus established sand collected from previous scraping events on top, exhibited the ability to remove indicator organisms more rapidly (Paper II). This SSF showed a similar community as an established SSF within 150 days, probably due to priming with the washed established sand, whereas a filter with completely new sand did not (Chan, 2018). It should, however, be noted that the sand was only sampled on the surface where the priming of new sand was placed and no sampling was carried out at deeper layers. These results indicate that priming a new SSF with sand from established SSFs may help to attain good performance more rapidly (Chan, 2018). This has also been observed for RSFs primed with enrichments of sand from older filters (Albers et al., 2018).

The biofilm community of biofilters has been observed to be different from those in the influent and effluent water (Chan, 2018; Haig et al., 2015a; Webster and Fierer, 2019), and has been characterized in several studies (Bai et al., 2013; Haig et al., 2015a; Oh et al., 2018). Well-functioning SSFs were associated with the genera *Acidovorax*, *Halomonas*, *Sphingobium*, and *Sphingomonas* and high species evenness (Haig et al., 2015a). Oh et al. (2018) found that *Bradyrhizobium* and *Nitrospira* were the most abundant genera in biofilters, including SSFs, and observed various bacteria within *Alphaproteobacteria* (*Afipia*, *Bradyrhizobium*, *Hyphomicrobium*, *Methylobacterium*, *Nitrobacter*, *Rhizobium*, *Rhodopseudomonas*, and *Sphingomonas*), *Betaproteobacteria* (*Acidovorax*, *Burkholderia*, and *Polaromonas*), and *Acidobacteria* (*Solibacter*). Some of these taxa, including *Sphingomonas, Hyphomicrobium* and *Nitrospira*, were also observed in DWDS pipe biofilms in water meters connected to the DWDS (Lührig et al., 2015) and in the DWDS pipe biofilm in one of the present studies (Paper III). Bai et al. (2013) found *Alphaproteobacteria* to be the most common class, and detected several aromatic degradation pathways, as well as nitrification and denitrification pathways. The biofilm community of biofilters is likely to depend on the ingoing water quality and nutrients such as nitrogen compounds, phosphorus and carbon, as well as the quality of the sand matrix, and may thus be DWTP specific. This is supported by a study by Webster and Fierer (2019) who found that the composition of the bacterial community in the sand filter varied depending on the nutrient levels (high or low concentrations of nitrogen, phosphorus and carbon) in the source water. Concentrations of nutrients, including carbon and nitrogen, have also been reported to decrease with increasing depth in a sand filter

(Bai et al., 2013), indicating possible niche environments for certain micro-organisms. Metabolic by-products from microorganisms in the top layers of a SSF may feed other organisms, depending on the depth and/or the retention time. Differences in the biofilm bacterial community with depth in BAC filters has been observed (Ma et al., 2020) whereas Haig et al. (2015a) reported a "marginal" effect of depth on the community composition in SSFs. This could perhaps be re-evaluated by obtaining core samples at different depths from several SSFs. However, it is difficult to obtain core samples from full-scale operating SSFs due to the depth of the water, and while they could be obtained during scraping or maintenance, this could disturb the function of the SSF by creating a potential pathway for untreated water to pass through the SSF. Lab-scale SSFs could be used instead since they have been shown to resemble full-scale SSFs well (Haig et al., 2014).

Chapter 4
Biofilms in the DWDS

Biofilms are ubiquitous in nature and microbial communities live on the surface of DWDS pipes as biofilms. Most of the biomass in DWDSs, estimated to be greater than 95%, has been estimated to reside in the pipe biofilm or as loose deposits (Flemming et al., 2002; G. Liu et al., 2014) and consists of up to 10^8 bacteria per cm^2 (Proctor and Hammes, 2015a). While biofilms can be beneficial in water treatment processes (e.g. as biofilters), the biofilm in DWDSs may have undesirable effects on the drinking water quality by changing the aesthetics of the water (Fish et al., 2017), providing a reservoir for opportunistic pathogens (Wingender and Flemming, 2011), deteriorating pipe material by corrosion (Kip and van Veen, 2015), and enhancing nitrification in chloraminated DWDSs (Carrico et al., 2008). The microbial dynamics and processes in the biofilms and bulk water of DWDSs may be influenced by many factors (Fig. 11), such as disinfectant residuals, nutrients, the type of microorganisms, attachment and detachment of cells to pipe walls, and predation. Although the DWDS biofilm may have undesirable effects on water quality, it can also inhibit corrosion (Kip and van Veen, 2015), and may play a role in further treatment of the water, through microbial activity, or by acting as a barrier against colonization by undesired microorganisms.

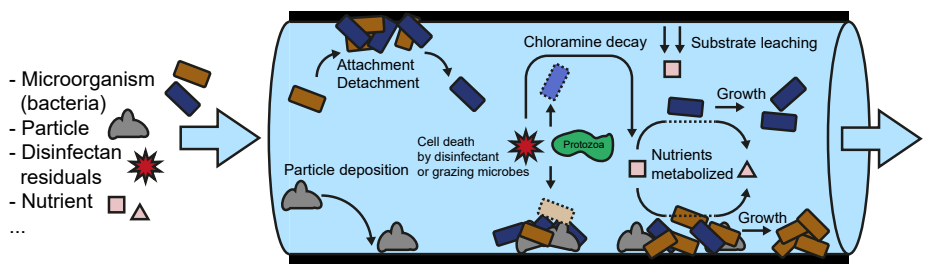

Figure 11. Schematic illustrating the microbial dynamics in a DWDS. Adapted from (Prest et al., 2016a) and (Proctor and Hammes, 2015b).

Sampling biofilms in a DWDS is difficult due to the inaccessibility of the pipes, and bulk water samples have thus mainly been used to study the microorganisms in DWDSs. These studies have indicated a broad diversity of bacteria in the bulk drinking water and at a high taxonomical level such as phyla or class, common bacteria are classified mostly as *Alphaproteobacteria* and *Betaproteobacteria* with a lower abundance of *Delta-, Epsilon-, and Gammaproteobacteria*, *Actinobacteria*, *Planctomycetes*, *Acidobacteria*, *Nitrospirae*, *Bacteroidetes*, and *Chloroflexi* (Bautista-de los Santos et al., 2016b; Henne et al., 2012; Lautenschlager et al., 2014; Lin et al., 2014). Although these studies are important in understanding the bacteriome in the bulk water of DWDSs, the DWDS biofilm has a different microbial composition from that in the bulk water (Henne et al., 2012; G. Liu et al., 2014; Waak et al., 2019a, Paper III) and a greater number of observed ASVs being observed in water than in the DWDS pipe biofilm (Paper III).

In this work, the installation of UF with coagulation (UF start) at a DWTP was found to remove almost all the cells from the finished water (Papers III, IV, & V). The UF start reduced the cell concentrations in the DWDS from 6.0×10^5 ($\pm$ 2.3×10^5) cells/mL to 6.0×10^3 ($\pm$ 8.3×10^3) cells/mL, and reduced most analyzed fractions of NOM in the finished water (Paper III). As the number of bacteria in the finished water was high, the pipe biofilm contributed only a very small fraction to the bulk water bacterial community in the DWDS, and could not be quantified before the UF start (Paper III). After UF start, very few cells were found in the finished water, and it was therefore concluded that most of the cells in the bulk water in the DWDS originated from the pipe biofilm, and that others were likely released from biofilms on storage tanks at the DWTP. The UF start together with sampling of the finished water at the DWTP and at different locations in the DWDS allowed the accumulated contribution of the pipe biofilm on the DWDS bulk water to be investigated. The bacteria released from the pipe biofilm and entering the bulk water included *Sphingomonas*, *Nitrospira*, *Nitrosomonadaceae*, *Mycobacterium*, and *Hyphomicrobium* (Paper IV). The detachment of cells may have been due to changes in the environmental conditions brought about by UF start, including changes in the organic matter. However, no destabilization of the biofilm, in terms of extreme detachment of cells or chunks of biofilm, was observed. The detachment of cells from the DWDS pipe biofilm may be influenced by flow rate, shear stress (Horn et al., 2003; Lehtola et al., 2006), and random attachment and detachment (Petrova and Sauer, 2016). However, in the system studied, UF start did not affect the hydraulic conditions, above and beyond the normal fluctuations in flow rates and shear stress caused by changes in water consumption throughout the day (Zhang and Liu, 2019).

Abundant amounts of *Sphingomonadaceae, Hyphomicrobium,* and *Nitrospira* have been detected in the biofilm on water meters connected to a DWDS (Lührig et al., 2015). When using coupons in a full-scale laboratory pipe system, the dominant phyla have been reported to be *Gammaproteobacteria, Betaproteobacteria, Alphaproteobacteria, Clostridia,* and *Bacilli*, and the genera *Pseudomonas* (Douterelo et al., 2013). Various bacteria have been detected in pipe biofilms in pipes excavated during maintenance or for research purposes, including *Nitrosomonas, Nitrospira, Hyphomicrobium, Mycobacterium, Legionella, Sphingomonas,* and *Pseudomonas* (Cruz et al., 2020; G. Liu et al., 2014; Liu et al., 2020; R. Liu et al., 2014; Ren et al., 2015; Waak et al., 2019a). In this work, the pipe biofilm on excavated operational pipe sections was analyzed, and the most abundant bacteria were found to be *Hyphomicrobium, Sphingomonas, Nitrosomonadaceae*, and *Nitrospira* (Paper III). While sampling of the pipe biofilm confirmed the previous results given in Paper IV, the composition of the pipe biofilms differed depending on the residence time and the local water quality. The taxa detected in the pipe biofilm have also been observed in other studies, and may be part of a core pipe biofilm microbiome. However, it would probably be difficult to define a core biofilm community as it is influenced by many factors such as disinfectant residuals, nutrients in the bulk water, hydraulic conditions and water temperature (Bautista-de los Santos et al., 2016b; Waak et al., 2019a; Wingender and Flemming, 2011). A large number of samples from diverse drinking water biofilms would have to be collected and analyzed. A drinking water microbiome project involving collaboration between laboratories from around the world has recently been suggested (Hull et al., 2019b).

Changes in the operation of the DWTP or transitions to other type of source water may affect the quality of the drinking water due to chemical or microbiological destabilization (G. Liu et al., 2017). The shift of source water with increased sulfate has caused discoloration of water (Li et al., 2010). This may have been due to changes in the microbial community, such as an increase in sulfur-oxidizing bacteria, which would affect the corrosion of iron pipes, resulting in the release of iron into the water (Yang et al., 2014). Microbial destabilization due to changes the in treatment or water quality may take months or years to become apparent (G. Liu et al., 2017). When the treatment process in the DWTP studied in this work was changed to include UF with coagulation, no consumer complaints were received. The community structure of the biofilm did change after UF start and a stable community was reached after 18 months (Fig. S12 in Paper III) showing a decrease in evenness and Shannon index (Fig. 5 in Paper III). While the number of observed ASVs decreased after UF start, no change was seen in the surface biofilm. Some bacteria did increase in relative abundance, such

as *Nitrosomonadacae_196* and *Hyphomicrobium_243* in biofilm (BF)1 and *Nitrospira_101* in BF4 while others decreased, for example, *Nitrosomonadacae_197* and *Sphingomonas_247* in BF1 and *Nitrospira_102* and *Nitrospira_103* in BF4 (Fig. 6 in Paper III). The changes in water quality due to UF start, including a decrease in the concentration of cells and reduction of most analyzed fractions of NOM in the DWDS, may have led to the selection of some bacteria that are better suited to the new environment, and caused others to diminish or disappear. Although changes were observed in the relative abundance of bacteria, the overall relative abundance of the abundant bacteria remained the same at family level (Fig. 2 in Paper III). This, together with the maintained turnover of nitrogen compounds (see below), indicates that the pipe biofilm maintained its functionality and adapted to the new water quality.

Various pipe materials are used in DWDSs, including cement, plastics (PVC, PE) and cast iron. It has been suggested in the literature that the pipe or coupon material affects the composition of the microbial community (Douterelo et al., 2020; Wang et al., 2014; Yu et al., 2010). However, no difference was observed in the composition of the bacterial community between PE and PVC pipes in the present work, despite the similar residence times (BF3 and BF4 in Paper III). This agrees with the findings by Aggarwal et al. (2018), showing that coupon material (CE, HDPE, and PVC) did not influence the bacterial community in bench-scale reactors. While the effect of pipe or coupon material on community composition may be debatable, the community composition in the biofilm is likely to depend on the nutrients available in the bulk water or the pipe material, for example, carbon or nitrogen compounds (see below). In very oligotrophic drinking water, leeching of for example assimilable organic carbon from plastic material (Neu and Hammes, 2020) will contribute relatively more to the carbon availability than to a carbon rich water and thus could shape the community composition of newly installed pipes whereas in other systems that have been installed for longer times may not be as influenced by leaching materials and reach a community composition that is more reflective of the bulk water environment (Proctor et al., 2016). Furthermore, a higher surface area due to the porosity of some materials (for example, cement) may affect the biofilm community (Wang et al., 2014).

Nitrification and nitrogen cycling in the DWDS

Disinfectant residuals are used in DWDSs to repress the growth of microorganisms, and are used in many countries. Chloramines (mostly monochloramine, NH_2Cl) and free chlorine ($HOCl/OCl^-$) are two frequently used disinfectants in drinking water (Kim et al., 2002). The use of disinfectant residual is debatable since it may form disinfection byproducts in combination with NOM (Li et al., 2019), select for resistant microorganisms (Chiao et al., 2014) and promote horizontal gene transfer of antimicrobial resistance genes (Jin et al., 2020). Chloramine is an unstable chemical compound that can auto-decompose (Valentine and Jafvert, 1992) or react with NOM resulting in ammonia (Ricca et al., 2019). This ammonia (NH_3) can in turn promote the growth of nitrifying bacteria and other microorganisms catalyzing chemical reactions in the biogeochemical nitrogen cycle (Fig. 12). Nitrogen (N) is essential in the biosynthesis of nucleic acids and proteins, and can exist in many different redox states. Nitrogen is abundant in the environment as nitrogen gas (N_2). Specific microorganisms can transform nitrogen between different redox states, and only a few bacteria and archaea can reduce nitrogen gas to its organic form as ammonia (Willey et al., 2011). When organic molecules are degraded and mineralized, ammonia is released as ammonium (NH_4^+).

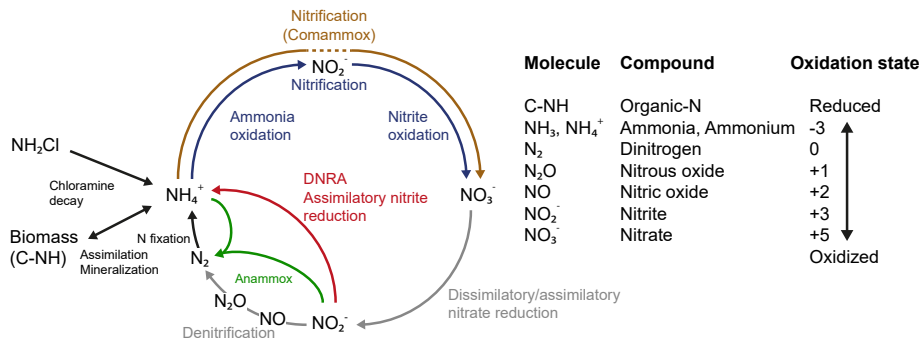

Figure 12. Overview of the processes in the nitrogen cycle and its intermediates, showing the oxidation states of nitrogen in various nitrogen compounds. The dashed line in comammox indicates that a single organism performs the nitrification step with nitrite as an intermediate. Abbreviations: Anammox, anaerobic ammonium oxidation; DNRA, dissimilatory nitrite reduction to ammonia; Comammox, complete ammonia oxidizer. Adapted from (Daims et al., 2016) and (Stein and Klotz, 2016).

Nitrification is the process in which NH_4^+ is oxidized to nitrate (NO_3^-) in a two-step process, with nitrite (NO_2^-) as an intermediate and oxygen as the electron acceptor (Daims et al., 2016). The first step of nitrification (NH_4^+ to NO_2^-) is catalyzed by ammonia-oxidizing microorganisms, i.e., ammonia-oxidizing bacteria (AOB) or ammonia-oxidizing archaea (AOA). Known AOB and AOA include for example *Nitrosomonadaceae, Nitrosococcus*, and *Thaumarcheota* (Stahl and de la Torre, 2012; Willey et al., 2011). The second step of nitrification (NO_2^- to NO_3^-) is catalyzed by nitrite-oxidizing bacteria (NOB), including *Nitrospira, Nitrobacter*, and *Nitrococcus*. Not only do AOB and AOA feed NOB with NO_2^-, other interactions have been observed between NOB and AOB. *Nitrospira moscoviensis* is able to convert urea to NH_4^+, which is utilized by urease-negative AOB and AOA, which in turn provide *Nitrospira* with NO_2^- (Koch et al., 2015). Species of *Nitrospira* have recently been found to be complete ammonia oxidizers (comammox), having the ability to oxidize ammonia to nitrate on their own (Daims et al., 2015; Van Kessel et al., 2015).

Nitrification was observed in the DWDS in the work presented in this thesis. Monochloramine was used in the DWTP studied, and higher concentrations of ammonium were measured in the finished water from the DWTP than in the DWDS, where the level of nitrite increased (Fig. 7 in Paper III). The metabolic activities of AOB (*Nitrosomonadaceae*) produced NO_2^-, in turn feeding the NOB (*Nitrospira*), which gradually dominated the community with increasing distance from the DWTP. The nitrite produced by AOB can further react and decrease monochloramine levels to produce ammonia and nitrate (Vikesland et al., 2001). The pipe biofilm community with mostly *Nitrosomonadaceae* (BF1) began to shift after 400 m (BF2), and a complete change in the relative abundance to *Nitrospira* was seen in the pipe biofilm in a distance of 1300 m, at BF3 (Fig. 2 & Fig. S8 in Paper III). Nitrogen compounds were assessed before and after UF start in the system, and since the turnover of nitrogen compounds remained the same (Fig. 7 in Paper III), it was concluded that nitrification was only performed by the pipe biofilm. The monochloramine concentration was expected to be highest in BF1 due to the shortest residence time, and lower alpha diversity (observed ASVs) was detected at this sampling point (Fig. S6 in Paper III). This is in line with the results of the study by Cruz et al. (2020), who also observed monochloramine-tolerant *Nitrosomonadaceae* in low alpha diversity samples. *Nitrosomonadaceae* were also present after exposure to UV irradiation (Paper I), indicating robustness to various disinfection methods. The genus *Sphingomonas* is commonly found in drinking water systems, and was detected in the biofilms described in this thesis. *Sphingomonas* has been found to play a central role in the initial formation of biofilms on reverse osmosis membranes (Bereschenko et al., 2010), and a meta-

bolic link has been proposed between *Nitrosomonas* producing tyrosine for degradation by *Sphingomonas* (Potgieter et al., 2020). It cannot be ruled out that the *Nitrospira* observed in the present work could be comammox *Nitrospira*, as they have been identified in numerous environments, including DWDSs (Pinto et al., 2015; Potgieter et al., 2020; Y. Wang et al., 2017).

Other biogeochemical processes included in the nitrogen cycle (Fig. 12) may also be performed by, for example, denitrifying *Hyphomicrobium* (Fesefeldt et al., 1998; Martineau et al., 2014), or assimilatory nitrate-reducing *Rhizobiales* or *Nitrospira* (Potgieter et al., 2020), all of which were observed in the biofilm samples (Paper III). *Hyphomicrobium* species are also facultative methylotrophs (i.e., they use C1-compounds for growth), which may give them an advantage in oligotrophic environments (Corpe and Jensen, 1996; Martineau et al., 2015). Denitrification is the process in which NO_3^- or NO_2^- is reduced to N_2 by a variety of heterotrophic microorganisms (Willey et al., 2011). These organisms use organic carbon as the electron donor and NO_3^- or NO_2^- as the electron acceptor. The reduction of NO_3^- or NO_2^- to N_2 is a multi-step process involving many enzymes for complete denitrification; intermediates include nitric oxide (NO) and nitrous oxide (N_2O). Many organisms in all domains of life are able to perform denitrification (Thamdrup, 2012). Assimilatory nitrite reduction is the process in which nitrate is incorporated into plant or microbial biomass. Dissimilatory nitrite reduction is performed by microorganisms using nitrite as the terminal electron acceptor during anaerobic respiration, reducing NO_2^- to NH_4^+. Anaerobic ammonium oxidation (anammox) is the process in which N_2 is the main product, and NO_2^- is used as an electron acceptor and NH_4^+ as an electron donor (Willey et al., 2011). The anammox process is catalyzed by a monophyletic group within the *Planctomycetes* phylum (Strous et al., 1999).

Further investigation of the genes of the microorganisms found in the pipe biofilm with metagenomics (Potgieter et al., 2020) or qPCR (Pjevac et al., 2017) could elucidate and confirm the potential and specific microbes participating in the different biogeochemical nitrogen processes. Nitrifying bacteria have been observed in pipe biofilms and nitrification in DWDSs in other monochloraminated systems (Regan et al., 2003; Waak et al., 2019a), including one in a tropical climate (Cruz et al., 2020). Based on the discussion above, it will probably be difficult for drinking water producers to maintain the level of chloramine in the DWDS due to nitrification by the pipe biofilm. Elevated concentrations of nitrite and nitrate may be hazardous (Ward et al., 2018), and in Sweden the limits on nitrite and nitrate in drinking water are 0.5 mg/L and 50 mg/L, respectively (Livsmedelsverket, 2001).

Impact of the DWDS biofilm

In the DWDS studied here, the TCC increased with both increasing contact area with the biofilm and residence time (Fig. 5 & Fig. 6 in Paper V). Although the TCC can be predicted from the residence time in a DWDS, the results of such models may be difficult to interpret since many parameters are likely to affect the release of bacteria from the biofilm, including hydraulics and seasonal variations (see below). The bacteria leaving the biofilm after short residence times in the DWTP (< 25 h) were identified as HNA bacteria (Fig. S5a in Paper III & Fig. S1 in Paper IV), which included *Nitrospira* and *Sphingomonadaceae*, in line with the findings of a previous study in which these bacteria were also identified as HNA bacteria (> 0.4 µm) (Proctor et al., 2018). The doubling time of bacteria in distributed water has been estimated to be 55 h (Boe-Hansen et al., 2002) and thus, the increase in HNA bacteria after residence times of less than 25 h was probably not due to regrowth. While an increase in HNA bacteria in the bulk water of the DWDS was correlated with short residence time, a shift to more LNA bacteria was observed with longer residence times of up to ~170 h (Paper V), indicating a different pipe biofilm community with increased residence time and/or regrowth of LNA in the DWDS. Similarly, J. Liu et al. (2017) reported that LNA bacteria dominated in the branch ends of a DWDS. At longer residence times, monochloramine is depleted and metabolic by-products from upstream biofilm microorganisms may affect nutrient availability. This has been observed in the same system, where the pH decreased and the conductivity increased with TCC (Schleich et al., 2020), indicating metabolic activity in the biofilm and possible mixed-acid fermentation forming weak acids (Willey et al., 2011). Contact time with biofilm and pH decrease was also observed in a SSF in the present work (Chapter 3 & Paper II). The results presented in this thesis indicate that metabolic activities, in terms of oxidation-reduction (redox) reactions throughout the DWDS, can change the environmental conditions and nutrients at different residence times, and affect the composition of the pipe biofilm community. This is in line with findings from other studies showing variations in community composition in a DWDS with distance (Pinto et al., 2014) or residence time (Lautenschlager et al., 2013).

Seasonal variation has been observed in DWDSs, and is an important factor affecting the microbial quality of drinking water (Henne et al., 2013; Nescerecka et al., 2018; Pinto et al., 2014; Prest et al., 2016b). Prest et al. (2016b) observed seasonal variations such as increased cell counts in the DWDS during summer (~May to September), and it was dominated by seasonal fluctuations in the

effluent water from the DWTP, with only small contributions from the pipe biofilm. Nescerecka et al. (2018) observed strong correlations between bacterial cell counts and temperature in samples collected from a distribution point throughout one year. Ozonation was utilized at this DWTP, probably inactivating and destroying most of the bacteria (Ramseier et al., 2011), but biofiltration and chlorination were also used as last steps (Nescerecka et al., 2018). The biofilter effluent may have contributed to cell counts in the finished water from the DWTP. An increase in bacterial cell counts with temperature was also observed in this work (Fig. 2 in Paper V), where the cells originated mainly from the pipe biofilm while a small fraction were from the storage tank biofilm in the DWTP. The higher temperature during summer probably led to an increase in the microbial activity, as a 10 °C increase in temperature doubles the rate of enzyme-catalyzed reactions (Willey et al., 2011). This could also affect the detachment of cells from the biofilm, as it has been found that the dispersion of cells from a biofilm can be caused by changes in environmental conditions (Chua et al., 2014). The increased temperature in the DWDS from 6 to almost 20 °C (Fig. S3 in Paper III & Fig. 2 in Paper V) may have led to regulated dispersion of cells from the biofilm.

Opportunistic pathogens may reside in DWDS biofilms (Wingender and Flemming, 2011). These include *Legionella spp.* and *Mycobacterium*, which have been detected in DWDS pipe biofilms (Gomez-Smith et al., 2015; Schwake et al., 2015; Waak et al., 2019b, 2018), and in both chlorinated and chloraminated bulk water (Donohue et al., 2019). DNA sequences from *Legionella* and *Mycobacterium* were also detected in DWDS pipe biofilm and bulk water in this work (Papers III & IV). *Mycobacterium* was observed to be resistant to UV irradiation (Paper I) and is known to be resistant to various disinfection methods (Taylor et al., 2000). While *Legionella* are considered to be more susceptible to chlorine and chloramine than *Mycobacterium* (Donohue et al., 2019), *Legionella* are able to grow within protozoa which provide protection (Steinert et al., 2002). Although it was shown in this work that *Legionella* and *Mycobacterium* DNA are present in the DWDS pipe biofilm, further studies are needed to investigate their viability and the risk of infection.

Biostability

Biostability often refers to maintaining the microbial quality of the finished water leaving a DWTP to the taps of the drinking water consumers (Prest et al., 2016a), and has been defined as follows: "Biologically stable water does not promote the growth of microorganisms during its distribution" (Rittmann and Snoeyink, 1984). Traditionally, biostability has been assessed using predictive approaches based on AOC and direct counts of bacteria, for example, HPCs (Prest et al., 2016a). While these tests provide a measure of the growth of heterotrophs, they do not account for most of the bacteria found in drinking water, and/or contributions from the biofilm in the DWDS. Recent developments in microbial analysis methods have improved our knowledge and understanding of the total bacterial community, and the ways in which the biofilm may contribute to the cells in the DWDS and affect water quality. At the DWTP where the water was treated with UF, the finished water was virtually cell-free (Papers III, IV, & V). Other treatments, such as UV irradiation, may influence the microbial dynamics in the DWDS by increasing nutrient availability through cell lysis (see "UV treatment", Chapter 3). As the finished water is flowing through the DWDS, the pipe biofilm in the DWDS may affect the cell concentration and change the water quality depending on various factors. This makes it impossible to achieve biostability as defined above. The definition of biostability should, therefore, be revised to include the natural dynamics in a DWDS that do not compromise public health (El-Chakhtoura et al., 2015). An improved understanding of how microbial dynamics should be monitored, in terms of modifiable baselines for specific drinking water systems depending on season, residence time, water quality, and other variables, is needed to enable a new definition of biostability to be formulated. Examples of monitoring strategies that could be applied today include on-line systems using FCM, ATP, and particle counts. More detailed, but time-consuming, methods such as qPCR and/or NGS could be used to verify and elucidate the results of simpler on-line measurements. Technological developments may lead to rational monitoring instruments for qPCR or NGS in the future. Microbial assessment could be combined with abiotic parameters, or measurements with more expensive and complex molecular microbial tools, in order to detect anomalies and predict water quality using machine learning.

Chapter 5
Conclusions

I have studied UV irradiation and slow sand filtration and their effect on the bacteriome of drinking water. I have also investigated how the pipe biofilm in a DWDS affects the drinking water quality and bacteriome as well as the effect of installation of UF with coagulation on the DWDS pipe biofilm community. The main conclusions are presented below.

- UV irradiation decreased the number of amplifiable target templates, and PCR-based techniques could thus be used for the assessment of UV damage to bacteria in drinking water. A higher GC content in bacteria was found to be a factor of UV resistance. Storage of UV-irradiated water showed a change in the composition of the bacterial community compared to non-irradiated water which did not change, indicating UV may affect the biostability of the water.
- FCM with cytometric fingerprinting was found to be a valuable method of assessing the bacterial communities associated with SSF treatment.
- Well-functioning SSFs that remove coliforms and *E. coli*, and lower the pH and TOC, cause a change in the effluent microbial community to a higher proportion of LNA bacteria. Removal of the *schmutzdecke* of a well-functioning SSF did not affect the performance or the ability to transform the effluent water. A newly constructed SSF containing new sand plus sand from established SSFs on top performed better in terms of coliforms and *E. coli* removal than a SSF with completely new sand, indicating that priming new SSFs with sand from established SSFs may be an efficient approach to achieve high performance in a shorter time.
- The pipe biofilm in a monochloraminated DWDS was dominated by *Nitrosomonadaceae*, *Nitrospira*, *Hyphomicrobium*, and *Sphingomonas.* DNA sequences of the opportunistic pathogens *Mycobacterium* and *Legionella* were also detected in the pipe biofilms and bulk water of the DWDS, but the risk to humans needs to be further investigated.

- Monochloramine decay and chemical reactions result in the formation of ammonia in monochloraminated systems. Ammonia in turn promotes the growth of nitrifying bacteria (*Nitrosomonadaceae* and *Nitrospira*), which are present in great abundance in the DWDS pipe biofilm. Nitrification is performed by the bacteria in the pipe biofilm, which affects the monochloramine residuals.
- Longer residence time and season (temperature) affect the number of bacteria in the DWDS. The metabolic activities in the pipe biofilm will affect the downstream water quality and the microbial community.
- UF with coagulation reduced the number of bacteria and reduced most analyzed fractions of NOM in the bulk water. The bacteria in the bulk water of the DWDS after UF start originated mainly from the pipe biofilm and a minor fraction from DWTP storage tank biofilm. The start of UF affected the bacterial composition of the pipe biofilm community, and a stable community was achieved after 18 months. Although some taxa were no longer present in the pipe biofilm, the nitrification functionality was retained.
- The concept of biostability in its former definition makes it difficult to achieve biostability, due to the contribution of bacteria and biological processes in pipe biofilm affecting the DWDS bulk water. A new definition should therefore be established that takes into account microbial dynamics through seasonal variation, residence time and other variables, without compromising the safety of drinking water.

Chapter 6
Outlook

The treatment processes in a DWTP and the pipe biofilm in a DWDS affect the microbiome of the water. The impact of UV irradiation and SSFs, as well as how the pipe biofilm in the DWDS affects the bacteriome and quality of drinking water have been studied here. The knowledge gained from these studies has improved our understanding of the bacteriome of drinking water but, at the same time, has given rise to new research questions.

Studies on the effects of UV irradiation have previously mainly been done at lab-scale with lab-grown microorganisms. It is difficult to study the efficiency of disinfection with UV irradiation in full-scale using conventional microbiological analysis methods, since these methods only analyze a fraction of the entire community. The efficiency of disinfection with UV irradiation could be quantified using qPCR to target bacteria known to be present in the water. This would give valuable insights into the UV irradiation process and the need for maintenance, for example, when the UV lamps need to be changed. Amplification of longer regions of the 16S rRNA gene combined with modern DNA sequencing techniques may be of interest in further studies on the bacterial community. Metagenomics or qPCR could be used to investigate whether UV irradiation affects virulence or antibiotic-resistance genes, or how eukaryotes are affected. In addition, lab-scale or pilot-scale DWDS setups could be used to study how UV irradiation affects the biostability in a DWDS pipe system.

SSFs have been used to treat drinking water for over 200 years, and recent developments in molecular biology analysis have made it possible to further our understanding of the biological processes taking place in SSFs. The functions of microorganisms in SSFs could be further studied, for example, by assessing the genes or other domains of life than bacteria with metagenomics, gene expression with metatranscriptomics, proteins with metaproteomics and visualizing active cells with stable isotope probing. This would not only provide insight into the biological processes and potential degradation pathways of undesirable chemicals, but also which types of microorganisms may be important for future priming of

new or poorly functioning SSFs. The impact of raw water quality and temperature on the SSF performance could be further investigated to improve our understanding of how SSF treatment may be affected in the future by climate change and increased NOM in raw water. It would also be of interest to study the microbial community and chemical parameters at different depths in a SSF to improve our understanding of how the water is treated spatially when passing through a SSF. This may provide important information on the depth of sand required or the optimal water flow through SSFs.

The bacterial community in the pipe biofilm of a DWDS was studied for short residence times of less than 25 h. It could be interesting to study the DWDS pipe biofilm at longer residence times, or with different chlorination regimes, as well as the contribution of the biofilm to the microbiome and water quality of the bulk water. Collecting samples of the biofilm from excavated pipes and bulk water at longer than those investigated in this work and at several residence times would be of interest. These samples could be analyzed with 16S rRNA gene amplicon sequencing or other omics-based analysis tools combined with cell counts and chemical data to provide important information on how microbial processes in the DWDS affect downstream biofilm taxa and quality of drinking water. Although omics-based studies are valuable in understanding the overall taxonomy and function of the biofilm, it would be interesting to investigate how microbial taxa are located spatially in the biofilm. This could be done using FISH imaging or other advanced microscopy techniques. The information obtained could help us to understand which taxa are detached from the biofilm during flushing of DWDSs or as the result of changes in the hydraulics.

Fast and informative monitoring of the water quality is important. Online FCM tools have recently been developed, as well as cytometric fingerprinting techniques. Other interesting methods of online analysis include particle counts and ATP measurements. It could be valuable to combine these tools with measurements of abiotic parameters to be able to predict drinking water quality in the DWDS, and for use as early warning systems by incorporating machine learning. Online measurement tools could be complemented with taxonomic identification or functional analysis using, for example, omics-based analysis tools or qPCR to increase our microbiological knowledge. Future technological developments might also lead to user-friendly NGS tools for taxonomic identification which can be applied in the field. New monitoring techniques will provide more information, leading to a better understanding of drinking water quality, which will be important if we are to be able to control and predict water quality, in order to continue to provide safe and clean drinking water in the future.

Hakuna matata

Acknowledgements

Writing these last few pages of my thesis was almost the hardest part. Throughout this work and this journey in my life, I've met, worked, laughed, reflected, discussed, exercised, and enjoyed nature with so many wonderful people, and it is difficult to acknowledge them all in a fitting way. To everyone: Thank you: this would not have been possible without you.

I'm truly grateful for the support of my main supervisor Peter and co-supervisor Catherine. Peter; thank you for giving me freedom and encouragement, guidance when needed, and for challenging me in various situations, which has led to my development in many ways. Thank you for always being available, both in your office and last summer, through on-line meetings. Catherine; thank you for introducing me to the world of research at the Division of Applied Microbiology (TMB) and for believing in me, starting with my ten-week project, Master's project to my PhD studies. I appreciate your skills and efficiency in planning and organization; you have inspired me and helped me tackle the projects we have been involved in.

To everyone at TMB, thanks for creating such a good working environment. I would like to thank present and former members of the Water Group, particularly Sandy, Janine, Mikael, Katharina, Sakarias, Mally, and Phantira. Working with you has been fun and has taught me a lot. To my office mates: Karen, Thitiwut, Nina, Yusak, Venkat, and Julia, and also our visitors, Nikhil, Yasmine, and Marie, thanks for contributing to maintaining a great balance between work, positivity, laughter, good/bad jokes and puzzles/games. During my work I've been involved in teaching various courses, to Sebastian, Eoin, Arne, and Celina, thanks for making these occasions enjoyable and developing. To Linda, for the exciting activities from floor ball to *mellandagspromenader*; to Maja, for the adventures; to Daniel, for the creative and fun time making the movie; to Magnus for your enthusiasm in almost anything, particularly flow cytometry; to Johannes for your expertise in PCR and interest in sports; to Anette for the administrative work and willingness to help; and to Christer for your technical solving skills and contagious laughter.

During my work I've had the pleasure to be involved in various projects with many outstanding people.

To everyone at the Swedish Defence Research Agency (FOI), thank you for fruitful collaboration and visits to Umeå. You always made me feel welcome, and I genuinely enjoyed your calm working environment. To Jon, for your positivity, support and openness, sharing your knowledge in bioinformatics and data analysis; to Emelie, for your kindness, helpfulness and skills in NGS library preparation.

To everyone in the Swedish water industry; I am so grateful to have been part of such a generous, open community. Thank you to everyone at Norrvatten, for our collaboration during the UV study, particularly Linda for your help and enthusiasm. To everyone at VIVAB, thank you for our collaboration during the UF and pipe studies, Alexander for your research mind, ability to make things happen, and inspiration while becoming co-supervisor towards the end of my work; and Caroline, Moshe and Jennie for your help with the field work during long working days. Thank you to everyone at Sydvatten, for help throughout my Master's project, Kenneth for your positivity and curiosity in water science; Britt-Marie, Tobias and Olivia for the great Christmas camps spiced with research discussions, good food and running. To my colleagues at Sweden Water Research (SWR), I've enjoyed our Wednesday breakfasts, SWR days, getting to know you and all our discussions, which have increased my knowledge in various areas of water science.

Emme, Issi ja Kaarel, olen alati tundnud teie tugevat toetust.

Emmy, I'm so happy when I'm with you, I love you.

References

Aggarwal, S., Gomez-Smith, C.K., Jeon, Y., Lapara, T.M., Waak, M.B., Hozalski, R.M., 2018. Effects of Chloramine and Coupon Material on Biofilm Abundance and Community Composition in Bench-Scale Simulated Water Distribution Systems and Comparison with Full-Scale Water Mains. Environmental Science and Technology 52, 13077–13088. https://doi.org/10.1021/acs.est.8b02607

Albers, C.N., Ellegaard-Jensen, L., Hansen, L.H., Sørensen, S.R., 2018. Bioaugmentation of rapid sand filters by microbiome priming with a nitrifying consortium will optimize production of drinking water from groundwater. Water Research 129, 1–10. https://doi.org/10.1016/j.watres.2017.11.009

Allen, M.J., Edberg, S.C., Reasoner, D.J., 2004a. Heterotrophic plate count bacteria - What is their significance in drinking water? International Journal of Food Microbiology 92, 265–274. https://doi.org/10.1016/j.ijfoodmicro.2003.08.017

Allen, M.J., Edberg, S.C., Reasoner, D.J., 2004b. Heterotrophic plate count bacteria - What is their significance in drinking water?, in: International Journal of Food Microbiology. pp. 265–274. https://doi.org/10.1016/j.ijfoodmicro.2003.08.017

Amalfitano, S., Fazi, S., Ejarque, E., Freixa, A., Romaní, A.M., Butturini, A., 2018. Deconvolution model to resolve cytometric microbial community patterns in flowing waters. Cytometry Part A 93, 194–200. https://doi.org/10.1002/cyto.a.23304

Ao, X., Chen, Z., Li, S., Li, C., Lu, Z., Sun, W., 2020. The impact of UV treatment on microbial control and DBPs formation in full-scale drinking water systems in northern China. Journal of Environmental Sciences 87, 398–410. https://doi.org/10.1016/j.jes.2019.08.003

Ashbolt, N.J., 2004. Microbial contamination of drinking water and disease outcomes in developing regions. Toxicology 198, 229–238. https://doi.org/10.1016/j.tox.2004.01.030

Aßhauer, K.P., Wemheuer, B., Daniel, R., Meinicke, P., 2015. Tax4Fun: Predicting functional profiles from metagenomic 16S rRNA data. Bioinformatics 31, 2882–2884. https://doi.org/10.1093/bioinformatics/btv287

Bai, Y., Liu, R., Liang, J., Qu, J., 2013. Integrated Metagenomic and Physiochemical Analyses to Evaluate the Potential Role of Microbes in the Sand Filter of a Drinking Water Treatment System. PLoS ONE 8. https://doi.org/10.1371/journal.pone.0061011

Baker, G.C., Smith, J.J., Cowan, D.A., 2003. Review and re-analysis of domain-specific 16S primers. Journal of Microbiological Methods 55, 541–555. https://doi.org/10.1016/j.mimet.2003.08.009

Bartram, J., Cotruvo, J., Exner, M., Fricker, C., Glasmacher, A., 2003. Heterotrophic Plate Counts and Drinking-Water Safety. IWA Publishing on behalf of the World Health Organization, London, UK.

Batté, M., Koudjonou, B., Laurent, P., Mathieu, L., Coallier, J., Prévost, M., 2003. Biofilm responses to ageing and to a high phosphate load in a bench-scale drinking water system. Water Research 37, 1351–1361. https://doi.org/10.1016/S0043-1354(02)00476-1

Bautista-de los Santos, Q.M., Schroeder, J.L., Blakemore, O., Moses, J., Haffey, M., Sloan, W., Pinto, A.J., 2016a. The impact of sampling, PCR, and sequencing replication on discerning changes in drinking water bacterial community over diurnal time-scales. Water Research 90, 216–224. https://doi.org/10.1016/j.watres.2015.12.010

Bautista-de los Santos, Q.M., Schroeder, J.L., Sevillano-Rivera, M.C., Sungthong, R., Ijaz, U.Z., Sloan, W.T., Pinto, A.J., 2016b. Emerging investigators series: microbial communities in full-scale drinking water distribution systems – a meta-analysis. Environmental Science: Water Research & Technology 2, 631–644. https://doi.org/10.1039/C6EW00030D

Beck, S.E., Rodriguez, R.A., Linden, K.G., Hargy, T.M., Larason, T.C., Wright, H.B., 2014. Wavelength dependent UV inactivation and DNA damage of adenovirus as measured by cell culture infectivity and long range quantitative PCR. Environmental Science and Technology 48, 591–598. https://doi.org/10.1021/es403850b

Ben Said, M., Masahiro, O., Hassen, A., 2010. Detection of viable but non cultivable Escherichia coli after UV irradiation using a lytic Qβ phage. Annals of Microbiology 60, 121–127. https://doi.org/10.1007/s13213-010-0017-4

Bereschenko, L.A., Stams, A.J.M., Euverink, G.J.W., Van Loosdrecht, M.C.M., 2010. Biofilm formation on reverse osmosis membranes is initiated and dominated by Sphingomonas spp. Applied and Environmental Microbiology 76, 2623–2632. https://doi.org/10.1128/AEM.01998-09

Berney, M., Hammes, F., Bosshard, F., Weilenmann, H.U., Egli, T., 2007. Assessment and interpretation of bacterial viability by using the LIVE/DEAD BacLight kit in combination with flow cytometry. Applied and Environmental Microbiology 73, 3283–3290. https://doi.org/10.1128/AEM.02750-06

Besmer, M.D., Weissbrodt, D.G., Kratochvil, B.E., Sigrist, J.A., Weyland, M.S., Hammes, F., Müller, S., Allen, L.-A.H., Farnleitner, A.H., 2014. The feasibility of automated online flow cytometry for in-situ monitoring of microbial dynamics in aquatic ecosystems. https://doi.org/10.3389/fmicb.2014.00265

Boe-Hansen, R., Albrechtsen, H.J., Arvin, E., Jørgensen, C., 2002. Bulk water phase and

biofilm growth in drinking water at low nutrient conditions. Water Research 36, 4477–4486. https://doi.org/10.1016/S0043-1354(02)00191-4

Bogosian, G., Bourneuf, E. V, 2001. A matter of bacterial life and death. EMBO reports 2, 770–774. https://doi.org/10.1093/embo-reports/kve182

Bohrerova, Z., Rosenblum, J., Linden, K.G., 2015. Importance of recovery of E. coli in water following ultraviolet light disinfection. Journal of Environmental Engineering (United States) 141, 1–6. https://doi.org/10.1061/(ASCE)EE.1943-7870.0000922

Bokulich, N.A., Subramanian, S., Faith, J.J., Gevers, D., Gordon, J.I., Knight, R., Mills, D.A., Caporaso, J.G., 2013. Quality-filtering vastly improves diversity estimates from Illumina amplicon sequencing. Nature Methods 10, 57–59. https://doi.org/10.1038/nmeth.2276

Bolyen, E., Rideout, J.R., Dillon, M.R., Bokulich, N.A., Abnet, C.C., Al-Ghalith, G.A., Alexander, H., Alm, E.J., Arumugam, M., Asnicar, F., Bai, Y., Bisanz, J.E., Bittinger, K., Brejnrod, A., Brislawn, C.J., Brown, C.T., Callahan, B.J., Caraballo-Rodríguez, A.M., Chase, J., Cope, E.K., Da Silva, R., Diener, C., Dorrestein, P.C., Douglas, G.M., Durall, D.M., Duvallet, C., Edwardson, C.F., Ernst, M., Estaki, M., Fouquier, J., Gauglitz, J.M., Gibbons, S.M., Gibson, D.L., Gonzalez, A., Gorlick, K., Guo, J., Hillmann, B., Holmes, S., Holste, H., Huttenhower, C., Huttley, G.A., Janssen, S., Jarmusch, A.K., Jiang, L., Kaehler, B.D., Kang, K. Bin, Keefe, C.R., Keim, P., Kelley, S.T., Knights, D., Koester, I., Kosciolek, T., Kreps, J., Langille, M.G.I., Lee, J., Ley, R., Liu, Y.-X., Loftfield, E., Lozupone, C., Maher, M., Marotz, C., Martin, B.D., McDonald, D., McIver, L.J., Melnik, A. V., Metcalf, J.L., Morgan, S.C., Morton, J.T., Naimey, A.T., Navas-Molina, J.A., Nothias, L.F., Orchanian, S.B., Pearson, T., Peoples, S.L., Petras, D., Preuss, M.L., Pruesse, E., Rasmussen, L.B., Rivers, A., Robeson, M.S., Rosenthal, P., Segata, N., Shaffer, M., Shiffer, A., Sinha, R., Song, S.J., Spear, J.R., Swafford, A.D., Thompson, L.R., Torres, P.J., Trinh, P., Tripathi, A., Turnbaugh, P.J., Ul-Hasan, S., van der Hooft, J.J.J., Vargas, F., Vázquez-Baeza, Y., Vogtmann, E., von Hippel, M., Walters, W., Wan, Y., Wang, M., Warren, J., Weber, K.C., Williamson, C.H.D., Willis, A.D., Xu, Z.Z., Zaneveld, J.R., Zhang, Y., Zhu, Q., Knight, R., Caporaso, J.G., 2019. Reproducible, interactive, scalable and extensible microbiome data science using QIIME 2. Nature Biotechnology 37, 852–857. https://doi.org/10.1038/s41587-019-0209-9

Bombach, P., Hübschmann, T., Fetzer, I., Kleinsteuber, S., Geyer, R., Harms, H., Müller, S., 2011. Resolution of natural microbial community dynamics by community fingerprinting, flow cytometry, and trend interpretation analysis. Advances in Biochemical Engineering/Biotechnology 124, 151–181. https://doi.org/10.1007/10_2010_82

Bosshard, F., Berney, M., Scheifele, M., Weilenmann, H.U., Egli, T., 2009. Solar disinfection (SODIS) and subsequent dark storage of Salmonella typhimurium and Shigella flexneri monitored by flow cytometry. Microbiology 155, 1310–1317. https://doi.org/10.1099/mic.0.024794-0

Boubetra, A., Nestour, F. Le, Allaert, C., Feinberg, M., 2011. Validation of alternative

methods for the analysis of drinking water and their application to Escherichia coli. Applied and Environmental Microbiology 77, 3360–3367. https://doi.org/10.1128/AEM.00020-11

Bourne, D.G., Blakeley, R.L., Riddles, P., Jones, G.J., 2006. Biodegradation of the cyanobacterial toxin microcystin LR in natural water and biologically active slow sand filters. Water Research 40, 1294–1302. https://doi.org/10.1016/j.watres.2006.01.022

Bowers, R.M., Kyrpides, N.C., Stepanauskas, R., Harmon-Smith, M., Doud, D., Reddy, T.B.K., Schulz, F., Jarett, J., Rivers, A.R., Eloe-Fadrosh, E.A., Tringe, S.G., Ivanova, N.N., Copeland, A., Clum, A., Becraft, E.D., Malmstrom, R.R., Birren, B., Podar, M., Bork, P., Weinstock, G.M., Garrity, G.M., Dodsworth, J.A., Yooseph, S., Sutton, G., Glöckner, F.O., Gilbert, J.A., Nelson, W.C., Hallam, S.J., Jungbluth, S.P., Ettema, T.J.G., Tighe, S., Konstantinidis, K.T., Liu, W.T., Baker, B.J., Rattei, T., Eisen, J.A., Hedlund, B., McMahon, K.D., Fierer, N., Knight, R., Finn, R., Cochrane, G., Karsch-Mizrachi, I., Tyson, G.W., Rinke, C., Lapidus, A., Meyer, F., Yilmaz, P., Parks, D.H., Eren, A.M., Schriml, L., Banfield, J.F., Hugenholtz, P., Woyke, T., 2017. Minimum information about a single amplified genome (MISAG) and a metagenome-assembled genome (MIMAG) of bacteria and archaea. Nature Biotechnology 35, 725–731. https://doi.org/10.1038/nbt.3893

Brandt, J., Albertsen, M., 2018. Investigation of Detection Limits and the Influence of DNA Extraction and Primer Choice on the Observed Microbial Communities in Drinking Water Samples Using 16S rRNA Gene Amplicon Sequencing. Frontiers in Microbiology 9, 2140. https://doi.org/10.3389/fmicb.2018.02140

Breitwieser, F.P., Lu, J., Salzberg, S.L., 2017. A review of methods and databases for metagenomic classification and assembly. Briefings in Bioinformatics. https://doi.org/10.1093/bib/bbx120

Bucheli-Witschel, M., Bassin, C., Egli, T., 2010. UV-C inactivation in Escherichia coli is affected by growth conditions preceding irradiation, in particular by the specific growth rate. Journal of Applied Microbiology 109, 1733–1744. https://doi.org/10.1111/j.1365-2672.2010.04802.x

Burtscher, M.M., Zibuschka, F., Mach, R.L., Lindner, G., Farnleitner, A.H., 2009. Heterotrophic plate count vs. in situ bacterial 16S rRNA gene amplicon profiles from drinking water reveal completely different communities with distinct spatial and temporal allocations in a distribution net. Water SA 35, 495–504. https://doi.org/10.4314/wsa.v35i4.76809

Bustin, S.A., Benes, V., Garson, J.A., Hellemans, J., Huggett, J., Kubista, M., Mueller, R., Nolan, T., Pfaffl, M.W., Shipley, G.L., Vandesompele, J., Wittwer, C.T., 2009. The MIQE Guidelines: Minimum Information for Publication of Quantitative Real-Time PCR Experiments. Clinical Chemistry 55, 611–622. https://doi.org/10.1373/clinchem.2008.112797

Callahan, B.J., Mcmurdie, P.J., Holmes, S.P., 2017. Exact sequence variants should replace operational taxonomic units in marker-gene data analysis. The ISME

Journal 11, 2639–2643. https://doi.org/10.1038/ismej.2017.119

Callahan, B.J., McMurdie, P.J., Rosen, M.J., Han, A.W., Johnson, A.J.A., Holmes, S.P., 2016. DADA2: High-resolution sample inference from Illumina amplicon data. Nature Methods 13, 581–583. https://doi.org/10.1038/nmeth.3869

Callahan, B.J., Wong, J., Heiner, C., Oh, S., Theriot, C.M., Gulati, A.S., McGill, S.K., Dougherty, M.K., 2019. High-throughput amplicon sequencing of the full-length 16S rRNA gene with single-nucleotide resolution. Nucleic acids research 47, e103. https://doi.org/10.1093/nar/gkz569

Caporaso, J.G., Kuczynski, J., Stombaugh, J., Bittinger, K., Bushman, F.D., Costello, E.K., Fierer, N., Peña, A.G., Goodrich, J.K., Gordon, J.I., Huttley, G.A., Kelley, S.T., Knights, D., Koenig, J.E., Ley, R.E., Lozupone, C.A., Mcdonald, D., Muegge, B.D., Pirrung, M., Reeder, J., Sevinsky, J.R., Turnbaugh, P.J., Walters, W.A., Widmann, J., Yatsunenko, T., Zaneveld, J., Knight, R., 2010. QIIME allows analysis of high- throughput community sequencing data. Nature Publishing Group 7, 335–336. https://doi.org/10.1038/nmeth0510-335

Carrico, B.A., Digiano, F.A., Love, N.G., Vikesland, P., Chandran, K., Fiss, M., Zaklikowski, A., 2008. Effectiveness of switching disinfectants for nitrification control. Journal / American Water Works Association 100. https://doi.org/10.1002/j.1551-8833.2008.tb09751.x

Chan, S., 2018. Processes governing the drinking water microbiome. Doctoral Thesis. Lund University.

Chatzigiannidou, I., Props, R., Boon, N., 2018. Drinking water bacterial communities exhibit specific and selective necrotrophic growth. npj Clean Water 1, 22. https://doi.org/10.1038/s41545-018-0023-9

Chen, P.F., Zhang, R.J., Huang, S. Bin, Shao, J.H., Cui, B., Du, Z.L., Xue, L., Zhou, N., Hou, B., Lin, C., 2020. UV dose effects on the revival characteristics of microorganisms in darkness after UV disinfection: Evidence from a pilot study. Science of the Total Environment 713, 136582. https://doi.org/10.1016/j.scitotenv.2020.136582

Chiao, T.H., Clancy, T.M., Pinto, A., Xi, C., Raskin, L., 2014. Differential resistance of drinking water bacterial populations to monochloramine disinfection. Environmental Science and Technology 48, 4038–4047. https://doi.org/10.1021/es4055725

Choi, Yonkyu, Choi, Young-june, 2010. The effects of UV disinfection on drinking water quality in distribution systems. Water Research 44, 115–122. https://doi.org/10.1016/J.WATRES.2009.09.011

Christensen, J., Linden, K.G., 2003. How particles affect UV light in the UV Disinfection of Unfiltered Drinking Water. Journal - American Water Works Association 95, 179–189. https://doi.org/10.1002/j.1551-8833.2003.tb10344.x

Chua, S.L., Liu, Y., Yam, J.K.H., Chen, Y., Vejborg, R.M., Tan, B.G.C., Kjelleberg, S., Tolker-Nielsen, T., Givskov, M., Yang, L., 2014. Dispersed cells represent a

distinct stage in the transition from bacterial biofilm to planktonic lifestyles. Nature Communications 5. https://doi.org/10.1038/ncomms5462

Clarridge, J.E., 2004. Impact of 16S rRNA Gene Sequence Analysis for Identification of Bacteria on Clinical Microbiology and Infectious Diseases Impact of 16S rRNA Gene Sequence Analysis for Identification of Bacteria on Clinical Microbiology and Infectious Diseases. Clinical Microbiology Reviews 17, 840–862. https://doi.org/10.1128/CMR.17.4.840

Corpe, W.A., Jensen, T.E., 1996. The diversity of bacteria, eukaryotic cells and viruses in an oligotrophic lake. Applied Microbiology and Biotechnology 46, 622–630. https://doi.org/10.1007/s002530050872

Craig Venter, J., Adams, M.D., Myers, E.W., Li, P.W., Mural, R.J., Sutton, G.G., Smith, H.O., Yandell, M., Evans, C.A., Holt, R.A., Gocayne, J.D., Amanatides, P., Ballew, R.M., Huson, D.H., Wortman, J.R., Zhang, Q., Kodira, C.D., Zheng, X.H., Chen, L., Skupski, M., Subramanian, G., Thomas, P.D., Zhang, J., Gabor Miklos, G.L., Nelson, C., Broder, S., Clark, A.G., Nadeau, J., McKusick, V.A., Zinder, N., Levine, A.J., Roberts, R.J., Simon, M., Slayman, C., Hunkapiller, M., Bolanos, R., Delcher, A., Dew, I., Fasulo, D., Flanigan, M., Florea, L., Halpern, A., Hannenhalli, S., Kravitz, S., Levy, S., Mobarry, C., Reinert, K., Remington, K., Abu-Threideh, J., Beasley, E., Biddick, K., Bonazzi, V., Brandon, R., Cargill, M., Chandramouliswaran, I., Charlab, R., Chaturvedi, K., Deng, Z., di Francesco, V., Dunn, P., Eilbeck, K., Evangelista, C., Gabrielian, A.E., Gan, W., Ge, W., Gong, F., Gu, Z., Guan, P., Heiman, T.J., Higgins, M.E., Ji, R.R., Ke, Z., Ketchum, K.A., Lai, Z., Lei, Y., Li, Z., Li, J., Liang, Y., Lin, X., Lu, F., Merkulov, G. V., Milshina, N., Moore, H.M., Naik, A.K., Narayan, V.A., Neelam, B., Nusskern, D., Rusch, D.B., Salzberg, S., Shao, W., Shue, B., Sun, J., Yuan Wang, Z., Wang, A., Wang, X., Wang, J., Wei, M.H., Wides, R., Xiao, C., Yan, C., Yao, A., Ye, J., Zhan, M., Zhang, W., Zhang, H., Zhao, Q., Zheng, L., Zhong, F., Zhong, W., Zhu, S.C., Zhao, S., Gilbert, D., Baumhueter, S., Spier, G., Carter, C., Cravchik, A., Woodage, T., Ali, F., An, H., Awe, A., Baldwin, D., Baden, H., Barnstead, M., Barrow, I., Beeson, K., Busam, D., Carver, A., Center, A., Lai Cheng, M., Curry, L., Danaher, S., Davenport, L., Desilets, R., Dietz, S., Dodson, K., Doup, L., Ferriera, S., Garg, N., Gluecksmann, A., Hart, B., Haynes, J., Haynes, C., Heiner, C., Hladun, S., Hostin, D., Houck, J., Howland, T., Ibegwam, C., Johnson, J., Kalush, F., Kline, L., Koduru, S., Love, A., Mann, F., May, D., McCawley, S., McIntosh, T., McMullen, I., Moy, M., Moy, L., Murphy, B., Nelson, K., Pfannkoch, C., Pratts, E., Puri, V., Qureshi, H., Reardon, M., Rodriguez, R., Rogers, Y.H., Romblad, D., Ruhfel, B., Scott, R., Sitter, C., Smallwood, M., Stewart, E., Strong, R., Suh, E., Thomas, R., Ni Tint, N., Tse, S., Vech, C., Wang, G., Wetter, J., Williams, S., Williams, M., Windsor, S., Winn-Deen, E., Wolfe, K., Zaveri, J., Zaveri, K., Abril, J.F., Guigo, R., Campbell, M.J., Sjolander, K. V., Karlak, B., Kejariwal, A., Mi, H., Lazareva, B., Hatton, T., Narechania, A., Diemer, K., Muruganujan, A., Guo, N., Sato, S., Bafna, V., Istrail, S., Lippert, R., Schwartz, R., Walenz, B., Yooseph, S., Allen, D., Basu, A., Baxendale, J., Blick, L., Caminha, M., Carnes-Stine, J., Caulk, P., Chiang, Y.H., Coyne, M., Dahlke, C., Deslattes Mays, A., Dombroski, M., Donnelly, M., Ely, D., Esparham, S., Fosler,

C., Gire, H., Glanowski, S., Glasser, K., Glodek, A., Gorokhov, M., Graham, K., Gropman, B., Harris, M., Heil, J., Henderson, S., Hoover, J., Jennings, D., Jordan, C., Jordan, J., Kasha, J., Kagan, L., Kraft, C., Levitsky, A., Lewis, M., Liu, X., Lopez, J., Ma, D., Majoros, W., McDaniel, J., Murphy, S., Newman, M., Nguyen, T., Nguyen, N., Nodell, M., Pan, S., Peck, J., Peterson, M., Rowe, W., Sanders, R., Scott, J., Simpson, M., Smith, T., Sprague, A., Stockwell, T., Turner, R., Venter, E., Wang, M., Wen, M., Wu, D., Wu, M., Xia, A., Zandieh, A., Zhu, X., 2001. The sequence of the human genome. Science 291, 1304–1351. https://doi.org/10.1126/science.1058040

Cross, K.L., Campbell, J.H., Balachandran, M., Campbell, A.G., Cooper, S.J., Griffen, A., Heaton, M., Joshi, S., Klingeman, D., Leys, E., Yang, Z., Parks, J.M., Podar, M., 2019. Targeted isolation and cultivation of uncultivated bacteria by reverse genomics. Nature Biotechnology 37, 1314–1321. https://doi.org/10.1038/s41587-019-0260-6

Cruz, M.C., Woo, Y., Flemming, H.C., Wuertz, S., 2020. Nitrifying niche differentiation in biofilms from full-scale chloraminated drinking water distribution system. Water Research 176, 115738. https://doi.org/10.1016/j.watres.2020.115738

D'Amore, R., Ijaz, U.Z., Schirmer, M., Kenny, J.G., Gregory, R., Darby, A.C., Shakya, M., Podar, M., Quince, C., Hall, N., 2016. A comprehensive benchmarking study of protocols and sequencing platforms for 16S rRNA community profiling. BMC Genomics 17. https://doi.org/10.1186/s12864-015-2194-9

Dai, T., Vrahas, M.S., Murray, C.K., Hamblin, M.R., 2012. Ultraviolet C irradiation: An alternative antimicrobial approach to localized infections? Expert Review of Anti-Infective Therapy 10, 185–195. https://doi.org/10.1586/eri.11.166

Dai, Z., Sevillano-Rivera, M.C., Calus, S.T., Bautista-De Los Santos, Q.M., Eren, A.M., Van Der Wielen, P.W.J.J., Ijaz, U.Z., Pinto, A.J., 2020. Disinfection exhibits systematic impacts on the drinking water microbiome. Microbiome 8, 1–19. https://doi.org/10.1186/s40168-020-00813-0

Daims, H., Lebedeva, E. V., Pjevac, P., Han, P., Herbold, C., Albertsen, M., Jehmlich, N., Palatinszky, M., Vierheilig, J., Bulaev, A., Kirkegaard, R.H., Von Bergen, M., Rattei, T., Bendinger, B., Nielsen, P.H., Wagner, M., 2015. Complete nitrification by Nitrospira bacteria. Nature 528, 504–509. https://doi.org/10.1038/nature16461

Daims, H., Lücker, S., Wagner, M., 2016. A New Perspective on Microbes Formerly Known as Nitrite-Oxidizing Bacteria. Trends in Microbiology 24, 699–712. https://doi.org/10.1016/j.tim.2016.05.004

Deines, P., Sekar, R., Husband, P.S., Boxall, J.B., Osborn, A.M., Biggs, C.A., 2010. A new coupon design for simultaneous analysis of in situ microbial biofilm formation and community structure in drinking water distribution systems. Applied Microbiology and Biotechnology 87, 749–756. https://doi.org/10.1007/s00253-010-2510-x

Delpla, I., Jung, A. V., Baures, E., Clement, M., Thomas, O., 2009. Impacts of climate

change on surface water quality in relation to drinking water production. Environment International 35, 1225–1233. https://doi.org/10.1016/j.envint.2009.07.001

Desantis, T.Z., Hugenholtz, P., Larsen, N., Rojas, M., Brodie, E.L., Keller, K., Huber, T., Dalevi, D., Hu, P., Andersen, G.L., 2006. Greengenes, a Chimera-Checked 16S rRNA Gene Database and Workbench Compatible with ARB. APPLIED AND ENVIRONMENTAL MICROBIOLOGY 72, 5069–5072. https://doi.org/10.1128/AEM.03006-05

Dias, M.F., Reis, M.P., Acurcio, L.B., Carmo, A.O., Diamantino, C.F., Motta, A.M., Kalapothakis, E., Nicoli, J.R., Ea, A., Nascimento, M.A., 2018. Changes in mouse gut bacterial community in response to different types of drinking water. https://doi.org/10.1016/j.watres.2017.12.052

Donohue, M.J., Vesper, S., Mistry, J., Donohue, J.M., 2019. Impact of Chlorine and Chloramine on the Detection and Quantification of Legionella pneumophila and Mycobacterium Species. Applied and Environmental Microbiology 85, 1–11. https://doi.org/10.1128/AEM.01942-19

dos Santos, P.R., Daniel, L.A., 2019. A review: organic matter and ammonia removal by biological activated carbon filtration for water and wastewater treatment. International Journal of Environmental Science and Technology 17, 591–606. https://doi.org/10.1007/s13762-019-02567-1

Douglas, G.M., Maffei, V.J., Zaneveld, J.R., Yurgel, S.N., Brown, J.R., Taylor, C.M., Huttenhower, C., Langille, M.G.I., 2020. PICRUSt2 for prediction of metagenome functions. Nature Biotechnology. https://doi.org/10.1038/s41587-020-0548-6

Douki, T., Cadet, J., 2001. Individual determination of the yield of the main UV-induced dimeric pyrimidine photoproducts in DNA suggests a high mutagenicity of CC photolesions. Biochemistry 40, 2495–2501. https://doi.org/10.1021/bi0022543

Douterelo, I., Boxall, J.B., Deines, P., Sekar, R., Fish, K.E., Biggs, C.A., 2014. Methodological approaches for studying the microbial ecology of drinking water distribution systems. Water Research 65, 134–156. https://doi.org/10.1016/j.watres.2014.07.008

Douterelo, I., Dutilh, B.E., Arkhipova, K., Calero, C., Husband, S., 2020. Microbial diversity, ecological networks and functional traits associated to materials used in drinking water distribution systems. Water Research 173, 115586. https://doi.org/10.1016/j.watres.2020.115586

Douterelo, I., Husband, S., Loza, V., Boxall, J., 2016. Dynamics of biofilm regrowth in drinking water distribution systems. Applied and Environmental Microbiology 82, 4155–4168. https://doi.org/10.1128/AEM.00109-16

Douterelo, I., Sharpe, R.L., Boxall, J.B., 2013. Influence of hydraulic regimes on bacterial community structure and composition in an experimental drinking water

distribution system. Water Research 47, 503–516. https://doi.org/10.1016/j.watres.2012.09.053

Edgar, R., 2018. Taxonomy annotation and guide tree errors in 16S rRNA databases. PeerJ 2018. https://doi.org/10.7717/peerj.5030

Edgar, R.C., 2010. Search and clustering orders of magnitude faster than BLAST. Bioinformatics 26, 2460–2461. https://doi.org/10.1093/bioinformatics/btq461

Edgar, R.C., Haas, B.J., Clemente, J.C., Quince, C., Knight, R., 2011. UCHIME improves sensitivity and speed of chimera detection. Bioinformatics 27, 2194–2200. https://doi.org/10.1093/bioinformatics/btr381

Eikebrokk, B., Vogt, R.D., Liltved, H., 2004. NOM increase in Northern European source waters: Discussion of possible causes and impacts on coagulation/contact filtration processes. Water Science and Technology: Water Supply 4, 47–54. https://doi.org/10.2166/ws.2004.0060

Eischeid, A.C., Meyer, J.N., Linden, K.G., 2009. UV Disinfection of Adenoviruses: Molecular Indications of DNA Damage Efficiency. APPLIED AND ENVIRONMENTAL MICROBIOLOGY 75, 23–28. https://doi.org/10.1128/AEM.02199-08

Eisenhofer, R., Minich, J.J., Marotz, C., Cooper, A., Knight, R., Weyrich, L.S., 2019. Contamination in Low Microbial Biomass Microbiome Studies: Issues and Recommendations. Trends in Microbiology 27, 105–117. https://doi.org/10.1016/j.tim.2018.11.003

Ekström, S.M., Kritzberg, E.S., Kleja, D.B., Larsson, N., Nilsson, P.A., Graneli, W., Bergkvist, B., 2011. Effect of acid deposition on quantity and quality of dissolved organic matter in soil-water. Environmental Science and Technology 45, 4733–4739. https://doi.org/10.1021/es104126f

El-Chakhtoura, J., Prest, E., Saikaly, P., Van Loosdrecht, M., Hammes, F., Vrouwenvelder, H., 2015. Dynamics of bacterial communities before and after distribution in a full-scale drinking water network. https://doi.org/10.1016/j.watres.2015.02.015

Elhadidy, A.M., Van Dyke, M.I., Chen, F., Peldszus, S., Huck, P.M., 2017. Development and application of an improved protocol to characterize biofilms in biologically active drinking water filters. Environmental Science: Water Research and Technology 3, 249–261. https://doi.org/10.1039/c6ew00279j

Elhadidy, A.M., Van Dyke, M.I., Peldszus, S., Huck, P.M., 2016. Application of flow cytometry to monitor assimilable organic carbon (AOC) and microbial community changes in water. Journal of Microbiological Methods 130, 154–163. https://doi.org/10.1016/j.mimet.2016.09.009

Elizaquível, P., Aznar, R., Sánchez, G., 2014. Recent developments in the use of viability dyes and quantitative PCR in the food microbiology field. Journal of Applied Microbiology 116, 1–13. https://doi.org/10.1111/jam.12365

Elliott, M.A., Stauber, C.E., Koksal, F., DiGiano, F.A., Sobsey, M.D., 2008. Reductions of E. coli, echovirus type 12 and bacteriophages in an intermittently operated household-scale slow sand filter. Water Research 42, 2662–2670. https://doi.org/10.1016/j.watres.2008.01.016

Eriksson, U., 2009. Råd och riktlinjer för UV-ljus vid vattenverk. Publikation. Svensk bearbetning av Norsk Vann Rapport 164.

Evans, C.D., Monteith, D.T., Cooper, D.M., 2005. Long-term increases in surface water dissolved organic carbon: Observations, possible causes and environmental impacts. Environmental Pollution 137, 55–71. https://doi.org/10.1016/j.envpol.2004.12.031

Fadrosh, D.W., Bing Ma, P.G., Sengamalay, N., Ott, S., Brotman, R.M., Ravel, J., 2014. An improved dual-indexing approach for multiplexed 16S rRNA gene sequencing on the Illumina MiSeq platform. Microbiome 2, 1–7.

Farell, E.M., Alexandre, G., 2012. Bovine serum albumin further enhances the effects of organic solvents on increased yield of polymerase chain reaction of GC-rich templates. BMC Research Notes 5, 1. https://doi.org/10.1186/1756-0500-5-257

Farhat, N., Hammes, F., Prest, E., Vrouwenvelder, J., 2018. A uniform bacterial growth potential assay for different water types. Water Research 142, 227–235. https://doi.org/10.1016/J.WATRES.2018.06.010

Farhat, N., Kim, L.H., Vrouwenvelder, J.S., 2020. Online characterization of bacterial processes in drinking water systems. npj Clean Water 3, 1–7. https://doi.org/10.1038/s41545-020-0065-7

Farrell, C., Hassard, F., Jefferson, B., Leziart, T., Nocker, A., Jarvis, P., 2018. Turbidity composition and the relationship with microbial attachment and UV inactivation efficacy. Science of the Total Environment 624, 638–647. https://doi.org/10.1016/j.scitotenv.2017.12.173

Favere, J., Buysschaert, B., Boon, N., De Gusseme, B., 2020. Online microbial fingerprinting for quality management of drinking water: Full-scale event detection. Water Research 170, 115353. https://doi.org/10.1016/j.watres.2019.115353

Fesefeldt, A., Kloos, K., Bothe, H., Lemmer, H., Gliesche, C.G., 1998. Distribution of denitrification and nitrogen fixation genes in Hyphomicrobium, spp. and other budding bacteria. Canadian Journal of Microbiology 44, 181–186. https://doi.org/10.1139/cjm-44-2-181

Fish, K., Osborn, A.M., Boxall, J.B., 2017. Biofilm structures (EPS and bacterial communities) in drinking water distribution systems are conditioned by hydraulics and influence discolouration. Science of the Total Environment 593–594, 571–580. https://doi.org/10.1016/j.scitotenv.2017.03.176

Fish, K.E., Collins, R., Green, N.H., Sharpe, R.L., Douterelo, I., Osborn, A.M., Boxall, J.B., 2015. Characterisation of the Physical Composition and Microbial Community Structure of Biofilms within a Model Full-Scale Drinking Water Distribution System. PLOS ONE 10, e0115824.

https://doi.org/10.1371/journal.pone.0115824

Flemming, H.-C., 2002. Biofouling in water systems – cases, causes and countermeasures. Applied Microbiology and Biotechnology 59, 629–640. https://doi.org/10.1007/s00253-002-1066-9

Flemming, H.-C., Wingender, J., Szewzyk, U., Steinberg, P., Rice, S.A., Kjelleberg, S., 2016. Biofilms: an emergent form of bacterial life. Nature Reviews Microbiology 14, 563–575. https://doi.org/10.1038/nrmicro.2016.94

Flemming, H.-C., Wuertz, S., 2019. Bacteria and archaea on Earth and their abundance in biofilms. Nature Reviews Microbiology 1. https://doi.org/10.1038/s41579-019-0158-9

Flemming, H.C., Percival, S.L., Walker, J.T., 2002. Contamination potential of biofilms in water distribution systems. Water Science and Technology: Water Supply 2, 271–280. https://doi.org/10.2166/ws.2002.0032

Flemming, H.C., Wingender, J., 2010. The biofilm matrix. Nature Reviews Microbiology 8, 623–633. https://doi.org/10.1038/nrmicro2415

Fowler, S.J., Palomo, A., Dechesne, A., Mines, P.D., Smets, B.F., 2018. Comammox Nitrospira are abundant ammonia oxidizers in diverse groundwater-fed rapid sand filter communities. Environmental Microbiology 20, 1002–1015. https://doi.org/10.1111/1462-2920.14033

Franzosa, E.A., Hsu, T., Sirota-Madi, A., Shafquat, A., Abu-Ali, G., Morgan, X.C., Huttenhower, C., 2015. Sequencing and beyond: Integrating molecular "omics" for microbial community profiling. Nature Reviews Microbiology 13, 360–372. https://doi.org/10.1038/nrmicro3451

Frossard, A., Hammes, F., Gessner, M.O., 2016. Flow Cytometric Assessment of Bacterial Abundance in Soils, Sediments and Sludge. Frontiers in Microbiology 7. https://doi.org/10.3389/fmicb.2016.00903

Gatza, E., Hammes, F., Prest, E., 2013. Assessing Water Quality with the BD Accuri™ C6 Flow Cytometer White Paper.

George, I., Petit, M., Servais, P., 2000. Use of enzymatic methods for rapid enumeration of coliforms in freshwaters. Journal of Applied Microbiology 88, 404–413. https://doi.org/10.1046/j.1365-2672.2000.00977.x

Gerba, C.P., Gramos, D.M., Nwachuku, N., 2002. Comparative inactivation of enteroviruses and adenovirus 2 by UV light. Applied and Environmental Microbiology 68, 5167–5169. https://doi.org/10.1128/AEM.68.10.5167-5169.2002

Gilbert, J.A., Jansson, J.K., Knight, R., 2014. The Earth Microbiome project: Successes and aspirations. BMC Biology 12, 1–4. https://doi.org/10.1186/s12915-014-0069-1

Glassman, S.I., Martiny, J.B.H., 2018. Broadscale Ecological Patterns Are Robust to Use of Exact. mSphere 3, e00148-18. https://doi.org/https://doi.org/10.1128/mSphere

.00148-18

Gloor, G.B., Macklaim, J.M., Pawlowsky-Glahn, V., Egozcue, J.J., 2017. Microbiome datasets are compositional: And this is not optional. Frontiers in Microbiology 8, 1–6. https://doi.org/10.3389/fmicb.2017.02224

Gohl, D.M., Vangay, P., Garbe, J., MacLean, A., Hauge, A., Becker, A., Gould, T.J., Clayton, J.B., Johnson, T.J., Hunter, R., Knights, D., Beckman, K.B., 2016. Systematic improvement of amplicon marker gene methods for increased accuracy in microbiome studies. Nature Biotechnology 34, 942–949. https://doi.org/10.1038/nbt.3601

Gomez-Smith, C.K., Lapara, T.M., Hozalski, R.M., 2015. Sulfate reducing bacteria and mycobacteria dominate the biofilm communities in a chloraminated drinking water distribution system. Environmental Science and Technology 49, 8432–8440. https://doi.org/10.1021/acs.est.5b00555

Goodrich, J.K., Di Rienzi, S.C., Poole, A.C., Koren, O., Walters, W.A., Caporaso, J.G., Knight, R., Ley, R.E., 2014. Conducting a microbiome study. Cell 158, 250–262. https://doi.org/10.1016/j.cell.2014.06.037

Goodwin, S., McPherson, J.D., McCombie, W.R., 2016. Coming of age: Ten years of next-generation sequencing technologies. Nature Reviews Genetics 17, 333–351. https://doi.org/10.1038/nrg.2016.49

Guo, F., Zhang, T., 2013. Biases during DNA extraction of activated sludge samples revealed by high throughput sequencing. Applied Microbiology and Biotechnology 97, 4607–4616. https://doi.org/10.1007/s00253-012-4244-4

Guo, L., Ye, C., Cui, L., Wan, K., Chen, S., Zhang, S., Yu, X., 2019. Population and single cell metabolic activity of UV-induced VBNC bacteria determined by CTC-FCM and D2O-labeled Raman spectroscopy. Environment International 130. https://doi.org/10.1016/j.envint.2019.05.077

Gutleben, J., Chaib De Mares, M., van Elsas, J.D., Smidt, H., Overmann, J., Sipkema, D., 2018. The multi-omics promise in context: from sequence to microbial isolate. Critical Reviews in Microbiology 44, 212–229. https://doi.org/10.1080/1040841X.2017.1332003

Hägglund, M., Bäckman, S., Macellaro, A., Lindgren, P., Borgmästars, E., Jacobsson, K., Dryselius, R., Stenberg, P., Sjödin, A., Forsman, M., Ahlinder, J., 2018. Accounting for Bacterial Overlap Between Raw Water Communities and Contaminating Sources Improves the Accuracy of Signature-Based Microbial Source Tracking. Frontiers in Microbiology 9, 2364. https://doi.org/10.3389/fmicb.2018.02364

Haig, S.J., 2014. Characterising the functional ecology of slow sand filters through environmental genomics. University of Glasgow.

Haig, S.J., Collins, G., Davies, R.L., Dorea, C.C., Quince, C., 2011. Biological aspects of slow sand filtration: Past, present and future. Water Science and Technology: Water Supply 11, 468–472. https://doi.org/10.2166/ws.2011.076

Haig, S.J., Quince, C., Davies, R.L., Dorea, C.C., Collins, G., 2014. Replicating the microbial community and water quality performance of full-scale slow sand filters in laboratory-scale filters. Water Research 61, 141–151. https://doi.org/10.1016/j.watres.2014.05.008

Haig, S.J., Quince, C., Davies, R.L., Dorea, C.C., Collinsa, G., 2015a. The relationship between microbial community evenness and function in slow sand filters. mBio 6, 1–12. https://doi.org/10.1128/mBio.00729-15

Haig, S.J., Schirmer, M., D'Amore, R., Gibbs, J., Davies, R.L., Collins, G., Quince, C., 2015b. Stable-isotope probing and metagenomics reveal predation by protozoa drives E. Coli removal in slow sand filters. ISME Journal 9, 797–808. https://doi.org/10.1038/ismej.2014.175

Halfvarson, J., Brislawn, C.J., Lamendella, R., Vázquez-Baeza, Y., Walters, W.A., Bramer, L.M., D'Amato, M., Bonfiglio, F., McDonald, D., Gonzalez, A., McClure, E.E., Dunklebarger, M.F., Knight, R., Jansson, J.K., 2017. Dynamics of the human gut microbiome in inflammatory bowel disease. Nature Microbiology 2, 17004. https://doi.org/10.1038/nmicrobiol.2017.4

Hammes, F., Berney, M., Wang, Y., Vital, M., Köster, O., Egli, T., 2008. Flow-cytometric total bacterial cell counts as a descriptive microbiological parameter for drinking water treatment processes. Water Research 42, 269–277. https://doi.org/10.1016/j.watres.2007.07.009

Hammes, F., Broger, T., Weilenmann, H.-U., Vital, M., Helbing, J., Bosshart, U., Huber, P., Peter Odermatt, R., Sonnleitner, B., 2012. Development and laboratory-scale testing of a fully automated online flow cytometer for drinking water analysis. Cytometry Part A 81A, 508–516. https://doi.org/10.1002/cyto.a.22048

Hammes, F., Egli, T., 2010. Cytometric methods for measuring bacteria in water: Advantages, pitfalls and applications. Analytical and Bioanalytical Chemistry 397, 1083–1095. https://doi.org/10.1007/s00216-010-3646-3

Hammes, F., Goldschmidt, F., Vital, M., Wang, Y., Egli, T., 2010. Measurement and interpretation of microbial adenosine tri-phosphate (ATP) in aquatic environments. Water Research 44, 3915–3923. https://doi.org/10.1016/j.watres.2010.04.015

Han, Z., An, W., Yang, M., Zhang, Y., 2020. Assessing the impact of source water on tap water bacterial communities in 46 drinking water supply systems in China. Water Research 172, 115469. https://doi.org/10.1016/j.watres.2020.115469

Harwood, V.J., Staley, C., Badgley, B.D., Borges, K., Korajkic, A., 2014. Microbial source tracking markers for detection of fecal contamination in environmental waters: Relationships between pathogens and human health outcomes. FEMS Microbiology Reviews 38, 1–40. https://doi.org/10.1111/1574-6976.12031

Hawinkel, S., Mattiello, F., Bijnens, L., Thas, O., 2019. A broken promise: Microbiome differential abundance methods do not control the false discovery rate. Briefings in Bioinformatics 20, 1–12. https://doi.org/10.1093/bib/bbx104

Hayes, S.L., Sivaganesan, M., White, K.M., Pfaller, S.L., 2008. Assessing the effectiveness of low-pressure ultraviolet light for inactivating Mycobacterium avium complex (MAC) micro-organisms. Letters in Applied Microbiology 47, 386–392. https://doi.org/10.1111/j.1472-765X.2008.02442.x

Hedegaard, M.J., Schliemann-Haug, M.A., Milanovic, N., Lee, C.O., Boe-Hansen, R., Albrechtsen, H.J., 2020. Importance of Methane Oxidation for Microbial Degradation of the Herbicide Bentazone in Drinking Water Production. Frontiers in Environmental Science 8. https://doi.org/10.3389/fenvs.2020.00079

Hedman, J., Knutsson, R., Ansell, R., Rådström, P., Rasmusson, B., 2013. Pre-PCR processing in bioterrorism preparedness: Improved diagnostic capabilities for laboratory response networks. Biosecurity and Bioterrorism 11, 87–102. https://doi.org/10.1089/bsp.2012.0090

Hedman, J., Rådström, P., 2013. Overcoming inhibition in real-time diagnostic PCR. Methods in Molecular Biology 943, 17–48. https://doi.org/10.1007/978-1-60327-353-4_2

Helm-Hansen, O., Booth, C.R., 1966. The measurement of adenosine triphosphate in the Ocean and of Adenosine Its Ecological Significance. Limnology and Oceanography 11, 510–519.

Henderson, G., Cox, F., Kittelmann, S., Miri, V.H., Zethof, M., Noel, S.J., Waghorn, G.C., Janssen, P.H., 2013. Effect of DNA extraction methods and sampling techniques on the apparent structure of cow and sheep rumen microbial communities. PloS one 8, 1–14. https://doi.org/10.1371/journal.pone.0074787

Henne, K., Kahlisch, L., Brettar, I., Höfle, M.G., 2012. Analysis of structure and composition of bacterial core communities in mature drinking water biofilms and bulk water of a citywide network in Germany. Applied and Environmental Microbiology 78, 3530–3538. https://doi.org/10.1128/AEM.06373-11

Henne, K., Kahlisch, L., Höfle, M.G., Brettar, I., 2013. Seasonal dynamics of bacterial community structure and composition in cold and hot drinking water derived from surface water reservoirs. Water Research 47, 5614–5630. https://doi.org/10.1016/j.watres.2013.06.034

Henry, R., Schang, C., Coutts, S., Kolotelo, P., Prosser, T., Crosbie, N., Grant, T., Cottam, D., O'Brien, P., Deletic, A., McCarthy, D., 2016. Into the deep: Evaluation of SourceTracker for assessment of faecal contamination of coastal waters. Water Research 93, 242–253. https://doi.org/10.1016/j.watres.2016.02.029

Hijnen, W.A.M., Beerendonk, E.F., Medema, G.J., 2006. Inactivation credit of UV radiation for viruses, bacteria and protozoan (oo)cysts in water: A review. Water Research 40, 3–22. https://doi.org/10.1016/j.watres.2005.10.030

Hijnen, W.A.M., Schijven, J.F., Bonné, P., Visser, A., Medema, G.J., 2004. Elimination of viruses, bacteria and protozoan oocysts by slow sand filtration. Water Science and Technology 50, 147–154. https://doi.org/10.2166/wst.2004.0044

Ho, J., Seidel, M., Niessner, R., Eggers, J., Tiehm, A., 2016. Long amplicon (LA)-qPCR

for the discrimination of infectious and noninfectious phix174 bacteriophages after UV inactivation. Water Research 103, 141–148. https://doi.org/10.1016/J.WATRES.2016.07.032

Hobbie, J.E., Daley, R.J., Jasper, S., 1977. Use of nuclepore filters for counting bacteria by fluorescence microscopy. Applied and Environmental Microbiology 33, 1225–1228. https://doi.org/10.1128/aem.33.5.1225-1228.1977

Holm, C., Jespersen, L., 2003. A Flow-Cytometric Gram-Staining Technique for Milk-Associated Bacteria 69, 2857–2863. https://doi.org/10.1128/AEM.69.5.2857

Horn, H., Reiff, H., Morgenroth, E., 2003. Simulation of growth and detachment in biofilm systems under defined hydrodynamic conditions. Biotechnology and Bioengineering 81, 607–617. https://doi.org/10.1002/bit.10503

Hugenholtz, P., 2002. Exploring prokaryotic diversity in the genomic era. Genome Biology 3, 1–8. https://doi.org/10.1186/gb-2002-3-2-reviews0003

Huisman, L., Wood, W.., 1974. Slow Sand Filtration. https://doi.org/10.1007/978-1-4614-5491-5_200157

Hull, N.M., Herold, W.H., Linden, K.G., 2019a. UV LED water disinfection: Validation and small system demonstration study. AWWA Water Science 1, 1–11. https://doi.org/10.1002/aws2.1148

Hull, N.M., Ling, F., Pinto, A.J., Albertsen, M., Jang, H.G., Hong, P.Y., Konstantinidis, K.T., LeChevallier, M., Colwell, R.R., Liu, W.T., 2019b. Drinking Water Microbiome Project: Is it Time? Trends in Microbiology 27, 670–677. https://doi.org/10.1016/j.tim.2019.03.011

Huttenhower, C., Gevers, D., Knight, R., Abubucker, S., Badger, J.H., Chinwalla, A.T., Creasy, H.H., Earl, A.M., Fitzgerald, M.G., Fulton, R.S., Giglio, M.G., Hallsworth-Pepin, K., Lobos, E.A., Madupu, R., Magrini, V., Martin, J.C., Mitreva, M., Muzny, D.M., Sodergren, E.J., Versalovic, J., Wollam, A.M., Worley, K.C., Wortman, J.R., Young, S.K., Zeng, Q., Aagaard, K.M., Abolude, O.O., Allen-Vercoe, E., Alm, E.J., Alvarado, L., Andersen, G.L., Anderson, S., Appelbaum, E., Arachchi, H.M., Armitage, G., Arze, C.A., Ayvaz, T., Baker, C.C., Begg, L., Belachew, T., Bhonagiri, V., Bihan, M., Blaser, M.J., Bloom, T., Bonazzi, V., Paul Brooks, J., Buck, G.A., Buhay, C.J., Busam, D.A., Campbell, J.L., Canon, S.R., Cantarel, B.L., Chain, P.S.G., Chen, I.M.A., Chen, L., Chhibba, S., Chu, K., Ciulla, D.M., Clemente, J.C., Clifton, S.W., Conlan, S., Crabtree, J., Cutting, M.A., Davidovics, N.J., Davis, C.C., Desantis, T.Z., Deal, C., Delehaunty, K.D., Dewhirst, F.E., Deych, E., Ding, Y., Dooling, D.J., Dugan, S.P., Michael Dunne, W., Scott Durkin, A., Edgar, R.C., Erlich, R.L., Farmer, C.N., Farrell, R.M., Faust, K., Feldgarden, M., Felix, V.M., Fisher, S., Fodor, A.A., Forney, L.J., Foster, L., Di Francesco, V., Friedman, J., Friedrich, D.C., Fronick, C.C., Fulton, L.L., Gao, H., Garcia, N., Giannoukos, G., Giblin, C., Giovanni, M.Y., Goldberg, J.M., Goll, J., Gonzalez, A., Griggs, A., Gujja, S., Kinder Haake, S., Haas, B.J., Hamilton, H.A., Harris, E.L., Hepburn, T.A., Herter, B., Hoffmann, D.E., Holder, M.E., Howarth, C., Huang, K.H., Huse, S.M., Izard, J., Jansson, J.K.,

Jiang, H., Jordan, C., Joshi, V., Katancik, J.A., Keitel, W.A., Kelley, S.T., Kells, C., King, N.B., Knights, D., Kong, H.H., Koren, O., Koren, S., Kota, K.C., Kovar, C.L., Kyrpides, N.C., La Rosa, P.S., Lee, S.L., Lemon, K.P., Lennon, N., Lewis, C.M., Lewis, L., Ley, R.E., Li, K., Liolios, K., Liu, B., Liu, Y., Lo, C.C., Lozupone, C.A., Dwayne Lunsford, R., Madden, T., Mahurkar, A.A., Mannon, P.J., Mardis, E.R., Markowitz, V.M., Mavromatis, K., McCorrison, J.M., McDonald, D., McEwen, J., McGuire, A.L., McInnes, P., Mehta, T., Mihindukulasuriya, K.A., Miller, J.R., Minx, P.J., Newsham, I., Nusbaum, C., Oglaughlin, M., Orvis, J., Pagani, I., Palaniappan, K., Patel, S.M., Pearson, M., Peterson, J., Podar, M., Pohl, C., Pollard, K.S., Pop, M., Priest, M.E., Proctor, L.M., Qin, X., Raes, J., Ravel, J., Reid, J.G., Rho, M., Rhodes, R., Riehle, K.P., Rivera, M.C., Rodriguez-Mueller, B., Rogers, Y.H., Ross, M.C., Russ, C., Sanka, R.K., Sankar, P., Fah Sathirapongsasuti, J., Schloss, J.A., Schloss, P.D., Schmidt, T.M., Scholz, M., Schriml, L., Schubert, A.M., Segata, N., Segre, J.A., Shannon, W.D., Sharp, R.R., Sharpton, T.J., Shenoy, N., Sheth, N.U., Simone, G.A., Singh, I., Smillie, C.S., Sobel, J.D., Sommer, D.D., Spicer, P., Sutton, G.G., Sykes, S.M., Tabbaa, D.G., Thiagarajan, M., Tomlinson, C.M., Torralba, M., Treangen, T.J., Truty, R.M., Vishnivetskaya, T.A., Walker, J., Wang, L., Wang, Z., Ward, D. V., Warren, W., Watson, M.A., Wellington, C., Wetterstrand, K.A., White, J.R., Wilczek-Boney, K., Wu, Y., Wylie, K.M., Wylie, T., Yandava, C., Ye, L., Ye, Y., Yooseph, S., Youmans, B.P., Zhang, L., Zhou, Y., Zhu, Y., Zoloth, L., Zucker, J.D., Birren, B.W., Gibbs, R.A., Highlander, S.K., Methé, B.A., Nelson, K.E., Petrosino, J.F., Weinstock, G.M., Wilson, R.K., White, O., 2012. Structure, function and diversity of the healthy human microbiome. Nature 486, 207–214. https://doi.org/10.1038/nature11234

Hwang, C., Ling, F., Andersen, G.L., LeChevallier, M.W., Liu, W.-T., 2012. Evaluation of Methods for the Extraction of DNA from Drinking Water Distribution System Biofilms. Microbes and Environments 27, 9–18. https://doi.org/10.1264/jsme2.ME11132

Ijpelaar, G.F., Van Der Veer, A.J., Medema, G.J., Kruithof, J.C., 2005. By-product formation during ultraviolet disinfection of a pretreated surface water. Journal of Environmental Engineering and Science 4. https://doi.org/10.1139/s04-066

Izano, E.A., Amarante, M.A., Kher, W.B., Kaplan, J.B., 2008. Differential roles of poly-N-acetylglucosamine surface polysaccharide and extracellular DNA in Staphylococcus aureus and Staphylococcus epidermidis biofilms. Applied and Environmental Microbiology 74, 470–476. https://doi.org/10.1128/AEM.02073-07

Jefferson, K.K., 2004. What drives bacteria to produce a biofilm? FEMS Microbiology Letters 236, 163–173. https://doi.org/10.1016/j.femsle.2004.06.005

Jin, M., Liu, L., Wang, D. ning, Yang, D., Liu, W. li, Yin, J., Yang, Z. wei, Wang, H. ran, Qiu, Z. gang, Shen, Z. qiang, Shi, D. yang, Li, H. bei, Guo, J. hua, Li, J. wen, 2020. Chlorine disinfection promotes the exchange of antibiotic resistance genes across bacterial genera by natural transformation. ISME Journal 14, 1847–1856. https://doi.org/10.1038/s41396-020-0656-9

Johnson, J.S., Spakowicz, D.J., Hong, B.Y., Petersen, L.M., Demkowicz, P., Chen, L., Leopold, S.R., Hanson, B.M., Agresta, H.O., Gerstein, M., Sodergren, E., Weinstock, G.M., 2019. Evaluation of 16S rRNA gene sequencing for species and strain-level microbiome analysis. Nature Communications 10. https://doi.org/10.1038/s41467-019-13036-1

Jungfer, C., Schwartz, T., Obst, U., 2007. UV-induced dark repair mechanisms in bacteria associated with drinking water. Water Research 41, 188–196. https://doi.org/10.1016/j.watres.2006.09.001

Karst, S.M., Dueholm, M.S., McIlroy, S.J., Kirkegaard, R.H., Nielsen, P.H., Albertsen, M., 2018. Retrieval of a million high-quality, full-length microbial 16S and 18S rRNA gene sequences without primer bias. Nature Biotechnology 36, 190–195. https://doi.org/10.1038/nbt.4045

Kaszubinski, S.F., Pechal, J.L., Schmidt, C.J., Jordan, H.R., Benbow, M.E., Meek, M.H., 2020. Evaluating Bioinformatic Pipeline Performance for Forensic Microbiome Analysis*,†,‡. Journal of Forensic Sciences 65, 513–525. https://doi.org/10.1111/1556-4029.14213

Kauser, I., Ciesielski, M., Poretsky, R.S., 2019. Ultraviolet disinfection impacts the microbial community composition and function of treated wastewater effluent and the receiving urban river. PeerJ 7, e7455. https://doi.org/10.7717/peerj.7455

Kelly, J.J., Minalt, N., Culotti, A., Pryor, M., Packman, A., 2014. Temporal variations in the abundance and composition of biofilm communities colonizing drinking water distribution pipes. PLoS ONE 9. https://doi.org/10.1371/journal.pone.0098542

Kim, B.R., Anderson, J.E., Mueller, S.A., Gaines, W.A., Kendall, A.M., 2002. Literature review - Efficacy of various disinfectants against Legionella in water systems. Water Research 36, 4433–4444. https://doi.org/10.1016/S0043-1354(02)00188-4

Kim, D., Hofstaedter, C.E., Zhao, C., Mattei, L., Tanes, C., Clarke, E., Lauder, A., Sherrill-Mix, S., Chehoud, C., Kelsen, J., Conrad, M., Collman, R.G., Baldassano, R., Bushman, F.D., Bittinger, K., 2017. Optimizing methods and dodging pitfalls in microbiome research. Microbiome 5, 1–14. https://doi.org/10.1186/s40168-017-0267-5

Kim, D.K., Kim, S.J., Kang, D.H., 2017. Bactericidal effect of 266 to 279 nm wavelength UVC-LEDs for inactivation of Gram positive and Gram negative foodborne pathogenic bacteria and yeasts. Food Research International 97, 280–287. https://doi.org/10.1016/j.foodres.2017.04.009

Kip, N., van Veen, J.A., 2015. The dual role of microbes in corrosion. The ISME Journal 9, 542–551. https://doi.org/10.1038/ismej.2014.169

Klindworth, A., Pruesse, E., Schweer, T., Peplies, J., Quast, C., Horn, M., Glockner, F.O., 2013. Evaluation of general 16S ribosomal RNA gene PCR primers for classical and next-generation sequencing-based diversity studies. Nucleic Acids Research 41, e1–e1. https://doi.org/10.1093/nar/gks808

Knights, D., Kuczynski, J., Charlson, E.S., Zaneveld, J., Mozer, M.C., Collman, R.G.,

Bushman, F.D., Knight, R., Kelley, S.T., 2011. Bayesian community-wide culture-independent microbial source tracking. Nature Methods 8, 761–765. https://doi.org/10.1038/nmeth.1650

Kobayashi, T., Mito, T., Watanabe, N., Suzuki, T., Shiraishi, A., Ohashi, Y., 2012. Use of 5-cyano-2,3-ditolyl-tetrazolium chloride staining as an indicator of biocidal activity in a rapid assay for anti-Acanthamoeba agents. Journal of Clinical Microbiology 50, 1606–1612. https://doi.org/10.1128/JCM.06461-11

Koch, C., Fetzer, I., Harms, H., Müller, S., 2013a. CHIC-an automated approach for the detection of dynamic variations in complex microbial communities. Cytometry Part A 83 A, 561–567. https://doi.org/10.1002/cyto.a.22286

Koch, C., Fetzer, I., Schmidt, T., Harms, H., Müller, S., 2013b. Monitoring functions in managed microbial systems by cytometric bar coding. Environmental Science and Technology 47, 1753–1760. https://doi.org/10.1021/es3041048

Koch, C., Harnisch, F., Schröder, U., Müller, S., 2014. Cytometric fingerprints: Evaluation of new tools for analyzing microbial community dynamics. Frontiers in Microbiology 5, 1–12. https://doi.org/10.3389/fmicb.2014.00273

Koch, H., Lücker, S., Albertsen, M., Kitzinger, K., Herbold, C., Spieck, E., Nielsen, P.H., Wagner, M., Daims, H., 2015. Expanded metabolic versatility of ubiquitous nitrite-oxidizing bacteria from the genus Nitrospira. Proceedings of the National Academy of Sciences of the United States of America 112, 11371–11376. https://doi.org/10.1073/pnas.1506533112

Koch, R., 1881. Methods for the study of pathogenic organisms 1881. Mittheilungen aus dem Kaiserlichen Gesundheitsamte 1, 1–48.

Köhler, S.J., Buffam, I., Seibert, J., Bishop, K.H., Laudon, H., 2009. Dynamics of stream water TOC concentrations in a boreal headwater catchment: Controlling factors and implications for climate scenarios. Journal of Hydrology 373, 44–56. https://doi.org/10.1016/j.jhydrol.2009.04.012

Koutchma, T., 2008. UV light for processing foods. Ozone: Science and Engineering 30, 93–98. https://doi.org/10.1080/01919510701816346

Kowalski, W., 2009. Ultraviolet germicidal irradiation handbook: UVGI for air and surface disinfection, Ultraviolet Germicidal Irradiation Handbook: UVGI for Air and Surface Disinfection. https://doi.org/10.1007/978-3-642-01999-9

Krehenwinkel, H., Pomerantz, A., Prost, S., 2019. Genetic biomonitoring and biodiversity assessment using portable sequencing technologies: Current uses and future directions. Genes 10. https://doi.org/10.3390/genes10110858

Lahr, D.J.G., Katz, L.A., 2009. Reducing the impact of PCR-mediated recombination in molecular evolution and environmental studies using a new-generation high-fidelity DNA polymerase. BioTechniques 47, 857–866. https://doi.org/10.2144/000113219

Langille, M.G.I., Zaneveld, J., Caporaso, J.G., McDonald, D., Knights, D., Reyes, J.A.,

Clemente, J.C., Burkepile, D.E., Vega Thurber, R.L., Knight, R., Beiko, R.G., Huttenhower, C., 2013. Predictive functional profiling of microbial communities using 16S rRNA marker gene sequences. Nature Biotechnology 31, 814–821. https://doi.org/10.1038/nbt.2676

Långmark, J., Storey, M. V., Ashbolt, N.J., Stenström, T.A., 2005. Accumulation and fate of microorganisms and microspheres in biofilms formed in a pilot-scale water distribution system. Applied and Environmental Microbiology 71, 706–712. https://doi.org/10.1128/AEM.71.2.706-712.2005

Laroche, O., Symonds, J.E., Smith, K.F., Banks, J.C., Mae, H., Bowman, J.P., Pochon, X., 2018. Understanding bacterial communities for informed biosecurity and improved larval survival in Pacific oysters. Aquaculture 497, 164–173. https://doi.org/10.1016/j.aquaculture.2018.07.052

Lautenschlager, K., Boon, N., Wang, Y., Egli, T., Hammes, F., 2010. Overnight stagnation of drinking water in household taps induces microbial growth and changes in community composition. Water Research 44, 4868–4877. https://doi.org/10.1016/j.watres.2010.07.032

Lautenschlager, K., Hwang, C., Ling, F., Liu, W.T., Boon, N., Köster, O., Egli, T., Hammes, F., 2014. Abundance and composition of indigenous bacterial communities in a multi-step biofiltration-based drinking water treatment plant. Water Research 62, 40–52. https://doi.org/10.1016/j.watres.2014.05.035

Lautenschlager, K., Hwang, C., Liu, W.-T., Boon, N., Köster, O., Vrouwenvelder, H., Egli, T., Hammes, F., 2013. A microbiology-based multi-parametric approach towards assessing biological stability in drinking water distribution networks. Water Research 47, 3015–3025. https://doi.org/10.1016/J.WATRES.2013.03.002

Lebaron, P., Parthuisot, N., Catala, P., 1998. Comparison of Blue Nucleic Acid Dyes for Flow Cytometric Enumeration of Bacteria in Aquatic Systems. Applied and Environmental Microbiology 64, 1725–1730. https://doi.org/10.1128/aem.64.5.1725-1730.1998

Lebaron, P., Servais, P., Agogué, H., Courties, C., Joux, F., 2001. Does the High Nucleic Acid Content of Individual Bacterial Cells Allow Us to Discriminate between Active Cells and Inactive Cells in Aquatic Systems? Applied and Environmental Microbiology 67, 1775–1782. https://doi.org/10.1128/AEM.67.4.1775-1782.2001

Lee, C.O., Boe-Hansen, R., Musovic, S., Smets, B., Albrechtsen, H.J., Binning, P., 2014. Effects of dynamic operating conditions on nitrification in biological rapid sand filters for drinking water treatment. Water Research 64, 226–236. https://doi.org/10.1016/j.watres.2014.07.001

Lehtola, M.J., Laxander, M., Miettinen, I.T., Hirvonen, A., Vartiainen, T., Martikainen, P.J., 2006. The effects of changing water flow velocity on the formation of biofilms and water quality in pilot distribution system consisting of copper or polyethylene pipes. Water Research 40, 2151–2160. https://doi.org/10.1016/j.watres.2006.04.010

Lehtola, M.J., Miettinen, I.T., Vartiainen, T., Rantakokko, P., Hirvonen, A., Martikainen, P.J., 2003. Impact of UV disinfection on microbially available phosphorus, organic carbon, and microbial growth in drinking water. Water Research 37, 1064–1070. https://doi.org/10.1016/S0043-1354(02)00462-1

Leuker, G., 1999. Description and application of biodosimetry - A testing procedure for UV systems. Journal of Water Supply: Research and Technology - AQUA 48, 154–160. https://doi.org/10.1046/j.1365-2087.1999.00141.x

Ley, C., Proctor, C., Singh, G., Ra, K., Noh, Y., Odimayomi, T., Salehi, M., Julien, R., Mitchell, J., Nejadhashemi, A.P., Whelton, A., Aw, T.G., 2020. Drinking water microbiology in a water-efficient building: Stagnation, seasonality, and physiochemical effects on opportunistic pathogen and total bacteria proliferation. Environmental Science: Water Research & Technology. https://doi.org/10.1039/d0ew00334d

Li, D., Li, Z., Yu, J., Cao, N., Liu, R., Yang, M., 2010. Characterization of bacterial community structure in a drinking water distribution system during an occurrence of red water. Applied and Environmental Microbiology 76, 7171–7180. https://doi.org/10.1128/AEM.00832-10

Li, G.Q., Wang, W.L., Huo, Z.Y., Lu, Y., Hu, H.Y., 2017. Comparison of UV-LED and low pressure UV for water disinfection: Photoreactivation and dark repair of Escherichia coli. Water Research 126, 134–143. https://doi.org/10.1016/j.watres.2017.09.030

Li, R.A., McDonald, J.A., Sathasivan, A., Khan, S.J., 2019. Disinfectant residual stability leading to disinfectant decay and by-product formation in drinking water distribution systems: A systematic review. Water Research 153, 335–348. https://doi.org/10.1016/j.watres.2019.01.020

Lin, W., Yu, Z., Zhang, H., Thompson, I.P., 2014. Diversity and dynamics of microbial communities at each step of treatment plant for potable water generation. Water Research 52, 218–230. https://doi.org/10.1016/j.watres.2013.10.071

Linden, K.G., Shin, G.A., Faubert, G., Cairns, W., Sobsey, M.D., 2002. UV disinfection of Giardia lamblia cysts in water. Environmental Science and Technology 36, 2519–2522. https://doi.org/10.1021/es0113403

Ling, F., Hwang, C., LeChevallier, M.W., Andersen, G.L., Liu, W.-T., 2016. Core-satellite populations and seasonality of water meter biofilms in a metropolitan drinking water distribution system. The ISME Journal 10, 582–595. https://doi.org/10.1038/ismej.2015.136

Ling, F., Whitaker, R., LeChevallier, M.W., Liu, W.-T., 2018. Drinking water microbiome assembly induced by water stagnation. The ISME Journal 2018 1. https://doi.org/10.1038/s41396-018-0101-5

Liu, G., Bakker, G.L., Li, S., Vreeburg, J.H.G., Verberk, J.Q.J.C., Medema, G.J., Liu, ‖ W T, Van Dijk, J.C., 2014. Pyrosequencing Reveals Bacterial Communities in Unchlorinated Drinking Water Distribution System: An Integral Study of Bulk

Water, Suspended Solids, Loose Deposits, and Pipe Wall Biofilm. https://doi.org/10.1021/es5009467

Liu, G., Zhang, Y., Knibbe, W.J., Feng, C., Liu, W., Medema, G., van der Meer, W., 2017. Potential impacts of changing supply-water quality on drinking water distribution: A review. Water Research 116, 135–148. https://doi.org/10.1016/j.watres.2017.03.031

Liu, G., Zhang, Y., Liu, X., Hammes, F., Liu, W., Medema, G., Wessels, P., 2020. 360-Degree Distribution of Bio fi lm Quantity and Community in an Operational Unchlorinated Drinking Water Distribution Pipe. https://doi.org/10.1021/acs.est.9b06603

Liu, G., Zhang, Y., van der Mark, E., Magic-Knezev, A., Pinto, A., van den Bogert, B., Liu, W., van der Meer, W., Medema, G., 2018. Assessing the origin of bacteria in tap water and distribution system in an unchlorinated drinking water system by SourceTracker using microbial community fingerprints. Water Research 138, 86–96. https://doi.org/10.1016/j.watres.2018.03.043

Liu, J., Zhao, R., Zhang, J., Zhang, G., Yu, K., Li, X., Li, B., 2018. Occurrence and fate of ultramicrobacteria in a full-scale drinking water treatment plant. Frontiers in Microbiology 9. https://doi.org/10.3389/fmicb.2018.02922

Liu, J., Zhao, Z., Chen, C., Cao, P., Wang, Y., 2017. In-situ features of LNA and HNA bacteria in branch ends of drinking water distribution systems. Journal of Water Supply: Research and Technology - AQUA 66, 300–307. https://doi.org/10.2166/aqua.2017.108

Liu, R., Zhu, J., Yu, Z., Joshi, D.R., Zhang, H., Lin, W., Yang, M., 2014. Molecular analysis of long-term biofilm formation on PVC and cast iron surfaces in drinking water distribution system. Journal of Environmental Sciences (China) 26, 865–874. https://doi.org/10.1016/S1001-0742(13)60481-7

Livsmedelsverket, 2017. Mikrobiologiska risker i ytråvatten.

Livsmedelsverket, 2001. SLVFS 2001:30 - Statens livsmedelsverks föreskrifter om dricksvatten.

Longnecker, K., Sherr, B.F., Sherr, E.B., 2005. Activity and phylogenetic diversity of bacterial cells with high and low nucleic acid content and electron transport system activity in an upwelling ecosystem. Applied and Environmental Microbiology 71, 7737–7749. https://doi.org/10.1128/AEM.71.12.7737-7749.2005

Love, M.I., Huber, W., Anders, S., 2014. Moderated estimation of fold change and dispersion for RNA-seq data with DESeq2. Genome Biology 15, 550. https://doi.org/10.1186/s13059-014-0550-8

Lührig, K., 2016. Bacterial communities in drinking water biofilms. Dissertation.

Lührig, K., Canbäck, B., Paul, C.J., Johansson, T., Persson, K.M., Rådström, P., 2015. Bacterial Community Analysis of Drinking Water Biofilms in Southern Sweden. Microbes and environments 30, 99–107. https://doi.org/10.1264/jsme2.ME14123

Lukumbuzya, M., Kristensen, J.M., Kitzinger, K., Pommerening-Röser, A., Nielsen, P.H., Wagner, M., Daims, H., Pjevac, P., 2020. A refined set of rRNA-targeted oligonucleotide probes for in situ detection and quantification of ammonia-oxidizing bacteria. Water Research 186. https://doi.org/https://doi.org/10.1016/j.watres.2020.116372

Ma, B., LaPara, T.M., Hozalski, R.M., 2020. Microbiome of Drinking Water Biofilters is Influenced by Environmental Factors and Engineering Decisions but has Little Influence on the Microbiome of the Filtrate. Environmental science & technology 54, 11526–11535. https://doi.org/10.1021/acs.est.0c01730

Malayeri, A.H., Mohseni, M., Cairns, B., Bolton, J.R., 2016. Fluence (UV Dose) Required to Achieve Incremental Log Inactivation of Bacteria, Protozoa, Viruses and Algae. IUVA News 18, 4–6.

Malorny, B., Tassios, P.T., Rådström, P., Cook, N., Wagner, M., Hoorfar, J., 2003. Standardization of diagnostic PCR for the detection of foodborne pathogens. International Journal of Food Microbiology 83, 39–48. https://doi.org/10.1016/S0168-1605(02)00322-7

Martineau, C., Mauffrey, F., Villemur, R., 2015. Comparative analysis of denitrifying activities of Hyphomicrobium nitrativorans, Hyphomicrobium denitrificans, and Hyphomicrobium zavarzinii. Applied and Environmental Microbiology 81, 5003–5014. https://doi.org/10.1128/AEM.00848-15

Martineau, C., Villeneuve, C., Mauffrey, F., Villemur, R., 2014. Complete genome sequence of Hyphomicrobium nitrativorans strain NL23, a denitrifying bacterium isolated from biofilm of a methanol-fed denitrification system treating seawater at the Montreal Biodome. Genome Announcements 2, 2–3. https://doi.org/10.1128/genomeA.e01165-13

Martiny, A.C., Jørgensen, T.M., Albrechtsen, H.J., Arvin, E., Molin, S., 2003. Long-Term Succession of Structure and Diversity of a Biofilm Formed in a Model Drinking Water Distribution System. Applied and Environmental Microbiology 69, 6899–6907. https://doi.org/10.1128/AEM.69.11.6899-6907.2003

Mason, J.M., Setlow, P., 1986. Essential Role of Small, Acid-Soluble Spore Proteins in Resistance of Bacillus subtilis Spores to UV Light.

McIlroy, S.J., Saunders, A.M., Albertsen, M., Nierychlo, M., McIlroy, B., Hansen, A.A., Karst, S.M., Nielsen, J.L., Nielsen, P.H., 2015. MiDAS: The field guide to the microbes of activated sludge. Database 2015, 1–8. https://doi.org/10.1093/database/bav062

Mckinney, C.W., Pruden, A., 2012. Ultraviolet Disinfection of Antibiotic Resistant Bacteria and Their Antibiotic Resistance Genes in Water and Wastewater. https://doi.org/10.1021/es303652q

McKinney, C.W., Pruden, A., 2012. Ultraviolet Disinfection of Antibiotic Resistant Bacteria and Their Antibiotic Resistance Genes in Water and Wastewater. Environmental Science & Technology 46, 13393–13400.

https://doi.org/10.1021/es303652q

McMurdie, P.J., Holmes, S., 2014. Waste Not, Want Not: Why Rarefying Microbiome Data Is Inadmissible. PLoS Computational Biology 10, e1003531. https://doi.org/10.1371/journal.pcbi.1003531

McMurdie, P.J., Holmes, S., 2013. phyloseq: An R Package for Reproducible Interactive Analysis and Graphics of Microbiome Census Data. PLoS ONE 8, e61217. https://doi.org/10.1371/journal.pone.0061217

Medema, G., Heijnen, L., Elsinga, G., Italiaander, R., Brouwer, A., 2020. Presence of SARS-Coronavirus-2 RNA in Sewage and Correlation with Reported COVID-19 Prevalence in the Early Stage of the Epidemic in The Netherlands. Environmental Science & Technology Letters. https://doi.org/10.1021/acs.estlett.0c00357

Metzker, M.L., 2010. Sequencing technologies the next generation. Nature Reviews Genetics 11, 31–46. https://doi.org/10.1038/nrg2626

Moeller, R., Setlow, P., Reitz, G., Nicholson, W.L., 2009. Roles of Small, Acid-Soluble Spore Proteins and Core Water Content in Survival of Bacillus subtilis Spores Exposed to Environmental Solar UV Radiation. APPLIED AND ENVIRONMENTAL MICROBIOLOGY 75, 5202–5208. https://doi.org/10.1128/AEM.00789-09

Mohamed, S., Syed, B.A., 2013. Commercial prospects for genomic sequencing technologies. Nature Reviews Drug Discovery 12, 341–342. https://doi.org/10.1038/nrd4006

Mooshammer, M., Kitzinger, K., Schintlmeister, A., Ahmerkamp, S., Nielsen, J.L., Nielsen, P.H., Wagner, M., 2020. Flow-through stable isotope probing (Flow-SIP) minimizes cross-feeding in complex microbial communities. ISME Journal. https://doi.org/10.1038/s41396-020-00761-5

Moreno, Y., Botella, S., Alonso, J.L., Ferrús, M.A., Hernández, M., Hernández, J., 2003. Specific detection of Arcobacter and Campylobacter strains in water and sewage by PCR and fluorescent in situ hybridization. Applied and Environmental Microbiology 69, 1181–1186. https://doi.org/10.1128/AEM.69.2.1181-1186.2003

Moss, T., Dimitrov, S.I., Houde, D., 1997. UV-Laser Crosslinking of Proteins to DNA. Methods 11, 225–234. https://doi.org/10.1006/meth.1996.0409

Muirheadi, K.A., Horan, P.K., Poste, G., 1985. Flow Cytometry: Present and future. Bio/Technology 3, 337–356. https://doi.org/10.1038/nbt0485-337

Mullis, K.B., 1990. The unusual origin of the polymerase chain reaction. Scientific American 262, 56–65. https://doi.org/10.1038/scientificamerican0490-56

Mullis, K.B., Faloona, F.A., 1987. Specific Synthesis of DNA in Vitro via a Polymerase-Catalyzed Chain Reaction. Methods in Enzymology 155, 335–350. https://doi.org/10.1016/0076-6879(87)55023-6

Murga, R., Forster, T.S., Brown, E., Pruckler, J.M., Fields, B.S., Donlan, R.M., 2001. Role of biofilms in the survival of Legionella pneumophila in a model potable-water

system. Microbiology 147, 3121–3126. https://doi.org/10.1099/00221287-147-11-3121

Nadkarni, M.A., Martin, E., Jacques, N.A., Hunter, N., 2002. Determination of bacterial load by real-time PCR using a broad-range (universal) probe and primers set. Microbiology 42, 6–257.

Nescerecka, A., Juhna, T., Hammes, F., 2018. Identifying the underlying causes of biological instability in a full-scale drinking water supply system. Water Research 135, 11–21. https://doi.org/10.1016/j.watres.2018.02.006

Neu, L., Bänziger, C., Proctor, C.R., Zhang, Y., Liu, W.-T., Hammes, F., 2018. Ugly ducklings—the dark side of plastic materials in contact with potable water. npj Biofilms and Microbiomes 4, 7. https://doi.org/10.1038/s41522-018-0050-9

Neu, L., Hammes, F., 2020. Feeding the Building Plumbing Microbiome : The Importance of Synthetic Polymeric Materials for Biofilm Formation and Management.

Neu, L., Proctor, C.R., Walser, J.C., Hammes, F., 2019. Small-scale heterogeneity in drinking water biofilms. Frontiers in Microbiology 10, 1–14. https://doi.org/10.3389/fmicb.2019.02446

Nevel, S. Van, Koetzsch, S., Weilenmann, H., Boon, N., Hammes, F., 2013. Routine bacterial analysis with automated fl ow cytometry. Journal of Microbiological Methods 94, 73–76. https://doi.org/10.1016/j.mimet.2013.05.007

Nichols, D., 2007. Cultivation gives context to the microbial ecologist. FEMS Microbiology Ecology 60, 351–357. https://doi.org/10.1111/j.1574-6941.2007.00332.x

Nishimura, Y., Kim, C., Nagata, T., 2005. Vertical and seasonal variations of bacterioplankton subgroups with different nucleic acid contents: Possible regulation by phosphorus. Applied and Environmental Microbiology 71, 5828–5836. https://doi.org/10.1128/AEM.71.10.5828-5836.2005

Nizri, L., Vaizel-Ohayon, D., Ben-Amram, H., Sharaby, Y., Halpern, M., Mamane, H., 2017. Development of a molecular method for testing the effectiveness of UV systems on-site. Water Research 127, 162–171. https://doi.org/10.1016/J.WATRES.2017.10.022

Nocker, A., Cheung, C.-Y., Camper, A.K., 2006. Comparison of propidium monoazide with ethidium monoazide for differentiation of live vs. dead bacteria by selective removal of DNA from dead cells. https://doi.org/10.1016/j.mimet.2006.04.015

Nocker, A., Shah, M., Dannenmann, B., Schulze-Osthoff, K., Wingender, J., Probst, A.J., 2018. Assessment of UV-C-induced water disinfection by differential PCR-based quantification of bacterial DNA damage. Journal of Microbiological Methods 149, 89–95. https://doi.org/10.1016/J.MIMET.2018.03.007

Oguma, K., Katayama, H., Mitani, H., Morita, S., Hirata, T., Ohgaki, S., 2001. Determination of Pyrimidine Dimers in Escherichia coli and Cryptosporidium

parvum during UV Light Inactivation, Photoreactivation, and Dark Repair. APPLIED AND ENVIRONMENTAL MICROBIOLOGY 67, 4630–4637. https://doi.org/10.1128/AEM.67.10.4630-4637.2001

Oh, S., Hammes, F., Liu, W.T., 2018. Metagenomic characterization of biofilter microbial communities in a full-scale drinking water treatment plant. Water Research 128, 278–285. https://doi.org/10.1016/j.watres.2017.10.054

Oksanen, J., Blanchet, F.G., Friendly, M., Kindt, R., Legendre, P., McGlinn, D., Minchin, P.R., O'Hara, R.B., Simpson, G.L., Solymos, P., Stevens, M.H.H., Szoecs, E., Wagner, H., 2019. vegan: Community Ecology Package. R package version 2.5-4.

Ortiz-Estrada, Á.M., Gollas-Galván, T., Martínez-Córdova, L.R., Martínez-Porchas, M., 2019. Predictive functional profiles using metagenomic 16S rRNA data: a novel approach to understanding the microbial ecology of aquaculture systems. Reviews in Aquaculture 11, 234–245. https://doi.org/10.1111/raq.12237

Pallen, M.J., Loman, N.J., Penn, C.W., 2010. High-throughput sequencing and clinical microbiology: Progress, opportunities and challenges. Current Opinion in Microbiology 13, 625–631. https://doi.org/10.1016/j.mib.2010.08.003

Petrova, O.E., Sauer, K., 2016. Escaping the biofilm in more than one way: Desorption, detachment or dispersion. Current Opinion in Microbiology 30, 67–78. https://doi.org/10.1016/j.mib.2016.01.004

Pfannes, K.R., Langenbach, K.M.W., Pilloni, G., Stührmann, T., Euringer, K., Lueders, T., Neu, T.R., Müller, J.A., Kästner, M., Meckenstock, R.U., 2015. Selective elimination of bacterial faecal indicators in the Schmutzdecke of slow sand filtration columns. Applied Microbiology and Biotechnology 99, 10323–10332. https://doi.org/10.1007/s00253-015-6882-9

Pinto, A.J., Marcus, D.N., Zeeshan Ijaz, U., Melina, Q., Santos, B.-D., Dick, G.J., Raskin, L., 2015. Metagenomic Evidence for the Presence of Comammox Nitrospira-Like Bacteria in a Drinking Water System. https://doi.org/10.1128/mSphere.00054-15

Pinto, A.J., Schroeder, J., Lunn, M., Sloan, W., Raskin, L., 2014. Spatial-temporal survey and occupancy-abundance modeling to predict bacterial community dynamics in the drinking water microbiomez. mBio 5. https://doi.org/10.1128/mBio.01135-14

Pinto, A.J., Xi, C., Raskin, L., 2012. Bacterial community structure in the drinking water microbiome is governed by filtration processes. Environmental Science and Technology 46, 8851–8859. https://doi.org/10.1021/es302042t

Pjevac, P., Schauberger, C., Poghosyan, L., Herbold, C.W., van Kessel, M.A.H.J., Daebeler, A., Steinberger, M., Jetten, M.S.M., Lücker, S., Wagner, M., Daims, H., 2017. AmoA-targeted polymerase chain reaction primers for the specific detection and quantification of comammox Nitrospira in the environment. Frontiers in Microbiology 8, 1–11. https://doi.org/10.3389/fmicb.2017.01508

Pollock, J., Glendinning, L., Wisedchanwet, T., Watson, M., 2018. The Madness of

Microbiome: Attempting To Find Consensus "Best Practice" for 16S Microbiome Studies. https://doi.org/10.1128/AEM.02627-17

Potgieter, S., Pinto, A., Sigudu, M., Ncube, E., Venter, S., 2018. Long-term spatial and temporal microbial community dynamics in a large-scale drinking water distribution system with multiple disinfectant regimes. Water Research 139, 406–419. https://doi.org/10.1016/j.watres.2018.03.077

Potgieter, S.C., Dai, Z., Venter, S.N., Sigudu, M., Pinto, A.J., 2020. Microbial Nitrogen Metabolism in Chloraminated Drinking Water Reservoirs. mSphere 5. https://doi.org/10.1128/mSphere.00274-20

Prest, E.I., El-Chakhtoura, J., Hammes, F., Saikaly, P.E., van Loosdrecht, M.C.M., Vrouwenvelder, J.S., 2014. Combining flow cytometry and 16S rRNA gene pyrosequencing: A promising approach for drinking water monitoring and characterization. Water Research 63, 179–189. https://doi.org/10.1016/j.watres.2014.06.020

Prest, E.I., Hammes, F., Kötzsch, S., van Loosdrecht, M.C.M., Vrouwenvelder, J.S., 2013. Monitoring microbiological changes in drinking water systems using a fast and reproducible flow cytometric method. Water Research 47, 7131–7142. https://doi.org/10.1016/j.watres.2013.07.051

Prest, E.I., Hammes, F., van Loosdrecht, M.C.M., Vrouwenvelder, J.S., 2016a. Biological stability of drinking water: Controlling factors, methods, and challenges. Frontiers in Microbiology. https://doi.org/10.3389/fmicb.2016.00045

Prest, E.I., Weissbrodt, D.G., Hammes, F., Van Loosdrecht, M.C.M., Vrouwenvelder, J.S., 2016b. Long-term bacterial dynamics in a full-scale drinking water distribution system. PLoS ONE 11, 1–20. https://doi.org/10.1371/journal.pone.0164445

Prévost, M., Rompré, A., Coallier, J., Servais, P., Laurent, P., Clément, B., Lafrance, P., 1998. Suspended bacterial biomass and activity in full-scale drinking water distribution systems: Impact of water treatment. Water Research 32, 1393–1406. https://doi.org/10.1016/S0043-1354(97)00388-6

Price, M.N., Dehal, P.S., Arkin, A.P., 2009. Fasttree: Computing large minimum evolution trees with profiles instead of a distance matrix. Molecular Biology and Evolution 26, 1641–1650. https://doi.org/10.1093/molbev/msp077

Proctor, C.R., Besmer, M.D., Langenegger, T., Beck, K., Walser, J.-C., Ackermann, M., Bürgmann, H., Hammes, F., 2018. Phylogenetic clustering of small low nucleic acid-content bacteria across diverse freshwater ecosystems. The ISME Journal. https://doi.org/10.1038/s41396-018-0070-8

Proctor, C.R., Gächter, M., Kötzsch, S., Rölli, F., Sigrist, R., Walser, J.C., Hammes, F., 2016. Biofilms in shower hoses-choice of pipe material influences bacterial growth and communities. Environmental Science: Water Research and Technology 2, 670–682. https://doi.org/10.1039/c6ew00016a

Proctor, C.R., Hammes, F., 2015a. Drinking water microbiology — from measurement to management. Current Opinion in Biotechnology 33, 87–94.

https://doi.org/10.1016/J.COPBIO.2014.12.014

Proctor, C.R., Hammes, F., 2015b. Drinking water microbiology — from measurement to management. Current Opinion in Biotechnology 33, 87–94. https://doi.org/10.1016/J.COPBIO.2014.12.014

Prodan, A., Tremaroli, V., Brolin, H., Zwinderman, A.H., Nieuwdorp, M., Levin, E., 2020. Comparing bioinformatic pipelines for microbial 16S rRNA amplicon sequencing. PLoS ONE 15, 1–19. https://doi.org/10.1371/journal.pone.0227434

Props, R., Kerckhof, F.-M., Rubbens, P., De Vrieze, J., Sanabria, E.H., Waegeman, W., Monsieurs, P., Hammes, F., Boon, N., 2016a. Absolute quantification of microbial taxon abundances. The ISME Journal 11, 584–587. https://doi.org/10.1038/ismej.2016.117

Props, R., Monsieurs, P., Mysara, M., Clement, L., Boon, N., 2016b. Measuring the biodiversity of microbial communities by flow cytometry. Methods in Ecology and Evolution 7, 1376–1385. https://doi.org/10.1111/2041-210X.12607

Props, R., Schmidt, M.L., Heyse, J., Vanderploeg, H.A., Boon, N., Denef, V.J., 2018. Flow cytometric monitoring of bacterioplankton phenotypic diversity predicts high population-specific feeding rates by invasive dreissenid mussels. Environmental Microbiology 20, 521–534. https://doi.org/10.1111/1462-2920.13953

Prosser, J.I., 2010. Replicate or lie. Environmental Microbiology 12, 1806–1810. https://doi.org/10.1111/j.1462-2920.2010.02201.x

Quast, C., Pruesse, E., Yilmaz, P., Gerken, J., Schweer, T., Yarza, P., Peplies, J., Glöckner, F.O., 2013. The SILVA ribosomal RNA gene database project: Improved data processing and web-based tools. Nucleic Acids Research 41, 590–596. https://doi.org/10.1093/nar/gks1219

Quinn, T.P., Richardson, M.F., Lovell, D., Crowley, T.M., 2017. Propr: An R-package for Identifying Proportionally Abundant Features Using Compositional Data Analysis. Scientific Reports 7. https://doi.org/10.1038/s41598-017-16520-0

R Core Team, 2020. R: A language and environment for statistical computing. R Foundation for Statistical Computing.

Ramseier, M.K., von Gunten, U., Freihofer, P., Hammes, F., 2011. Kinetics of membrane damage to high (HNA) and low (LNA) nucleic acid bacterial clusters in drinking water by ozone, chlorine, chlorine dioxide, monochloramine, ferrate(VI), and permanganate. Water Research 45, 1490–1500. https://doi.org/10.1016/j.watres.2010.11.016

Ravanat, J.-L., Douki, T., Cadet, J., 2001. Direct and indirect effects of UV radiation on DNA and its components. Journal of Photochemistry and Photobiology B: Biology 63, 88–102. https://doi.org/10.1016/S1011-1344(01)00206-8

Reasoner, D.J., 1990. Monitoring Heterotrophic Bacteria in Potable Water. In: McFeters G.A. (eds) Drinking Water Microbiology. Brock/Springer Series in Contemporary Bioscience. Springer, New York, NY. https://doi.org/https://doi.org/10.1007/978-

1-4612-4464-6_22

Reckhow, D.A., Linden, K.G., Kim, J., Shemer, H., Makdissy, G., 2010. Effect of UV treatment on DBP formation. Journal - American Water Works Association 102, 100–113. https://doi.org/10.1002/j.1551-8833.2010.tb10134.x

Reed, N.G., 2010. The history of ultraviolet germicidal irradiation for air disinfection. Public Health Reports 125, 15–27. https://doi.org/10.1177/003335491012500105

Regan, J.M., Harrington, G.W., Baribeau, H., Leon, R. De, Noguera, D.R., 2003. Diversity of nitrifying bacteria in full-scale chloraminated distribution systems. Water Research 37, 197–205. https://doi.org/10.1016/S0043-1354(02)00237-3

Ren, H., Wang, W., Liu, Y., Liu, S., Lou, L., Cheng, D., He, X., Zhou, X., Qiu, S., Fu, L., Liu, J., Hu, B., 2015. Pyrosequencing analysis of bacterial communities in biofilms from different pipe materials in a city drinking water distribution system of East China. Applied Microbiology and Biotechnology 99, 10713–10724. https://doi.org/10.1007/s00253-015-6885-6

Renaud, G., Stenzel, U., Maricic, T., Wiebe, V., Kelso, J., 2015. deML: robust demultiplexing of Illumina sequences using a likelihood-based approach. Bioinformatics 31, 770–772. https://doi.org/10.1093/bioinformatics/btu719

Ricca, H., Aravinthan, V., Mahinthakumar, G., 2019. Modeling chloramine decay in full-scale drinking water supply systems. Water Environment Research 91, 441–454. https://doi.org/10.1002/wer.1046

Riesenman, P.J., Nicholson, W.L., 2000. Role of the Spore Coat Layers in Bacillus subtilis Spore Resistance to Hydrogen Peroxide, Artificial UV-C, UV-B, and Solar UV Radiation, APPLIED AND ENVIRONMENTAL MICROBIOLOGY.

Rittmann, B.E., Snoeyink, V.L., 1984. Achieving biologically stable drinking water. Journal / American Water Works Association 76, 106–114. https://doi.org/10.1002/j.1551-8833.1984.tb05427.x

Rockey, N., Young, S., Kohn, T., Pecson, B., Wobus, C.E., Raskin, L., Wigginton, K.R., 2020. UV Disinfection of Human Norovirus: Evaluating Infectivity Using a Genome-Wide PCR-Based Approach. https://doi.org/10.1021/acs.est.9b05747

Rodrigues, A., Brito, A., Janknecht, P., Proena, M.F., Nogueira, R., 2009. Quantification of humic acids in surface water: Effects of divalent cations, pH, and filtration]. Journal of Environmental Monitoring 11, 377–382. https://doi.org/10.1039/b811942b

Roeselers, G., Coolen, J., van der Wielen, P.W.J.J., Jaspers, M.C., Atsma, A., de Graaf, B., Schuren, F., 2015. Microbial biogeography of drinking water: Patterns in phylogenetic diversity across space and time. Environmental Microbiology 17, 2505–2514. https://doi.org/10.1111/1462-2920.12739

Rogers, W.T., Holyst, H.A., 2009. FlowFP: A Bioconductor Package for Fingerprinting Flow Cytometric Data. Advances in Bioinformatics 2009, 1–11. https://doi.org/10.1155/2009/193947

Rubbens, P., Schmidt, M.L., Props, R., Biddanda, B.A., Boon, N., Waegeman, W., Denef, V.J., 2019. Randomized Lasso Links Microbial Taxa with Aquatic Functional Groups Inferred from Flow Cytometry. mSystems 4, e00093-19. https://doi.org/10.1128/mSystems.00093-19

Salter, S.J., Cox, M.J., Turek, E.M., Calus, S.T., Cookson, W.O., Moffatt, M.F., Turner, P., Parkhill, J., Loman, N.J., Walker, A.W., 2014. Reagent and laboratory contamination can critically impact sequence-based microbiome analyses. BMC Biology 12. https://doi.org/10.1186/s12915-014-0087-z

Sanger, F., Air, G.M., Barrell, B.G., Brownt, N.L., Coulson, A.R., Fiddes, J.C., Iii, C.A.H., Slocombe, P.M., Smith, M., 1977a. Nucleotide sequence of bacteriophage ϕX174 DNA 265, 687–695.

Sanger, F., Nicklen, S., Coulson, A.., 1977b. DNA sequencing with chain-terminating. Proc Natl Acad Sci USA 74, 5463–5467.

Schleich, C., Chan, S., Pullerits, K., Habagil, M., Lindgren, J., Paul, C.J., Keucken, A., Rådström, P., 2020. Biofilmens funktion och korrelation med dricksvattnets kvalitet. Svenskt Vatten Utveckling 2020–2.

Schloss, P.D., 2020. Reintroducing mothur: 10 years later. Applied and Environmental Microbiology 86. https://doi.org/10.1128/AEM.02343-19

Schumann, J., Koch, C., Fetzer, I., Müller, S., 2020. flowCHIC: Analyze flow cytometric data using histogram information. http://www.ufz.de/index.php?en=16773.

Schwake, D.O., Alum, A., Abbaszadegan, M., 2015. Impact of environmental factors on legionella populations in drinking water. Pathogens 4, 269–282. https://doi.org/10.3390/pathogens4020269

Schwartz, T, Hoffmann, S., Obst, U., Schwartz, Thomas, 2003. Formation of natural biofilms during chlorine dioxide and u.v. disinfection in a public drinking water distribution system. Journal of Applied Microbiology 95, 591–601. https://doi.org/10.1046/j.1365-2672.2003.02019.x

Servais, P., Billen, G., Bouillot, P., 1994. Biological Colonization of Granular Activated Carbon Filters in Drinking-Water Treatment. Journal of Environmental Engineering 120, 888–899.

Servais, P., Casamayor, E., Courties, C., Catala, P., Parthuisot, N., Lebaron, P., 2003. Activity and diversity of bacterial cells with high and low nucleic acid content. Aquatic Microbial Ecology 33, 41–51. https://doi.org/10.3354/ame033041

Shakya, M., Quince, C., Campbell, J.H., Yang, Z.K., Schadt, C.W., Podar, M., 2013. Comparative metagenomic and rRNA microbial diversity characterization using archaeal and bacterial synthetic communities. Environmental Microbiology 15, 1882–1899. https://doi.org/10.1111/1462-2920.12086

Shaw, J.P., Malley, J.P., Willoughby, S.A., 2000. Effects of UV irradiation on organic matter. Journal / American Water Works Association 92, 157–167. https://doi.org/10.1002/j.1551-8833.2000.tb08930.x

Sidstedt, M., Jansson, L., Nilsson, E., Noppa, L., Forsman, M., Rådström, P., Hedman, J., 2015. Humic substances cause fluorescence inhibition in real-time polymerase chain reaction. Analytical Biochemistry 487, 30–37. https://doi.org/10.1016/j.ab.2015.07.002

Sidstedt, M., Rådström, P., Hedman, J., 2020. PCR inhibition in qPCR, dPCR and MPS—mechanisms and solutions. Analytical and Bioanalytical Chemistry 412, 2009–2023. https://doi.org/10.1007/s00216-020-02490-2

Sinha, R.P., Häder, D.P., 2002. UV-induced DNA damage and repair: A review. Photochemical and Photobiological Sciences. https://doi.org/10.1039/b201230h

Smith, C.M., Hill, V.R., 2009. Dead-end hollow-fiber ultrafiltration for recovery of diverse microbes from water. Applied and Environmental Microbiology 75, 5284–5289. https://doi.org/10.1128/AEM.00456-09

Smyth, R.P., Schlub, T.E., Grimm, A., Venturi, V., Chopra, A., Mallal, S., Davenport, M.P., Mak, J., 2010. Reducing chimera formation during PCR amplification to ensure accurate genotyping. Gene 469, 45–51. https://doi.org/10.1016/j.gene.2010.08.009

Sommer, R., Lhotsky, M., Haider, T., Cabaj, A., 2000. UV Inactivation, Liquid-Holding Recovery, and Photoreactivation of Escherichia coli O157 and Other Pathogenic Escherichia coli Strains in Water, Journal of Food Protection.

Song, K., Mohseni, M., Taghipour, F., 2016. Application of ultraviolet light-emitting diodes (UV-LEDs) for water disinfection: A review. Water Research 94, 341–349. https://doi.org/10.1016/J.WATRES.2016.03.003

Stahl, D.A., de la Torre, J.R., 2012. Physiology and Diversity of Ammonia-Oxidizing Archaea. Annual Review of Microbiology 66, 83–101. https://doi.org/10.1146/annurev-micro-092611-150128

Staley, J.T., Konopka, A., 1985. Measurements of in situ activities of nonphotosynthetic microorganisms in aquatic and terrestrial habitats. Annual review of microbiology 39, 321–346.

Stein, L.Y., Klotz, M.G., 2016. The nitrogen cycle. Current Biology 26, R94–R98. https://doi.org/10.1016/j.cub.2015.12.021

Steinert, M., Hentschel, U., Hacker, J., 2002. Legionella pneumophila: An aquatic microbe goes astray. FEMS Microbiology Reviews 26, 149–162. https://doi.org/10.1016/S0168-6445(02)00093-1

Stoodley, P., Sauer, K., Davies, D.G., Costerton, J.W., 2002. Biofilms as Complex Differentiated Communities. Annual Review of Microbiology 56, 187–209. https://doi.org/10.1146/annurev.micro.56.012302.160705

Strous, M., Planet, E., Mechanics, T., America, M., Appl, P., Island, A., Islands, A., Init, O.D.P., Rica, C., 1999. Missing lithotroph identified as new planctomycete. Nature 400.

Sulzberger, B., Durisch-Kaiser, E., 2009. Chemical characterization of dissolved organic

matter (DOM): A prerequisite for understanding UV-induced changes of DOM absorption properties and bioavailability. Aquatic Sciences 71, 104–126. https://doi.org/10.1007/s00027-008-8082-5

Süß, J., Volz, S., Obst, U., Schwartz, T., 2009. Application of a molecular biology concept for the detection of DNA damage and repair during UV disinfection. Water Research 43, 3705–3716. https://doi.org/10.1016/j.watres.2009.05.048

Sutton, S., 2010. Microbiology Topics. The Most Probable Number Method and Its Uses in Enumeration, Qualification, and Validation. Journal of Validation Technology.

Suzuki, T., Fujikura, K., Higashiyama, T., Takata, K., 1997. DNA staining for fluorescence and laser confocal microscopy. Journal of Histochemistry and Cytochemistry 45, 49–53. https://doi.org/10.1177/002215549704500107

Svenskt Vatten, 2017. Värt att veta om vatten - Frågor och svar om vårt dricksvatten. Svenskt Vatten 22.

Sze, M.A., Schloss, P.D., 2019. The Impact of DNA Polymerase and Number of Rounds of Amplification in PCR on 16S rRNA Gene Sequence Data. mSphere 4, 1–13. https://doi.org/10.1128/msphere.00163-19

Tamaki, H., 2019. Cultivation renaissance in the post-metagenomics era: Combining the new and old. Microbes and Environments 34, 117–120. https://doi.org/10.1264/jsme2.ME3402rh

Tan, G., Opitz, L., Schlapbach, R., Rehrauer, H., 2019. Long fragments achieve lower base quality in Illumina paired-end sequencing. Scientific Reports 9, 1–7. https://doi.org/10.1038/s41598-019-39076-7

Tanaka, T., Kawasaki, K., Daimon, S., Kitagawa, W., Yamamoto, K., Tamaki, H., Tanaka, M., Nakatsu, C.H., Kamagata, Y., 2014. A hidden pitfall in the preparation of agar media undermines microorganism cultivability. Applied and Environmental Microbiology 80, 7659–7666. https://doi.org/10.1128/AEM.02741-14

Taylor Eighmy, T., Robin Collins, M., Spanos, S.K., Fenstermacher, J., 1992. Microbial populations, activities and carbon metabolism in slow sand filters. Water Research 26, 1319–1328. https://doi.org/10.1016/0043-1354(92)90126-O

Taylor, R.H., Falkinham Iii, J.O., Norton, C.D., Lechevallier, M.W., 2000. Chlorine, Chloramine, Chlorine Dioxide, and Ozone Susceptibility of Mycobacterium avium Downloaded from, APPLIED AND ENVIRONMENTAL MICROBIOLOGY.

Temmerman, R., Vervaeren, H., Noseda, B., Boon, N., Verstraete, W., 2006. Necrotrophic growth of Legionella pneumophila. Applied and Environmental Microbiology 72, 4323–4328. https://doi.org/10.1128/AEM.00070-06

Thamdrup, B., 2012. New Pathways and Processes in the Global Nitrogen Cycle. Annual Review of Ecology, Evolution, and Systematics 43, 407–428. https://doi.org/10.1146/annurev-ecolsys-102710-145048

Thayanukul, P., Kurisu, F., Kasuga, I., Furumai, H., 2013. Evaluation of microbial regrowth potential by assimilable organic carbon in various reclaimed water and distribution systems. Water Research 47, 225–232. https://doi.org/10.1016/j.watres.2012.09.051

Thorsen, J., Brejnrod, A., Mortensen, M., Rasmussen, M.A., Stokholm, J., Al-Soud, W.A., Sørensen, S., Bisgaard, H., Waage, J., 2016. Large-scale benchmarking reveals false discoveries and count transformation sensitivity in 16S rRNA gene amplicon data analysis methods used in microbiome studies. Microbiome 4, 62. https://doi.org/10.1186/s40168-016-0208-8

Thrash, J.C., 2020. Towards culturing the microbe of your choice. Environmental microbiology reports. https://doi.org/10.1111/1758-2229.12898

Tyagi, V.K., Khan, A.A., Kazmi, A.A., Mehrotra, I., Chopra, A.K., 2009. Slow sand filtration of UASB reactor effluent: A promising post treatment technique. Desalination 249, 571–576. https://doi.org/10.1016/j.desal.2008.12.049

Tyson, G.W., Chapman, J., Hugenholtz, P., Allen, E.E., Ram, R.J., Richardson, P.M., Solovyev, V. V., Rubin, E.M., Rokhsar, D.S., Banfield, J.F., 2004. Community structure and metabolism through reconstruction of microbial genomes from the environment. Nature 428, 37–43. https://doi.org/10.1038/nature02340

Urfer, D., Huck, P.M., Booth, S.D.J., Coffey, B.M., 1997. Biological filtration for BOM and particle removal: A critical review: The authors review key parameters and engineering variables influencing biological filtration and identify areas requiring further research. Journal / American Water Works Association 89, 83–98. https://doi.org/10.1002/j.1551-8833.1997.tb08342.x

Urrutia-Cordero, P., Ekvall, M.K., Hansson, L.A., 2016. Local food web management increases resilience and buffers against global change effects on freshwaters. Scientific Reports 6, 1–9. https://doi.org/10.1038/srep29542

USEPA, 2006. Ultraviolet disinfection guidance manual for the final long term 2 enhanced surface water treatment rule. Environmental Protection EPA 815-R-06-007.

Valentine, R.L., Jafvert, C.T., 1992. Reaction Scheme for the Chlorination of Ammoniacal Water. Environmental Science and Technology 26, 577–586. https://doi.org/10.1021/es00027a022

Van der Kooij, D., 1992. Assimilable organic carbon as an indicator of bacterial regrowth. J Am Water Works Assoc 84, 57–65.

Van Der Kooij, D., Visser, A., Hijnen, W.A.M., 1982a. Determining the Concentration of Easily Assimilable Organiccarbon in Drinking Water. J Am Water Works Assoc V 74, 540–545. https://doi.org/10.1002/j.1551-8833.1982.tb05000.x

Van Der Kooij, D., Visser, A., Hijnen, W.A.M., 1982b. Determining the Concentration of Easily Assimilable Organic carbon in Drinking Water. J Am Water Works Assoc V 74, 540–545. https://doi.org/10.1002/j.1551-8833.1982.tb05000.x

Van Der Kooij, D., Vrouwenvelder, J.S., Veenendaal, H.R., 2003. Elucidation and control of biofilm formation processes in water treatment and distribution using the unified biofilm approach. Water Science and Technology 47, 83–90. https://doi.org/10.2166/wst.2003.0287

Van Kessel, M.A.H.J., Speth, D.R., Albertsen, M., Nielsen, P.H., Op Den Camp, H.J.M., Kartal, B., Jetten, M.S.M., Lücker, S., 2015. Complete nitrification by a single microorganism. https://doi.org/10.1038/nature16459

Van Nevel, S., Koetzsch, S., Proctor, C.R., Besmer, M.D., Prest, E.I., Vrouwenvelder, J.S., Knezev, A., Boon, N., Hammes, F., 2017. Flow cytometric bacterial cell counts challenge conventional heterotrophic plate counts for routine microbiological drinking water monitoring. Water Research 113, 191–206. https://doi.org/10.1016/j.watres.2017.01.065

Velten, S., Boller, M., Köster, O., Helbing, J., Weilenmann, H.U., Hammes, F., 2011. Development of biomass in a drinking water granular active carbon (GAC) filter. Water Research 45, 6347–6354. https://doi.org/10.1016/j.watres.2011.09.017

Verma, S., Daverey, A., Sharma, A., 2017. Slow sand filtration for water and wastewater treatment–a review. Environmental Technology Reviews 6, 47–58. https://doi.org/10.1080/21622515.2016.1278278

Vert, M., Doi, Y., Hellwich, K.H., Hess, M., Hodge, P., Kubisa, P., Rinaudo, M., Schué, F., 2012. Terminology for biorelated polymers and applications (IUPAC recommendations 2012). Pure and Applied Chemistry 84, 377–410.

Vignola, M., Werner, D., Hammes, F., King, L.C., Davenport, R.J., 2018. Flow-cytometric quantification of microbial cells on sand from water biofilters. Water Research 143, 66–76. https://doi.org/10.1016/j.watres.2018.05.053

Vikesland, P.J., Ozekin, K., Valentine, R.L., 2001. Monochloramine decay in model and distribution system waters. Water Research 35, 1766–1776. https://doi.org/10.1016/S0043-1354(00)00406-1

Vila-Costa, M., Gasol, J.M., Sharma, S., Moran, M.A., 2012. Community analysis of high- and low-nucleic acid-containing bacteria in NW Mediterranean coastal waters using 16S rDNA pyrosequencing. Environmental Microbiology. https://doi.org/10.1111/j.1462-2920.2012.02720.x

Vital, M., Dignum, M., Magic-Knezev, A., Ross, P., Rietveld, L., Hammes, F., 2012. Flow cytometry and adenosine tri-phosphate analysis: Alternative possibilities to evaluate major bacteriological changes in drinking water treatment and distribution systems. Water Research 46, 4665–4676. https://doi.org/10.1016/j.watres.2012.06.010

Waak, M., Hozalski, R.M., Hallé, C., Lapara, T.M., 2019a. Comparison of the microbiomes of two drinking water distribution systems - With and without residual chloramine disinfection. Microbiome 7. https://doi.org/10.1186/s40168-019-0707-5

Waak, M., Lapara, T.M., Hallé, C., Hozalski, R.M., 2019b. Nontuberculous

Mycobacteria in Two Drinking Water Distribution Systems and the Role of Residual Disinfection. Environmental Science and Technology 53, 8563–8573. https://doi.org/10.1021/acs.est.9b01945

Waak, M., LaPara, T.M., Hallé, C., Hozalski, R.M., 2018. Occurrence of Legionella spp. in Water-Main Biofilms from Two Drinking Water Distribution Systems. Environmental Science and Technology 52, 7630–7639. https://doi.org/10.1021/acs.est.8b01170

Wagner, F.B., Diwan, V., Dechesne, A., Fowler, S.J., Smets, B.F., Albrechtsen, H.J., 2019. Copper-Induced Stimulation of Nitrification in Biological Rapid Sand Filters for Drinking Water Production by Proliferation of Nitrosomonas spp. Environmental Science and Technology 53, 12433–12441. https://doi.org/10.1021/acs.est.9b03885

Wagner, M., Erhart, R., Manz, W., Amann, R., Lemmer, H., Wedi, D., Schleifer, K.H., 1994. Development of an rRNA-targeted oligonucleotide probe specific for the genus Acinetobacter and its application for in situ monitoring in activated sludge. Applied and Environmental Microbiology 60, 792–800. https://doi.org/10.1128/aem.60.3.792-800.1994

Wakelin, S., Page, D., Dillon, P., Pavelic, P., Abell, G.C.J., Gregg, A.L., Brodie, E., DeSantis, T.Z., Goldfarb, K.C., Anderson, G., 2011. Microbial community structure of a slow sand filter schmutzdecke: A phylogenetic snapshot based on rRNA sequence analysis. Water Science and Technology: Water Supply 11, 426–436. https://doi.org/10.2166/ws.2011.063

Wang, H., Bédard, E., Prévost, M., Camper, A.K., Hill, V.R., Pruden, A., 2017. Methodological approaches for monitoring opportunistic pathogens in premise plumbing: A review. Water Research 117, 68–86. https://doi.org/10.1016/j.watres.2017.03.046

Wang, H., Masters, S., Edwards, M.A., Falkinham, J.O., Pruden, A., 2014. Effect of disinfectant, water age, and pipe materials on bacterial and eukaryotic community structure in drinking water biofilm. Environmental Science and Technology 48, 1426–1435. https://doi.org/10.1021/es402636u

Wang, Q., Garrity, G.M., Tiedje, J.M., Cole, J.R., 2007. Naïve Bayesian classifier for rapid assignment of rRNA sequences into the new bacterial taxonomy. Applied and Environmental Microbiology 73, 5261–5267. https://doi.org/10.1128/AEM.00062-07

Wang, Y., Hammes, F., Boon, N., Chami, M., Egli, T., 2009. Isolation and characterization of low nucleic acid (LNA)-content bacteria. The ISME Journal 3, 889–902. https://doi.org/10.1038/ismej.2009.46

Wang, Y., Hammes, F., De Roy, K., Verstraete, W., Boon, N., 2010. Past, present and future applications of flow cytometry in aquatic microbiology. Trends in Biotechnology 28, 416–424. https://doi.org/10.1016/j.tibtech.2010.04.006

Wang, Y., Ma, L., Mao, Y., Jiang, X., Xia, Y., Yu, K., Li, B., Zhang, T., 2017.

Comammox in drinking water systems. Water Research 116, 332–341. https://doi.org/10.1016/j.watres.2017.03.042

Ward, M.H., Jones, R.R., Brender, J.D., de Kok, T.M., Weyer, P.J., Nolan, B.T., Villanueva, C.M., van Breda, S.G., 2018. Drinking water nitrate and human health: An updated review. International Journal of Environmental Research and Public Health 15, 1–31. https://doi.org/10.3390/ijerph15071557

Warnecke, F., Sommaruga, R., Sekar, R., Hofer, J.S., Pernthaler, J., 2005. Abundances, Identity, and Growth State of Actinobacteria in Mountain Lakes of Different UV Transparency. Applied and Environmental Microbiology 71, 5551–5559. https://doi.org/10.1128/AEM.71.9.5551-5559.2005

Webster, T.M., Fierer, N., 2019. Microbial dynamics of biosand filters and contributions of the microbial food web to effective treatment of wastewater-impacted water sources. Applied and Environmental Microbiology 85, 1–14. https://doi.org/10.1128/AEM.01142-19

Wellinger, R., Thoma, F., 1996. Taq DNA polymerase blockage at pyrimidine dimers. Nucleic Acids Research 24, 1578–1579. https://doi.org/10.1093/nar/24.8.1578

Wemheuer, F., Taylor, J.A., Daniel, R., Johnston, E., Meinicke, P., Thomas, T., Wemheuer, B., 2020. Tax4Fun2: prediction of habitat-specific functional profiles and functional redundancy based on 16S rRNA gene sequences. Environmental Microbiome.

White, C.P., DeBry, R.W., Lytle, D.A., 2012. Microbial survey of a full-scale, biologically active filter for treatment of drinking water. Applied and Environmental Microbiology 78, 6390–6394. https://doi.org/10.1128/AEM.00308-12

WHO, 2003. Emerging Issues in Water and Infectious Disease 24.

Wickham, H., 2017. tidyverse: Easily Install and Load the "Tidyverse". R package version 1.2.1 [WWW Document]. URL https://cran.r-project.org/package=tidyverse

Wickham, H., 2016. ggplot2: Elegant Graphics for Data Analysis. Springer-Verlag New York.

Widder, S., Allen, R.J., Pfeiffer, T., Curtis, T.P., Wiuf, C., Sloan, W.T., Cordero, O.X., Brown, S.P., Momeni, B., Shou, W., Kettle, H., Flint, H.J., Haas, A.F., Laroche, B., Kreft, J.-U., Rainey, P.B., Freilich, S., Schuster, S., Milferstedt, K., van der Meer, J.R., Groβkopf, T., Huisman, J., Free, A., Picioreanu, C., Quince, C., Klapper, I., Labarthe, S., Smets, B.F., Wang, H., Soyer, O.S., 2016. Challenges in microbial ecology: building predictive understanding of community function and dynamics. The ISME Journal 10, 2557–2568. https://doi.org/10.1038/ismej.2016.45

Willey, J.M., Sherwood, L., Woolverton, C.J., 2011. Prescott's microbiology, 10th Editi. ed. New York: McGraw-Hill.

Wingender, J., Flemming, H.C., 2011. Biofilms in drinking water and their role as

reservoir for pathogens. International Journal of Hygiene and Environmental Health 214, 417–423. https://doi.org/10.1016/j.ijheh.2011.05.009

Wingender, J., Flemming, H.C., 2004. Contamination potential of drinking water distribution network biofilms. Water Science and Technology 49, 277–286. https://doi.org/10.2166/wst.2004.0861

Woese, C.R., 1987. Bacterial evolution. Microbiological Reviews 51, 221–271. https://doi.org/10.1128/mmbr.51.2.221-271.1987

Wotton, R.S., 2002. Water purification using sand. Hydrobiologia 469, 193–201. https://doi.org/10.1023/A:1015503005899

Yang, B., Wang, Y., Qian, P.Y., 2016. Sensitivity and correlation of hypervariable regions in 16S rRNA genes in phylogenetic analysis. BMC Bioinformatics 17, 1–8. https://doi.org/10.1186/s12859-016-0992-y

Yang, C., Sun, W., Ao, X., 2020. Bacterial inactivation, DNA damage, and faster ATP degradation induced by ultraviolet disinfection. Frontiers of Environmental Science and Engineering 14, 1–10. https://doi.org/10.1007/s11783-019-1192-6

Yang, F., Shi, B., Bai, Y., Sun, H., Lytle, D.A., Wang, D., 2014. Effect of sulfate on the transformation of corrosion scale composition and bacterial community in cast iron water distribution pipes. Water Research 59, 46–57. https://doi.org/10.1016/j.watres.2014.04.003

Yarza, P., Yilmaz, P., Pruesse, E., Glöckner, F.O., Ludwig, W., Schleifer, K.H., Whitman, W.B., Euzéby, J., Amann, R., Rosselló-Móra, R., 2014. Uniting the classification of cultured and uncultured bacteria and archaea using 16S rRNA gene sequences. Nature Reviews Microbiology 12, 635–645. https://doi.org/10.1038/nrmicro3330

Yu, J., Kim, D., Lee, T., 2010. Microbial diversity in biofilms on water distribution pipes of different materials. Water Science and Technology 61, 163–171. https://doi.org/10.2166/wst.2010.813

Zhang, Y., Liu, W.T., 2019. The application of molecular tools to study the drinking water microbiome–Current understanding and future needs. Critical Reviews in Environmental Science and Technology 49, 1188–1235. https://doi.org/10.1080/10643389.2019.1571351

Paper I

npj | Clean Water

www.nature.com/npjcleanwater

ARTICLE OPEN

Impact of UV irradiation at full scale on bacterial communities in drinking water

Kristjan Pullerits[1,2], Jon Ahlinder[3], Linda Holmer[4], Emelie Salomonsson[3], Caroline Öhrman[3], Karin Jacobsson[5,7], Rikard Dryselius[5,8], Mats Forsman[3], Catherine J. Paul[1,6]✉ and Peter Rådström[1]

Water in a full-scale drinking water treatment plant was irradiated with ultraviolet (UV) doses of 250, 400, and 600 J/m^2, and the effect on bacterial communities investigated using 16s rRNA gene amplicon sequencing, heterotrophic plate counts (HPCs), coliform, and *Escherichia coli* counts. The bacteria in the irradiated water were also analyzed following storage for 6 days at 7 °C, to approximate the conditions in the distribution system. The $\log_{10}$ reduction of HPCs at 400 J/m^2 was 0.43 ± 0.12. Phylogenetic examination, including DESeq2 analysis, showed that *Actinobacteria* was more resistant to UV irradiation, whereas *Bacteroidetes* was sensitive to UV. Phylum *Proteobacteria* contained monophyletic groups that were either sensitive or resistant to UV exposure. The amplicon sequence variants (ASVs) resistant to UV irradiation had a greater average GC content than the ASVs sensitive to UV, at 55% ± 1.7 ($n = 19$) and 49% ± 2.5 ($n = 16$), respectively. Families *Chitinophagaceae*, *Pelagibacteraceae*, *Holophagaceae*, *Methylophilaceae*, and *Cytophagaceae* decreased linearly in relative abundance, with increasing UV dose ($P < 0.05$, Pearson's correlation). When irradiated water was stored, *Chitinophagaceae*, *Comamonadaceae*, and *Flavobacteriaceae* families decreased in relative abundance, whereas *ACK-M1*, *Mycobacteriaceae*, and *Nitrosomonadaceae* were increasing in relative abundance. This suggests that the impact of UV irradiation cannot only be considered directly after application but that this treatment step likely continues to influence microbial dynamics throughout the distribution system.

npj Clean Water (2020)3:11 ; https://doi.org/10.1038/s41545-020-0057-7

INTRODUCTION

Ultraviolet (UV) irradiation is widely used as a disinfection method for drinking water treatment. The technique became increasingly popular in the 1990s when its ability to disinfect water containing *Cryptosporidium* and *Giardia* was recognized[1]. Unlike other disinfection methods such as chlorination or ozonation, UV irradiation requires no addition of chemicals and low-pressure UV produces insignificant amounts of disinfection byproducts[1,2]. Various bacteria have different UV susceptibility: a 4 − $\log_{10}$ reduction of a lab-grown environmental isolate of *Mycobacterium avium* requires a dose of 128 J/m^2 UV 254 nm[3], whereas for the same reduction, cultivated environmental isolate of *Escherichia coli* requires a dose of 81 J/m^2 [4]. The dose required for disinfection can also be affected by suspended particles in the water, which can absorb and scatter UV light and affect UV efficiency[5,6].

The disinfection mechanism resulting from exposure to UV is mainly damage to nucleic acids by irradiation[7]. Nucleotides absorb UV light with wavelengths of between 200 and 300 nm with a peak absorption between 260 and 265 nm[8]. The absorption of light triggers the formation of mutagenic DNA lesions, such as cyclobutane pyrimidine dimers and 6–4 photoproducts[9]. Both pyrimidines and purines can absorb UV light, although pyrimidines are considered to be more photoreactive[10,11]. When nucleotides are damaged by UV light, the DNA replication is blocked, resulting in cell inactivation[12,13]. Some microorganisms are able to repair UV damage either by photoreactivation or dark repair[9,14].

The impact of UV on target microorganisms has largely been studied using cultivation-based techniques of monocultures at laboratory scale[1]. At full scale, a biodosimetry test is used to calibrate the irradiation dose for UV reactors by spiking a known concentration of a specific cultured microorganism and calculating the log-reduction. This is compared with results from a calibrated laboratory UV reactor to calculate the final UV dose of the full-scale UV reactor at a specific UV transmission and flow[15]. The validity of these tests to assess disinfection of drinking water, however, is debatable, as the majority of microorganisms in drinking water cannot currently be cultivated[16], bacteria in drinking water are diverse, and bacteria in the environment have an increased UV resistance compared with laboratory-cultivated strains[1]. Exposure to UV can also cause some bacteria to enter a viable but nonculturable state as a response to environmental stress[17,18].

Molecular DNA-based methods analyze the microbial community without the need for cultivation and, as UV irradiation causes DNA lesions and reduces the number of amplifiable target templates in the PCR reaction[13,19], amplicon-based methods can describe which types of bacteria and genes are affected by UV[20–22]. Microbial inactivation of *Pseudomonas aeruginosa* and *Enterococcus faecium* by UV was assessed by cultivation and quantitative PCR (qPCR)[19] and impact of UV on adenovirus concentrations were measured by cell culture infectivity and long-range PCR with subsequent qPCR[23]. The impact of UV irradiation on the number of bacteria in drinking water has been quantified with 16s rRNA gene amplification[24].

[1]Applied Microbiology, Department of Chemistry, Lund University, P.O. Box 124, SE-221 00 Lund, Sweden. [2]Sweden Water Research AB, Ideon Science Park, Scheelevägen 15, SE-223 70 Lund, Sweden. [3]FOI, Swedish Defence Research Agency, Cementvägen 20, SE-906 21 Umeå, Sweden. [4]Norrvatten, Box 2093, SE-169 02 Solna, Sweden. [5]Swedish Food Agency, Box 622, SE-751 26 Uppsala, Sweden. [6]Water Resources Engineering, Department of Building and Environmental Technology, Lund University, P.O. Box 118, SE-221 00 Uppsala, Sweden. [7]Present address: Swedish University of Agricultural Sciences, Box 7036, SE-750 07 Uppsala, Sweden. [8]Present address: Health Agency of Sweden, SE-171 82 Solna, Sweden ✉email: catherine.paul@tvrl.lth.se

Published in partnership with King Fahd University of Petroleum & Minerals

npj nature partner journals

Although the value of UV irradiation for reduction of microbial pathogens in drinking water is not disputed, it is not known how UV irradiation impacts other bacteria that are undesirable. Some bacteria can cause water quality issues, by producing unpleasant odors and tastes[25], or exacerbate corrosion of infrastructure[26]. Descriptions of the bacterial community in water using 16s rRNA gene amplicon sequencing have described changes in drinking water during distribution[27]; however, few studies exist, examining the impact of UV exposure on the bacterial community in drinking water. An initial study using 16s rRNA gene amplicon sequencing conducted by Nocker et al.[21] showed how some phyla of bacteria were affected by a single dose of UV in a full-scale drinking water treatment plant. The approach of using 16S rRNA gene amplicon sequencing has been used to observe changes in the bacterial community for UV wastewater disinfection[22] and UV irradiation of marine water[28].

The current study is a detailed examination of the impact of three different UV irradiation doses (250, 400, and 600 J/m^2) in drinking water at full scale. The contents and diversity of the bacterial community was assessed using 16S rRNA gene amplicon sequencing. The results of this molecular analysis were compared with traditional cultivation-based methods determining heterotrophic plate counts (HPCs), coliforms, and *E. coli*. To understand how changes might occur during distribution of water irradiated with UV, bacterial communities of irradiated water, stored at temperatures simulating those of a distribution system, were also investigated.

RESULTS

Effect of UV irradiation on bacterial community structure

The bacterial community in water irradiated with different UV doses (250, 400, and 600 J/m^2) and following 6 days water storage at 7 °C was investigated using 16S rRNA gene amplicon sequencing (Fig. 1). Canonical correspondance analysis (CCA) of the relative abundances of amplicon sequence variants (ASVs), which takes into account the parameters of UV dose and storage, showed increasingly dissimilar bacterial communities with higher UV dose ($P < 0.001$, CCA followed by analysis of variance (ANOVA)). This was also observed with ordination analysis using the Bray–Curtis distance between samples (Supplementary Fig. 1). Although storage of the water affected the community composition of the UV-irradiated samples (Supplementary Fig. 2A, $P < 0.001$, $R^2 = 0.62$, Analysis of Dissimilarities (ADONIS), storage had no impact on the bacterial community that had not been irradiated by UV according to Bray–Curtis analysis (Supplementary Fig. 2B, $P = 0.36$, $R^2 = 0.10$, ADONIS).

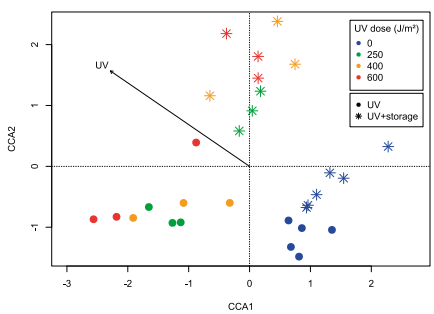

Fig. 1 Canonical correspondence analysis (CCA) of bacterial communities and UV dose. UV dose is used as a numeric variable and sample type as a factor. Bacterial communities were analyzed from water exposed to UV (0, 250, 400, and 600 J/m^2; blue, green, orange, and red circles, respectively) or after storage (6 day storage at 7 °C, stars); $n = 5$ for UV dose of 0 J/m^2 and $n = 6$ for storage not exposed to UV; $n = 3$ for all UV doses >0 and sample type.

To further investigate how irradiation shaped the bacterial community structures, alpha diversity was assessed by comparing evenness (Pielou's measure), species richness (number of observed ASVs), and diversity (Shannon index) (Supplementary Fig. 3). When all water samples exposed to UV irradiation (250, 400, and 600 J/m^2) were grouped, the evenness of the community increased compared with the non-irradiated water from 0.49 ± 0.016 to 0.54 ± 0.025 ($P < 0.001$, one-way ANOVA). Species richness in water samples ranged from 109 to 140, but no changes in species richness were observed by UV irradiation ($P > 0.05$, one-way ANOVA). Changes in Shannon diversity reflected those in evenness, with UV exposure resulting in increased Shannon diversity in the bacterial communities, from 2.33 ± 0.094 for non-irradiated communities to 2.61 ± 0.12 when all water samples exposed to UV were grouped for analysis ($P < 0.001$, one-way ANOVA).

The effects of UV irradiation were observed as changes in the relative abundance of specific bacterial taxa as the UV dose increased (Fig. 2). Following agglomeration of ASVs into phylum level, *Bacteroidetes* decreased in relative abundance ($P < 0.05$, Pearson's correlation), whereas *Actinobacteria* increased in relative abundance ($P < 0.05$, Pearson's correlation). Five families showed linear decreases in relative abundance ($P < 0.05$, Pearson's correlation), including *Pelagibacteraceae* ($R = -0.74$), *Chitinophagaceae* ($R = -0.96$), *Holophagaceae* ($R = -0.71$), *Methylophilaceae* ($R = -0.61$), and *Cytophagaceae* ($R = -0.8$). Within the *Chitinophagaceae* family, the *Sediminibacterium* genus showed a strong linear decrease in relative abundance ($R = -0.97$, $P < 0.05$, Pearson's correlation; Supplementary Fig. 10).

Phylogenetic relationships of bacteria impacted by UV

ASVs from bacteria affected by UV irradiation were identified by differential abundance analysis using DESeq2 where negative and positive $\log_2$ fold changes were defined as sensitive- and resistant to UV, respectively. Thirty-five out of 164 ASVs with a significant change in differential abundance ($P_{adjusted} < 0.05$) were identified (Supplementary Figs 4 and 5). Specific clades were identified by their sensitivity to UV (Fig. 3), phylum *Bacteroidetes* was sensitive to UV, with ASVs identified as *Sediminibacterium*, *Sphingobacteriaceae*, and *Cytophagaceae* having a negative $\log_2$ fold change. Phylum *Actinobacteria* was resistant to UV with ASVs classified as families *ACK-M1* and *C111* with a positive $\log_2$ fold change. The *Proteobacteria* phylum included ASVs that were both sensitive and resistant to UV: ASVs classified as *Pelagibacteraceae* (order *Ricketsiales*, *Alphaproteobacteria*), *Methylophilaceae* (*Betaproteobacteria*), and *Limnohabitans* (*Betaproteobacteria*) showed a negative $\log_2$ fold change, whereas others including *Rhodospirillaceae* (*Alphaproteobacteria*), *Ralstonia* (*Betaproteobacteria*), *Polynucleobacter* (*Betaproteobacteria*), and *Rhodoferax* (*Betaproteobacetria*) demonstrated positive $\log_2$ fold changes. Phylogeny was determined to be a cause for UV sensitivity when the community sensitive to UV, which consisted of 16 ASVs showed a difference in composition compared with all identified ASVs in the samples at phylum level ($P = 0.020$, Fisher's exact test). The GC content of the 16S rRNA gene region of ASVs identified by DESeq2 analysis was calculated (Supplementary Table 2) where ASVs with positive $\log_2$ fold change ($n = 19$) had a significantly greater average GC content compared with ASVs with negative $\log_2$ fold change ($n = 16$), 55% ± 1.7 and 49% ± 2.5, respectively ($P < 0.001$, one-way ANOVA).

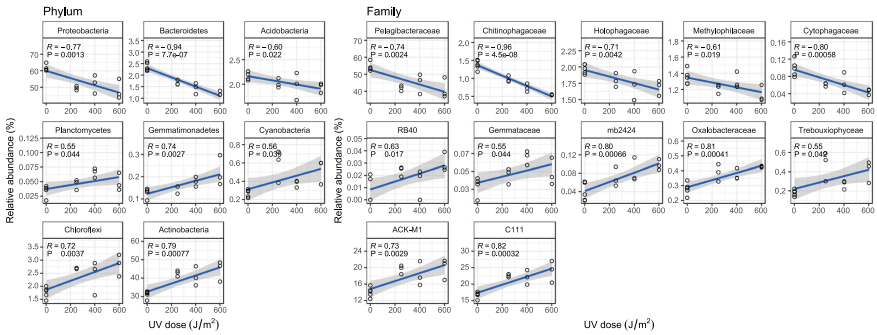

Fig. 2 Impact of UV dose at phylum and family level. Linear regressions (blue line) of the relative taxonomic abundance again UV dose are shown, with the gray transparent area showing the 95% confidence interval. Reads were agglomerated to phylum or family level. Only phyla and families with significant regression correlation ($P < 0.05$, Pearson's correlation) are shown; see Supplementary Figs 6–10 for full data set at all taxonomic ranks. Taxa are ordered with the greatest negative slope correlation in top left with subsequent increase. $n = 3$ for each UV-irradiated sample, $n = 5$ for the non-irradiated samples.

Impact of water storage on bacterial communities exposed to UV irradiation

As water exposed by UV irradiation is often distributed to the consumer over a period of days and at low temperatures, changes that could occur in the bacterial community following irradiation and distribution were assessed (Fig. 1). To replicate these conditions, water samples were stored for 6 days at 7 °C following UV exposure. The alpha diversity measure evenness recovered after storage to similar levels as before UV irradiation when the UV-irradiated and -stored samples were grouped together and compared with the non-irradiated samples, 0.49 ± 0.026 (mean ± SD) and 0.48 ± 0.034, respectively (Supplementary Fig. 3). The storage did not affect the species richness ($P > 0.05$, one-way ANOVA). As with evenness, the Shannon diversity also recovered after storage for the grouped irradiated and stored samples to the same levels as the non-irradiated samples, Shannon index 2.36 ± 0.14 and 2.29 ± 0.16, respectively.

To assess which bacteria were able to repair the UV damage or regrow faster than other members in the community, the relative abundance of ASVs representing bacterial taxa in the UV-irradiated water were compared before and after storage (Fig. 4). Following UV irradiation, the *Pelagibacteraceae* family comprised 37–50% of the community (Fig. 2) but after storage this increased to 46–59% (Fig. 4, $P < 0.05$, one-way ANOVA). The families *Flavobacteriaceae*, *Trebouxiophyceae*, *C111*, and *Hyphomicrobiaceae* were not initially affected or increased in relative abundance by UV irradiation (Fig. 2 and Supplementary Fig. 9), but decreased in relative abundance after storage (Fig. 4, $P < 0.05$, one-way ANOVA). A relative decrease in the *Trebouxiophyceae* family and changes in relative abundance for 6 (out of 34) additional families ($P < 0.05$, one-way ANOVA) were observed when the water that had not been UV-irradiated was stored (Supplementary Fig. 16).

To assess the impact of UV exposure on the bacterial community in distributed water, the relative abundance of bacterial taxa in stored water that had, or had not been irradiated with UV were compared (Fig. 5). Five families of bacteria decreased in relative abundance when water exposed to UV was stored, including *Flavobacteriaceae, Chitinophagaceae, Cytophagaceae, Comamonadaceae*, and *Sphingobacteriaceae* (one-way ANOVA, $P < 0.05$), and 11 families increased in relative abundance following UV exposure and storage, including *ACK-M1, Oxalobacteraceae, Nitrosomonadaceae, Rhodospirillaceae, mb2424, Sinobacteraceae, LD19 Trebouxiophyceae, Gemmatimonadaceae, Mycobacteriaceae*, and *Acetobacteraceae* ($P < 0.05$, one-way ANOVA).

Impact of UV on conventional microbial indicators

HPCs were assessed for water irradiated with 250, 400, and 600 J/m^2, and after storage. HPCs in the UV-exposed water decreased to an average of 1.2 ± 0.83 CFU/mL from 4.5 ± 1.4 CFU/mL (Fig. 6, $P < 0.001$, one-way ANOVA). There was no significant change in HPCs between the three different doses ($P > 0.05$, one-way ANOVA, followed by a Tukey's test): $\log_{10}$ reductions in HPCs were 0.53 ± 0.12 and 0.43 ± 0.12 for 250 J/m^2 and 400 J/m^2, respectively. Although the number of heterotrophic bacteria increased during storage in the non-irradiated samples, from 4.5 ± 1.4 to 8.7 ± 6.2 CFU/mL, this was not statistically significant ($P > 0.05$, one-way ANOVA). HPCs in water that had been UV-irradiated did not change during storage, regardless of dose ($P > 0.05$, one-way ANOVA, followed by a Tukey's test). No differences in fast growing HPCs after 3 days were seen for any of the samples ($P > 0.05$, one-way ANOVA, followed by a Tukey's test; Supplementary Fig. 17). To assess coliform counts, 60 L of water was concentrated using dead-end hollow-fiber ultrafiltration[29] following exposure of the water to 0, 400, and 600 J/m^2 ($n = 3$ for each dose). Coliforms (1.7 ± 0.57 coliforms/10 L) and *E. coli* (0.97 ± 0.93 *E. coli*/10 L) were detected in the concentrates of the untreated water but not in any sample of water exposed to UV (Supplementary Table 1).

DISCUSSION

As bacteria in drinking water are diverse and likely have different susceptibility to UV[1], this study examined bacterial communities in water irradiated with different UV doses, using 16S rRNA gene amplicon sequencing. The impact of storage on the relative abundance of different taxa was also determined to describe how exposing water to UV irradiation could alter the microbiology of the distributed water. The community descriptions were compared with conventional methods using indicator bacteria to assess and compare how these approaches reflect the impact of UV irradiation on microbial water quality.

Examining the relationship between phylogeny and UV exposure revealed bacterial clades that were both sensitive and resistant to UV. *Actinobacteria* phylum was resistant, *Bacteroidetes* phylum showed sensitivity to UV, whereas some monophyletic groups in the *Proteobacteria* phylum showed sensitivity and others

Fig. 3 Phylogenetic tree of ASVs identified as sensitive and resistant to UV. The inferred phylogenetic tree with branches colored by sensitivity and resistant to UV was created with ASVs recognized as having a signficant change with differential abundance analysis using DESeq2 ($P_{adjusted} < 0.05$). Samples not exposed to UV ($n = 5$) were compared to UV irradiated samples ($n = 9$), with the dose as a numeric parameter. A negative log2fold change was considered a UV-sensitive taxa (red) and positive log2fold change as a UV-resistant taxa (blue). The scale bar shows an estimate of the substitutions per nucleotide position. See Supplementary Fig. 4 and Supplementary Table 2 for output data from DESeq2. See Supplementary Fig. 5 depicting the ASVs classified as sensitive and resistant to UV among all identified ASVs.

resistance to UV (Fig. 3). Low and high GC content calculated from the different ASV DNA sequences correlated with how the taxa were categorized as sensitive or resistant to UV, respectively (Supplementary Table 2). It has been proposed that the high genomic GC content in *Actinobacteria* contributes to their UV resistance[30], perhaps as TT and TC nucleotide sites are more photoreactive[31]. Reichenberger et al.[32] proposed that phyla could be classified into GC-rich (*Actinobacteria*), GC-intermediate (*Proteobacteria*), and GC-poor (*Bacteroidetes*), linking UV sensitivity to a genomic, and thus heritable, trait. Nocker et al.[21] showed resistance of *Actinobacteria* to UV in drinking water and suggested that the *Proteobacteria* phylum is sensitive to UV. In addition to GC content, *Actinobacteria*, *Bacteroidetes*, and *Proteobacteria* have distinct membrane structures that can result in these bacteria having different degrees of resistance to UV[33]. A study from McKinney and Pruden[20] observed that two Gram-positive organisms (*Staphylococcus aureus* and *E. faecium*, both *Firmicutes*) were more resistant to UV irradiation than two Gram-negative bacteria (*E. coli* and *P. aeruginosa*, phylum *Proteobacteria* and *Firmicutes*, respectively), which could be due to the thicker peptidoglycan layer in Gram-positive organisms protecting the cells from UV damage. *Actinobacteria* are Gram-positive and have been isolated in environments exposed to strong solar UV radiation[30,34]. In addition, *Actinobacteria* are spore forming[35] and this can also contribute to their resistance to UV[36,37]. In contrast the phyla *Bacteroidetes* are Gram-negative rods that do not form endospores[38] and this combination could be a reason for the sensitivity to UV demonstrated by the members of the *Bacteroidetes* phylum observed in the current study. Strains classified in the *Bacteroidetes* phylum are abundant in high-altitude lakes receiving strong UV radiation from the sun[39], suggesting tolerance to UV exposure; however, the *Bacteroidetes* phylum is diverse and the members of the *Bacteroidetes* in this study may be UV-sensitive, as the source water used in the treatment plant in this study is from a low-altitude lake. *Proteobacteria* are Gram-negative and the division is the largest and most diverse among prokaryotes[40]. In this study within the *Proteobacteria*, the response to UV seemed largely related to GC content. In *Alphaproteobacteria*, the *Rickettsiales* order was sensitive to UV (low GC content, ranging from ~30% to 40%[41]), whereas the *Rhodospirillaceae* family (high GC content of ~65%[41]) was resistant to UV, and in *Betaproteobacteria*, the *Methylophilaceae* family showed sensitivity to UV (low GC content of ~35–40%[42]), whereas *Ralstonia* and *Rhodoferax* were resistant to UV (high GC content of ~67%[43] and ~60%[44], respectively). The exceptions were the sensitivity of *Polynucleobacter*, with a GC content of ~45%[45] to UV, and that members of *Limnohabitans* (GC content of 59%[44]) were both resistant and sensitive. These observations could be due, in part, to the few isolates of these bacteria that have been sequenced, to determine GC content, which may differ from those present in this study.

Depending on the time for drinking water to reach consumers, some bacteria in the water could repair UV damage[46] received at the treatment plant. In this study, the evenness and diversity of the bacterial community were affected by UV, although both metrics indicated that the community rebounded following storage. This could largely be attributed to changes in the relative abundance of *Pelagibacteraceae*, which was highly abundant in the community. The relative abundance of this family recovered after UV exposure and storage (Fig. 4), possibly due to the ability of these bacteria to repair UV damage and/or by surviving the UV exposure, and then regrowing faster than the other surviving taxa. As *Pelagibacteraceae*, or the SAR11 clade, are abundant in drinking water[47] and marine water[48,49]; they may have acquired UV resistance to survive the UV exposure from the sun in their preferred niche and, with a large surface-to-volume ratio, efficient nutrient uptake in oligotrophic environments[50] allows them to grow faster than other members of the bacterial community[51].

The relative abundance of families *Flavobacteriaceae*, *Trebouxiophyceae*, *C111*, and *Hyphomicrobiaceae* was initially not affected or increased by UV irradiation (Supplementary Fig. 14) but during storage decreased in relative abundance (Fig. 4). The initial relative UV resistance of these taxa could be due to the 16S rRNA gene not

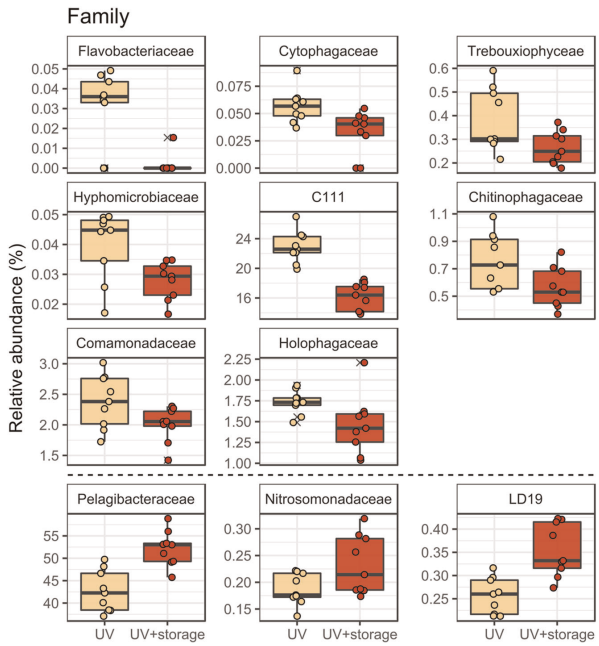

Fig. 4 Comparison of bacterial taxa at family level, in water samples exposed to UV, with and without storage. Relative abundance of bacterial taxa in water samples exposed to UV, and then stored for 6 days at 7 °C (red), or not stored (gold), were compared. Only families with significant difference in relative abundance between groups ($P < 0.05$, one-way ANOVA) are shown, see Supplementary Figs 11–15 for full data set. Families are ordered with the most relative change in the top left with subsequent decrease. The boxes show the interquartile range, the line inside each box represents the median, whiskers show maximum and minimum values, and the crosses show outliers. $n = 9$ for water samples exposed to UV and $n = 9$ for water exposed to UV and incubated. Samples irradiated at different UV doses were grouped for this analysis.

receiving any DNA lesions, but damage by UV irradiation can also cause cell death via by, e.g., creating protein–DNA crosslinks[52], which would not be detected with 16S rRNA gene amplicon sequencing. In addition, although valuable in many applications, the use of viability dyes (e.g., propidium monoazide (PMA) and propidium iodide (PI)) together with qPCR or flow cytometry (Supplementary Table 5) to assess UV disinfection is difficult, as UV irradiation damages DNA and not cell membranes.

UV irradiation is increasingly considered as a disinfection process for drinking water, and with specific observations of how the bacterial community would change during distribution from a treatment plant applying UV, it was also important to understand how this community compared with distributed water that had not been UV-irradiated water. After storage, some families, including *Chitinophagaceae*, *Comamonadaceae*, and *Flavobacteriaceae* decreased in relative abundance in water that had been UV-irradiated compared with untreated, stored water, whereas other families increased in relative abundance, including *ACK-M1*, *Mycobacteriaceae*, and *Nitrosomonadaceae* (Fig. 5). The *ACK-M1* family is included in the *Actinomycetales* order and the presence of *Actinomycetes* has been associated with taste and odor problems, due to their production of odorants, including 2-methylisoborneol (2-MIB)[25]. 2-MIB is an odorant that is difficult to remove with conventional water treatment processes; however, *Chitinophagaceae bacterium*, among other bacteria isolated from an activated carbon filter, are able to biodegrade 2-MIB[53]. This suggests that UV treatment may both increase the abundance of bacteria associated with production of odorants and decrease those with the potential to biodegrade the problematic compounds. This may be a concern for drinking water treatment plants, as preventing taste and odor problems in drinking water is of great importance[25].

In addition to aesthetic compounds, the presence of opportunistic pathogens such as *Legionellae*, *Mycobacteria*, and *P. aeruginosa* are a concern in distributed water and can also persist in biofilms[54]. In this study, family *Mycobacteriaceae* (classified as *Mycobacterium*; Supplementary Fig. 15) was detected in higher relative abundance in water after UV exposure and storage, than in untreated, stored water (Fig. 5). Shin et al.[55] have described *M. avium* as more resistant to UV irradiation than other waterborne pathogens, and as this species has also shown resistance to other disinfection methods such as chlorine, monochloramine, chlorine dioxide, and ozone[56], it could be of concern for drinking water producers.

Not much is known about how a UV installation will affect the biofilm in the drinking water distribution system (DWDS) in the long term[57]. The biofilm community in DWDS is complex and can differ depending on location and material[58,59]. The genus *Nitrosomonas*, included in the *Nitrosomonadaceae* family, which increased in relative abundance by UV irradiation and storage (Fig. 5), has been found in DWDS biofilms[60,61]. *Comamonadaceae* has been observed in DWDS biofilms[62] and *Flavobacterium*,

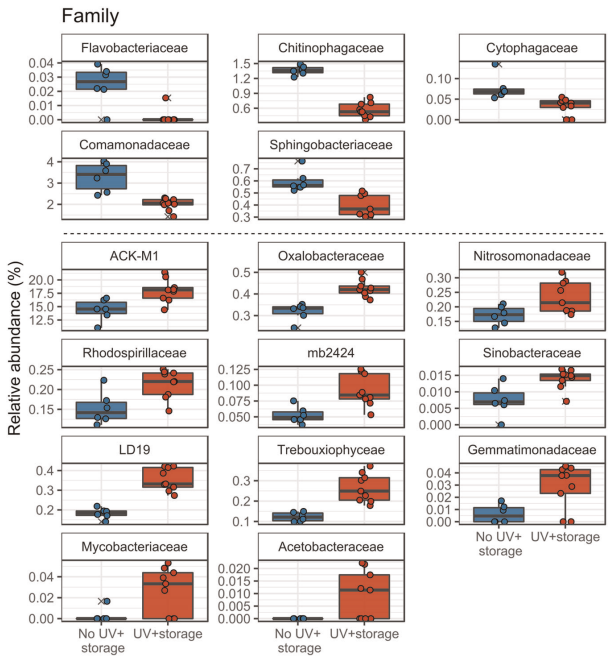

Fig. 5 Comparison of bacterial taxa at family level following storage of water. Relative abundance of bacterial taxa in water samples that were stored for 6 days at 7 °C, and were either not exposed (blue) or exposed (red) to UV. Only families with significant difference in relative abundance between groups ($P < 0.05$, one-way ANOVA) are shown; see Supplementary Figs 11–15 for full data set. Families are ordered with the most relative change in the top left with subsequent decrease. The boxes show the interquartile range, the line inside each box represents the median, whiskers show maximum and minimum values, and the crosses show outliers. $n = 6$ for no UV samples and $n = 9$ for UV-irradiated samples. Samples irradiated at different UV doses were grouped for this analysis.

included in the *Flavobacteriaceae* family, has been observed in drinking water wells[63], both decreasing in relative abundance by UV irradiation and storage in this study. If a treatment plant using UV disinfection selects for certain bacteria, this will inevitably shape the DWDS biofilm, which will affect the water quality in the end.

Despite the observation in this, and other studies that bacteria are affected differently by UV irradiation, biodosimetry tests are based on single target organisms. This makes it difficult to assess UV irradiation in full scale[21,24,64]. However, in this study families *Chitinophagaceae*, *Pelagibacteraceae*, *Holophagaceae*, *Methylophilaceae*, and *Cytophagaceae* showed sensitivity to UV in a linear correlation with dose (Fig. 2). These bacterial families have been widely observed in drinking water, freshwater, and river water[65–68], and the 16S rRNA gene from these families could be a feasible target biomarker for evaluating UV irradiation dose at full scale. As water treatment plants have their own unique microbiome[69], 16S rRNA gene amplicon sequencing to screen for these families, and potentially other biomarker target organisms, could then support targeted gene analysis, e.g., qPCR, to be applied routinely to assess UV disinfection. Longer fragment length of the qPCR target (compared with that used in this sequencing-based study) could increase the resolution of the methodology, as more UV damage can be observed with qPCR of longer amplicons[19].

The need for molecular biology techniques was supported by observations in this study and others[70] of HPCs, where log reductions attributed to UV irradiation were lower than previously determined with lab-cultivated organisms[1]. Several taxa that have been identified from drinking water by growth on HPCs[71–73] were among the taxa identified by sequencing in this study as UV-sensitive, including *Methylophilaceae*, *Sphingobacteriales*, and *Comamonadaceae* correlating with the reduction in HPCs by UV irradiation (Fig. 6); however, no change in HPCs was observed when comparing the UV-irradiated water before and after storage, which was seen by molecular techniques (Fig. 1). Mofidi and Linden[74] showed regrowth of HPCs following UV disinfection at 200, 600, and 1400 J/m^2, and 7 days of storage at 20 °C to the same counts as the non-irradiated control, with regrowth attributed to the robustness of the natural bacterial community in drinking water, and likely temperatures, as this was not observed in the current study, where a lower temperature was used for storage. Thus, HPCs are particularly unsuitable for monitoring quality of UV-irradiated water in systems where water temperatures are low, with overall low numbers making log-reduction comparison difficult or meaningless. This was also the case for coliforms and *E. coli*, which were completely removed by UV irradiation, as expected[4,75].

Although UV treatment is widely used in full-scale drinking water treatment plants, it is difficult to apply traditional

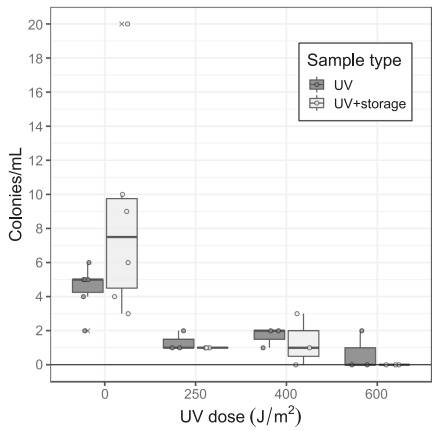

Fig. 6 Heterotrophic plate counts of water exposed to different UV doses, and following storage. Water exposed to different UV doses (dark gray), and following storage for 6 days at 7 °C (light gray). $n = 6$ for UV dose of 0 J/m^2 and $n = 6$ for storage not exposed to UV. $n = 3$ for all UV doses >0 and sample type. The boxes show the interquartile range, the line inside each box represents the median, whiskers show maximum and minimum values, and the crosses show outliers.

microbiological methods to assess dose and quality of the distributed water. A variety of treatment processes produce water containing microorganisms with different UV susceptibility and different wavelengths of UV can be more efficient on certain organisms[76]. In addition to treatment plants, additional applications of UV disinfection include point-of-use and within the pipe network to prevent regrowth of opportunistic pathogens, including UV LED devices[57]. The need to assess the impact of these technologies, both for process monitoring purposes and to investigate the bacterial community that is exposed to consumers through water, could use a molecular biology approach, based on biomarkers for specific taxa. In addition, as the 16S rRNA gene is a fraction of the complete genome in bacteria, shotgun metagenomics examining the genome of UV-irradiated bacteria could investigate the role of GC content on survival, the sensitivity of specific genes involved in biofilm formation, DNA repair, antibiotic resistance, and virulence to understand how UV irradiation affects the microbiota and quality of drinking water. As the DWDS biofilm also interacts with drinking water quality, the impact of UV-exposed water on biofilm formation and composition, in lab- or full scale, would also be of interest.

METHODS

Sampling of water

Drinking water was sampled at Görvälnverket waterworks in Stockholm, Sweden. The waterworks operated by Norrvatten AB produces 1.6 m^3/s drinking water from the surface water taken from Lake Mälaren. Water is produced using flocculation with aluminum sulfate, followed by sedimentation, rapid sand filtration, granulated activated carbon, UV irradiation, addition of monochloramine, and pH adjustment. The UV aggregate is a low-pressure UV (Trojan UV) emitting light at a wavelength of 254 nm with the USEPA standard[8], routinely at a UV dose of 400 J/m^2. The aggregate is 1000 mm in diameter consisting of ten rows of four UV lamps diagonally placed through the pipe. The UV intensities are measured with five light intensity meters evenly distributed throughout the aggregate measuring UV intensity at 200–300 nm. When sampling was conducted, the flow rate through the UV aggregate was ~500 L/s and UV transmittance ~84%. Water exposed to three different doses of UV irradiation (250, 400, and 600 J/m^2) and water that had not been irradiated (0 J/m^2) were sampled both directly after exposure and following storage for 6 days at 7 °C. The conditions for storage were chosen to resemble the water temperature (~1–8 °C) in spring (February–April) and residence time (maximum 14 days) in this distribution system. General water quality data can be found in Supplementary Table 4. Sampling was done in March on two successive days with sampling for 0 J/m^2 ($n = 3$ for all analyses except $n = 2$ for DNA analysis) and 250 J/m^2 ($n = 3$) on day 1 and 0, 400, and 600 J/m^2 ($n = 3$, for each dose) on day 2. Each sample was collected in 1 L sterile borosilicate bottles for DNA analysis, 500 mL sterile borosilicate bottles for HPCs, and 6 × 10 L sterile plastic cans for dead-end ultrafiltration and Colilert analysis. For the storage experiment, water was collected in 2 L sterile borosilicate bottles for DNA and HPC analyses, wrapped in aluminum foil for 6 days at 7 °C (0 J/m^2 $n = 6$ and each UV dose $n = 3$). For DNA analysis, 1 L water samples were filtered onto 0.22 µm filters (Merck, Germany) and filters were stored at −20 °C until DNA extraction. Dead-end ultrafiltration[29] was done using 60 L of water exposed to UV irradiation doses of 0, 400, and 600 J/m^2. Rexeed 25AX filters (Asahi Kasei Corporation, Tokyo, Japan) were pretreated with fetal calf serum (PAA Laboratories, Waltham, MA, USA) to prevent adhesion of microorganisms. After filtration, the concentrate was eluted by back-flushing with 500 mL elution buffer (phosphate-buffered saline containing 1% Tween 80 and 0.01% Antifoam A (both from Sigma-Aldrich, St. Louis, MO, USA). The final volume typically consisted of 600–700 mL.

Conventional water quality parameters

HPCs were determined by the SS-EN ISO 6222:1999 standard with the pour plate method using 1 mL of water and addition of melted yeast peptone agar, followed by incubation at 22 °C for 3 (72 h) and 7 days (168 h) in triplicate. Concentrations of coliforms and *E. coli* were assessed using 100 mL of the dead-end ultrafiltered eluate water with the Colilert®−18 (IDEXX Laboratories Sverige AB) according to the manufacturer's instructions.

Bacterial community analysis

DNA was extracted from filter papers using the FastDNA Spin Kit for Soil (MP Biomedicals). Filters were cut into strips and added to Lysing Matrix E tubes with pre-added sodium phosphate, then extracted following the manufacturer's instructions. Empty filters were extracted for use as negative controls. Extracted DNA was stored at −20 °C. The V3–V4 region of the 16S rRNA gene was amplified using primers 341 F (5′-CCTACGGGNGGCWGCAG-3′) and 785 R (5′-GACTACHVGGGTATCTAATCC-3′)[77]. The PCR reaction (25 µL) contained 12.6 µL MilliQ-water, 10 µL 5 Prime Hot MasterMix (Quantabio, USA), 0.4 µL (20 mg mL^{-1}) bovine serum albumin, 0.5 µL (10 µM) forward and reverse primers, and 1 µL template DNA. The PCR cycling settings were 94 °C for 3 min and 35 cycles of 94 °C for 45 s, 50 °C for 1 min, 72 °C for 1.5 min, and a final step of 72 °C for 10 min. Samples were analyzed in triplicate PCR reactions and pooled together. Pooled amplicons were visualized by agarose gel and DNA concentration quantified using a Qubit 2.0 dsDNA BR Assay Kit (Thermo Fisher Scientific, USA). No amplicons were visible on the agarose gel for the negative controls, which were then excluded from further analyses. Fifty nanograms of each pooled amplicon were pooled together, purified using Select-A-size DNA clean and concentrator (Zymo Research, catalog #4080), and quantified using Qubit. The concentration was adjusted to 2 nM and the library was denatured and diluted according to the manufacturer's instruction (Illumina, USA), with 10% PhiX added to the sequencing run and sequenced using the MiSeq Reagent Kit v3 (600-cycles) (Illumina), according to the manufacturer's instructions.

Bioinformatics and statistics

Raw data from sequencing was demultiplexed with deML[78]. Demultiplexed reads were imported and processed in QIIME 2, version 2018.8.0[79]; forward and reverse reads were truncated using DADA2[80] at 250 bp, classified using the Greengenes database[81], and phylogenetic tree created with FastTree[82]. The feature table and phylogenetic tree from QIIME 2 were imported to the Phyloseq package[83] in R[84]. Singletons and ASVs at a frequency <0.005% of the total number of reads[85] and ASVs with <15 reads in 4 samples were removed. Reads were normalized with the transform_sample_counts function to relative abundances. CCA was done using the vegan package[86] with the ASV table, UV as a numeric variable, and sample type (after UV exposure or stored for 6 days at 7 °C) as a factor,

the CCA output was followed by an ANOVA permutation test for CCA. Principal Coordinates Analysis plot using Bray–Curtis dissimilarity was done and visualized using Phyloseq and the ggplot2 package[87], and ADONIS statistics performed using the vegan package. Data were agglomerated at different taxonomic ranks in Phyloseq and wrangled using Tidyverse R package[88]. Linear regression plots were plotted in R with ggplot2[87], ggpubr[89], and ggpmisc[90] packages, and the linear regression model calculated with the lm function, Pearson's correlation, and correlation coefficient calculated using the cor.test function in R. All other statistical analyses were done using base R. Non-normalized reads were used for differential abundance analysis using DESeq2[91] within Phyloseq ($P_{adjusted} < 0.05$), excluding samples which were stored and accounting for the UV dose as a numeric parameter and visualized in ggplot2. Output ASVs from DESeq2 were visualized in a phylogenetic tree using ggtree[92]. Species diversity indices were calculated with non-normalized reads with the Phyloseq package (Shannon Index and observed ASVs) and custom scripts (Pielou's measure).

Log reductions of HPCs (H) were calculated using Eq. 1:

$$H = \log_{10}(N_0) - \log_{10}(N) \quad (1)$$

where N_0 is the HPCs of the non-irradiated water and N the HPCs of the irradiated water at a specific dose. The SDs of log reductions (σ) were calculated with Eq. (2):

$$\sigma = \sqrt{\left(\frac{\sigma_{N_0}^2}{n_0} + \frac{\sigma_N^2}{n}\right)} \quad (2)$$

using $\log_{10}$ values of HPCs where σ_{N_0} is the SD of N_0 and σ_N the SD of N, n_0 is the sample size of the non-irradiated water, and n the sample size of the irradiated water at a specific dose.

DATA AVAILABILITY

DNA sequences are available at the NCBI Sequence Read Archive, accession number: PRJNA579449.

Received: 12 November 2019; Accepted: 21 February 2020;
Published online: 19 March 2020

REFERENCES

1. Hijnen, W. A. M., Beerendonk, E. F. & Medema, G. J. Inactivation credit of UV radiation for viruses, bacteria and protozoan (oo)cysts in water: a review. *Water Res.* **40**, 3–22 (2006).
2. Reckhow, D. A., Linden, K. G., Kim, J., Shemer, H. & Makdissy, G. Effect of UV treatment on DBP formation. *J. Am. Water Works Assoc.* **102**, 100–113 (2010).
3. Hayes, S. L., Sivaganesan, M., White, K. M. & Pfaller, S. L. Assessing the effectiveness of low-pressure ultraviolet light for inactivating *Mycobacterium avium* complex (MAC) micro-organisms. *Lett. Appl. Microbiol.* **47**, 386–392 (2008).
4. Sommer, R., Lhotsky, M., Haider, T. & Cabaj, A. UV inactivation, liquid-holding recovery, and photoreactivation of *Escherichia coli* O157 and other pathogenic *Escherichia coli* strains in water. *J. Food Protect.* **63**, 1015–1020 (2000).
5. Christensen, J. & Linden, K. G. How particles affect UV light in the UV disinfection of unfiltered drinking water. *J. Am. Water Works Assoc.* **95**, 179–189 (2003).
6. Farrell, C. et al. Turbidity composition and the relationship with microbial attachment and UV inactivation efficacy. *Sci. Total Environ.* **624**, 638–647 (2018).
7. Jungfer, C., Schwartz, T. & Obst, U. UV-induced dark repair mechanisms in bacteria associated with drinking water. *Water Res.* **41**, 188–196 (2007).
8. USEPA. *Ultraviolet Disinfection Guidance Manual for the Final Long Term 2 Enhanced Surface Water Treatment Rule.* 815-R-06-007 (Environmental Protection Agency, 2006).
9. Sinha, R. P. & Häder, D. P. UV-induced DNA damage and repair: A review. *Photochem. Photobiol. Sci.* **1**, 225–236 (2002).
10. Rastogi, R. P., Richa, Kumar, A., Tyagi, M. B. & Sinha, R. P. Molecular mechanisms of ultraviolet radiation-induced DNA damage and repair. *J. Nucleic Acids* **2010**, 592980 (2010).
11. Ravanat, J.-L., Douki, T. & Cadet, J. Direct and indirect effects of UV radiation on DNA and its components. *J. Photochem. Photobiol. B Biol.* **63**, 88–102 (2001).
12. Jungfer, C., Schwartz, T. & Obst, U. UV-induced dark repair mechanisms in bacteria associated with drinking water. *Water Res.* https://doi.org/10.1016/j.watres.2006.09.001 (2007).
13. Wellinger, R. & Thoma, F. Taq DNA polymerase blockage at pyrimidine dimers. *Nucleic Acids Res.* **24**, 1578–1579 (1996).
14. Harm, W. Effects of dose fractionation on ultraviolet survival of *Escherichia coli*. *Photochem. Photobiol.* **7**, 73–86 (1968).
15. Leuker, G. Description and application of biodosimetry - a testing procedure for UV systems. *J. Water Supply. Res. Technol. Aqua* **48**, 154–160 (1999).
16. Van Nevel, S. et al. Flow cytometric bacterial cell counts challenge conventional heterotrophic plate counts for routine microbiological drinking water monitoring. *Water Res.* https://doi.org/10.1016/j.watres.2017.01.065 (2017).
17. Ben Said, M., Masahiro, O. & Hassen, A. Detection of viable but non cultivable *Escherichia coli* after UV irradiation using a lytic Qβ phage. *Ann. Microbiol.* **60**, 121–127 (2010).
18. Guo, L. et al. Population and single cell metabolic activity of UV-induced VBNC bacteria determined by CTC-FCM and D2O-labeled Raman spectroscopy. *Environ. Int.* **130**, 104883 (2019).
19. Süß. J., Volz, S., Obst, U. & Schwartz, T. Application of a molecular biology concept for the detection of DNA damage and repair during UV disinfection. *Water Res.* **43**, 3705–3716 (2009).
20. McKinney, C. W. & Pruden, A. Ultraviolet disinfection of antibiotic resistant bacteria and their antibiotic resistance genes in water and wastewater. *Environ. Sci. Technol.* **46**, 13393–13400 (2012).
21. Nocker, A. et al. Assessment of UV-C-induced water disinfection by differential PCR-based quantification of bacterial DNA damage. *J. Microbiol. Methods* **149**, 89–95 (2018).
22. Kauser, I., Ciesielski, M. & Poretsky, R. S. Ultraviolet disinfection impacts the microbial community composition and function of treated wastewater effluent and the receiving urban river. *PeerJ* **7**, e7455 (2019).
23. Beck, S. E. et al. Wavelength dependent UV inactivation and DNA damage of adenovirus as measured by cell culture infectivity and long range quantitative PCR. *Environ. Sci. Technol.* **48**, 591–598 (2014).
24. Nizri, L. et al. Development of a molecular method for testing the effectiveness of UV systems on-site. *Water Res.* **127**, 162–171 (2017).
25. Zaitlin, B. & Watson, S. B. Actinomycetes in relation to taste and odour in drinking water: myths, tenets and truths. *Water Res.* **40**, 1741–1753 (2006).
26. Kip, N. & van Veen, J. A. The dual role of microbes in corrosion. *ISME J.* **9**, 542–551 (2015).
27. Pinto, A. J., Xi, C. & Raskin, L. Bacterial community structure in the drinking water microbiome is governed by filtration processes. *Environ. Sci. Technol.* **46**, 8851–8859 (2012).
28. Laroche, O. et al. Understanding bacterial communities for informed biosecurity and improved larval survival in Pacific oysters. *Aquaculture* **497**, 164–173 (2018).
29. Smith, C. M. & Hill, V. R. Dead-end hollow-fiber ultrafiltration for recovery of diverse microbes from water. *Appl. Environ. Microbiol.* **75**, 5284–5289 (2009).
30. Warnecke, F., Sommaruga, R., Sekar, R., Hofer, J. S. & Pernthaler, J. Abundances, identity, and growth state of actinobacteria in mountain lakes of different UV transparency. *Appl. Environ. Microbiol.* **71**, 5551–5559 (2005).
31. Douki, T. & Cadet, J. Individual determination of the yield of the main UV-induced dimeric pyrimidine photoproducts in DNA suggests a high mutagenicity of CC photolesions. *Biochemistry* https://doi.org/10.1021/bi0022543 (2001).
32. Reichenberger, E. R., Rosen, G., Hershberg, U. & Hershberg, R. Prokaryotic nucleotide composition is shaped by both phylogeny and the environment. *Genome Biol. Evol.* **7**, 1380–1389 (2015).
33. Arrage, A. A., Phelps, T. J., Benoit, R. E. & White, D. C. Survival of subsurface microorganisms exposed to UV radiation and hydrogen peroxide. *Appl. Environ. Microbiol.* **59**, 3545–3550 (1993).
34. Rasuk, M. C. et al. UV-resistant Actinobacteria from high-altitude Andean Lakes: isolation, characterization and antagonistic activities. *Photochem. Photobiol.* **93**, 865–880 (2017).
35. Barka, E. A. et al. Taxonomy, physiology, and natural products of Actinobacteria. *Microbiol. Mol. Biol. Rev.* **80**, 1–43 (2016).
36. Mason, J. M. & Setlow, P. Essential role of small, acid-soluble spore proteins in resistance of *Bacillus subtilis* spores to UV light. *J. Bacteriol.* **167**, 174–178 (1986).
37. Riesenman, P. J. & Nicholson, W. L. Role of the spore coat layers in Bacillus subtilis spore resistance to hydrogen peroxide, artificial UV-C, UV-B, and solar UV radiation. *Appl. Environ. Microbiol.* **66**, 620–626 (2000).
38. Krieg, N. R., et al. (eds) *Bergey's Manual® of Systematic Bacteriology* (Springer, New York, NY, 2010). https://doi.org/10.1007/978-0-387-68572-4_3.
39. Ordoñez, O. F., Flores, M. R., Dib, J. R., Paz, A. & Farías, M. E. Extremophile culture collection from Andean Lakes: extreme pristine environments that host a wide diversity of microorganisms with tolerance to UV radiation. *Microb. Ecol.* **58**, 461–473 (2009).
40. Gupta, R. S. The phylogeny of proteobacteria: relationships to other eubacterial phyla and eukaryotes. *FEMS Microbiol. Rev.* https://doi.org/10.1111/j.1574-6976.2000.tb00547.x (2014).
41. Gupta, R. S. & Mok, A. Phylogenomics and signature proteins for the alpha Proteobacteria and its main groups. *BMC Microbiol.* **7**, 106 (2007).

42. Salcher, M. M., Schaefle, D., Kaspar, M., Neuenschwander, S. M. & Ghai, R. Evolution in action: habitat transition from sediment to the pelagial leads to genome streamlining in Methylophilaceae. *ISME J.* https://doi.org/10.1038/s41396-019-0471-3 (2019).
43. Guarischi-Sousa, R. et al. Complete genome sequence of the potato pathogen Ralstonia solanacearum UY031. *Stand. Genomic Sci.* **11**, 7 (2016).
44. Jara, E. et al. The complex pattern of codon usage evolution in the family Comamonadaceae. *Ecol. Genet. Genomics* **6**, 1–8 (2018).
45. Hahn, M. W., Jezberová, J., Koll, U., Saueressig-Beck, T. & Schmidt, J. Complete ecological isolation and cryptic diversity in Polynucleobacter bacteria not resolved by 16S rRNA gene sequences. *ISME J.* **10**, 1642–1655 (2016).
46. Oguma, K. et al. Determination of pyrimidine dimers in *Escherichia coli* and *Cryptosporidium parvum* during UV light inactivation, photoreactivation, and dark repair. *Appl. Environ. Microbiol.* **67**, 4630–4637 (2001).
47. Liu, J. et al. Occurrence and fate of ultramicrobacteria in a full-scale drinking water treatment plant. *Front. Microbiol.* **9**, 2922 (2018).
48. Ortmann, A. C. & Santos, T. T. L. Spatial and temporal patterns in the Pelagibacteraceae across an estuarine gradient. *FEMS Microbiol. Ecol.* **92**, 133 (2016).
49. Morris, R. M. et al. SAR11 clade dominates ocean surface bacterioplankton communities. *Nature* **420**, 806–810 (2002).
50. Giovannoni, S. J. et al. Genetics: genome streamlining in a cosmopolitan oceanic bacterium. *Science* **309**, 1242–1245 (2005).
51. Malmstrom, R. R., Cottrell, M. T., Elifantz, H. & Kirchman, D. L. Biomass production and assimilation of dissolved organic matter by SAR11 bacteria in the Northwest Atlantic Ocean. *App. Environ. Microbiol.* **71**, 2979–2986 (2005).
52. Moss, T., Dimitrov, S. I. & Houde, D. UV-laser crosslinking of proteins to DNA. *Methods* **11**, 225–234 (1997).
53. Du, K., Liu, J., Zhou, B. & Yuan, R. Isolation of bacteria capable of removing 2-methylisoborneol and effect of cometabolism carbon on biodegradation. *Environ. Eng. Res.* **21**, 256–264 (2016).
54. Wingender, J. Biofilms in drinking water and their role as reservoir for pathogens. *Int. J. Hyg. Environ. Health* **214**, 417–423 (2011).
55. Shin, G.-A., Lee, J.-K., Freeman, R. & Cangelosi, G. A. Inactivation of *Mycobacterium avium* complex by UV irradiation. *Appl. Environ. Microbiol.* **74**, 7067–7069 (2008).
56. Taylor, R. H., Falkinham Iii, J. O., Norton, C. D. & Lechevallier, M. W. Chlorine, chloramine, chlorine dioxide, and ozone susceptibility of *Mycobacterium avium*. *Appl. Environ. Microbiol.* **66**, 1702–1705 (2000).
57. Linden, K. G., Hull, N. & Speight, V. Thinking outside the treatment plant: UV for water distribution system disinfection. *Acc. Chem. Res.* https://doi.org/10.1021/acs.accounts.9b00060 (2019).
58. Henne, K., Kahlisch, L., Brettar, I. & Höfle, M. G. Analysis of structure and composition of bacterial core communities in mature drinking water biofilms and bulk water of a citywide network in Germany. *Appl. Environ. Microbiol.* https://doi.org/10.1128/AEM.06373-11 (2012).
59. Liu, G., et al. Pyrosequencing reveals bacterial communities in unchlorinated drinking water distribution system: an integral study of bulk water, suspended solids, loose deposits, and pipe wall biofilm. *Environ. Sci. Technol.* https://doi.org/10.1021/es5009467 (2014).
60. Regan, J. M., Harrington, G. W., Baribeau, H., Leon, R. D. & Noguera, D. R. Diversity of nitrifying bacteria in full-scale chloraminated distribution systems. *Water Res.* **37**, 197–205 (2003).
61. Lipponen, M. T. T. et al. Occurrence of nitrifiers and diversity of ammonia-oxidizing bacteria in developing drinking water biofilms. *Water Res.* **38**, 4424–4434 (2004).
62. Ling, F., Hwang, C., LeChevallier, M. W., Andersen, G. L. & Liu, W.-T. Core-satellite populations and seasonality of water meter biofilms in a metropolitan drinking water distribution system. *ISME J.* **10**, 582–595 (2016).
63. Navarro-Noya, Y. E. et al. Pyrosequencing analysis of the bacterial community in drinking water wells. *Microb. Ecol.* **66**, 19–29 (2013).
64. Bohrerova, Z., Bohrer, G., Mohanraj, S. M., Ducoste, J. & Linden, K. G. Experimental measurements of fluence distribution in a UV reactor using fluorescent microspheres. *Environ. Sci. Technol.* **39**, 8925–8930 (2005).
65. Qin, K., Struewing, I., Domingo, J. S., Lytle, D. & Lu, J. Opportunistic pathogens and microbial communities and their associations with sediment physical parameters in drinking water storage tank sediments. *Pathogens* **6**, pii: E54 (2017).
66. Zeng, D. N. et al. Analysis of the bacterial communities associated with different drinking water treatment processes. *World J. Microbiol. Biotechnol.* **29**, 1573–1584 (2013).
67. Zaremba-Niedzwiedzka, K. et al. Single-cell genomics reveal low recombination frequencies in freshwater bacteria of the SAR11 clade. *Genome Biol.* **14**, R130 (2013).
68. Henson, M. W. et al. Nutrient dynamics and stream order influence microbial community patterns along a 2914 kilometer transect of the Mississippi River. *Limnol. Oceanogr.* **63**, 1837–1855 (2018).
69. Proctor, C. R. & Hammes, F. Drinking water microbiology—from measurement to management. *Curr. Opin. Biotechnol.* **33**, 87–94 (2015).
70. Lehtola, M. J. et al. Impact of UV disinfection on microbially available phosphorus, organic carbon, and microbial growth in drinking water. *Water Res.* **37**, 1064–1070 (2003).
71. Tokajian, S. T., Hashwa, F. A., Hancock, I. C. & Zalloua, P. A. Phylogenetic assessment of heterotrophic bacteria from a water distribution system using 16S rDNA sequencing. *Can. J. Microbiol.* **51**, 325–335 (2005).
72. Ultee, A., Souvatzi, N., Maniadi, K. & König, H. Identification of the culturable and nonculturable bacterial population in ground water of a municipal water supply in Germany. *J. Appl. Microbiol.* **96**, 560–568 (2004).
73. Tokajian, S. & Hashwa, F. Microbiological quality and genotypic speciation of heterotrophic bacteria isolated from potable water stored in household tanks. *Water Qual. Res. J. Can.* **39**, 64–73 (2004).
74. Mofidi, A. A. & Linden, K. G. Disinfection effectiveness of ultraviolet (UV) light for heterotrophic bacteria leaving biologically active filters. *J. Water Supply. Res. Technol. Aqua.* **53**, 553–566 (2004).
75. Butler, R. C., Lund, V. & Carlson, D. A. Susceptibility of Campylobacter jejuni and Yersinia enterocolitica to UV Radiation. *Appl. Environ. Microbiol.* **53**, 375–378 (1987).
76. Rattanakul, S. & Oguma, K. Inactivation kinetics and efficiencies of UV-LEDs against *Pseudomonas aeruginosa*, *Legionella pneumophila*, and surrogate microorganisms. *Water Res.* https://doi.org/10.1016/j.watres.2017.11.047 (2018).
77. Klindworth, A. et al. Evaluation of general 16S ribosomal RNA gene PCR primers for classical and next-generation sequencing-based diversity studies. *Nucleic Acids Res.* **41**, e1 (2013).
78. Renaud, G., Stenzel, U., Maricic, T., Wiebe, V. & Kelso, J. deML: robust demultiplexing of Illumina sequences using a likelihood-based approach. *Bioinformatics* **31**, 770–772 (2015).
79. Bolyen, E. et al. Reproducible, interactive, scalable and extensible microbiome data science using QIIME 2. *Nat. Biotechnol.* **37**, 852–857 (2019).
80. Callahan, B. J. et al. DADA2: high-resolution sample inference from Illumina amplicon data. *Nat. Methods* **13**, 581–583 (2016).
81. Desantis, T. Z. et al. Greengenes, a chimera-checked 16S rRNA gene database and workbench compatible with ARB. *Appl. Environ. Microbiol.* **72**, 5069–5072 (2006).
82. Price, M. N., Dehal, P. S. & Arkin, A. P. Fasttree: computing large minimum evolution trees with profiles instead of a distance matrix. *Mol. Biol. Evolution* **26**, 1641–1650 (2009).
83. McMurdie, P. J. & Holmes, S. phyloseq: an R package for reproducible interactive analysis and graphics of microbiome census data. *PLoS ONE* **8**, e61217 (2013).
84. R Core Team. *R: A Language and Environment for Statistical Computing* (R Foundation for Statistical Computing, 2018).
85. Bokulich, N. A. et al. Quality-filtering vastly improves diversity estimates from Illumina amplicon sequencing. *Nat. Methods* **10**, 57–59 (2013).
86. Oksanen, J. et al. *vegan: Community Ecology Package. R. Package Version 2.5-4* (2019).
87. Wickham, H. *ggplot2: Elegant Graphics for Data Analysis* (Springer-Verlag, New York, 2016).
88. Wickham, H. tidyverse: Easily Install and Load the 'Tidyverse'. R package version 1.2.1. Available at: https://cran.r-project.org/package=tidyverse (2017).
89. Kassambara, A. *ggpubr: 'ggplot2' Based Publication Ready Plots* (2018).
90. Aphalo, P. J. *Learn R…as you learnt your mother tongue.* (Leanpub, 2016).
91. Love, M. I., Huber, W. & Anders, S. Moderated estimation of fold change and dispersion for RNA-seq data with DESeq2. *Genome Biol.* **15**, 550 (2014).
92. Yu, G., Smith, D. K., Zhu, H., Guan, Y. & Lam, T. T.-Y. ggtree: an r package for visualization and annotation of phylogenetic trees with their covariates and other associated data. *Methods Ecol. Evol.* **8**, 28–36 (2017).

ACKNOWLEDGEMENTS

We thank the employees at Norrvatten AB for contributions in planning the experiments at full scale with a special thanks to Jamileh Mirzai and lab colleagues for assistance in the lab. This study was funded by Sweden Water Research AB, DRICKS center for drinking water research, Swedish Water and Wastewater Association (SVU), Swedish Civil Contingencies Agency (MSB), and Norrvatten AB. Open access funding provided by Lund University.

AUTHOR CONTRIBUTIONS

K.P., L.H., R.D., M.F., C.J.P., and P.R. planned the experiments. K.P., L.H., and R.D. conducted the sampling. K.P., K.J., R.D., and E.S. did the experimental work. K.P., J.A., and C.Ö. performed data analysis. K.P., C.J.P., and P.R. drafted the manuscript. All authors contributed to the final manuscript.

COMPETING INTERESTS

The authors declare no competing interests.

ADDITIONAL INFORMATION

Supplementary information is available for this paper at https://doi.org/10.1038/s41545-020-0057-7.

Correspondence and requests for materials should be addressed to C.J.P.

Reprints and permission information is available at http://www.nature.com/reprints

Publisher's note Springer Nature remains neutral with regard to jurisdictional claims in published maps and institutional affiliations.

Supplementary information – Figures and Tables

Impact of UV irradiation at full scale on bacterial communities in drinking water

Kristjan Pullerits[1,2], Jon Ahlinder[3], Linda Holmer[4], Emelie Salomonsson[3], Caroline Öhrman[3], Karin Jacobsson[5], Rikard Dryselius[6], Mats Forsman[3], Catherine J. Paul[1,7,*], Peter Rådström[1]

[1]Applied Microbiology, Department of Chemistry, Lund University, P.O. Box 124, SE-221 00 Lund, Sweden

[2]Sweden Water Research AB, Ideon Science Park, Scheelevägen 15, SE-223 70 Lund, Sweden

[3]FOI, Swedish Defence Research Agency, Cementvägen 20, SE-906 21 Umeå, Sweden

[4]Norrvatten, Box 2093, SE-169 02 Solna, Sweden

[5]Swedish Food Agency, Box 622, SE-751 26 Uppsala, Sweden, current address: Swedish University of Agricultural Sciences, Box 7036, SE-750 07 Uppsala, Sweden

[6]Swedish Food Agency, Box 622, SE-751 26 Uppsala, Sweden, current address: Public Health Agency of Sweden, SE-171 82 Solna, Sweden

[7]Water Resources Engineering, Department of Building and Environmental Technology, Lund University, P.O. Box 118, SE-221 00 Lund, Sweden

**corresponding author*

Table of contents

Supplementary Figure 1 – PCoA plot using Bray Curtis distance.

Supplementary Figure 2 – PCoA plot using Bray Curtis distance with ADONIS.

Supplementary Figure 3 – Alpha diversity measures.

Supplementary Figure 4 – DESeq2 output figure.

Supplementary Figure 5 – Phylogenetic tree showing all identified ASVs.

Supplementary Figure 6 – Impact of UV dose at Phylum level.

Supplementary Figure 7 – Impact of UV dose at Class level.

Supplementary Figure 8 – Impact of UV dose at Order level.

Supplementary Figure 9 – Impact of UV dose at Family level.

Supplementary Figure 10 – Impact of UV dose at Genus level.

Supplementary Figure 11 – Impact of UV irradiation and storage at Phylum level.

Supplementary Figure 12 – Impact of UV irradiation and storage at Class level.

Supplementary Figure 13 – Impact of UV irradiation and storage at Order level.

Supplementary Figure 14 – Impact of UV irradiation and storage at Family level.

Supplementary Figure 15 – Impact of UV irradiation and storage at Genus level.

Supplementary Figure 16 – Impact of storage at Family level for non-irradiated samples.

Supplementary Figure 17 – Heterotrophic plate counts after 3 days incubation.

Supplementary Table 1 – Coliform and *Escherichia coli* counts.

Supplementary Table 2 – Output data from DESeq2 analysis.

Supplementary Table 3 – Representative sequences from each ASVid from DESeq2 analysis.

Supplementary Table 4 – Water quality parameters.

Supplementary Table 5 – Flow cytometry microbial data

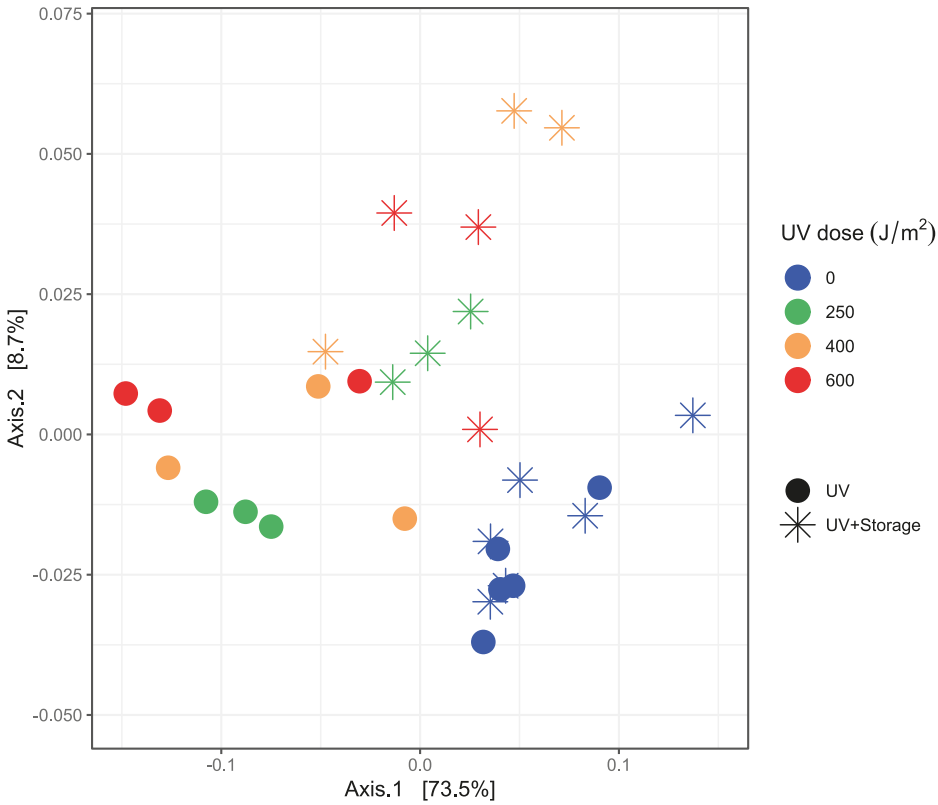

Supplementary Figure 1. Principal coordinates analysis (PCoA) plot based on Bray Curtis-dissimilarity of the bacterial communities which were analyzed from water exposed to UV (0, 250, 400 and 600 J/m^2, blue, green, orange and red, circles) or after storage (6 day storage in 7 °C, stars). n = 3 for each UV dose and sample type, n = 5 UV 0 J/m^2 and n = 6 for storage 0 J/m^2.

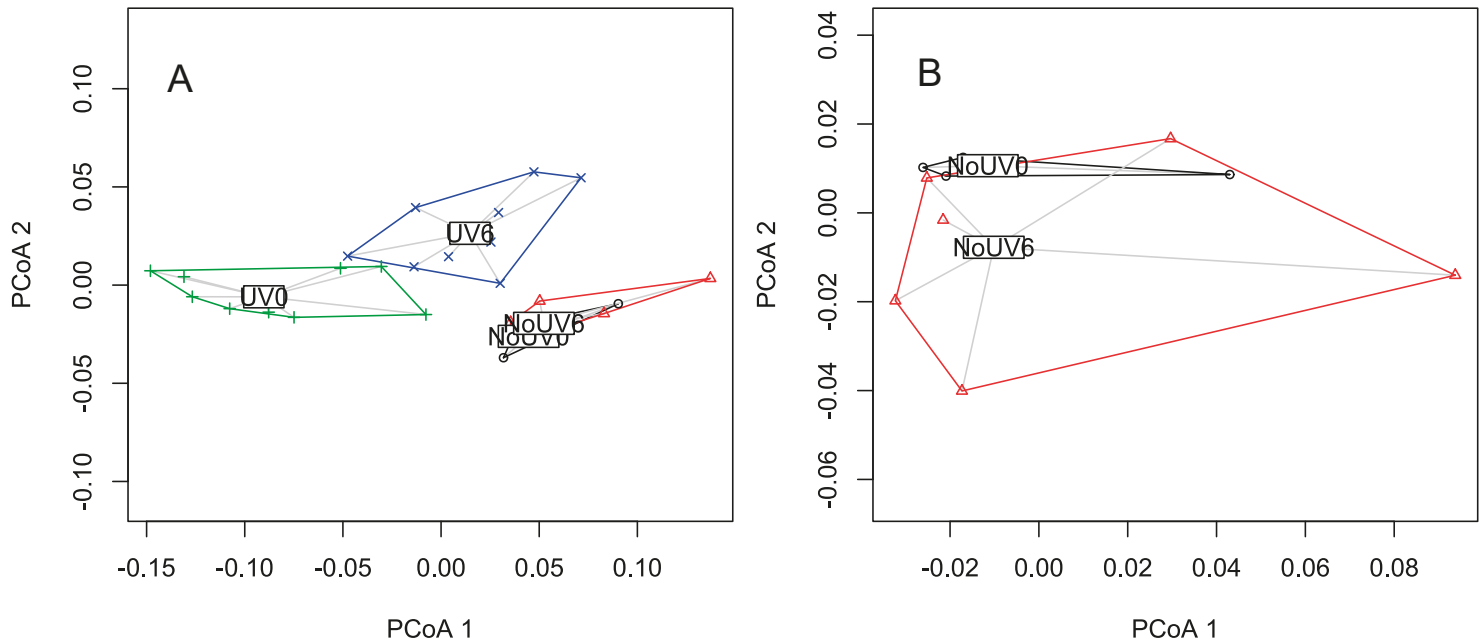

Supplementary Figure 2. Principal coordinates analysis (PCoA) plot based on Bray Curtis-dissimilarity of the bacterial communites showing samples treated at different UV doses. UV0 = UV treated samples (n = 9), UV6 = UV treated and stored samples (n = 9), NoUV0 = non-irradiated samples (n = 5) and NoUV6 = non-irradiated, stored samples (n = 6). (A) shows a significant clustering by UV0, UV6, NoUV0 and NoUV6, $P < 0.001$, $R^2 = 0.62$ (ADONIS). (B) shows a non-significant clustering by filtering out NoUV0 and NoUV6 samples, $P = 0.36$, $R^2 = 0.10$ (ADONIS).

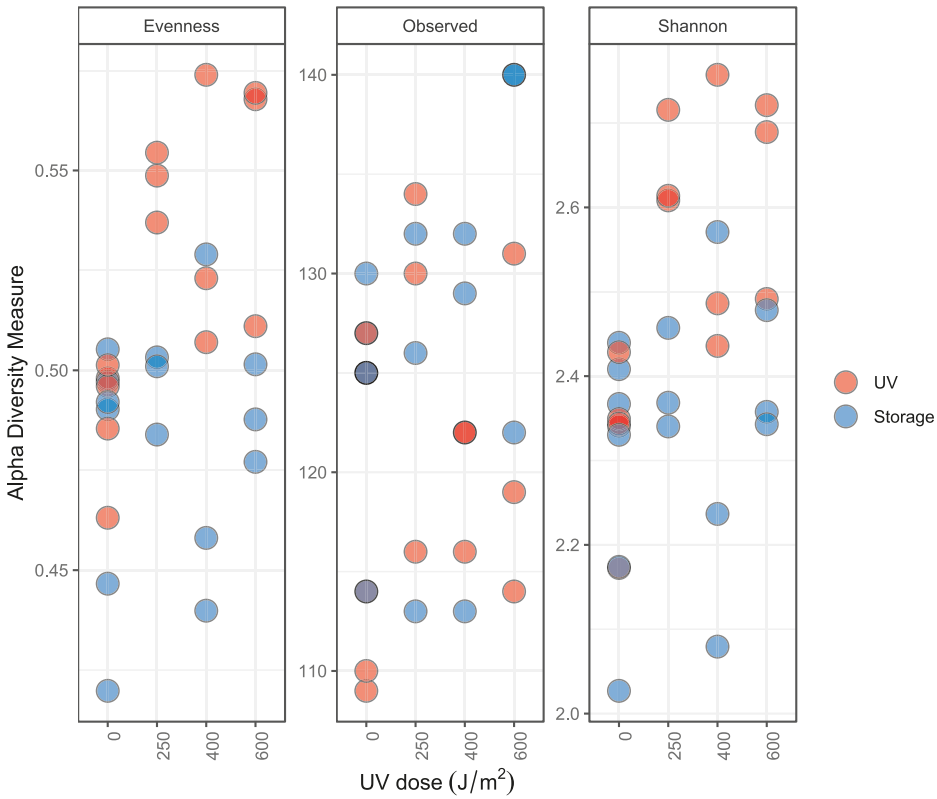

Supplementary Figure 3. Alpha diversity measures calculated from 16S rRNA gene amplicon sequencing of samples irradiated at different UV doses (blue) or after storage (red, 6 day storage in 7 °C).

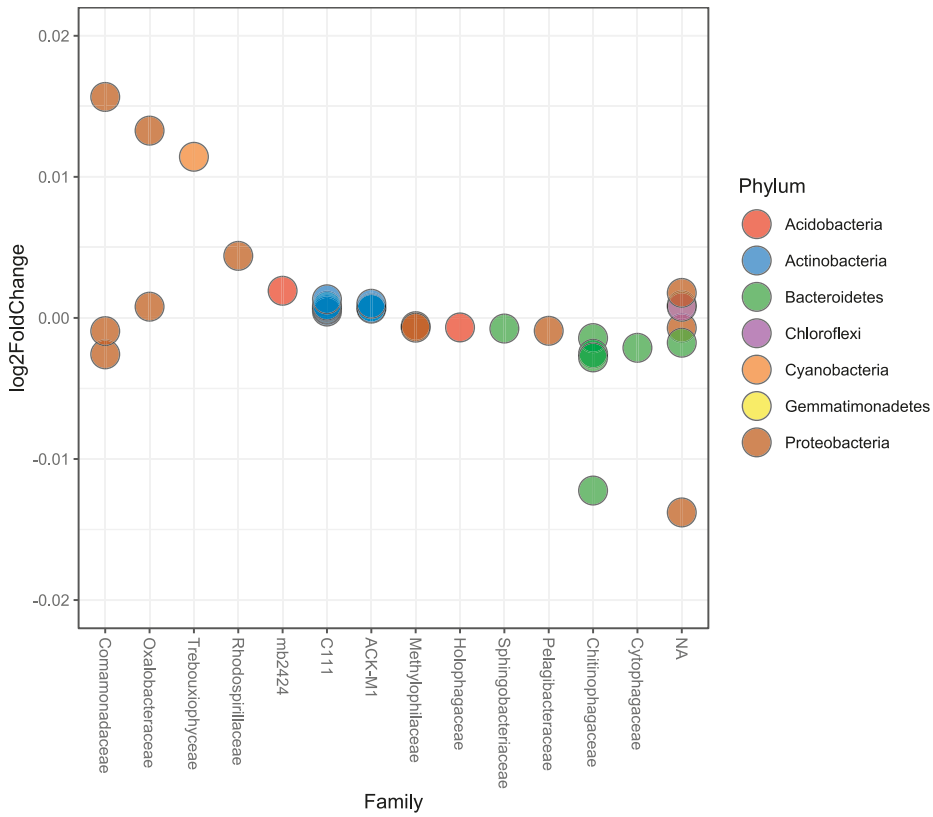

Supplementary Figure 4. Differential abundance analysis of the bacterial community using DESeq2 and comparing water samples exposed (n = 9) and not exposed to UV (n = 5) ($P_{adjusted} < 0.05$). Showing the log2fold change of the significant amplicon sequence variants (ASVs) displaying Families. One ASV identified as *Pelagibacteraceae* with a log2fold change of -26 is not shown in the figure.

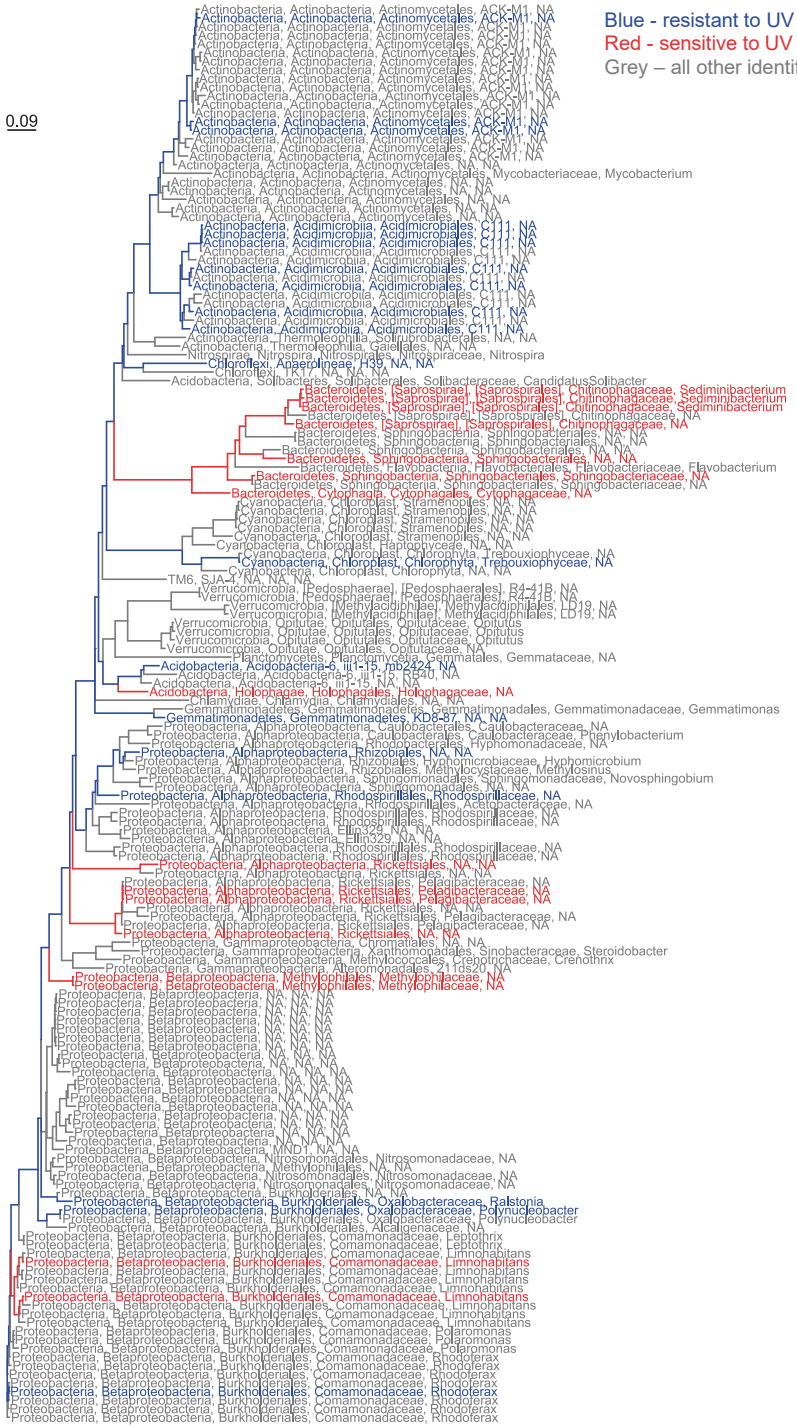

Supplementary Figure 5. Inferred phylogenetic tree showing ASVs identified as sensitive and resistant to UV from DESeq2 analysis (Supplementary Figure 4 and Supplementary Table 2). A negative log2fold change was considered a UV-sensitive taxa (red) and positive log2fold change as a UV-resistant taxa (blue), grey taxa are all other taxa identified in the study. The scale bar shows an estimate of the substitutions per nucleotide position.

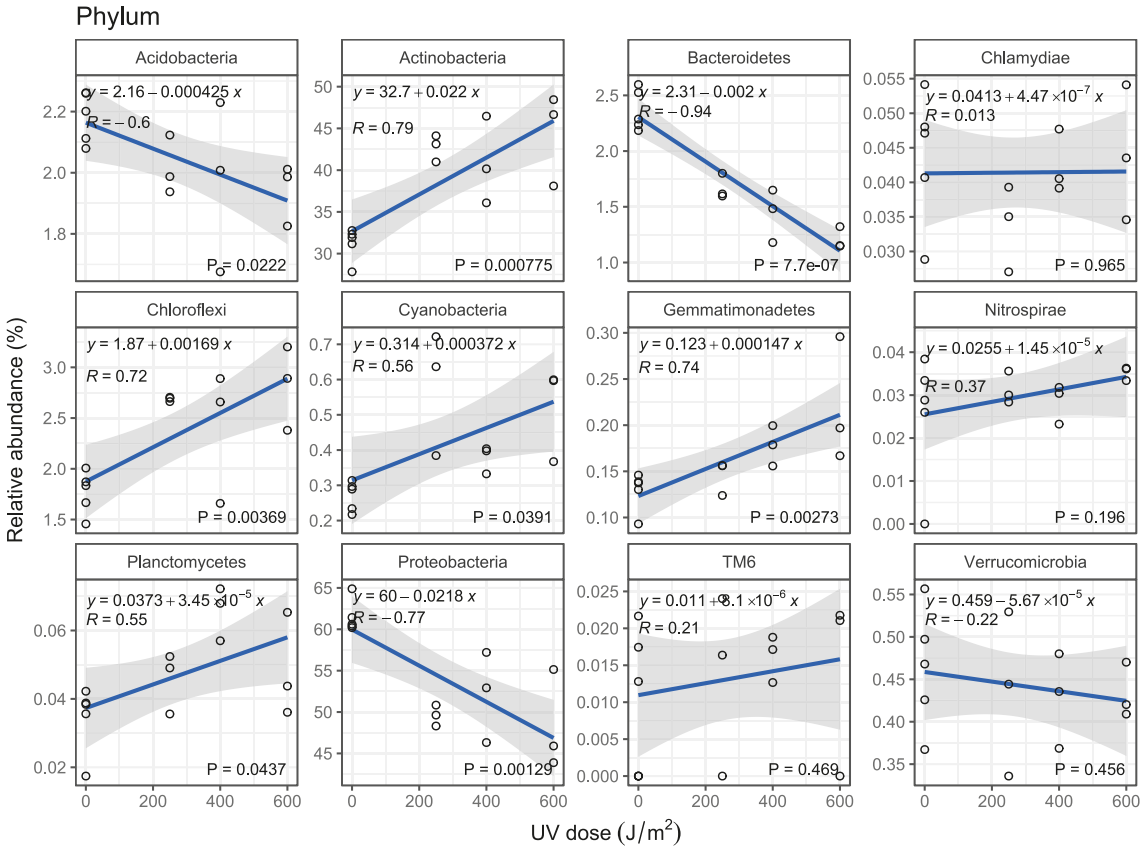

Supplementary Figure 6. Impact of UV dose at Phylum level showing linear regressions (blue line) of the relative taxonomic abundance against UV dose. The grey transparent area shows the 95% confidence interval for the regression line. Taxa are ordered in alphabetical order.

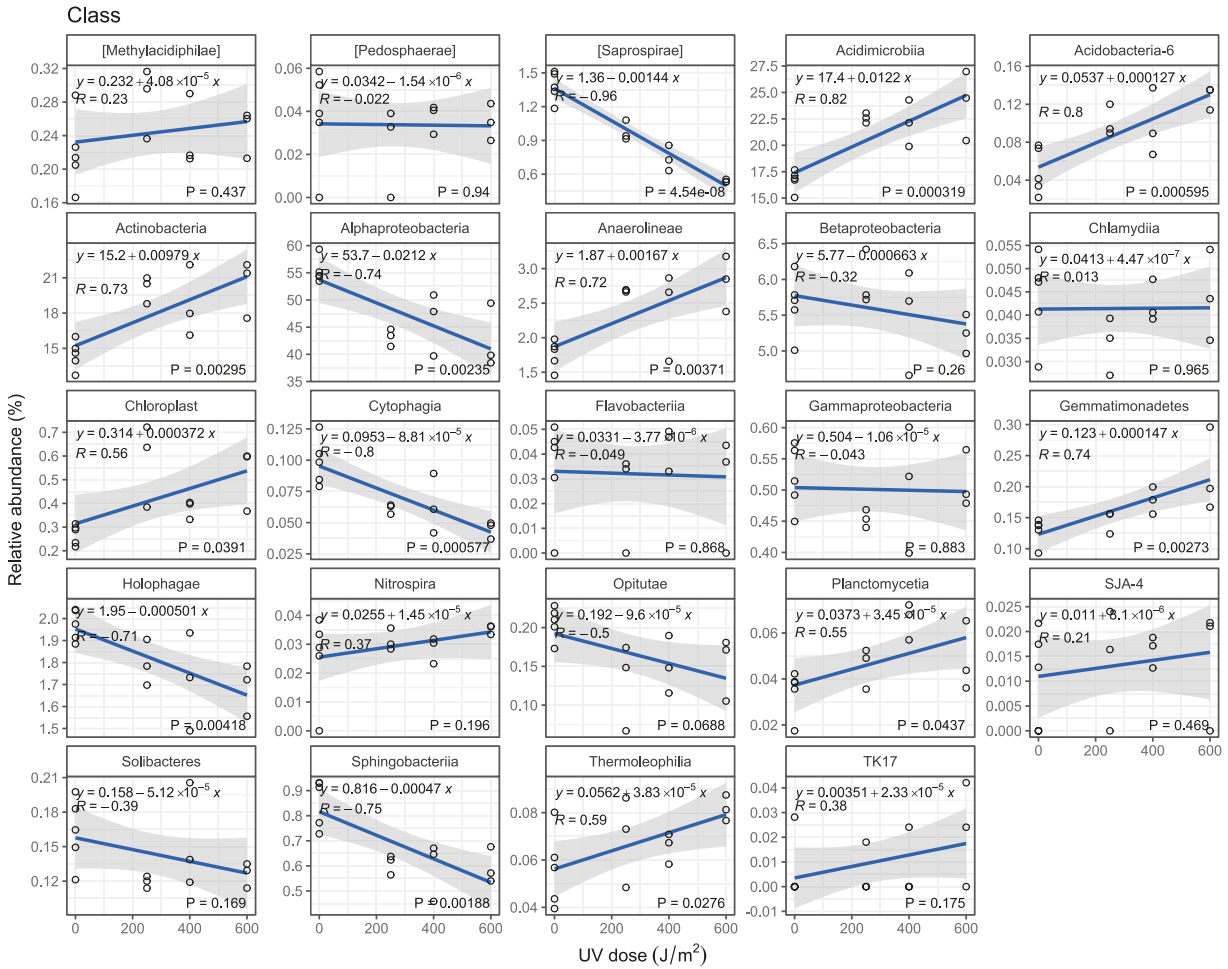

Supplementary Figure 7. Impact of UV dose at Class level showing linear regressions (blue line) of the relative taxonomic abundance against UV dose. The grey transparent area shows the 95% confidence interval for the regression line. Taxa are ordered in alphabetical order.

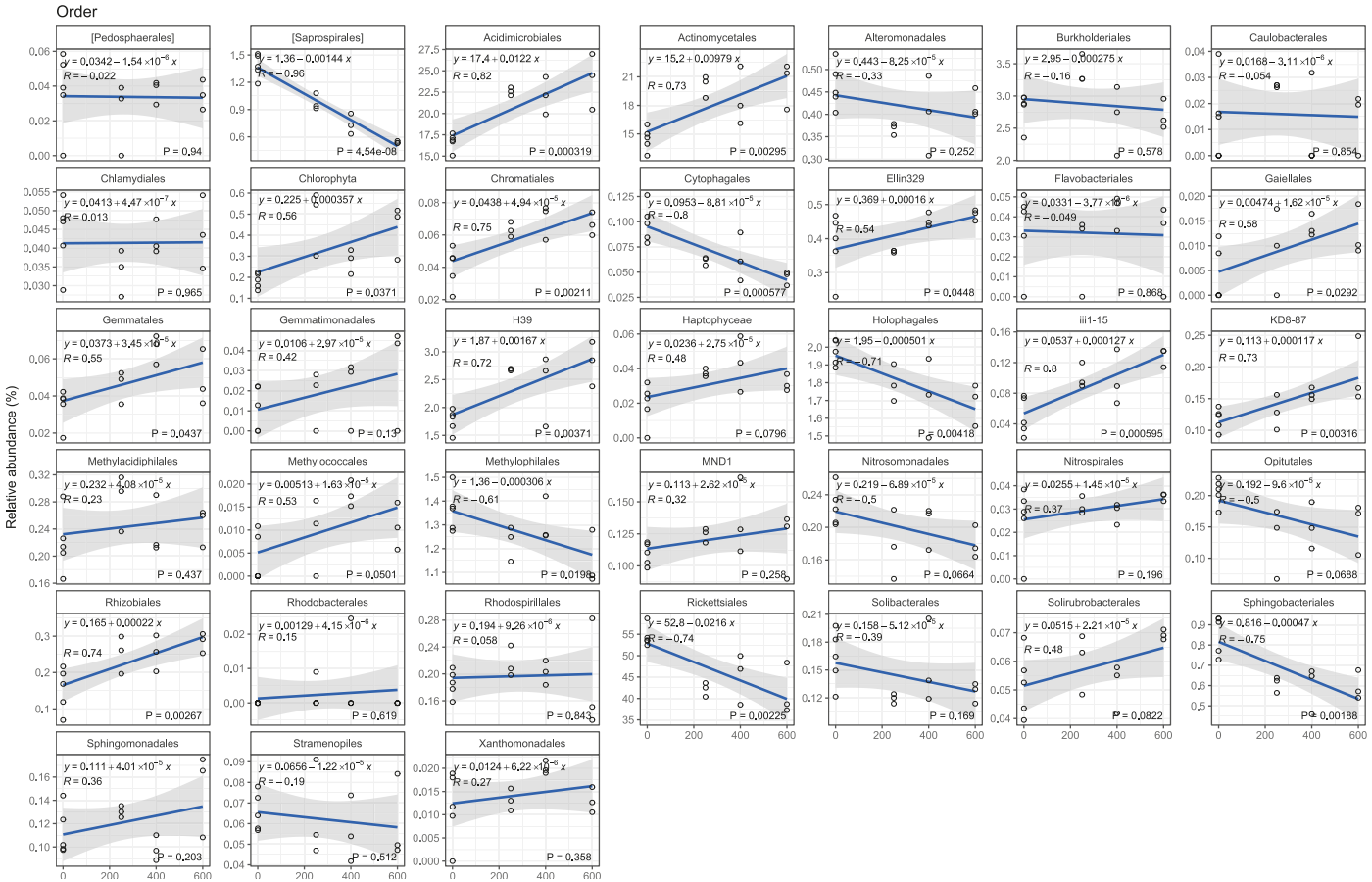

Supplementary Figure 8. Impact of UV dose at Order level showing linear regressions (blue line) of the relative taxonomic abundance against UV dose. The grey transparent area shows the 95% confidence interval for the regression line. Taxa are ordered in alphabetical order.

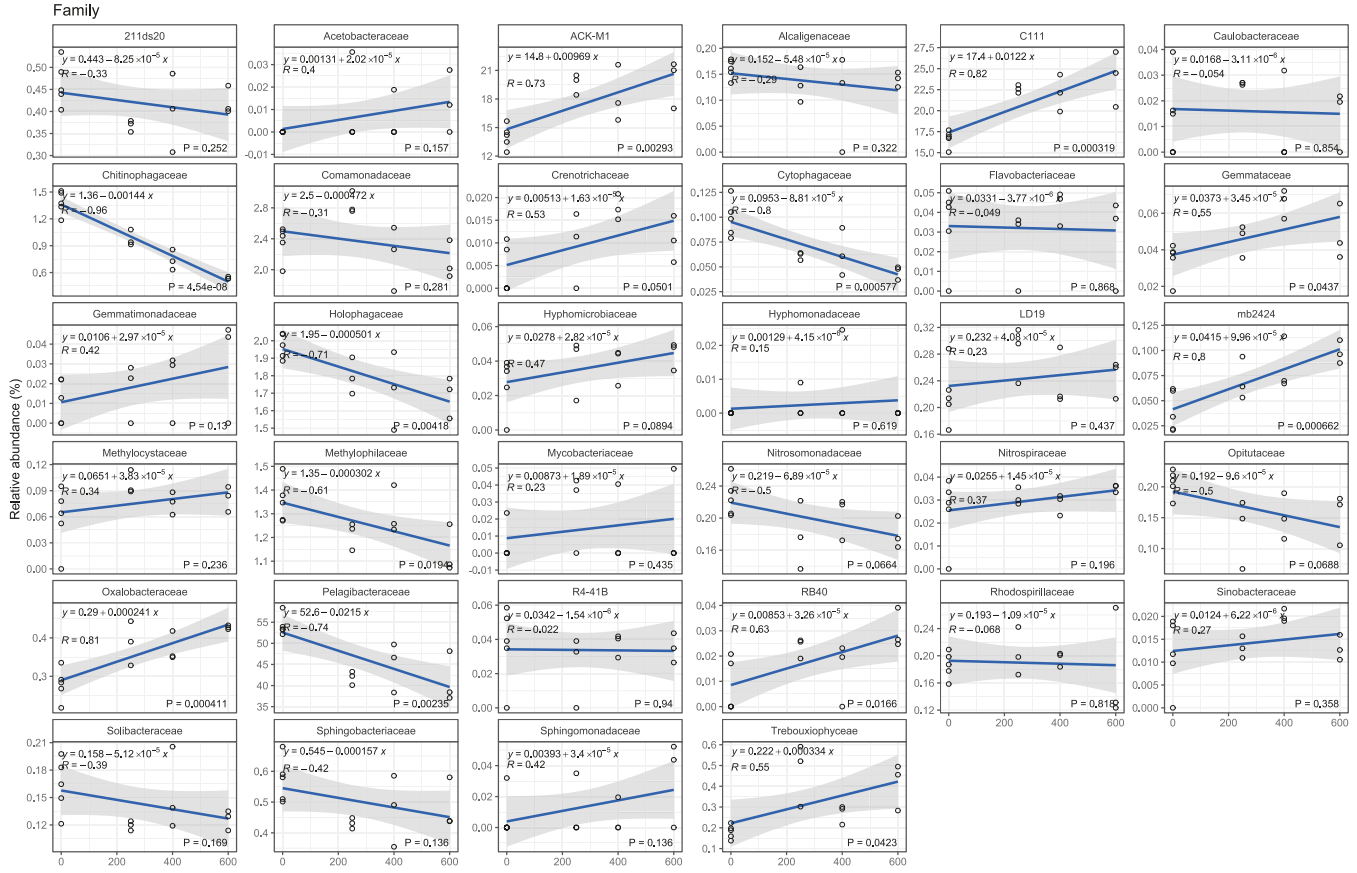

Supplementary Figure 9. Impact of UV dose at Family level showing linear regressions (blue line) of the relative taxonomic abundance against UV dose. The grey transparent area shows the 95% confidence interval for the regression line. Taxa are ordered in alphabetical order.

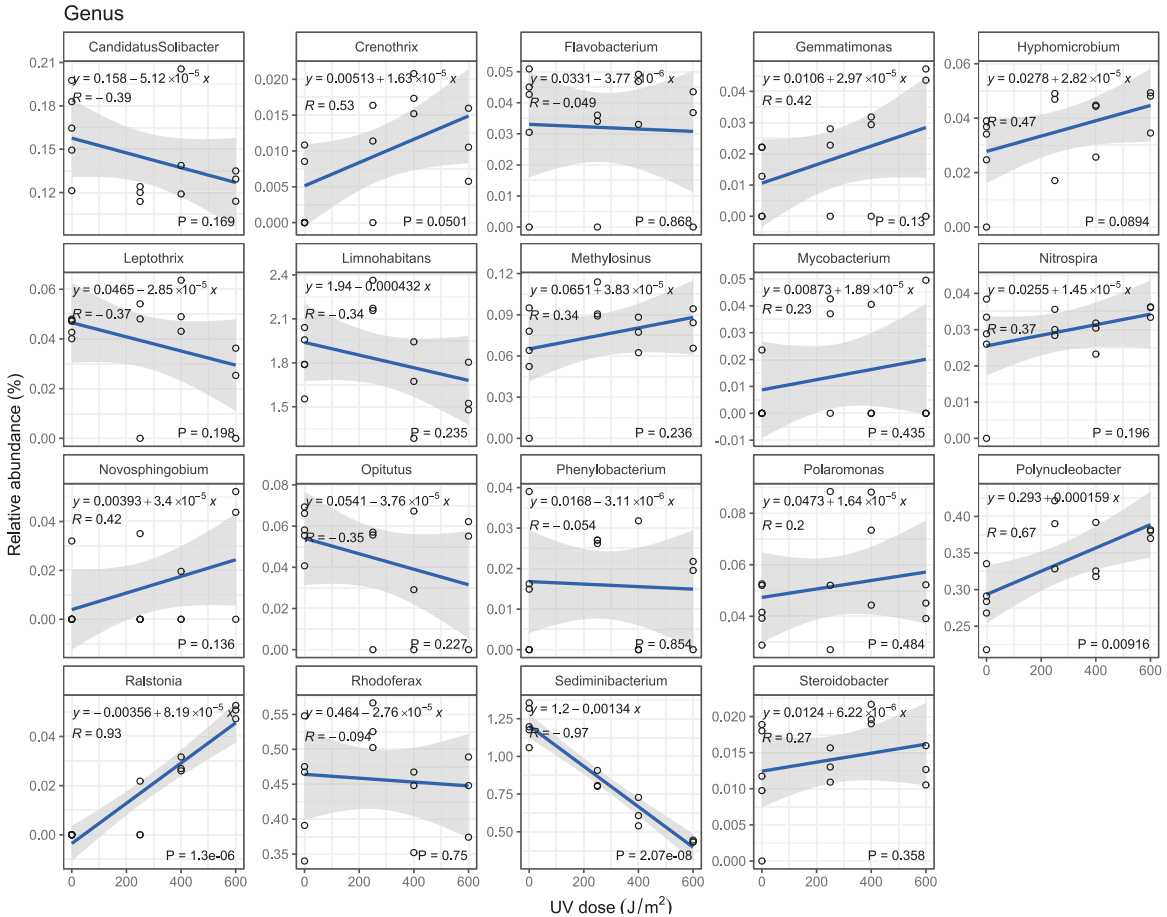

Supplementary Figure 10. Impact of UV dose at Genus level showing linear regressions (blue line) of the relative taxonomic abundance against UV dose. The grey transparent area shows the 95% confidence interval for the regression line. Taxa are ordered in alphabetical order.

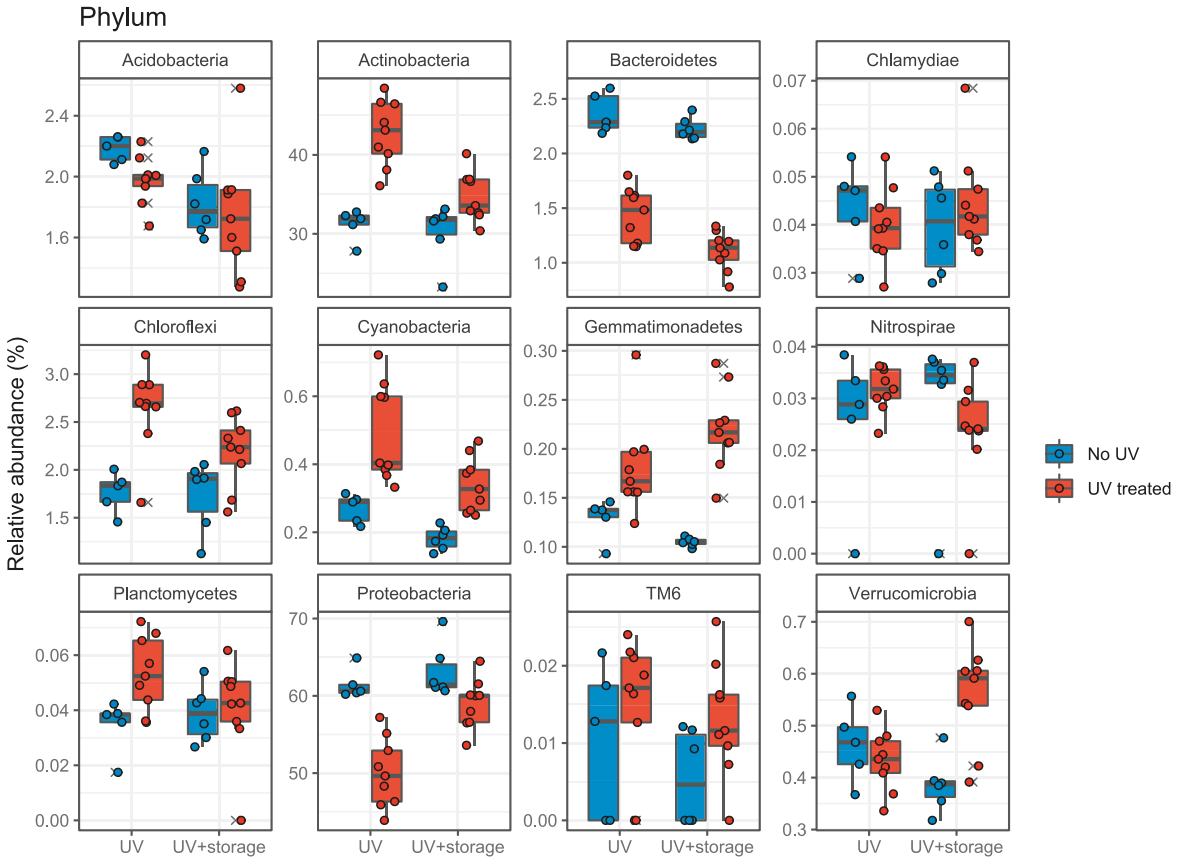

Supplementary Figure 11. Impact of UV treatment and storage on the relative taxonomic abundance at phylum level. Taxa are ordered in alphabetical order. The boxes show the interquartile range, the line inside each box represents the median, whiskers show maximum and minimum values and the crosses show outliers. Samples irradiated at different UV doses were grouped for this analysis.

Supplementary Figure 12. Impact of UV treatment and storage on the relative taxonomic abundance at class level. Taxa are ordered in alphabetical order. The boxes show the interquartile range, the line inside each box represents the median, whiskers show maximum and minimum values and the crosses show outliers. Samples irradiated at different UV doses were grouped for this analysis.

Supplementary Figure 13. Impact of UV treatment and storage on the relative taxonomic abundance at order level. Taxa are ordered in alphabetical order. The boxes show the interquartile range, the line inside each box represents the median, whiskers show maximum and minimum values and the crosses show outliers. Samples irradiated at different UV doses were grouped for this analysis.

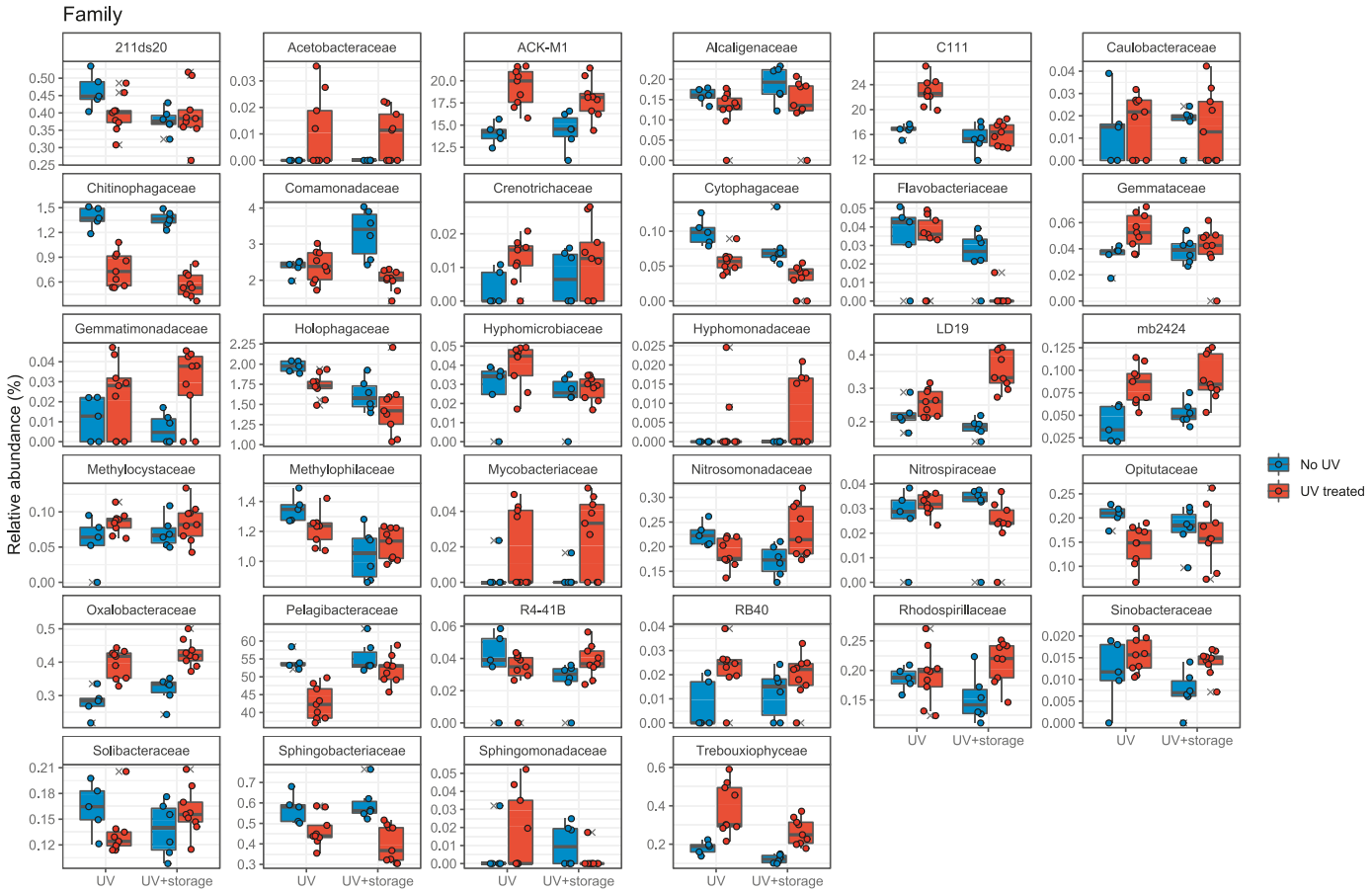

Supplementary Figure 14. Impact of UV treatment and storage on the relative taxonomic abundance at family level. Taxa are ordered in alphabetical order. The boxes show the interquartile range, the line inside each box represents the median, whiskers show maximum and minimum values and the crosses show outliers. Samples irradiated at different UV doses were grouped for this analysis.

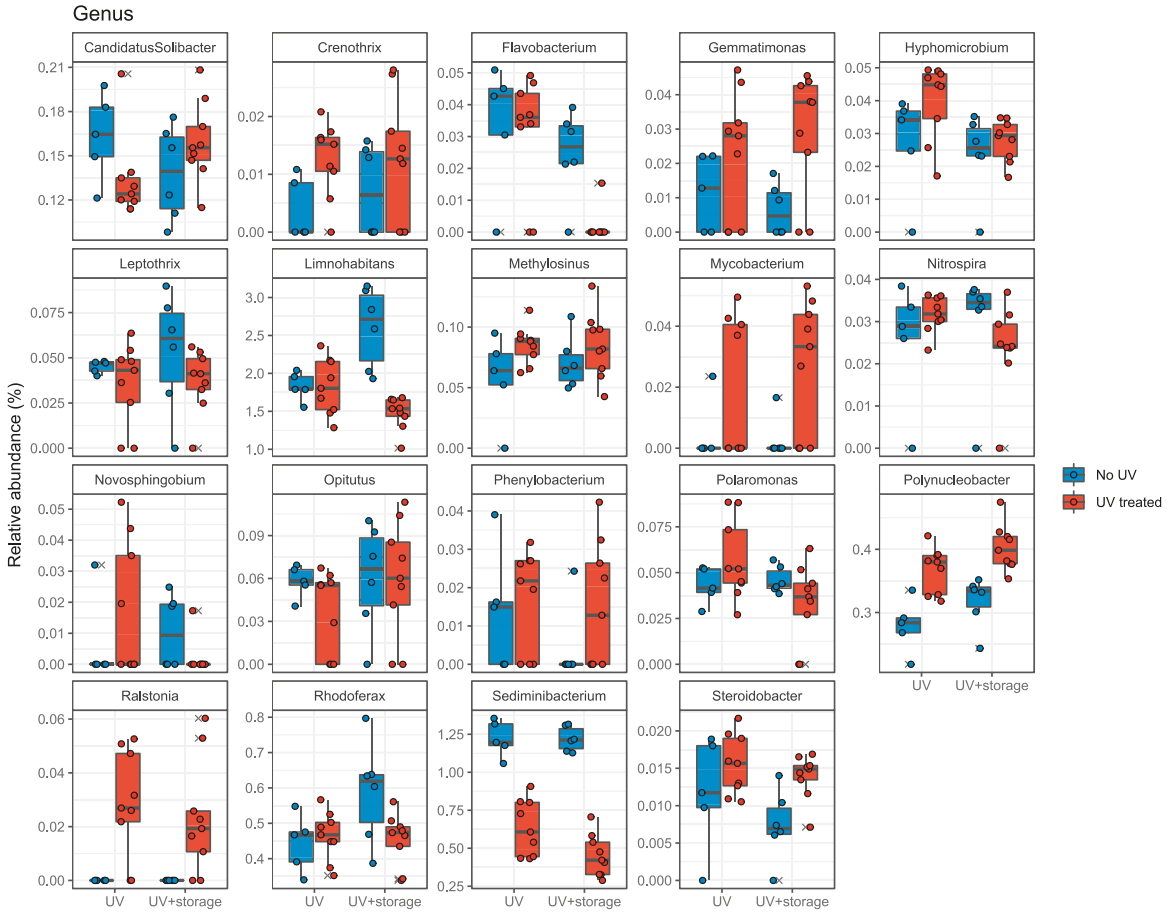

Supplementary Figure 15. Impact of UV treatment and storage on the relative taxonomic abundance at genus level. Taxa are ordered in alphabetical order. The boxes show the interquartile range, the line inside each box represents the median, whiskers show maximum and minimum values and the crosses show outliers. Samples irradiated at different UV doses were grouped for this analysis.

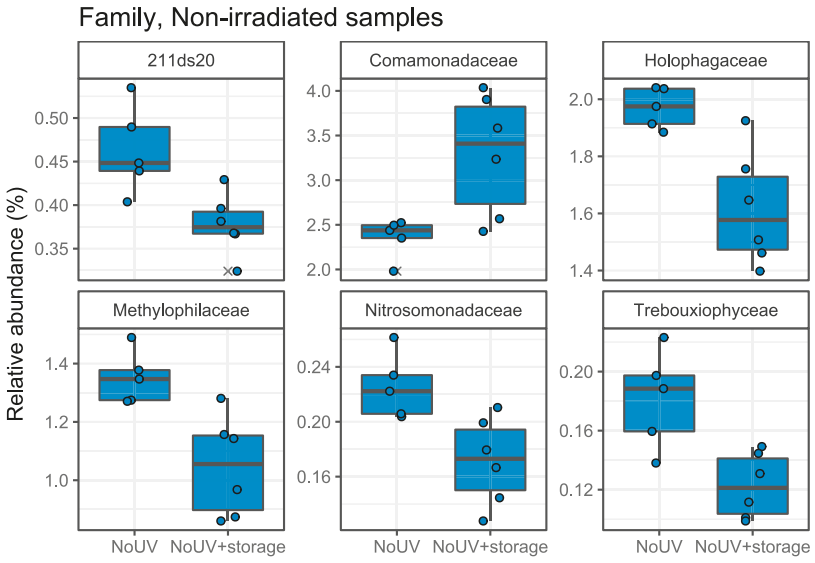

Supplementary Figure 16. Impact of storage on the relative taxonomic abundance at genus level for the non-irradiated samples. Only taxa that had a significant change are shown (P<0.05, one-way ANOVA). Taxa are ordered in alphabetical order. The boxes show the interquartile range, the line inside each box represents the median, whiskers show maximum and minimum values and the crosses show outliers. NoUV samples means no storage and NoUV+storage samples have been stored.

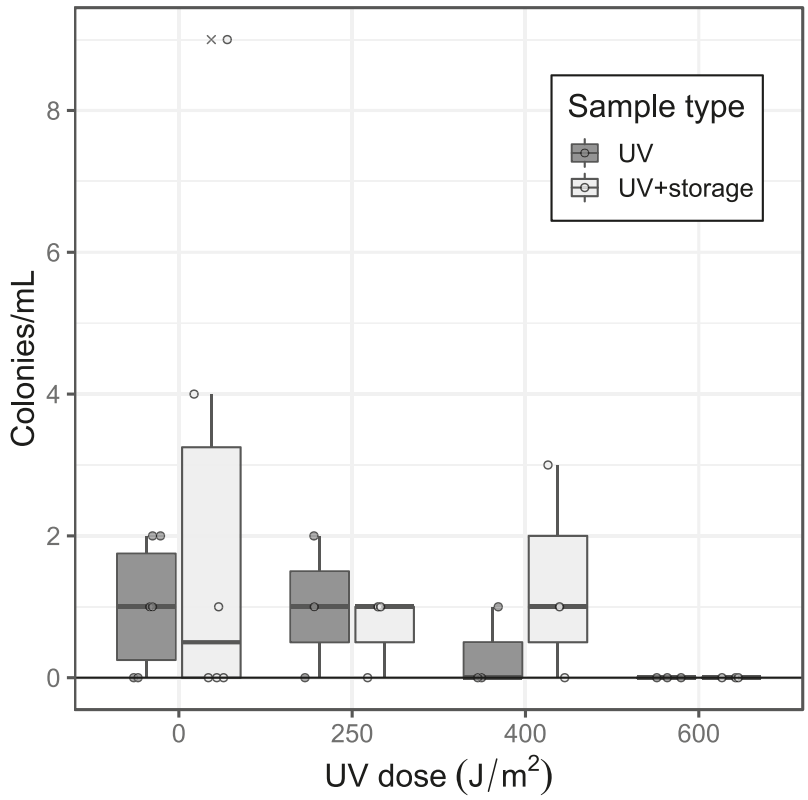

Supplementary Figure 17. Heterotrophic plate counts after 3 days incubation at different UV doses. Water was exposed to different UV doses (dark grey) or exposed and then stored for 6 days at 7 °C (light grey). n = 5 for UV dose of 0 J/m2 and n = 6 for storage not exposed to UV. n = 3 for all UV doses >0 and sample type. The boxes show the interquartile range, the line inside each box represents the median, whiskers show maximum and minimum values and the crosses show outliers.

Supplementary Table 1. Coliforms and *Escherichia coli* counts for the different samples.

Sample	Filtered volume	Volume of eluate	Coliforms	E. coli
Before UV repl. 1	60 L	640 ml	2.0 in 9.38 L	<1.0 in 9.38 L
Before UV repl. 2	60 L	620 ml	1.0 in 9.68 L	1.0 in 9,68 L
Before UV repl. 3	60 L	560 ml	2.0 in 10.72 L	2.0 in 10.72 L
UV 400 J/m^2 repl. 1	60 L	580 ml	<1.0 in 10.34 L	<1.0 in 10.34 L
UV 400 J/m^2 repl. 2	60 L	580 ml	<1.0 in 10.34 L	<1.0 in 10.34 L
UV 400 J/m^2 repl. 3	60 L	600 ml	<1.0 in 10.0 L	<1.0 in 10.0 L
UV 600 J/m^2 repl. 1	60 L	590 ml	<1.0 in 10.17 L	<1.0 in 10.17 L
UV 600 J/m^2 repl. 2	60 L	600 ml	<1.0 in 10.0 L	<1.0 in 10.0 L
UV 600 J/m^2 repl. 3	60 L	600 ml	<1.0 in 10.0 L	<1.0 in 10.0 L

Supplementary Table 2. Output data from DESeq2 analysis. ASVs are ordered with descending log2fold change. A negative log2fold change was considered a UV-sensitive taxa and positive log2fold change as a UV-resistant taxa. The GC content was calculated from the representative sequences obtained from QIIME2. The bold line separates from a positive to negative log2fold change. See Supplementary Table 3 for full DNA sequences for the different ASVids.

ASVid	baseMean	log2FoldChange	pvalue	padj	Domain	Phylum	Class	Order	Family	Genus	Species	GC content (%)
787ec8478ea75e9a298de113ec8abeca	21.9333836	0.015665358	0.00118714	0.00910139	Bacteria	Proteobacteria	Betaproteobacteria	Burkholderiales	Comamonadaceae	Rhodoferax	NA	52.9274
3638f2062c305c79df283ef573a10b97	13.5399138	0.013276245	4.12E-06	8.30E-05	Bacteria	Proteobacteria	Betaproteobacteria	Burkholderiales	Oxalobacteraceae	Ralstonia	NA	53.39579
1f18cf29076957c15e3c64478934c53f	13.7491699	0.011422062	0.00642603	0.03233095	Bacteria	Cyanobacteria	Chloroplast	Chlorophyta	Trebouxiophyceae	NA	NA	52.83951
d8534dd07e84a8fee208828b561e691a	22.4134379	0.004397365	0.00877791	0.04156599	Bacteria	Proteobacteria	Alphaproteobacteria	Rhodospirillales	Rhodospirillaceae	NA	NA	57.46269
73ccfd0bf411b690447a30d9c9f59e00	51.1004044	0.001923987	0.00022934	0.002172	Bacteria	Acidobacteria	Acidobacteria-6	iii1-15	mb2424	NA	NA	55.37383
98fb8bf25b5baca1e947628c9a1e2d13	85.6984301	0.001772723	1.20E-05	0.00016869	Bacteria	Proteobacteria	Alphaproteobacteria	Rhizobiales	NA	NA	NA	54.22886
970ed30e2fa7430e8d50f91b564fe97f	777.487376	0.001319083	1.19E-07	4.79E-06	Bacteria	Actinobacteria	Acidimicrobiia	Acidimicrobiales	C111	NA	NA	56.82382
ae71bf7c99d3583a2d8841e5911c5716	6445.5958	0.001001855	9.17E-06	0.00014762	Bacteria	Actinobacteria	Actinobacteria	Actinomycetales	ACK-M1	NA	NA	53.56265
adee15fbdd4b70ff88b7e68a51afab75	110.258285	0.000901658	0.0070062	0.03418179	Bacteria	Gemmatimonadetes	Gemmatimonadetes	KD8-87	NA	NA	NA	59.18854
55ff6faf3d171ef953a5f98ffa6d7dd1	2553.47802	0.000869351	2.19E-07	7.06E-06	Bacteria	Actinobacteria	Acidimicrobiia	Acidimicrobiales	C111	NA	NA	56.82382
75776764065cf5111d6a186068cbb3ff	86.3220136	0.000796375	0.0041171	0.02367332	Bacteria	Proteobacteria	Betaproteobacteria	Burkholderiales	Oxalobacteraceae	Polynucleobacter	NA	53.52113
dfb115cfb1c595fd0a2611c733c58d00	1762.90728	0.000783882	0.00127437	0.00932606	Bacteria	Chloroflexi	Anaerolineae	H39	NA	NA	NA	55.97015
88b5b5240649749ca876d10823045b01	393.560744	0.000777699	8.84E-06	0.00014762	Bacteria	Actinobacteria	Acidimicrobiia	Acidimicrobiales	C111	NA	NA	56.57568
d76a3d4c5d8913aeb4deac6f162ca3c4	76.3349585	0.000725619	0.00626984	0.03233095	Bacteria	Actinobacteria	Acidimicrobiia	Acidimicrobiales	C111	NA	NA	56.0794
0167e1bd8560c962ee9e440f30318dfb	382.805674	0.000719881	0.00449022	0.02492844	Bacteria	Actinobacteria	Actinobacteria	Actinomycetales	ACK-M1	NA	NA	54.05405
c366064866eaed18a54d15640272ab34	529.647152	0.000658888	2.17E-05	0.00026916	Bacteria	Actinobacteria	Actinobacteria	Actinomycetales	ACK-M1	NA	NA	55.52826
a68b37133e9d3da604674d143353033d	2123.27196	0.000650322	1.26E-05	0.00016869	Bacteria	Actinobacteria	Acidimicrobiia	Acidimicrobiales	C111	NA	NA	54.47761
887bc7033b46d960e893caceb711700b	1107.10402	0.000585103	2.35E-05	0.00027073	Bacteria	Actinobacteria	Acidimicrobiia	Acidimicrobiales	C111	NA	NA	54.72637
921175c5e69a32e289e597a77764eac9	6957.01272	0.000452618	3.28E-05	0.00035176	Bacteria	Actinobacteria	Acidimicrobiia	Acidimicrobiales	C111	NA	NA	54.22886
fdf79b2352da82f67612a0d3fa98c598	678.509997	-0.000582302	0.00282661	0.01820334	Bacteria	Proteobacteria	Betaproteobacteria	Methylophilales	Methylophilaceae	NA	NA	52.45902
7a4df51ab28e00fbe0fbf630eedd63c7	1407.9248	-0.000674692	0.00030281	0.00270845	Bacteria	Acidobacteria	Holophagae	Holophagales	Holophagaceae	NA	NA	52.45902
03c021662d88f96cbdfdacd21420f0cd	301.064157	-0.000691472	0.00146696	0.01026875	Bacteria	Proteobacteria	Betaproteobacteria	Methylophilales	Methylophilaceae	NA	NA	52.69321
1c14e085e85aef7ec5a50101b7d9f363	126.783097	-0.000714745	0.00547804	0.0293988	Bacteria	Proteobacteria	Alphaproteobacteria	Rickettsiales	NA	NA	NA	48.50746
bbdd9b6e83118f34fd27596a877f64e0	279.548091	-0.000753045	0.01057449	0.04864265	Bacteria	Bacteroidetes	Sphingobacteriia	Sphingobacteriales	Sphingobacteriaceae	NA	NA	49.76303
aca380d3d06d653c6296f75364e4e6fb	36052.7432	-0.00091385	0.00108409	0.0087269	Bacteria	Proteobacteria	Alphaproteobacteria	Rickettsiales	Pelagibacteraceae	NA	NA	47.01493
bdfac780ed7ad9d5d57bccef8f271bf6	82.3875369	-0.000937381	0.0030854	0.01910574	Bacteria	Proteobacteria	Betaproteobacteria	Burkholderiales	Comamonadaceae	Limnohabitans	NA	53.86417
d451827eb1e44147c6c2f657cc7e6587	84.3338686	-0.001429358	1.90E-06	5.11E-05	Bacteria	Bacteroidetes	[Saprospirae]	[Saprospirales]	Chitinophagaceae	NA	NA	46.91943
8a388b2fedb1e9ce85fd666ae0bd9e47	57.0044225	-0.001757148	0.00016534	0.00166369	Bacteria	Bacteroidetes	Sphingobacteriia	Sphingobacteriales	NA	NA	NA	49.05213
5ff2cac14309cf649d4337bfd19c3e03	56.3131683	-0.00212013	3.86E-06	8.30E-05	Bacteria	Bacteroidetes	Cytophagia	Cytophagales	Cytophagaceae	NA	NA	48.21853
a9a366c63a209df0aa5d56031c1dbd26	276.277718	-0.002537623	2.57E-31	1.38E-29	Bacteria	Bacteroidetes	[Saprospirae]	[Saprospirales]	Chitinophagaceae	Sediminibacterium	NA	47.39337
7ab841730b2f0b5d19633a00b11b0034	37.0218451	-0.002581117	0.00375622	0.02239819	Bacteria	Proteobacteria	Betaproteobacteria	Burkholderiales	Comamonadaceae	Limnohabitans	NA	52.45902
f41db34cba53df323bb0a10bbc00a20c	373.720808	-0.002798543	1.12E-49	9.05E-48	Bacteria	Bacteroidetes	[Saprospirae]	[Saprospirales]	Chitinophagaceae	Sediminibacterium	NA	47.39337
e0f5477563201220539c5435473bd1c0	10.6703598	-0.012237761	0.00222397	0.0149191	Bacteria	Bacteroidetes	[Saprospirae]	[Saprospirales]	Chitinophagaceae	Sediminibacterium	NA	46.91943
f42a06190ba088bc6602ddc22d71ac67	18.1898168	-0.013789319	0.000736	0.00623661	Bacteria	Proteobacteria	Alphaproteobacteria	Rickettsiales	NA	NA	NA	49.25373
9ae0313caea2bd14b9be59e90546070c	17.5364626	-26.48102828	0	0	Bacteria	Proteobacteria	Alphaproteobacteria	Rickettsiales	Pelagibacteraceae	NA	NA	46.76617

Supplementary Table 3. Representative sequences obtained from QIIME2 for each ASVid in Supplementary Table 2.

ASVid	DNA sequence
787ec8478ea75e9a298de113ec8abeca	TGGGGAATTTTGGACAATGGGCGCAAGCCTGATCCAGCAATGCCGCGTGCAGGATGAAGGCCTTCGGGTTGTAAACTGCTTTTGTACGGAGCGAAACGGTCTACTTTAATACAGTGGGCTAATGACGGTACCGTAAGAATAAGCACCGGCTAACTACGTGCCAGCAGCCGCGGTAATACGTAGGGTGCGAGCGTTAATCGGAATTACTGGGCGTAAAGCGTGCGCAGGCGGTTATATAAG
3638f2062c305c79df283ef573a10b97	TGGGGAATTTTGGACAATGGGCGAAAGCCTGATCCAGCAATGCCGCGTGTGTGAAGAAGGCCTTCGGGTTGTAAAGCACTTTTGTCCGGAAAGAAATGGCTCTGGTTAATACCTGGGGTCGATGACGGTACCGGAAGAATAAGGACCGGCTAACTACGTGCCAGCAGCCGCGGTAATACGTAGGGTCCAAGCGTTAATCGGAATTACTGGGCGTAAAGCGTGCGCAGGCGGTTGTGCAA
1f18cf29076957c15e3c64478934c53f	TGAGGAATTTTCCGCAATGGGCGAAAGCCTGACGGAGCAATGCCGCGTGGAGGAGGAAGGCCTGTGGGTCGTAAACTCCTTTTCTCAGAGAAGAAGTTCTGACGGTATCTGAGGAATAAGCATCGGCTAACTCTGTGCCAGCAGCCGCGGTAATACGGAGGATGCAAGCGTTATCCGGAATTATTGGGCGTAAAGCGTCCTGAGGTGGCTTACCCAGTCGACTGTGAAAGCTCAAGGCTT
d8534dd07e84a8fee208828b561e691a	TGGGGAATATTGGACAATGGGGCAACCCTGATCCAGCAATGCCGCGTGAGTGATGAAGGCCTTAGGGTTGTAAAGCTCTTTTACCGGGGACGATGATGACGGTACCCGAGAATAAGCCCCGGCTAACTTCGTGCCAGCAGCCGCGGTAATACGAAGGGGGCGAGCGTTGTTCGGAATTACTGGGCGTAAAGGGCGCGTAGGCGGCGCTCCAAGTTAGGCGTGAAAGCCCCGGGCTCA
73ccfd0bf411b690443a30d9c9f59e00	TGGGGAATTGTTCACAATGGGCGCAAGCCTGATGACGCAACGCCGCGTGGGGGATGAAGGTCTTCGGATCGTAAACCCCTGTCGAATGGGACGAATAGCCTTCGAATTAATACCTCGGAGGAATGACGGTACCGTTAAAGGAAGCCACGGCTAACTCTGTGCCAGCAGCCGCGGTAATACAGAGGTGGCAAGCGTTGTTCGGAATTACTGGGCGTAAAGGGCGCGTAGGCGGCATCTA
98fb8bf25b5baca1e94762 8c9a1e2d13	TGGGGAATCTTGGACAATGGGCGCAAGCCTGATCCAGCCATGCCGCGTGAGTGAAGAAGGTCTTCGGATTGTAAAGCTCTTTACCGGGACGATAATGACGGTACCTGGAGAATAAGCCCCGGCAAACTTCGTGCCAGCAGCCGCGGTAATACGAAGGGGGCTAGCGTTGTTCGGAATTACTGGGCGTAAAGCGCACGTAGGCGGGTCGTTAAGTCAGGGGTGAAATCCCGGAGCTCA
970ed30e2fa7430e8d50f91b564fe97f	TGGGGAATCTTGCGCAATGGGCGAAAGCCTGACGCAGCAACGCCGCGTGCGGGAAGAAGGCCTTCGGGTTGTAAACCGCTTTCAGCAGGAACGAAAATGACGGTACCTGCAGAAGAAGTGCGGCCAACTATGTGCCAGCAGCCGCGGTAATACAGGCACCAAGCGTTGTCCGGATTTATTGGGCGTAAAGAGCTCGTAGGCGGTTCAGTCAGTCGGGTGTGAAAACTCTGGGCTTA
ae71bf7c99d3583a2d8841e5911c5716	TGGGGAATATTGGGCAATGGAGGAAACTCTGACCAGCGACGCCGCGTGCGGGATGAAGGCCTTCGGGTTGTAAAGCTCTTCAGTAGGGAAGAAGCGAAAGTGACGGTACCTAACAAAGGAGCACGGCTAACTACGTGCCAGCAGCCGCGGTAATACGTAGGGTGCAAGCGTTGTCCGGAATTATTGGGCGTAAAGAGCTGCAGGCGGTTTGTTACGTCGGATGTGAAAGCCCGAGGCTCA
adee15fbdd4b70ff88b7e68a51afab75	TGGGGAATATTGCGCAATGGACGAAAGTCTGACGCAGCGACGCCGCGTGTGGGGATGAAGGCTTCGGGGTGTAAACCACTTGTCAGCAGGAAGAAACTCTGATTCGTCGACGGTACCTGCAGAAGAAGCACCGGCTAACTACGTGCCAGCAGCCGCGGTAATACGAAGGGGTGCGAGCGTTGTCCGGAATTACTGGGCGTAAAGGGCGCGTAGGTGGCGGGATAAGTGTGTG
55ff6faf3d171ef953a5f98ffa6d7dd1	TGGGGAATCTTGCGCAATGGGCGAAAGCCTGACGCAGCGACGCCGCGTGGGGATGAAGGCCTTCGGGTTGTAAACCGCTTTCAGCAGGAACGAAAAGGAGGCGGCCAACTACGTGCCAGCAGCCGCGGTAATACGTAGGGTCCAAGCGTTGTCCGGATTTATTGGGCGTAAAGAGCTCGTAGGCGGTTTGTTAAGTCGGGTGTTAAAACTCTGGGCTCA
75776764065cf5111d6a186068cbb3ff	ACCCGGAGAGGCCATCCGATACTGCTGTGACTTGAGTTCAGGAGGGGAGCGGGGGAATTCCTAGTGTAGCGGTGAAATGCGCAGATATTAGGAGGAACACCGGTGGCGAAGGCGCCGCTCTGGACTGAAACTGACGCTGAGGAGCGAAAGCATGGGTAGCAAACA
dfb115cfb1c595fd0a2611c733c58d00	TAGGGAATATTGGTCAATGGGCGAAAGCCTGAACCAGCAACGCCGCGTGCGGATGAAGGCCTTCGGGTCGTAAAGCGCTTTGCAGCAGGAAGAAGAAGGTGACGGTACCTGCAGAAGAAGCACCGGCTAACTACGTGCCAGCAGCCGCGGTAATACGTAGGGTGCGAGCGTTGTCCGGAATTATTGGGCGTAAAGGGCGTGTAGGAGGTTGGCAAGTCGGCCATGAAAGTCCCGGCTCA
88b5b524064974bca876d10823045b01	TGGGGAATCTTGCGCAATGGGCGAAAGCCTGACGCAGCGACGCCGCGTGCGGGATGAAGGCCTTCGGGTTGTAAACCGCTTTCAGCAGGAAGAAAATGACGGTACCTGAGAAGAAGGACGGCCAACTACGTGCCAGCAGCCGCGGTAACACGTAGGCTCAAGCGTTGTCCGGATTTATTGGGCGTAAAGAGCTCGTAGGCGGTTGAGTAAGTCGGGTGTGAAAACTCTGGGCTTA
76d10823045b01	ACCCGGAGACGCCATCCGATACTGCTGACTAGAGTTCAGGAGGGGAGTGGGGAATTCCTAGTGTAGCGGTGAAATGCGCAGATATTAGGAGGAACACCGGTGGCGAAGGCGCCACTCTGGACTGAAACTGACGCTGAGGAGCGAAAGCATGGGTAGCAAACA
d76a3d4c5d8913aeb4deac6f162ca3c4	TGGGGAATCTTGCGCAATGGGCGAAAGCCTGACGCAGCGACGCCGCGTGCGGGATGAAGGCCTAGGGTTGTAAACCGCTTTCAGCAGGAACGAAAATGACGGTACCTGTAGAATAAGGTGCGGCCAACTACGTGCCAGCAGCCGCGGTAACACGTAGGCACCAAGCGTTGTCCGGATTTATTGGGCGTAAAGAGCTCGTAGGCGGTTTGTCAGTAAGTCGGGTGTGAAAACTCGGGCTCA
0167e1bd8560c962ee9e440f30318dfb	TGGGGAATATTGGGCAATGGAGGAAACTCTGACCCAGCGACGCCGCGTGCGGGATGAAGGCCTTCGGGTTGTAAACCGCTTTCAGTAGGGAAGAAGCGAAAGTGACGGTACCTAACTATGTGCCAGCAGCCGCGGTAATACATAGGGTGCAAGCGTTGTCCGGAATTATTGGGCGTAAAGAGCTCGTAGGCGGTTCGTCGCCAGTCGGATGTGAAACCTGAG
9e440f30318dfb	GCTCAACCTCAGGCCTGCATTCGATACGAGGAACTAGAGTTTGGTAGGGGAGACTGGAATTCCTGGTGTAGCGGTGGAATGCGCAGATATCAGGAGGAACACCAACGGCGAAGGCAGGTCTCTGGGCCATACTGACACTGAGGAGCGAAAGCTGGGGAGCGAACA
c366064866eaed18a54d1564027 2ab34	TGGGGAATATTGGGCAATGGAGGAAACTCTGACCCAGCGACGCCGCGTGCGGGATGAAGGCCTTCGGGTTGTAAACCGCTTTCAGCAGGGAAGAAGCGAAAGTGACGGTACCTGACAGAAGAAGCCCGGCTAACTATGTGCCAGCAGCCGCGGTAATACATAGGGTGCAAGCGTTGTCCGGAATTATTGGGCGTAAAGAGCTCGTAGGTGGTTCGTCACGTCGGATGTGAAACCTGGG
a68b37133e9d3da604674d143353033d	ACCCAGAGACGCCACCCGATACTGCTTAACTTGAGTTCGATAGGGGAGTGGGGAATTCCTAGTGTAGCGGTGAAATGCGCAGATATTAGGAGGAACACCGGTGGCGAAGGCGACTCTGGATCGATACTGACGCTGAGGAGCGAAAGCATGGGTAGCAAACA
887bc7033b46d960e893caceb711700b	TGGGGAATCTTGCGCAATGGGCGAAAGCCTGACGCAGCAACGCCGCGTGCGGGAAGAAGGCTTCGGGCTGTAAACCGCTTTCAGCAGGAACGAAAATGACGGTACCTGACAGAAGAAGGACGGCCAACTATGTGCCAGCAGCCGCGGTAATACATAGGCTCGAAGCGTTGTCCGGATTATTGGGCGTAAAGAGTTCGTAGGCGGTCGAGTAAGTCGGGTGTGAAAATTCCGGGCTCA
921175c5e69a32e289e597a77764eae3	TGGGGAATCTTGCGCAATGGGCGAAAGCCTGACGCAGCAACGCCGCGTGCGGGAAGAAGGCTTCGGGCTGTAAACCGCTTTCAGCAGGAACGAAAATGACGGTACCTGACAGAAGAAGGACGGCCAACTATGTGCCAGCAGCCGCGGTAATACATAGGCTCGAAGCGTTGTCCGGATTATTGGGCGTAAAGAGTTCGTAGGCGGTCGAGTAAGTCGGGTGTGAAAATTCCGGGCTCA
fdf79b2352da82f67612a0d3fa98c598	TGGGGAATTTTGGACAATGGGGCAACCCTGATCCAGCCATTCCGCGTGAGTGAAGAAGGCCTTCGGGTTGTAAAGCTCTTTCGCAAGGGAAGAAAACTTATGATCGAATAAATCATGAGGTTGACGGTACCTTGAAGAAGCACCGGCTAACTACGTGCCAGCAGCCGCGGTAATACGTAGGGTGCGAGCGTTAATCGGAATTACTGGGCGTAAAGCGTGCGCAGGCGGTTTTGTAAG
03c021662d88f96cbdfdacd21420f0cd	TGGGGAATTTTGGACAATGGGGCAACCCTGATCCAGCCATTCCGCGTGAGTGAAGAAGGCCTTCGGGTTGTAAAGCTCTTTCGCAGGGAGGAAAACTTATGATCGAATAAATCATGAGGTTGACGGTACCTTGAAGAAGCACCGGCTAACTACGTGCCAGCAGCCGCGGTAATACGTAGGGTGCGAGCGTTAATCGGAATTACTGGGCGTAAAGCGTGCGCAGGCGGTTTTGTAAG
1c14e085e85aef7ec5a50101b7d9f363	TGGGGAATATTGGACAATGGGCGCAAGCCTGATCCAGCAATCCGCGTGAGTGATGAAGGCTTCGGATCGTAAAGCTCTTTAGTGGAAGATAATGACGGTATCCACAGAAAAAGCACCGGCAAACTTCGTGCCAGCAGCCGCGGTAATACGAAGGGTGCTAGCGTTGTTCGGAATTATTGGGCGTAAAGCGTAGCAGGCGGTTTAGTAAGTCGATTGTGAAATACCCGAGCTCAAC
8dd09b6e83118f34fd27596a877f64e0	TTGGGAATTGCAATCCGAACTGCTTGCTAGAGTTTAGTGGGGTAGTGGAATTCCTAGTGTAGCGGTGAAATGCGCAGATATCAGGAGGAACACCAGTGGCGAAGGCGACTATCTAGCGTAACTGACGCTGAGGAGCGAAAGCGTGGGGAGCGAACA
aca380d3d06d653c6296f75364e4e6fb	TGGGGAATCTTGCACAATGGAGGAAACTCTGATGCAGCGATGCCGCGTGAGTGAAGAAGGCCTTTGGGTTGTAAAGCTCTTTTGTAGGGAAGAATAATGACTGTACCTACAAGAAAGTCCGGCTAACTTCGTGCCAGCAGCCGCGGTAATACGAAGGGACCTAGCGTAGTTCGGAATTACTGGGCGTAAAGCGCGCGTAGGCGGTTTGTCAAGTCAGATGTGAAATCCCCGAGCTTAAC
bdfac780ed7ad9d5d57bccef8f271bf6	TGGGGAATTTTGGACAATGGACGCAAGTCTGATCCAGCCATGCCGCGTGCAGGACGAAGGCCTTCGGGTTGTAAACTGCTTTTGTACGGAACGAAAAGCCTTGGCTAATACGTCCAGGGTCCAAGTCGACGGTACCGTAAGAATAAGCACCGGCTAACTACGTGCCAGCAGCCGCGGTAATACGTAGGGTGCGAGCGTTAATCGGAATTACTGGGCGTAAAGCGTGCGCAGGCGGTTATATAAG
d451827eb1e44147c6c2f657cc7e6587	TAAGGAATATTGGTCAATGGACGCAAGTCTGAACCAGCCATGCCGCGTGAAGGATGAAGGCCCTTCGGGTTGTAAACTTCTTTTATCTGGGACGAAAAACGGGCTTCTAGCTCACTTGACGGTACCAGAGGAATAAGCACCGGCTAACTCCGTGCCAGCAGCCGCGGTAATACGGAGGGTGCAAGCGTTATCCGGATTTACTGGGTCGTAAAGGGTGCGTAGGTGGGTAGGTAAGTCAGTG
c2f657cc7e6587	GTGAAATCTTCAAGCTTAACTTGGAAACTGCCATTGATACTATCTATCTTGAATACTTTGGAGGTAAGCGGAATATGTCATGTAGCGGTGAAATGCTTAGATATGACATAGAACACCAATTGCGAAGGCAGCTTACTACACAGTTATTGACACTGAGGCACGAAAGCGTGGGGATCAAACA
8a388b2fedb1e9ce85fd666ae0bd9e47	TAAGGAATATTGGACAATGCCGCAAGGGTATCCAGCCATGCCGCGTGCAGGAAGAAGGCATTATGGGTCGTAAACTGCTTTTACCCGGAGAAGAAGCATCGGCTAACTTCGTGCCAGCAGCCGCGGTAAGACGAAGGTCGAAGCGTTATCCGGATTTATTGGGCGTAAAGCGAGCGTAGGTGGACTGATAAGTCAGGTGTGAAATCCATCGGCTCAACCGATGG
5ff24cc14309cfb49d337bfd19c3e03	TAGGGAATATTGGGCAATGGACGCAAGTCTGACCCAGCCATGCCGCGTGCAGGATGAAGGCGTTATGCGTCGTAAACTGCTTTTATACAGGAAGAAACGACTCTTGCGAGAGCGATTGACGGTACTGTATGAATAAGCACCGGCTAACTCCGTGCCAGCAGCCGCGGTAATACGGAGGGTGCAAGCGTTGTCCGGAATTATTGGGTTTAAAGGGAGCGCAGGTGGTTTATTAAGTCAGTGG
7ab84173bb2f0b5d19633a00b11b0034	TGGGGAATTTTGGACAATGGACGCAAGTCTGATCCAGCCATTCCGCGTGCAGGATGAAGGCCCTCGGGTTGTAAACTGCTTTTGTACGGAACGAAAAGGTCTCTTCGAGAGGCTATGACGGTACCGTAACTAGTGCCAGCAGCCGCGGTAATACGAAGGGTGCAAGCGTTAATCGGAATTACTGGGCGTAAAGCGTGCGCAGGCGGTTATATAAGA
f41db34cba53df323b0a10bbc00a20c	TAAGGAATATTGGTCAATGGACGCAAGTCTGAACCAGCTATGCCGCGTGAAGGATTAAGGTCCTCTGGATTGTAAACTTCTTTTATCTGGGACGAAAAAAGGTCTTCTAGACCCCTGACGGTACCAGTGAATAACGCACCGGCTAACTCCGTGCCAGCAGCCGCGGTAATACGGAGGGTGCAAGCGTTATCCGGATTCACTGGGTTTAAAGGGTGCGTAGGCGGGTAGGTAAGTCAGTG
b0a10bbc00a20c	GTGAAATCCTGGAGCTCAACTCCAGAACTGCCATTGATACTATCTATCTTGAATATTGTGGAGGTAAGCGGAATATGTCATGTAGCGGTGAAATGCTTAGATATGACATAGAACACCATTGCGAAGGCAGCTTACTACGCATTATTGACGCTGAGGCACGAAAGCGTGGGGATCAAACA
e0f547756320122053c9c5435473bd1c0	TAAGGAATATTGGTCAATGGACGCAAGTCTGAACCAGCTATGCCGCGTGAAGGATTAAGGTCCTCTGGATTGTAAACTTCTTTTATAGGGACGAAAACAGATCTTTCTAGATCCTTTGACGGTACCATATGAATAAGCACCGGCTAACTCCGTGCCAGCAGCCGCGGTAATACGGAGGGTGCAAGCGTTATCCGGATTCACTGGGTTTAAAGGGTGCGTAGGCGGGCAGGTAAGTCAGTGG
9c5435473bd1c0	TGAAATCCTGGAGCTCAACTCCAGAACTGCCATTGATACTATCTGTCTTGAATATTGTGGAGGTAAGCGGAATATGTCATGTAGCGGTGAAATGCTTAGATATGACATAGAACACCATTGCGAAGGCAGCTTACTACGCATTATTGACGCTGAGGCACGAAAGCGTGGGGATCAAACA
f42a06190ba088bbc66d2ddc22d71ac67	TGGGGAATCTTGCACAATGGAGGAAACTCTGATGCAGCGATGCCGCGTGAGTGAAGAAGGCCTTTGGGTTGTAAAGCTCTTTTGTAGGGAAGATAATGACTGTACCTACAAGAATAAGGTCCGGCTAACTTCGTGCCAGCAGCCGCGGTAATACGAAGGGACCTAGCGTAGTTCGGAATTACTGGGCGTAAAGCGCGCGTAGGCGGTTGAGTTAGTTAATTGTGAAATCCCAAGCTTAAC
9ae0313caea2bd14b9be59e90546070c	TGGGGAATCTTGCACAATGGAGGAAACTCTGATGCAGCGATGCCGCGTGAGTGAAGAAGGCCTTTGGGTTGTAAAGCTCTTTTGTAGGGAAGATAATGACTGTACCTACAAGAATAAGGTCCGGCTAACTTCGTGCCAGCAGCCGCGGTAATACGAAGGGACCTAGCGTAGTTCGGAATTACTGGGCGTAAAGCGCGCGTAGGCGGTTGAGTTAGTTAATTGTGAAATCCCAAGCTTAAC
TTTGGAACTGCAATTAAAACTGCTCAACTAGAGTTTGATAGAGGAAAGCGGAATACATAGTGTAGAGGTGAAATTCGTAGATATTATGTAGAACACCAGTTGCGAAGGCGGCTTCTGGATCAACACTGACGCTGAGGCGCGAAAGTATGGGTAGCAAAGA	

Supplementary Table 4. Quality parameters of the outgoing drinking water from the treatment plant during the sampling in March. DWTP = drinking water treatment plant.

Temperature (°C)	1.2
Turbidity (FNU)	<0.1
UV absorbance 254 nm, 5 cm (A.U)	0.367
pH after rapid sand filtration (before the UV aggregate)	6.8
pH outgoing water DWTP	8.05
Alkalinity mg (HCO_3/L)	55.5
Hardness (°dH)	4.6
TOC (mg/L)	4.1
COD-Mn (mg O_2/L)	2.55
Ammonium (mg/L)	0.0635
Ammonium-nitrogen (mg/L)	0.049
Nitrite (mg/L)	<0.01
Nitrite-nitrogen (mg/L)	<0.003
Aluminium (mg/L)	0.029
Iron (mg/L)	<0.01
Manganese (mg/L)	<0.005
Calcium (mg/L)	26
Magnesium (mg/L)	4.25

Supplementary Table 5. Flow cytometry data of total cell concentrations (TCC) and percentage intact cells (%IC) of the samples not exposed to UV and UV irradiated samples. TCC and %IC were measured according to the protocols by Prest et al.[1] and Gatza et al.[2]

UV dose (J/m^2)	TCC (cells/mL)	%IC
0	563083 ± 9549	49 ± 3.1
250	559053 ± 4527	59 ± 0.48
400	560713 ± 2963	47 ± 0.64
600	564213 ± 4060	49 ± 0.57

1. Prest, E. I., Hammes, F., Kötzsch, S., van Loosdrecht, M. C. M. & Vrouwenvelder, J. S. Monitoring microbiological changes in drinking water systems using a fast and reproducible flow cytometric method. *Water Research* **47**, 7131–7142 (2013).

2. Gatza, E., Hammes, F. & Prest, E. Assessing Water Quality with the BD Accuri™ C6 Flow Cytometer White Paper. (2013).

Paper II

Water Research 138 (2018) 27–36

Contents lists available at ScienceDirect

Water Research

journal homepage: www.elsevier.com/locate/watres

Monitoring biofilm function in new and matured full-scale slow sand filters using flow cytometric histogram image comparison (CHIC)

Sandy Chan [a, b, c], Kristjan Pullerits [a, b, c], Janine Riechelmann [a], Kenneth M. Persson [b, c, d], Peter Rådström [a], Catherine J. Paul [a, d, *]

[a] Applied Microbiology, Department of Chemistry, Lund University, P.O. Box 124, SE-221 00 Lund, Sweden
[b] Sweden Water Research AB, Ideon Science Park, Scheelevägen 15, SE-223 70 Lund, Sweden
[c] Sydvatten AB, Hyllie Stationstorg 21, SE-215 32 Malmö, Sweden
[d] Water Resources Engineering, Department of Building and Environmental Technology, Lund University, P.O. Box 118, SE-221 00 Lund, Sweden

ARTICLE INFO

Article history:
Available online 13 March 2018

Keywords:
Slow sand filters
Drinking water
Flow cytometry
Schmutzdecke
Cytometric histogram image comparison (CHIC)
Biofilm

ABSTRACT

While slow sand filters (SSFs) have produced drinking water for more than a hundred years, understanding of their associated microbial communities is limited. In this study, bacteria in influent and effluent water from full-scale SSFs were explored using flow cytometry (FCM) with cytometric histogram image comparison (CHIC) analysis; and routine microbial counts for heterotrophs, total coliforms and *Escherichia coli*. To assess if FCM can monitor biofilm function, SSFs differing in age and sand composition were compared. FCM profiles from two established filters were indistinguishable. To examine biofilm in the deep sand bed, SSFs were monitored during a scraping event, when the top layer of sand and the *schmutzdecke* are removed to restore flow through the filter. The performance of an established SSF was stable: total organic carbon (TOC), pH, numbers of heterotrophs, coliforms, *E. coli*, and FCM bacterial profile were unaffected by scraping. However, the performance of two newly-built SSFs containing new and mixed sand was compromised: breakthrough of both microbial indicators and TOC occurred following scraping. The compromised performance of the new SSFs was reflected in distinct effluent bacterial communities; and, the presence of microbial indicators correlated to influent bacterial communities. This demonstrated that FCM can monitor SSF performance. Removal of the top layer of sand did not alter the effluent water from the established SSF, but did affect that of the SSFs containing new sand. This suggests that the impact of the surface biofilm on effluent water is greater when the deep sand bed biofilm is not established.

1. Introduction

One of the oldest technologies for the treatment of drinking water is the use of slow sand filters (SSFs) (Huisman and Wood, 1974). These filters combine multiple cleaning mechanisms including mechanical filtration and sedimentation but are primarily considered as biological filters where a microbial ecosystem develops as biofilm on the sand particles and contributes to the cleaning process (Haig et al., 2015b). As SSFs remove a broad range of microbial contaminants including *Escherichia coli*, *Clostridium* spp., *Cryptosporidium* spp., viral pathogens and toxins (Bourne et al., 2006; Elliott et al., 2008; Hijnen et al., 2007), as well as total organic carbon (TOC) (Wotton, 2002), monitoring the performance of these filters is crucial for the drinking water producer. This type of monitoring however, is complicated by limitations in both knowledge regarding the microbial diversity in these filters; and the analytical methods that are able to follow this diversity in real-time, or near real-time, resolution. Understanding these human-built aquatic ecosystems would facilitate both routine monitoring for quality control as well as optimised design for SSFs. These are both required to produce safe drinking water in a future with climate-related changes such as altered natural organic matter, water temperatures, and pathogen contamination in source water; at a time when urbanization will increase demand for treated water (Ritson et al., 2014; Sterk et al., 2013; van Leeuwen, 2013).

* Corresponding author. Applied Microbiology, Department of Chemistry, Lund University, P.O. Box 124, SE-221 00 Lund, Sweden.
E-mail addresses: sandy.chan@tmb.lth.se (S. Chan), kristjan.pullerits@tmb.lth.se (K. Pullerits), janine.riechelmann@gmx.de (J. Riechelmann), kenneth_m.persson@tvrl.lth.se (K.M. Persson), peter.radstrom@tmb.lth.se (P. Rådström), catherine.paul@tmb.lth.se (C.J. Paul).

https://doi.org/10.1016/j.watres.2018.03.032

Knowledge about the dynamics of bacterial communities in SSFs is limited by the ability of the current routine analyses to describe the microbial processes occurring in the biofilm and water phases with respect to both diversity and time. Heterotrophic plate counts (HPC), and counts of coliforms and *E. coli*, can analyse microbes passing through the SSFs and satisfy traditions of common usage and regulations, however these methods only capture a small fraction of the total microbial population (Allen et al., 2004), and at least 24 h incubation time is required. Studies using molecular techniques have described laboratory and pilot-plant scale SSF systems (Bourne et al., 2006; Calvo-Bado et al., 2003; Wakelin et al., 2011) or focused on elements of the filter, such as the uppermost biofilm, or *schmutzdecke* (Unger and Collins, 2008; Wakelin et al., 2011). Other studies have focused on microbial contaminant removal by SSFs (Bauer et al., 2011; Elliott et al., 2008; Hijnen et al., 2004). Several metagenomic DNA sequencing studies of the microbial community in full-scale SSFs in operating drinking water treatment plants have shown that a highly diverse community dominated by bacteria is living in these biological filters (Bai et al., 2013; Haig et al., 2014, 2015b; Oh et al., 2018). The presence of bacteriophage, protozoa and fungi and their role in SSF ecology has also been examined (Haig et al., 2015a; Prenafeta-Boldú et al., 2017). These studies are invaluable for providing a deep understanding of the microbial ecosystems in SSFs however, the methods used are expensive, with time-consuming laboratory work and demanding data analysis. This currently prevents their use for online routine monitoring.

Flow cytometry (FCM) with DNA staining is used to study the microbial communities of numerous aquatic systems (Berney et al., 2008; Boi et al., 2016; De Corte et al., 2016) including microbial dynamics in both treatment and distribution of drinking water (Besmer et al., 2014; El-Chakhtoura et al., 2015; Lautenschlager et al., 2014). Total cell count (TCC) has been proposed for monitoring drinking water treatment processes (Van Nevel et al., 2017b) and online measurement has been demonstrated (Besmer and Hammes, 2016). Additional quantitative FCM parameters describe the bacteria in a water sample, including the number of intact cells, and a fluorescent fingerprint describing the distribution of DNA content in the bacterial community (Prest et al., 2013).

During SSF operation, the bacteria in the sand consume organic matter and multiply, and over a period of months or years (depending on season and source water) the filter becomes clogged with biomass. To restore the water flow, the top layer of the SSF is removed by mechanical scraping (Huisman and Wood, 1974). This procedure may disturb the filter function, and effluent water from the disturbed SSFs is not used until water quality parameters comply with regulations. The ability to follow SSF function in real, or near-real, time would minimise the time filters are offline to both ensure maximum supply of treated water and reduce costs. This is particularly relevant in Sweden, where SSFs require scraping 2–3 times per year. In this study, three SSFs differing in microbial community maturation and sand composition were followed over a period of several weeks during summer, before and after a scraping procedure. Water quality of influent and effluent were assessed using FCM and conventional microbial and chemical parameters. FCM parameters together with Cytometric Histogram Image Comparison (CHIC) analysis were analysed to assess if this method could resolve dynamic changes in the bacterial communities of the effluent water. In order to examine if this method could be used to monitor the function of the biofilm in SSFs, these profiles were correlated to different traditional microbial water quality indicators. In addition, by observing the different SSFs before and after the removal of the top layer of sand, including *schmutzdecke*, the specific contribution of the deep sand bed biofilms to SSF function could be observed.

2. Materials and methods

2.1. Description of SSFs and sampling

The full-scale SSFs in this study are located in Sweden, at Ringsjö Waterworks, Stehag, Sweden, and operated by Sydvatten AB (Hyllie Stationstorg 21, Malmö, Sweden). During the study, the treatment plant produced 1300 L/sec of drinking water from surface water (Lake Bolmen, Småland, Sweden), supplemented with a small fraction of groundwater. The plant receives the source water through an 82 km tunnel and treated using flocculation with ferric chloride, lamellar sedimentation, rapid sand filtration, slow sand filtration and disinfection with hypochlorite before distribution (Sydvatten AB, 2016). Each SSF at the treatment plant is scraped 2–3 times per year, usually in the summer, when the resistance of flow through the filter is unacceptable. The SSFs are scraped to remove the top layer of sand, including the *schmutzdecke* and then refilled with water from below the sand bed.

In winter 2015, two new SSFs were built at Ringsjö Waterworks. One was constructed using only purchased virgin sand (Sibelco Nordic AB, Baskarp, Sweden), (NEW) while the second SSF (MIX) was constructed with first a layer of virgin sand, topped with a layer of washed sand collected during previous scraping of established SSFs. A third SSF, a well-established working SSF (EST) in the same production line as the newly constructed filters and used for drinking water production over 20 years (built 1995), was included in sampling as a control (Persson, 2013). Water samples were collected during July and August 2015 from above the sand beds, using a telescopic sampler; and after filtration, from continuously running taps. Samples were collected using sterilized borosilicate bottles one day before, and for up to three weeks after, the scraping of each SSF. As scraping for each filter was not carried out on the same calendar day, data and comparisons are presented relative to the day of scraping, with day 1 being the day before scraping, day 2 being the day of the scraping activity and so forth. All three SSFs were scraped within the same three week period of stable ambient temperatures (data not shown).

In summer 2016 (April–August), EST and a second mature SSF from the same treatment line (EST2) were sampled in the same way as describe above except that water samples were collected directly into 50 mL Falcon tubes and not transferred from the borosilicate bottles.

2.2. Water quality measurements

Water samples for conventional microbial parameters were processed by the treatment plant staff according to a routine schedule and coincided in time with the flow cytometry analysis. Heterotrophic plate counts (HPC) were determined by mixing 1 mL of water with R2A agar, with incubation at 22 °C for 72 h (Bartram et al., 2003). Concentration of coliforms and *E. coli* were determined with the Colilert method from IDEXX laboratories, using the Quanti-Tray/2000® and sealed with Quanti-Tray sealer ® according to the manufacturer's instructions (Idexx Laboratories, Westbrook, USA).

Chemical water quality parameters were determined by VA SYD, Malmö, Sweden using standard methods, (Table S1). The temperature of the water over the studied period was measured online in the bulk water at the outlet of the treatment plant.

2.3. Flow cytometry

Samples of 50 mL water for flow cytometry were transferred and stored in sterile 50 mL Falcon tubes on ice and analyzed within 7 h of sampling. Water samples were stained in triplicate for measurement of total cell count and fingerprints according to Prest et al. (2013). Briefly, 5 μL mL^{-1} of SYBR Green I at 100 X diluted with DMSO (stock concentration 10 000 X, Invitrogen AG, Switzerland) was added to samples at room temperature, to a final concentration of 1 X SYBR Green I, before incubation in the dark at 37 °C for 15 min. For intact cell measurements, a working solution of SYBR Green I (100 X) and propidium iodide (PI) (1 mg/mL, Sigma-Aldrich, Germany) was prepared with final concentrations of 1 X SYBR Green I and 3 μM PI in the sample and incubated as above (Gillespie et al., 2014). Live and ethanol-killed *E. coli* were used as controls for examination of cells with intact membranes, referred to hereafter as intact cells, as well as MilliQ water as a control for background fluorescence were used in every run. All measurements were performed using a BD Accuri C6 flow cytometer (Becton Dickinson, Belgium) with a 50 mW laser with an emission wavelength at 488 nm. A quality control of the flow cytometer using Spherotech 8-peak and 6-peak validation beads (BD Biosciences) was conducted each day measurements were taken in order to allow samples from different days to be compared. 50 μL of 500 μL samples were measured in triplicate for each sample at a flow rate of 35 μL min^{-1} and a threshold of 500 arbitrary units on the green fluorescence channel.

2.4. Data analysis

Data processing and gating were performed with FlowJo software (Tree Star Inc, USA). Signals were collected and analyzed by gating on the dot plot with green fluorescence (FL1, 533 ± 30 nm) and red fluorescence (FL3, >670 nm). Gating was done following the gating strategy described in (Prest et al., 2013) and identical gating was applied on all samples. The gated data visualized by the green fluorescence histogram plot is referred to as the fluorescent fingerprint. Percentage of bacteria with low nucleic acid content (LNA) and bacteria with high nucleic acid content (HNA) were determined as described in Prest et al. (2013). Statistical analysis was performed on all data (TCC, ICC and HNA concentration) using one-way ANOVA, followed by Tukey test in R (R Development Core Team, 2017).

Cytometric histogram image comparison (CHIC) analysis on dot plots was performed using R packages flowCHIC and flowCore (Ellis et al., 2016), and visualized by ggplot2 (Wickham, 2009) according to Schumann et al. (2015) and Koch et al. (2013). Gated populations of the flow cytometric dot plots (green fluorescence at x-axis and red fluorescence at y-axis) were converted into 300 × 300 pixel images with 64-channel gray scale resolution for image comparison and to generate values describing the differences between water samples. A nonmetric multidimensional scaling (NMDS) plot based on Bray-Curtis dissimilarity was created from the results and analysis of similarities (ANOSIM) was performed with the formed clusters. All statistical calculations were performed in R (R Development Core Team, 2017). The correlation between the nonmetric multidimensional scaling (NMDS) of the FCM data and the conventional microbial parameters (HPC, coliforms and *E. coli*) was determined using the R function *envfit*, vegan package (Oksanen et al., 2017). Only parameters from plate counts with a significant effect (P-value < 0.05) are presented. After the sampling and FCM analysis were completed, plate count data collected as part of the routine monitoring schedule were obtained from the laboratory at Ringsjö Waterworks. Only FCM profiles and plate counts obtained on the same sampling day were used for the correlation analysis.

3. Results

3.1. Conventional water quality assessments

Water quality parameters, including specific microbial indicators, were measured during a routine scraping event and subsequent operation period for three SSFs (Fig. 1). Influent water showed variations in the concentration of microbial indicators (i.e. HPC, coliforms and *E. coli*), between filters and over time, despite the fact that all SSFs received water from the same process line at the treatment plant.

Effluent water samples from the three SSFs contained heterotrophs during the entire sampling period. The established SSF, hereafter referred to as EST, had the lowest mean value of heterotrophs calculated over time of the three filters, at 1.8 ± 1.6 CFU/mL. Counts for coliforms and *E. coli* above zero were detected in effluent water from the established filter only once during the 35 days of sampling, at 1 CFU per 100 mL of breakthrough coliforms. The SSF with mixed sand (MIX), both coliforms and *E. coli* were detected in the effluent water following the scraping event with a steady decrease of indicators detected over operation time and no detection of *E. coli* after day 8. The SSF containing all new sand (NEW) showed frequent breakthroughs of coliforms and *E. coli* in effluent water during the entire sampling period.

Chemical parameters for water quality were measured in the influent and effluent water for each filter (Table S1). The three SSFs showed similar values for parameters such as nitrite, total phosphorus and conductivity but differed with respect to TOC and pH. TOC and pH of the effluent water of EST were lower and more stable than effluent from MIX and NEW. TOC across EST was reduced 0.6 mg/L ± 0.2 mg/L, from a mean value of 2.9 mg/L ± 0.09 mg/L in the influent water to 2.2 mg/L ± 0.09 mg/L in effluent. This was in contrast to that observed for the new SSFs, where there was less reduction of TOC. MIX gave a reduction in TOC of 0.2 mg/L ± 0.0 mg/L (mean value of TOC in influent 2.9 mg/L ± 0.1 mg/L to effluent 2.7 ± 0.1 mg/L mg/L) and TOC was reduced 0.1 mg/L ± 0.0 mg/L for NEW (mean value of TOC in influent 2.8 mg/L ± 0.05 mg/L to effluent 2.7 mg/L ± 0.05 mg/L).

In EST, pH was lowered from a mean value of 7.8 to 7.4, while the pH of the influent and effluent water of both MIX and NEW were unaffected by filtration and remained with a mean value of 7.7.

3.2. Flow cytometric bacterial counts

Total cell counts (TCC) were determined by FCM to assess changes in the number of bacterial cells in the influent and effluent water of the three SSFs during the routine scraping event (Fig. 2). TCCs of the influent and effluent water of EST peaked one day after scraping (sampling day 3), with $6 \times 10^5 \pm 1.5 \times 10^4$ cells mL^{-1} in the influent and $3.9 \times 10^5 \pm 1.9 \times 10^3$ cells mL^{-1} in the effluent water. This was the highest TCC observed in this study. TCC values in effluent from the newly built filters were in the same order of magnitude, with an average of $2.7 \times 10^5 \pm 5.3 \times 10^4$ cells mL^{-1} in effluent water across the three filters.

After scraping (sampling days 7–10 for EST and MIX, sampling days 6–11 for NEW) the average reduction in TCC performed by EST was 16% ± 1%, compared to MIX, at 25% ± 3%, and NEW, at 30% ± 1%. TCC in the effluent water from EST reached a steady-state level at 5 days after the scraping event (sampling day 7), with almost no change in bacterial numbers over the following sampling days. This was not observed for the two newly constructed filters. Calculating the slope values from linear regression of TCC/time showed the stability of the effluent TCC from EST, giving a rate of change for EST TCC over 10 times lower than that observed for either of the newly built SSFs (EST:1090; MIX: -13100; NEW: -17800).

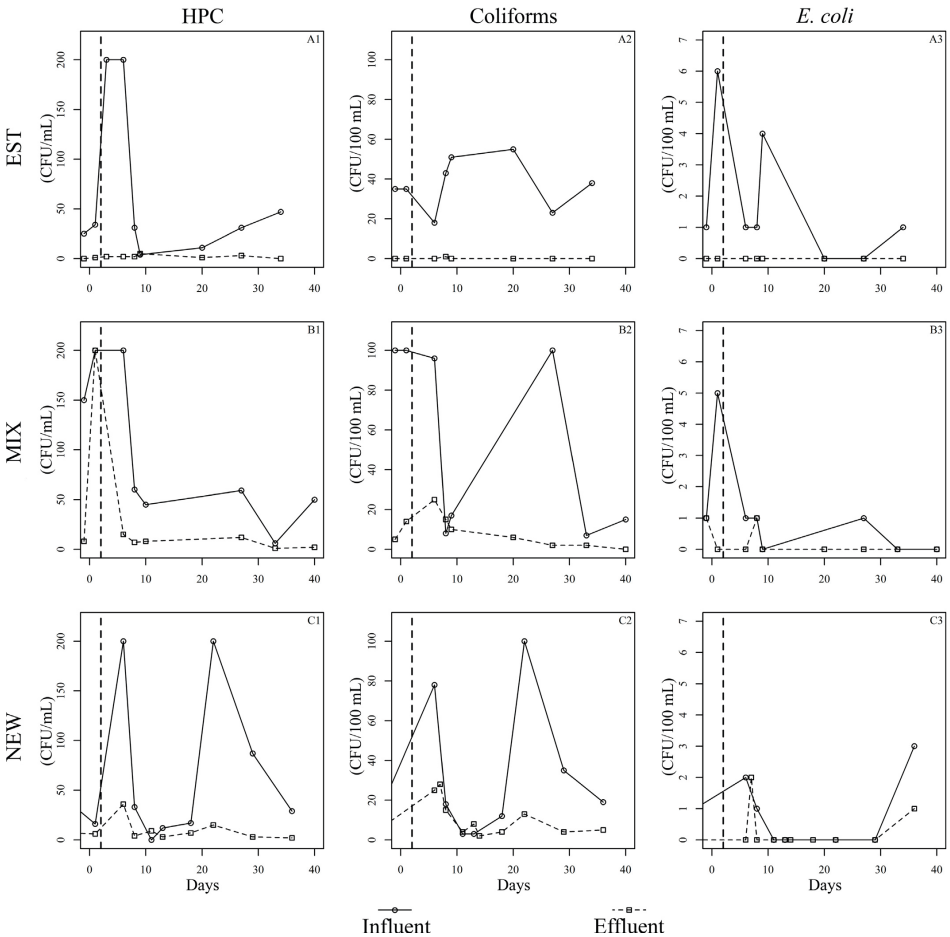

Fig. 1. Conventional microbial water quality assessment Measured microbial parameters, from left to right: heterotrophic plate count (HPC), coliforms and *E. coli* in influent (○ solid line) and effluent (□ dashed line) water of EST (A1-3), MIX (B1-3) and NEW (C1-3). The days on the x-axis correspond to the scraping of the filters that occurred in day 2 (vertical dashed line).

Intact cell counts showed similar trends as TCC (data not shown). Effluent water from EST had on average 80% intact cells, with a statistically significantly higher *P*-value < 0.05 than both MIX and NEW (averages of 73% and 76% intact cells respectively). The percentage of intact cells in effluent waters from MIX and NEW were not statistically different from each other (Fig. 3). Effluent water from all filters contained, on average, more intact cells than influent, with one exception from MIX before the scraping event (sampling day 1), where the influent had a higher ICC.

3.3. Profiling bacterial communities by flow cytometric measurements

Fluorescence distribution histograms from FCM were used to compare DNA-stained bacterial cells in the SSF influent and effluent waters. Each histogram image represents a cumulative fluorescent profile of the individual cells in the bacterial community of a water samples (Prest et al., 2013). Histograms were visualised by FCM as fluorescence fingerprints. Fingerprints obtained from 64 influent

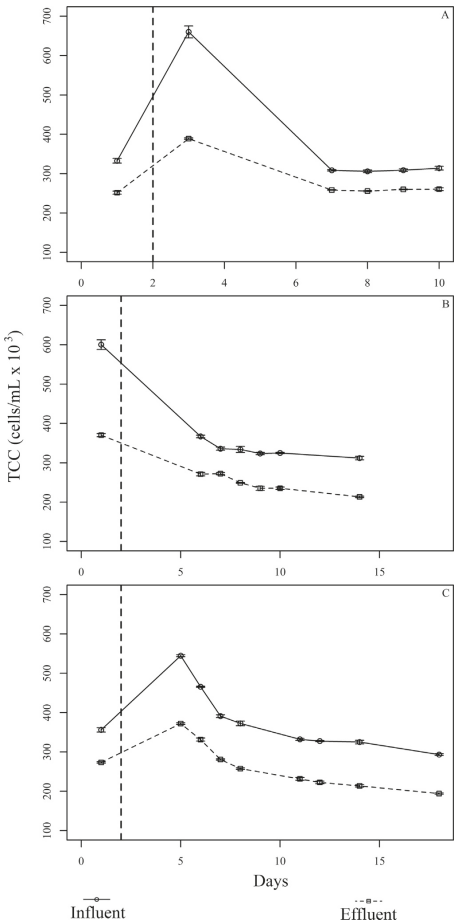

Fig. 2. Cell concentrations in water from slow sand filters. Total cell concentrations (TCC) of influent (○ solid line) and effluent (□ dashed line) water of EST (A), MIX (B) and NEW (C) measured by flow cytometry. X-axis is defined by a scraping event occurring on day 2 (dashed line).

water samples from three SSFs showed similar patterns, indicating comparable bacterial communities with no significant differences in concentration of high nucleic acid bacteria (HNA) (Fig. S1). One exception was influent water for EST, sampled one day after scraping (sample day 3), with an altered fingerprint and HNA concentration of 48.8 ± 0.95%. This anomaly was likely due to cells entering the influent due to disturbance of the SSF biofilm when the SSF was refilled from below after scraping.

Fluorescence fingerprints of effluent from EST and MIX showed a lower concentration of HNA, with a dramatic shift in community composition towards bacteria with low nucleic acid content (LNA) (Fig. 4). The effluent from EST had, on average, 29.6 ± 2.78% HNA bacteria, and MIX effluent had 39.5 ± 3.09% HNA, although only EST maintained a steady-state level of LNA bacteria after the scraping event. In contrast, effluent water from NEW increased in the concentration of HNA bacteria over time and always contained a higher HNA concentration than the other effluent waters, with an average of 46.6 ± 4.43% HNA.

All gated cell dot plots were analyzed using CHIC and presented in an NMDS plot to quantitatively compare the changes and dynamics in the bacterial communities (Fig. 5). CHIC analysis identified four distinct clusters associated with effluent water, and depending on the origin of the SSFs, and one cluster which encompassed all influent water samples. Correlation analysis between traditional plate counts and FCM profiles showed higher levels of indicator bacteria associated with the influent water cluster (In). Analysis of similarities (ANOSIM) confirmed significant separation between all groups (R-value = 0.933; P-value = 0.001). Data from effluent water samples of EST (E) and MIX (M) were distinct from those of the influent cluster (In), and each other. NEW effluent waters split into two clusters in the NMDS plot. N1 was associated with samples taken before and shortly after the scraping procedure in time. N2 contained samples taken several days after the scraping, and showed water profiles that were most similar to those of the influent (In) water. This division in profile character for NEW effluent water was also observed in the fingerprints over time (Fig. 4).

The effluent water from EST had visually identical fingerprints regardless of whether the samples were taken before or after scraping. This uniformity was also reflected in the compact cluster of group E in the CHIC analysis, and the steady-state behavior of this SSF observed by other parameters (i.e. coliform count). The cluster representing the effluent water of MIX grouped between those of EST and NEW, with day before scraping (sample day 1) and the last sampling points (day 10 and 14) being closer to the EST cluster.

To determine if FCM shows the same bacterial profile for established SSFs at this treatment plant, effluent water was analyzed from EST and a second well-established SSF (EST2), over a five month period. CHIC analysis with all previous SSF effluent water data (Fig. S2) again separated effluent waters from new and established filters, and all histograms describing effluent from established filters clustered together, regardless of sampling date. CHIC analysis of data from only the established filters (EST, 2015, 2016 and EST2 2016), separated into two clusters representing the communities of the influent and effluent water from both filters, and confirmed by ANOSIM (R-value = 0.957; P-value = 0.001; data not shown).

4. Discussion

Next generation sequencing (NGS) studies of drinking water biofilters have previously shown that the effluent water community reflects the content of the biofilm (Haig et al., 2015b; Li et al., 2017; Oh et al., 2018; Pinto et al., 2012). Some studies have examined the use of FCM to characterize the influent and effluent communities from biofilters (Lautenschlager et al., 2014; Park et al., 2016). The goal of the current study was to examine if FCM can monitor biofilm status and function in SSFs with sand beds of differing maturity and sand composition, including their response to a scraping event. Using FCM, the bacterial communities in the influent and effluent water from four SSFs were followed through time. CHIC analysis was used for statistical comparison to compare total number of cells and distribution of nucleic acid in these cells. This grouped the influent water separately from the effluent water, and each SSF produced effluent water with a unique bacterial profile. The influent water to each SSF was the same, and

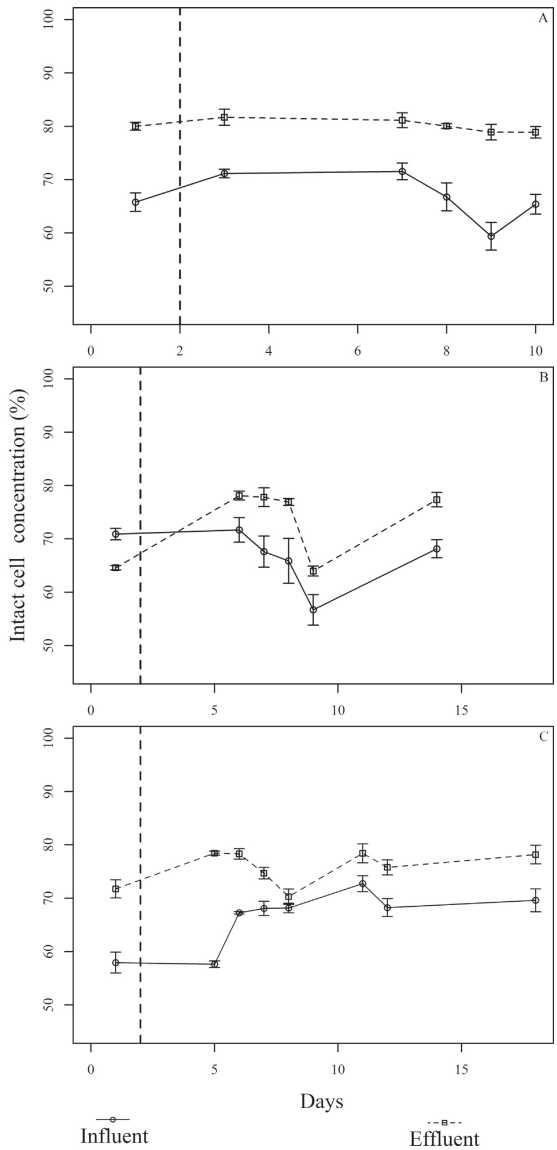

Fig. 3. Intact cell concentrations in water from slow sand filters. Intact cell concentration of influent (○ line) and effluent (□ dashed line) water for EST (A), MIX (B) and NEW (C) measured by flow cytometry during a scraping event occurred in day 2 (dashed line) in the x-axis.

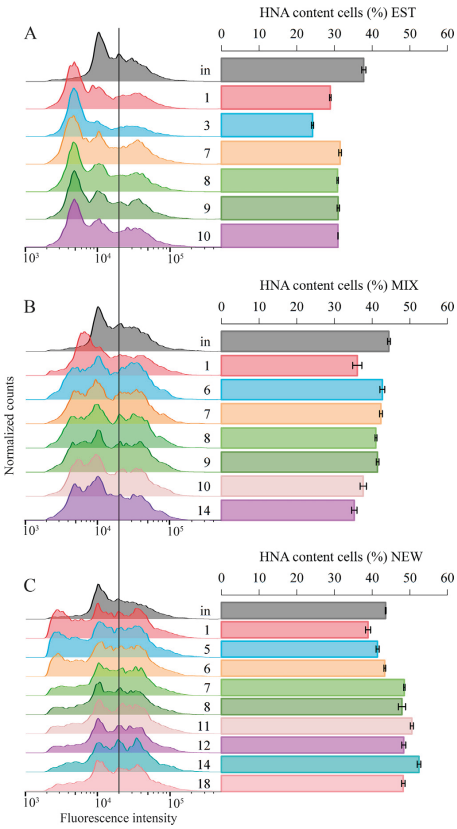

Fig. 4. Fingerprint analysis of effluent water from slow sand filters. Fluorescence distribution histograms from flow cytometry are combined over time for the effluent water of EST (A), MIX (B) and NEW (C) on the left. Percentage of HNA cells separated by a black line adapted from Prest et al., 2013 (around 2×10^4 a.u) are shown on the right as bar plots. The first sample for each filter (in grey) are influent water from sampling day 6. Sampling days corresponding to scraping (occurring in day 2) are shown in the middle of the figure.

differences in the effluents between filters indicated that a distinct microbial biofilm inhabited each of the examined SSFs.

The bacterial profiles in the effluent water of the two established SSFs were similar to each other regardless of sampling year. Closer examination of one of these filters showed consistent chemical and biological transformation of the water quality across the sand bed including: removal of microbial indicators; a lowering of pH; an increase in percentage of intact cells; and decreased HNA content, regardless of fluctuations in the influent water. Importantly, the transformation of the water quality was not dependent on the upper layer of sand: scraping did not result in changes to the FCM bacterial profiles of effluent water, or breakthrough of microbial indicators. This was in contrast to observations in the newly built SSFs, particularly the SSF containing all new sand. In this SSF, removal of the top layer of sand, including the *schmutzdecke,* preceded breakthrough of microbial indicators and FCM profiles showed that the community in the effluent water became more similar to that of the influent. This suggests that the sand bed biofilm in these newly-built filters was not able to transform the influent water to the extent observed for the established filter. The role of the *schmutzdecke* in water purification has long been attributed to the activity of microbes living as biofilm in this region of the SSF (Barrett et al., 1991; Bauer et al., 2011; Huisman and Wood, 1974; Oh et al., 2018). As the function of the mature SSF was not disrupted by scraping, the functional microbial community of this filter resided in the sand bed and not only in the *schmutzdecke*. An NGS study of two full-scale SSFs showed that the bacterial communities between sand samples are highly similar even when sampled from different depths (Haig et al., 2015b) and together with the results in the current study, it seems these core communities contain the essential functionality of SSFs. However, as studies characterizing the ecology of the SSF sand bed have used extracted DNA, without the ability to distinguish between living and dead cells or free DNA, it is difficult to say which mechanisms within the sand bed ecosystem are responsible for effluent water quality. Stable isotope probing showed that removal of *E. coli* from laboratory SSFs was mediated via multiple direct and indirect mechanisms including protozoal grazing, viral killing, reactive oxygen species produced by algae, and mutualistic fungi-algal interactions (Haig et al., 2015a). This study also suggested that ecosystem-wide associations on multiple trophic levels are required for pathogen removal and that the absence of this complexity could explain compromised function, in less diverse filter ecosystems. It is also known that SSF function improves with time; virus removal improved over time in constructed model systems as the *schmutzdecke* and deeper sand biofilm developed (Bauer et al., 2011); and, seven week old freshwater biofilms showed greater enzyme activity for removal of DOC than four week old biofilms (Peter et al., 2011). These observations are supported by the current study as the SSF which had a top layer of washed sand from other SSFs (MIX) was more effective at removing indicator organisms at the end of the study period. CHIC analysis showed the bacterial profile in the effluent from this SSF migrated towards that of the established filters in the days following the scraping event. This suggests that the biofilm community in the mixed SSF may have been approaching that of the established filter biofilm, including acquisition of ecosystem-wide associations required for pathogen removal. Further investigation is required however, to determine if the microbial ecology and/or specific pathogen removal mechanisms differ between the SSFs in this study.

The washed sand used in construction of one SSF (MIX) appears to have inoculated the biofilm with a community preconditioned for SSF function, promoting a more rapid development of a biofilm core community similar to that in the established sand filters. Interestingly, Pagaling et al., (2014) showed that the colonization of a microbial community was predictable, and similar to the original community, when it was introduced to an environment to which it had previously been exposed. The idea that inoculation with preconditioned microbial biomass can lead to rapid establishment of SSF function is supported by laboratory studies by Haig et al. (2014). Lab scale SSF columns constructed using sand from a full-scale SSF differed: non-sterile columns removed indicators after a period of 4–6 weeks, whereas sterile columns required 7–10 weeks to reach the same level of performance.

While the biofilm in the deep sand is essential for shaping the effluent water from well-functioning SSFs, the removal of the top layer of sand and *schmutzdecke* did impact the function of the new SSFs. In the SSF containing all new sand (NEW), CHIC analysis

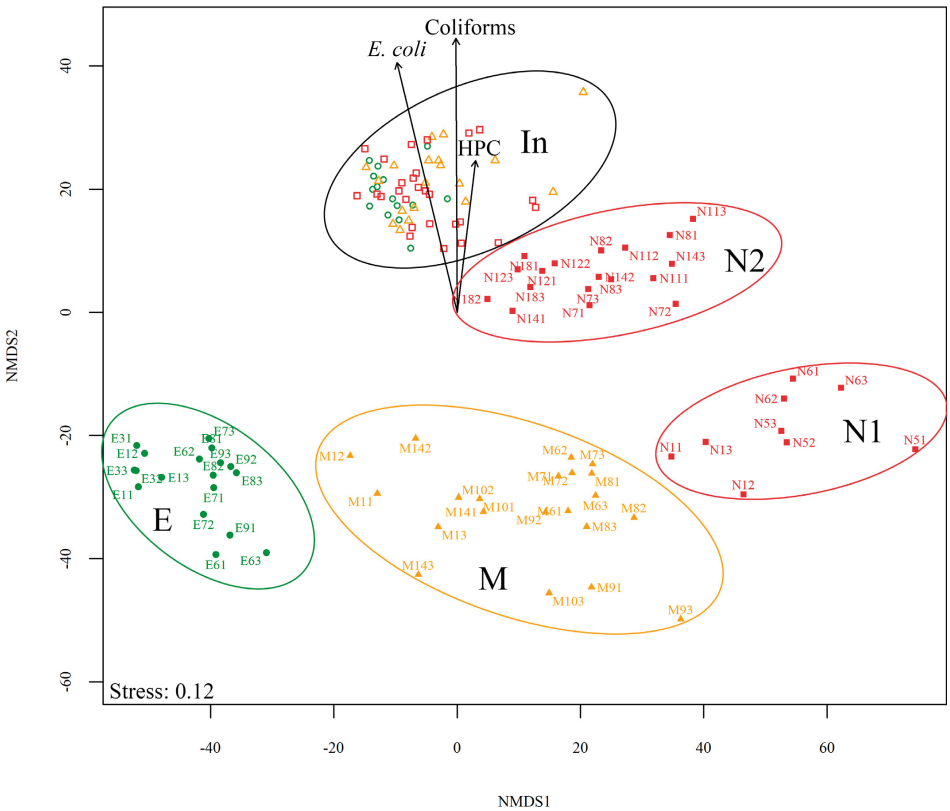

Fig. 5. Non-metric multidimensional scaling (NMDS) ordination plot from CHIC analysis of water samples from different slow sand filters. Profiling bacterial communities by flow cytometric measurements and CHIC analysis grouped water samples into five clusters: a combined cluster of all influent water (black), effluent water from EST (E, green), effluent water from MIX (M, yellow) and two clusters formed by effluent water of NEW (N1, N2, red). The first one or two numbers (if name consist of three numbers) of each effluent sample name indicate days corresponding to the scraping (occurred in day 2), n = 127. Vectors describing the linear relationships between the FCM and plate count data (heterotrophs, coliforms and *E. coli*) are indicated by labelled arrows. (For interpretation of the references to colour in this figure legend, the reader is referred to the web version of this article.)

showed that after the scraping event, the effluent profiles began approaching that of the influent water. This suggests that without the *schmutzdecke*, the deep sand bed in this SSF had minimal impact on the bacterial community in the water. In an NGS study examining response of established full-scale SSFs to scraping, overlap between communities in the influent and effluent water was concomitant with coliform breakthrough (Haig et al., 2015b). Thus, in filters without a well-functioning microbial community in the deep sand bed, the biofilm may not be able to sufficiently impact the effluent water and changes in the effluent water could be more coupled to the status of the *schmutzdecke*. This could explain the emphasis placed on the role of the *schmutzdecke* in water filtration: studies examining its function have largely been conducted on filters that are not performing optimally; or at lab or pilot scale, where a sand bed community has not had years to establish (Haig et al., 2015b; Pfannes et al., 2015; Unger and Collins, 2006). The study showing effective removal of faecal indicators from wastewater identified the *schmutzdecke* as the essential feature of 14 week-old model slow sand filters, but again, the communities in the influent and effluent water were indistinguishable by t-RFLP analysis of bacterial 16S rRNA (Pfannes et al., 2015). The study by Unger and Collins (2006) also showed that the removal of *schmutzdecke* changed filter function although again, these experiments were conducted at lab-scale and over a period of weeks. It is not surprising that the *schmutzdecke* plays an important role in filtration by new SSFs as substrate concentrations and the biomass acting on the substrates are highest at the surface of the sand bed (Bai et al., 2013; Lautenschlager et al., 2014). In filters where for any number of reasons (time, inoculation) the deep sand bed biofilm cannot significantly transform the influent water,

the influence of *schmutzdecke* on filter function may thus be more obvious. As biofilms in both the *schmutzdecke* and sand bed can entrap particles and cells, and support antagonistic microbial interactions (Pfannes et al., 2015; Prenafeta-Boldú et al., 2017), the overall function of the filter is likely a balance between the functions of the biofilm ecosystems in these different regions. A recent metagenomics study predicted that the minimum generation time for a mature SSF sand bed community was shorter than that predicted for the associated *schmutzdecke* metagenome (Oh et al., 2018) suggesting that the degradation of organic material which fuels microbial growth in a mature filter is higher in the sand bed then on the surface. Although the bacterial content in *schmutzdecke* is denser than in the sand bed (10^{11} copies/mL and 10^{8}-10^{9} copies/g respectively) (Pfannes et al., 2015), the total volume of the deep sand is many times greater than that occupied by the *schmutzdecke*. Instead of being dominated by the function in the *schmutzdecke*, the activity of the SSF community in the deeper sand is likely more significant for overall SSF performance than previously thought. Conclusions from lab-based experiments may thus overestimate the impact of the *schmutzdecke*, emphasizing the need for studies conducted at full scale for complete assessment of drinking water treatment by SSFs.

The question still remains: to what extent does the biofilm transform the influent water community to obtain desirable effluent water quality? In this, and other studies (Haig et al., 2015b), an overlap between the bacterial communities of the influent and effluent water were concomitant with indicator breakthrough. It may be a specific and significant transformation of the bacterial community between influent and effluent water that is the signature of a well-functioning SSF. The established filter showed the least reduction of total cells, with an increase in the amount of intact cells, and a decrease in HNA content, suggesting an exchange of communities in the water as it passed this biofilm. An increase in intact cells following SSF has also been reported Lautenschlager et al. (2014). CHIC analysis showed that the bacterial communities from each SSF differed in HNA, suggesting that the distinct biofilms in each individual sand bed altered this aspect of the effluent. HNA and LNA bacteria are thought to be both phylogenetically and physiologically different (Schattenhofer et al., 2011; Wang et al., 2009; Vila-Costa et al., 2012). Changes in the ratio of HNA to LNA bacteria, with LNA bacteria dominating in effluent water, have been observed following biofiltration (Lautenschlager et al., 2014; Vital et al., 2012). The seeding of the treated drinking water with bacteria during biofiltration is thought to be important for the quality of the distributed water (El-Chakhtoura et al., 2015; Lautenschlager et al., 2014; Pinto et al., 2012). The ability of a biofilter to shift the community to include increased numbers of LNA bacteria could be essential to achieve a desirable microbial water quality. The effluent water from the established filter in this study showed this typical change to higher LNA content. In contrast, both new filters had more HNA bacteria in their effluent water compared to influent. The HNA content from the new filter containing mixed sand decreased over the study period, to more closely resemble that of the established filter. The new filter containing new sand, however, had continually increasing HNA content in effluent water. These changes in HNA content appeared to coincide with the ability of the new SSFs to remove indicators. Observing a shift in the distribution of nucleic acid content could provide an alternative way to monitor SSFs, although the relationship between DNA content and SSF function requires more investigation.

The ability of different disinfectants to inflict membrane damage on HNA and LNA cells was examined (Ramseier et al., 2011). This study postulated that HNA bacteria contain higher proportions of, or more accessible, thiol or other non-amine groups in their membrane proteins, and that this difference could increase the sensitivity of HNA cells to chlorine dioxide and permanganate disinfection. When ozonation was examined in more detail, LNA cells were more sensitive to low doses of ozone than HNA cells (Lee et al., 2016). Understanding the origin of the distribution of HNA and LNA bacteria in the SSF effluent may thus impact downstream disinfection as SSFs are often the last biological treatment step with the potential to shape the bacterial community entering the distribution system.

The rapid FCM method used here captured dynamic microbial changes in the SSF biofilm and effluent water. These changes reflected SSF function and could potentially impact downstream disinfection. FCM would thus be useful for process control of SSF in drinking water treatment plants, providing advantages over current methods utilizing routine plating, including cost, speed, and the potential for online monitoring (Besmer et al., 2014; Van Nevel et al., 2017b). FCM has been specifically proposed for monitoring of maintenance in distribution networks (Van Nevel et al., 2017a). Time and water volume lost during maintenance and reconnection of the SSF into the production line could be minimized, reducing the overall cost for water treatment. This would be a particular advantage in countries such as Sweden where scraping of SSFs is required 2–3 times per year. Zonal distributions created by CHIC analysis can establish a baseline profile, with deviations from this profile indicating possible changes in microbial water quality. Understanding how much variation can be expected in the bacterial profile, including the influence of seasonal or operational changes, is required. Given that many factors, including local weather patterns or source water, could impact the bacterial community, the use of FCM with CHIC for process control may require each drinking water producer to establish unique baselines customized for individual treatment plants.

5. Conclusions

- Established SSFs showed consistent performance by FCM bacterial profiling that was not altered by removal of the *schmutzdecke* suggesting that a mature biofilm in the deep sand bed is required for consistent microbial water quality from SSFs.
- Inoculation with sand previously used in SSF at the same treatment plant could explain the more rapidly improved functioning of one new SSF. Improvement in function was not observed for a new SSF constructed only with new sand.
- Alteration of FCM bacterial profiles in effluents from SSFs could indicate compromised function of the filter.
- Using routine CHIC analysis would simplify and reduce bias in assessing microbial water quality, facilitating use of FCM for process control.

Acknowledgements

This study was financially supported by the Swedish Research Council (Grant 621-2013-587), the Swedish Water and Wastewater Association Development Fund, The Crafoord Foundation, Sweden Water Research AB and Sydvatten AB. The authors would like to thank the employees at Ringsjö Waterworks, especially Agneta Jönsson and Marianne Franke for their assistance with sampling and analysis of conventional data.

Appendix A. Supplementary data

Supplementary data related to this article can be found at https://doi.org/10.1016/j.watres.2018.03.032.

References

Allen, M.J., Edberg, S.C., Reasoner, D.J., 2004. Heterotrophic plate count bacteria—what is their significance in drinking water? Int. J. Food Microbiol. 92 (3), 265–274.

Bai, Y., Liu, R., Liang, J., Qu, J., 2013. Integrated metagenomic and physiochemical analyses to evaluate the potential role of microbes in the sand filter of a drinking water treatment system. PLoS One 8 (4), e61011.

Barrett, J.M., Bryck, J., Collins, M.R., Janonis, B.A., Logsdon, G.S., 1991. Manual of Design for Slow Sand Filtration. AWWA Research Foundation and American Water Works Association, USA.

Bartram, J., Cotruvo, J., Exner, M., 2003. Heterotrophic Plate Counts and Drinking-water Safety: The Significance of HPCs for Water Quality and Human Health. IWA Pub.

Bauer, R., Dizer, H., Graeber, I., Rosenwinkel, K.-H., López-Pila, J.M., 2011. Removal of bacterial fecal indicators, coliphages and enteric adenoviruses from waters with high fecal pollution by slow sand filtration. Water Res. 45 (2), 439–452.

Berney, M., Vital, M., Hulshoff, I., Weilenmann, H.U., Egli, T., Hammes, F., 2008. Rapid, cultivation-independent assessment of microbial viability in drinking water. Water Res. 42 (14), 4010–4018.

Besmer, M.D., Hammes, F., 2016. Short-term microbial dynamics in a drinking water plant treating groundwater with occasional high microbial loads. Water Res. 107, 11–18.

Besmer, M.D., Weissbrodt, D.G., Kratochvil, B.E., Sigrist, J.A., Weyland, M.S., Hammes, F., 2014. The feasibility of automated online flow cytometry for in-situ monitoring of microbial dynamics in aquatic ecosystems. Front. Microbiol. 5, 265.

Boi, P., Amalfitano, S., Manti, A., Semprucci, F., Sisti, D., Rocchi, M.B., Balsamo, M., Papa, S., 2016. Strategies for water quality assessment: a multiparametric analysis of microbiological changes in river waters. River Res. Appl. 32 (3), 490–500.

Bourne, D.G., Blakeley, R.L., Riddles, P., Jones, G.J., 2006. Biodegradation of the cyanobacterial toxin microcystin LR in natural water and biologically active slow sand filters. Water Res. 40 (6), 1294–1302.

Calvo-Bado, L.A., Pettitt, T.R., Parsons, N., Petch, G.M., Morgan, J.A., Whipps, J.M., 2003. Spatial and temporal analysis of the microbial community in slow sand filters used for treating horticultural irrigation water. Appl. Environ. Microbiol. 69 (4), 2116–2125.

De Corte, D., Sintes, E., Yokokawa, T., Lekunberri, I., Herndl, G.J., 2016. Large-scale distribution of microbial and viral populations in the South Atlantic Ocean. Environ. Microbiol. Rep. 8 (2), 305–315.

El-Chakhtoura, J., Prest, E., Saikaly, P., van Loosdrecht, M., Hammes, F., Vrouwenvelder, H., 2015. Dynamics of bacterial communities before and after distribution in a full-scale drinking water network. Water Res. 74, 180–190.

Elliott, M.A., Stauber, C.E., Koksal, F., DiGiano, F.A., Sobsey, M.D., 2008. Reductions of E. coli, echovirus type 12 and bacteriophages in an intermittently operated household-scale slow sand filter. Water Res. 42 (10–11), 2662–2670.

Ellis, B., Haaland, P., Hahne, F., Meur, N.L., Gopalakrishnan, N., Spidlen, J., Jiang, M., 2016. flowCore: basic structures for flow cytometry data. Bioconductor R. package version 1.40.0.

Gillespie, S., Lipphaus, P., Green, J., Parsons, S., Weir, P., Juskowiak, K., Jefferson, B., Jarvis, P., Nocker, A., 2014. Assessing microbiological water quality in drinking water distribution systems with disinfectant residual using flow cytometry. Water Res. 65, 224–234.

Haig, S.-J., Quince, C., Davies, R.L., Dorea, C.C., Collins, G., 2014. Replicating the microbial community and water quality performance of full-scale slow sand filters in laboratory-scale filters. Water Res. 61, 141–151.

Haig, S.-J., Schirmer, M., D'Amore, R., Gibbs, J., Davies, R.L., Collins, G., Quince, C., 2015a. Stable-isotope probing and metagenomics reveal predation by protozoa drives E. coli removal in slow sand filters. ISME J. 9 (4), 797–808.

Haig, S.J., Quince, C., Davies, R.L., Dorea, C.C., Collins, G., 2015b. The relationship between microbial community evenness and function in slow sand filters. MBio 6 (5).

Hijnen, W.A., Schijven, J.F., Bonne, P., Visser, A., Medema, G.J., 2004. Elimination of viruses, bacteria and protozoan oocysts by slow sand filtration. Water Sci. Technol. 50 (1), 147–154.

Hijnen, W.A., Dullemont, Y.J., Schijven, J.F., Hanzens-Brouwer, A.J., Rosielle, M., Medema, G., 2007. Removal and fate of Cryptosporidium parvum, Clostridium perfringens and small-sized centric diatoms (Stephanodiscus hantzschii) in slow sand filters. Water Res. 41 (10), 2151–2162.

Huisman, L., Wood, W.E., 1974. Slow Sand Filtration. World Health Organization, Geneva Switzerland.

Koch, C., Fetzer, I., Harms, H., Müller, S., 2013. CHIC—an automated approach for the detection of dynamic variations in complex microbial communities. Cytom. Part A 83A (6), 561–567.

Lautenschlager, K., Hwang, C., Ling, F., Liu, W.T., Boon, N., Koster, O., Egli, T., Hammes, F., 2014. Abundance and composition of indigenous bacterial communities in a multi-step biofiltration-based drinking water treatment plant. Water Res. 62, 40–52.

Lee, Y., Imminger, S., Czekalski, N., von Gunten, U., Hammes, F., 2016. Inactivation efficiency of Escherichia coli and autochthonous bacteria during ozonation of municipal wastewater effluents quantified with flow cytometry and adenosine tri-phosphate analyses. Water Res. 101, 617–627.

Li, C., Ling, F., Zhang, M., Liu, W.-T., Li, Y., Liu, W., 2017. Characterization of bacterial community dynamics in a full-scale drinking water treatment plant. J. Environ. Sci. 51 (Suppl. C), 21–30.

Oh, S., Hammes, F., Liu, W.-T., 2018. Metagenomic characterization of biofilter microbial communities in a full-scale drinking water treatment plant. Water Res. 128, 278–285.

Oksanen, J., Blanchet, F.G., Friendly, M., Kindt, R., Legendre, P., McGlinn, D., Minchin, P.R., O'Hara, R.B., Simpson, G.L., Solymos, P., Stevens, M.H.H., Szoecs, E., Wagner, H., 2017. Vegan: Community Ecology Package.

Pagaling, E., Strathdee, F., Spears, B.M., Cates, M.E., Allen, R.J., Free, A., 2014. Community history affects the predictability of microbial ecosystem development. ISME J. 8 (1), 19–30.

Park, J.W., Kim, H.C., Meyer, A.S., Kim, S., Maeng, S.K., 2016. Influences of NOM composition and bacteriological characteristics on biological stability in a full-scale drinking water treatment plant. Chemosphere 160, 189–198.

Persson, K.M., 2013. Vattnet ska fram!: 50 år med Ringsjöverket. Sydvatten AB.

Peter, H., Ylla, I., Gudasz, C., Romaní, A.M., Sabater, S., Tranvik, L.J., 2011. Multifunctionality and diversity in bacterial biofilms. PLoS One 6 (8), e23225.

Pfannes, K.R., Langenbach, K.M., Pilloni, G., Stuhrmann, T., Euringer, K., Lueders, T., Neu, T.R., Muller, J.A., Kastner, M., Meckenstock, R.U., 2015. Selective elimination of bacterial faecal indicators in the Schmutzdecke of slow sand filtration columns. Appl. Microbiol. Biotechnol. 99 (23), 10323–10332.

Pinto, A.J., Xi, C., Raskin, L., 2012. Bacterial community structure in the drinking water microbiome is governed by filtration processes. Environ. Sci. Technol. 46 (16), 8851–8859.

Prenafeta-Boldú, F.X., Trillas, I., Viñas, M., Guivernau, M., Cáceres, R., Marfà, O., 2017. Effectiveness of a full-scale horizontal slow sand filter for controlling phytopathogens in recirculating hydroponics: from microbial isolation to full microbiome assessment. Sci. Total Environ. 599–600, 780–788.

Prest, E.I., Hammes, F., Kotzsch, S., van Loosdrecht, M.C.M., Vrouwenvelder, J.S., 2013. Monitoring microbiological changes in drinking water systems using a fast and reproducible flow cytometric method. Water Res. 47, 7131–7142.

R Development Core Team, 2017. R: a Language and Environment for Statistical Computing. R Foundation for Statistical Computing, Vienna, Austria.

Ramseier, M.K., von Gunten, U., Freihofer, P., Hammes, F., 2011. Kinetics of membrane damage to high (HNA) and low (LNA) nucleic acid bacterial clusters in drinking water by ozone, chlorine, chlorine dioxide, monochloramine, ferrate(VI), and permanganate. Water Res. 45 (3), 1490–1500.

Ritson, J.P., Graham, N.J.D., Templeton, M.R., Clark, J.M., Gough, R., Freeman, C., 2014. The impact of climate change on the treatability of dissolved organic matter (DOM) in upland water supplies: a UK perspective. Sci. Total Environ. 473–474, 714–730.

Schattenhofer, M., Wulf, J., Kostadinov, I., Glöckner, F.O., Zubkov, M.V., Fuchs, B.M., 2011. Phylogenetic characterisation of picoplanktonic populations with high and low nucleic acid content in the North Atlantic Ocean. Syst. Appl. Microbiol. 34 (6), 470–475.

Schumann, J., Koch, C., Fetzer, I., Müller, S., 2015. flowCHIC - Analyze flow cytometric data of complex microbial communities based on histogram images. Bioconductor R. package version 1.8.0.

Sterk, A., Schijven, J., de Nijs, T., de Roda Husman, A.M., 2013. Direct and indirect effects of climate change on the risk of infection by water-transmitted pathogens. Environ. Sci. Technol. 47 (22), 12648–12660.

Sydvatten AB, 2016. Ringsjöverket. Sydvatten AB.

Unger, M., Collins, M.R., 2006. In: Gimbel, R., Graham, N., Collins, M.R. (Eds.), Recent progress in Slow Sand and Alternative Biofiltration Processes. IWA Publishing.

Unger, M., Collins, M.R., 2008. Assessing *Escherichia coli* removal in the schmutzdecke of slow-rate biofilters. J. AWWA Am. Water Works Assoc. 100 (12), 60–73.

van Leeuwen, C.J., 2013. City blueprints: baseline assessments of sustainable water management in 11 cities of the future. Water Resour. Manag. 27 (15), 5191–5206.

Van Nevel, S., Buysschaert, B., De Roy, K., De Gusseme, B., Clement, L., Boon, N., 2017a. Flow cytometry for immediate follow-up of drinking water networks after maintenance. Water Res. 111, 66–73.

Van Nevel, S., Koetzsch, S., Proctor, C.R., Besmer, M.D., Prest, E.I., Vrouwenvelder, J.S., Knezev, A., Boon, N., Hammes, F., 2017b. Flow cytometric bacterial cell counts challenge conventional heterotrophic plate counts for routine microbiological drinking water monitoring. Water Res. 113, 191–206.

Vila-Costa, M., Gasol, J.M., Sharma, S., Moran, M.A., 2012. Community analysis of high- and low-nucleic acid-containing bacteria in NW Mediterranean coastal waters using 16S rDNA pyrosequencing. Environ. Microbiol. 14 (6), 1390–1402.

Vital, M., Dignum, M., Magic-Knezev, A., Ross, P., Rietveld, L., Hammes, F., 2012. Flow cytometry and adenosine tri-phosphate analysis: alternative possibilities to evaluate major bacteriological changes in drinking water treatment and distribution systems. Water Res. 46 (15), 4665–4676.

Wakelin, S., Page, D., Dillon, P., Pavelic, P., Abell, G.C.J., Gregg, A.L., Brodie, E., DeSantis, T.Z., Goldfarb, K.C., Anderson, G., 2011. Microbial community structure of a slow sand filter schmutzdecke: a phylogenetic snapshot based on rRNA sequence analysis. Water Sci. Technol. Water Supply 11 (4), 426–436.

Wang, Y., Hammes, F., Boon, N., Chami, M., Egli, T., 2009. Isolation and characterization of low nucleic acid (LNA)-content bacteria. ISME J. 3 (8), 889–902.

Wickham, H., 2009. ggplot2: elegant graphics for data analysis. Springer, New York.

Wotton, R.S., 2002. Water purification using sand. Hydrobiologia 469 (1), 193–201.

APPENDICES

Table A.1. Conventional chemical parameters. Chemical data of influent and effluent water from three sampling points of EST (top) and NEW (bottom). MIX (middle) was only sampled twice during this study for the conventional chemical parameters.

Sample	EST in	EST out	EST in	EST out	EST in	EST out	
Date	2015-07-29	2015-07-29	2015-07-31	2015-07-31	2015-08-03	2015-08-03	
Washing days	1	1	3	3	6	6	analysis method
pH	7.8	7.4	7.7	7.4	7.8	7.4	SS 028122
Conductivity (mS/m)	14	14	14	14	14	14	SS-EN 27888
Ammonium (mg/l)	<0.01	<0.01	0.02	<0.01	<0.01	<0.01	SS-EN ISO 11732:2005
Nitrite (mg/l)	<0.004	<0.004	<0.004	<0.004	<0.004	<0.004	SS-EN ISO 13395
Nitrate (mg/l)	1.1	1.3	1.3	1.8	1.1	1.2	SS-EN ISO 10304
COD (mg/l)	2	2	2	2	2	2	Fd SS 028118
TOC (mg/l)	2.8	2.3	3	2.1	2.8	2.3	SS EN 1484
Total phosphorus (µg/l)	<10	<10	<10	<10	<10	<10	SS-EN ISO 6878:2005
Iron (mg/l)	0.03	<0.01	0.03	<0.01	0.03	<0.01	SS-EN ISO 11885
Manganese (mg/l)	<0.01	<0.01	0.02	<0.01	0.01	<0.01	SS-EN ISO 11885
Calcium (mg/l)	15	15	18	17	16	16	SS-EN ISO 11885
Magnesium (mg/l)	1.4	1.4	1.7	1.6	1.6	1.5	SS-EN ISO 11885
Hardness (°dH)	2.4	2.4	2.9	2.7	2.6	2.6	SS 028121

Sample	MIX in	MIX out	MIX in	MIX out	
Date	2015-07-06	2015-07-06	2015-07-13	2015-07-13	
Washing days	-15	-15	-8	-8	analysis method
pH	7.5	7.6	7.7	7.7	SS 028122
Conductivity (mS/m)	14	14	14	14	SS-EN 27888
Ammonium (mg/l)	<0.01	<0.01	<0.01	<0.01	SS-EN ISO 11732:2005
Nitrite (mg/l)	<0.004	<0.004	<0.004	<0.004	SS-EN ISO 13395
Nitrate (mg/l)	1.2	1.2	1.2	1.3	SS-EN ISO 10304
COD (mg/l)	3	2.7	2	2	Fd SS 028118
TOC (mg/l)	2.9	2.7	2.8	2.6	SS EN 1484
Total phosphorus (µg/l)	<10	<10	<10	<10	SS-EN ISO 6878:2005
Iron (mg/l)	0.05	0.01	0.04	<0.01	SS-EN ISO 11885
Manganese (mg/l)	0.01	<0.01	<0.01	<0.01	SS-EN ISO 11885
Calcium (mg/l)	14	14	14	15	SS-EN ISO 11885
Magnesium (mg/l)	1.4	1.4	1.4	1.5	SS-EN ISO 11885
Hardness (°dH)	2.3	2.3	2.3	2.4	SS 028121

Sample	NEW in	NEW out	NEW in	NEW out	NEW in	NEW out	
Date	2015-07-06	2015-07-06	2015-07-13	2015-07-13	2015-08-03	2015-08-03	
Washing days	-10	-10	-3	-3	18	18	analysis method
pH	7.4	7.6	7.7	7.7	7.8	7.8	SS 028122
Conductivity (mS/m)	14.0	14.0	14	14	14	10	SS-EN 27888
Ammonium (mg/l)	<0.01	<0.01	<0.01	<0.01	<0.01	<0.01	SS-EN ISO 11732:2005
Nitrite (mg/l)	<0.004	<0.004	<0.004	<0.004	<0.004	<0.004	SS-EN ISO 13395
Nitrate (mg/l)	1.2	1.2	1.2	1.3	1.1	<0.01	SS-EN ISO 10304
COD (mg/l)	3.0	2.0	3	3.7	2	2	Fd SS 028118
TOC (mg/l)	2.9	2.8	2.8	2.7	2.8	2.7	SS EN 1484
Total phosphorus (µg/l)	<10	<10	<10	<10	<10	<10	SS-EN ISO 6878:2005
Iron (mg/l)	0.05	0.03	0.04	0.02	0.03	<0.01	SS-EN ISO 11885
Manganese (mg/l)	0.01	<0.01	<0.01	<0.01	0.01	<0.01	SS-EN ISO 11885
Calcium (mg/l)	14	14	15	15	16	16	SS-EN ISO 11885
Magnesium (mg/l)	1.4	1.4	1.4	1.5	1.5	1.6	SS-EN ISO 11885
Hardness (°dH)	2.3	2.3	2.4	2.4	2.6	2.6	SS 028121

Figure A.1. Flourescence fingerprint of influent water. The distribution of the fluorescence intensity plotted against the total cell concentration (fingerprints) for one of the three technical triplicates of each influent sample over time. Number of days according to scraping maintenance (occurred in day 2) (left) and concentration of HNA bacteria (right) are shown for each sampling point. The * highlights the sampling point from EST at Day 3, when the influent water was sampled directly after the scraping maintenance and included back rinsed water.

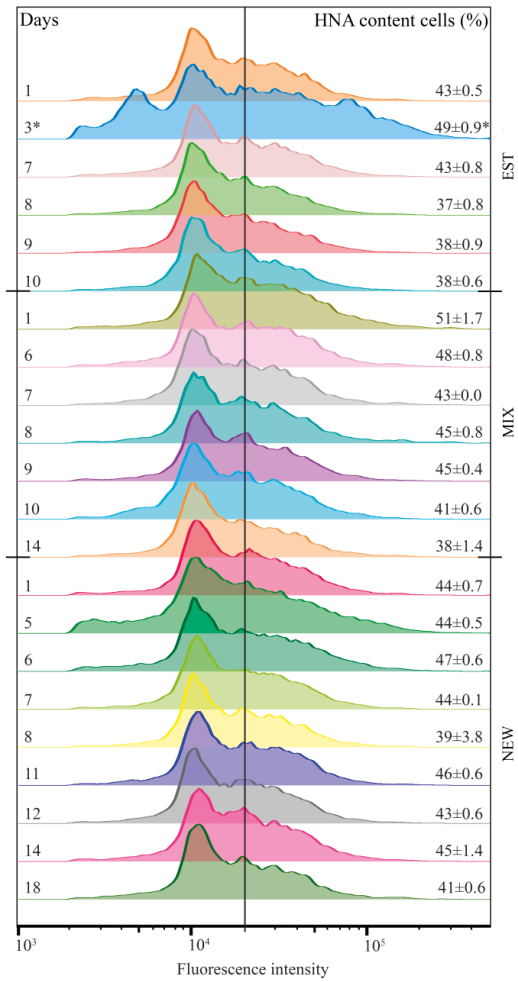

Figure A.2. Non-metric multidimensional scaling (NMDS) ordination plot from CHIC analysis of established filters from different years. Profiling bacterial communities by flow cytometric measurements of effluent water samples of EST (black circle), MIX and NEW (grey star) from 2015 combined with influent (empty) and effluent (filled) EST (E1, green) and EST2 (E2, blue) sampled 2016. The cluster of effluent water from established filters (EST 2015, 2016 and EST2 2016) are grouped in green. n=132

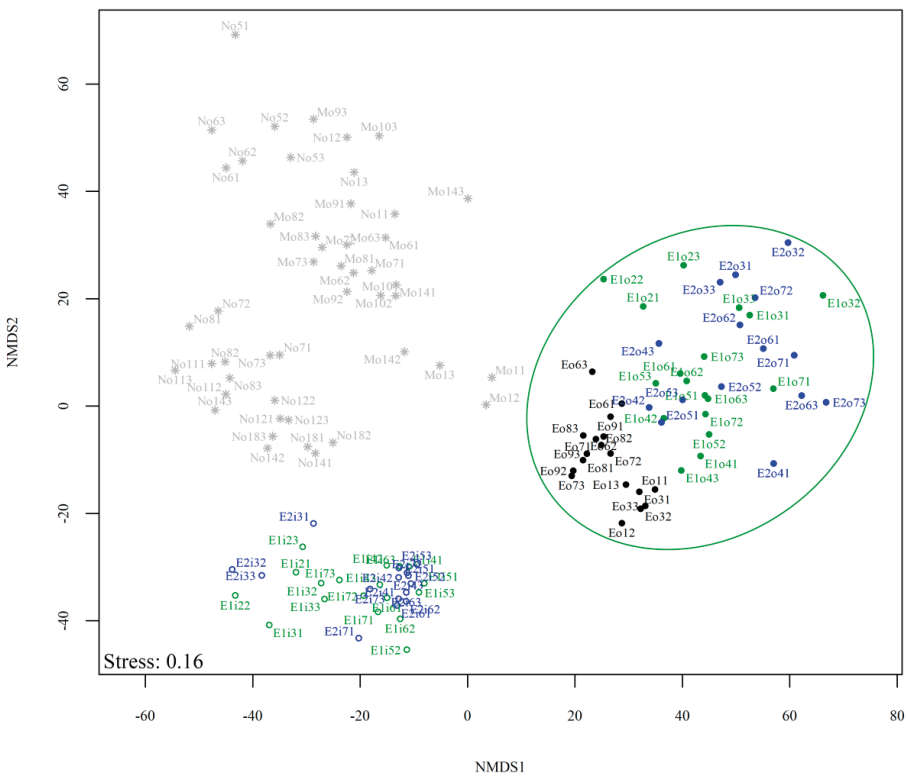

Paper III

Environmental Science
Water Research & Technology

PAPER

View Article Online
View Journal

Cite this: DOI: 10.1039/d0ew00622j

Impact of coagulation–ultrafiltration on long-term pipe biofilm dynamics in a full-scale chloraminated drinking water distribution system†

Kristjan Pullerits,[ab] Sandy Chan,‡[ab] Jon Ahlinder,[c] Alexander Keucken,[de] Peter Rådström[a] and Catherine J. Paul *[ae]

While pipe biofilms in DWDSs (drinking water distribution systems) are thought to affect the quality of distributed water, studies regarding the microbial processes are impeded by the difficulties in accessing biofilm undisturbed by DWDS maintenance. In this study, pipe sections were removed from a fully operational DWDS for biofilm sampling over two years and three months, and before and after start of ultrafiltration (UF) with coagulation treatment in the drinking water treatment plant (DWTP). Water (n = 31), surface biofilm (obtained by swabbing, n = 34) and deep pipe biofilm (obtained by scraping, n = 34) were analyzed with 16S rRNA gene amplicon sequencing; with flow cytometry, and chemical and natural organic matter (NOM) analysis as additional parameters for water quality. UF with coagulation decreased the total cell concentration in the DWDS bulk water from $6.0 \times 10^5 \pm 2.3 \times 10^5$ cells per ml to $6.0 \times 10^5 \pm 8.3 \times 10^5$ cells per ml, including fluctuations due to seasonal change, as well as decreasing most analyzed fractions of NOM. UF treatment of the water revealed that 75% ± 18% of the cells in the water originated from DWDS biofilm, confirmed by SourceTracker analysis, with the rest of the cells likely released from biofilm on DWTP storage tanks. Following UF start, the ASVs (amplicon sequence variants) in the deep pipe biofilm decreased, and Evenness and Shannon diversity indices decreased, reflecting the community's response to the new environment created by the altered water quality. The pipe biofilm community was dominated by ASVs classified as *Nitrosomonadaceae*, *Nitrospira*, *Hyphomicrobium* and *Sphingomonas*, with relative abundances ranging from 5–78%, and also included ASVs of genus *Mycobacterium*, genus *Legionella* and order *Legionellales*. This community composition, together with the observation that turnover of nitrogen compounds was unchanged by UF start, indicate that nitrification in the DWDS was localized to the pipe biofilm.

Received 1st July 2020,
Accepted 10th September 2020

DOI: 10.1039/d0ew00622j

rsc.li/es-water

Water impact

Pipe biofilm in a full-scale DWDS did not result in any significant biofilm detachment following installation of coagulation and ultrafiltration in the treatment plant. The bacterial community did alter, with nitrifiers adapting to maintain turn-over of nitrogen compounds at pre-UF levels. Since removal of cells by UF didn't impact nitrification, this was localized to the biofilm in this system.

1. Introduction

The surface of pipes in drinking water distribution systems (DWDSs) are colonized by microorganisms as biofilm. It has been estimated that >95% of the biomass in DWDSs is found in pipe biofilm and loose deposits[1,2] and biofilm may include up to 10^8 bacteria per cm^2.[2,3] Pipe biofilm is of great importance and has been linked to the drinking water quality by altering aesthetics of the bulk water,[4] enhancing nitrification in chloraminated systems,[5] serving as a reservoir for persistent opportunistic pathogens such as *Legionella* and *Mycobacteria*[6] and influencing corrosion.[7]

Due to their location, sampling of pipe biofilm in a DWDS is challenging. To address this difficulty, studies have investigated different types of biofilms in the DWDS that are more accessible, including biofilm on water meters[8] and coupons recovered from pilot- and full-scale systems,[9,10] as well as estimations of the biofilm community by sampling

[a] *Applied Microbiology, Department of Chemistry, Lund University, P.O. Box 124, SE-221 00 Lund, Sweden. E-mail: catherine.paul@tvrl.lth.se*
[b] *Sweden Water Research AB, Ideon Science Park, Scheelevägen 15, SE-223 70 Lund, Sweden*
[c] *FOI, Swedish Defence Research Agency, Cementvägen 20, SE-906 21 Umeå, Sweden*
[d] *Vatten & Miljö i Väst AB, P.O. Box 110, SE-311 22 Falkenberg, Sweden*
[e] *Water Resources Engineering, Department of Building and Environmental Technology, Lund University, P.O. Box 118, SE-221 00 Lund, Sweden*
† Electronic supplementary information (ESI) available. See DOI: 10.1039/d0ew00622j
‡ Present address: Sydvatten AB, Hyllie Stationstorg 21, SE-215 32 Malmö, Sweden.

water at different locations in the DWDS.[11,12] Grab samples of pipe biofilm, obtained for research purposes or during pipe maintenance, have also been investigated.[1,8,13–15]

Maintaining disinfectant residuals such as chloramine to repress growth of problematic organisms in the DWDS is common practice. This use is however debatable since resistant microorganisms can be selected[16] and, in combination with organic matter, cause undesirable disinfection byproducts to form.[17] The use of chloramine generates ammonia in the DWDS by excess ammonia, from chloramine formation, and chloramine decay, which can stimulate growth of nitrifying bacteria and subsequent undesirable production of nitrite and nitrate.[18] The ammonia is converted to nitrite by AOB (ammonia oxidizing bacteria) or AOA (ammonia oxidizing archaea); this nitrite can then support continued decay of monochloramine, and growth of NOB (nitrate oxidizing bacteria), producing both nitrate and growth of biofilm.[18] Bacteria in chloraminated drinking water included a community with diverse approaches to nitrogen metabolism dominated by *Nitrosomonas* (AOB), and *Nitrospira* (NOB) and accompanied by heterotrophs such as *Sphingomonas*[19] and these taxa were recently identified as actively conducting nitrification in diverse pipe biofilms.[13]

When a drinking water treatment plant (DWTP) in Varberg, Sweden, installed an ultrafiltration (UF) facility with two-stage filtration and in-line coagulation at the primary membrane stage,[20] the new finished water (FW) contained virtually no bacteria, and less and different natural organic matter (NOM).[11] The impact of this change on the bacterial community was examined by collecting water, swabbing the surface of the biofilm, and scraping to remove deep biofilm from multiple sections of pipe in series and excavated from the operational DWDS. In this drinking water system, we previously reported which bacteria were entering the water phase from the biofilm[11] and how seasonal variations and residence time affect the water quality.[21] In this study we examine how installation of the coagulation and ultrafiltration processes in the DWTP impacted the DWDS biofilm. The nature of the water quality in the DWDS was characterized in detail in order to determine if these changes could be linked to specific roles for the bacteria in the pipe biofilm, and we show that the bacterial biofilm alone can impact both biotic and abiotic aspects of water quality.

2. Methods

2.1 Study site and sampling

Samples were collected from the DWDS and DWTP (Kvarnagården) in Varberg, Sweden operated by Vatten & Miljö i Väst AB (VIVAB). Treatment consisted of pH adjustment, rapid sand filtration, storage tank 1 with addition of monochloramine, followed by storage tank 2 and 3 and UV disinfection (for more details see ref. 20). In November 2016, UF was added, hereafter defined as UF start, resulting in a treatment chain of rapid sand filtration, storage tank 1, coagulation and UF, pH adjustment, storage tank 2 with addition of monochloramine, storage tank 3 and UV disinfection (Fig. 1A). The monochloramine residual concentration in the finished water (FW) was between 0.13 and 0.21 mg L^{-1} as total chlorine. UF feed water was used for pH adjustment until March 2017 after which UF permeate water was used.[11]

Pipe biofilm (BF) was sampled in four locations in the DWDS on six occasions over 27 months (Fig. 1A). Biofilms BF1, BF2 and BF3 were sampled from a 25–30 year-old PVC pipe, while BF4 was sampled from a 15 year-old PE pipe. Before UF start, BF1, BF2, BF3 and BF4 were sampled two (n = 8), none, one (n = 4) and two (n = 8) occasions, respectively. After UF start BF1, BF2, BF3 and BF4 were sampled four (n = 16), two (n = 8), two (n = 8) and four (n = 16) occasions, respectively. All sampled pipes had a diameter of 160 mm. Biofilm was collected from multiple adjacent sections, 5–10 m upstream of each previous sampling location; and with swabbing through 360° in the field and with duplicate cotton swabs (Fig. S1A†) for surface biofilm samples; a strategy supported by both Neu *et al.*[22] and Liu *et al.*[15] Following surface sampling, sections of at least 70 cm excavated pipes were sealed with parafilm and transported to the lab. Deep biofilm was then sampled from 50 cm of the bottom half of each section (total area: 0.13 m^2) of excavated pipe (Fig. S1B†) within one hour, using a flame-sterilized custom-made metal scraper (Fig. S2†). Biofilm suspension was homogenized and collected using a 1 mL pipette with cut-off tips to avoid clogging the tips and suspensions were aliquoted into 1.5 mL Eppendorf tubes and duplicates used for sequencing. Cotton swabs and scraped biofilm were stored at −20 °C until DNA extraction.

Water was collected in the DWTP and from three distribution points (DPs; DP1, DP2 and DP3) in the DWDS (Fig. 1A) for conventional water quality analysis (n = 1, Eurofins Environment Testing Sweden AB, Linköping), NOM characterization (n = 1, LC-OCD-OND (liquid chromatography-organic carbon detection-organic nitrogen detection) at DOC-Labor (Germany)), flow cytometry (FCM) (n = 1, technical triplicates) and DNA sequencing (n = 1 and n = 2 for FW and DP3). FCM samples were collected in 15 mL Falcon tubes and when applicable, chlorine residuals were quenched with 1% (v/v) sodium thiosulfate (20 g L^{-1}). Samples were stored on ice or at 4 °C for less than 12 hours before analysis. Water for sequencing was collected in sterilized borosilicate bottles (1 L before UF start, and feed/RW, 5 L after UF start), filtered onto 0.22 μm pore size filters (Merck, Germany) and stored at −20 °C until DNA extraction. Raw data of flow cytometry-, conventional- and LC OCD-analyses are available through figshare (https://doi.org/10.6084/m9.figshare.12555353).

2.2 FCM analysis

FCM analysis was conducted on raw water, feed to the UF, FW and three DPs according to Prest *et al.*[23] and Gatza *et al.*[24] using a BD Accuri C6 flow cytometer (Becton Dickinson, Belgium) with a 50 mW laser at a wavelength of

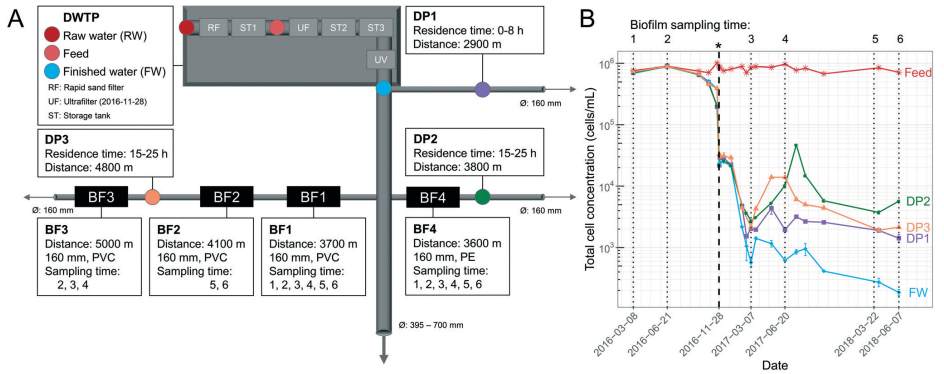

Fig. 1 Overview of sampling locations and total cell concentrations (TCC) over time. (A) Schematic illustration of the drinking water treatment plant (DWTP) process steps, and distribution points (DPs) in the DWDS, indicating locations where water was sampled, as well as biofilm (BF) points, where pipe sections were excavated for biofilm sampling. Ø indicates pipe diameter, arrows indicate water flow direction, and pipe material was polyethylene (PE) or polyvinyl chloride (PVC). The ultrafilter (UF) started November 28, 2016. (B) TCC in the water, determined by flow cytometry, and indicating in time when biofilm was sampled (dotted lines) and the UF start (*, bold, dashed line). Error bars show standard deviations of technical triplicates. Before the UF start, raw-water (RW) is labelled "Feed". Parts of this data are also shown in Chan *et al.* (2019)[11] and Schleich *et al.* (2019).[21]

488 nm. Total cell concentrations (TCC) were measured by staining bacteria in water samples with SYBR Green I at a final concentration of 1× in triplicate, final volume of 500 μL. Intact cell concentrations (ICC) were measured by staining bacteria with SYBR Green I (1× final concentration, 500 μL final volume) and propidium iodide (0.3 mM final concentration, 500 μL final volume) in triplicate. Stained samples were incubated at 37 °C for 15 min and 50–250 μL was analyzed (to ensure >1000 cells per analysis) using a threshold of 500 arbitrary units in green fluorescence. FCS files were analyzed using FlowJo (Tree Star Inc., USA) and gated identically on green fluorescence (533 ± 30 nm) and red fluorescence (>670 nm). High nucleic acid (HNA) bacteria were measured by a cut-off in green fluorescence at $>2 \times 10^4$ arbitrary units.[23] The contribution of cells from the pipe biofilm (BFcells) was calculated using eqn (1) where cells_{DP} is the TCC at the distribution point and cells_{FW} the TCC in the Finished Water:

$$\text{BFcells} = \text{cells}_{DP} - \text{cells}_{FW} \quad (1)$$

The relative contribution of cells from the pipe biofilm (BFcells (%)) was calculated using eqn (2)

$$\text{BFcells}\ (\%) = \frac{\text{BFcells}}{\text{cells}_{DP}} \quad (2)$$

where BFcells was calculated with eqn (1).

2.3 Bacterial community analysis

All DNA was extracted using the FastDNA Spin Kit for soil (MP Biomedicals, USA) following the manufacturer's instructions. Sodium phosphate was added to Lysing Matrix E tubes and either the cut-off tip of the cotton swabs; 120 μL of the scraped biofilm; or, filter papers cut into strips, were added to the tubes. Empty filters and unused cotton swabs were extracted as negative controls. DNA was stored at −20 °C. The V3-V4 region of the 16S rRNA gene was amplified with primers 341F (5-CCTACGGGNGGCWGCAG-3) and 785R (5-GACTACHVGGGTATCTAATCC-3).[25] The PCR reaction (25 μL) included 12.6 μL MilliQ-water, 10 μL 5 Prime Hot MasterMix (Quantabio, USA), 0.4 μL (20 mg mL^{-1}) bovine serum albumin, 0.5 μL (10 μM) forward and reverse primers and 1 μL template DNA or 5 μL template DNA in low biomass samples. PCR settings were 94 °C for 3 min and 35 cycles of 94 °C for 45 s, 50 °C for 1 min, 72 °C for 1.5 min and a final step of 72 °C for 10 min. Three PCR reactions were performed for each sample, pooled together, visualized by agarose gel, with DNA concentration quantified using a Qubit 2.0 dsDNA BR Assay Kit (Thermo Fisher Scientific, USA). Some primer dimers were observed following amplification from low biomass samples (FW, after UF start), although these were minimal in the amplicons from biofilm. Fifty ng of each pooled amplicon were pooled together and purified using Select-a-Size DNA clean and concentrator (Zymo Research, catalog #4080) and quantified using Qubit. Purified amplicon concentrations were adjusted to 2 nM, the library was denatured and diluted according to manufacturer's instruction (Illumina, USA), 10% PhiX was added to the sequencing run and amplicons sequenced using the MiSeq Reagent Kit v3 (600-cycles) (Illumina) according to the manufacturer's instructions.

2.4 Bioinformatics and statistics

Raw sequencing reads were demultiplexed with deML[26] and processed in QIIME2,[27] version 2018.8.0. Reads were

truncated at 280 and 215 bp for forward and reverse reads, respectively, and classified with the Greengenes database.[28] Additional analyses were done with the Phyloseq package[29] in R.[30] Samples were visualized in a PCoA plot using Bray Curtis dissimilarity. Negative controls clustered with low biomass samples (FW, after UF start) having low read counts. Thus, samples with fewer than 2600 reads and all FW samples after UF start (eight negative controls and nine FW samples) were not included in further data analyses. Singletons and ASVs at a frequency less than 0.005% of the total number of reads[31] and ASVs occurring in less than four samples were removed, resulting in 289 ASVs in 99 samples. Each ASV was identified with a number from 1–289 and letter to indicate its taxonomy when available (g = genus, f = family, o = order and c = class). Reads were normalized to relative abundances. R packages used for visualizations and calculations were; ggplot2,[32] ggnomics,[33] microbiome[34] and VennDiagram.[35] R script and plots from Kantor *et al.*[36] were used as inspiration in some figures. Species diversity indices were calculated using Phyloseq (Shannon Index and observed ASVs) and the microbiome package (Pielou's measure) with non-normalized reads as suggested by McMurdie and Holmes[37] since these indices are based on observations and not fractions. Differential abundance analysis was conducted with DESeq2,[38] using non-normalized reads ($P_{adjusted} < 0.05$). A Bayesian signature based microbial source tracking method (SourceTracker[39]) was utilized using default settings with the exception of a rarefaction depth set to 10 000. The source library included 68 biofilm communities, five raw-water communities and seven negative control communities (to account for possible contamination[40]).

Pearson correlation (paired *t*-test) was calculated with the cor.test function, and the Welch *t*-test, were done in R. Locally weighted least squares (loess) regression was done using geom_smooth function in ggplot2 with the span parameter at 0.9. DNA sequences are available at the NCBI sequence read archive with the project accession number: PRJNA622401.

3. Results

3.1 Impact of UF start on water quality

Most water quality parameters responded predictably, based on expected changes introduced by UF start (Fig. S16† and Chan *et al.*, (2019)[11]). The UF with coagulation removed 32% ± 4.4 of the dissolved organic carbon (DOC), from 2700 ± 300 ppb-C (feed) to 1800 ± 140 ppb-C (permeate) (Fig. S17†). Following UF start, DOC, chromatographic dissolved organic carbon (CDOC), chemical oxygen demand (COD-Mn), absorbance and color decreased in the DPs (Table 1). Throughout the study the UF feed water or raw water had a TCC of 820 000 ± 90 000 (± standard deviation) (Fig. 1B). Before UF start, the finished water (FW) and water from the DWDS (DP1, DP2, DP3) had similar mean TCC, at 630 000 ± 200 000 cells per mL and 600 000 ± 230 000 cells per mL, with minimal contribution of cells from pipe biofilm (−0.13% ± 0.33; eqn (2)). After UF start, most cells in the FW originated from UF feed water used for pH regulation[11] while after March 2017, UF permeate was used for pH regulation, and the TCC in the FW was 900 ± 560 cells per mL, likely originating from biofilm in DWTP storage tanks. Each DP had water with TCC of an overall mean of 6000 ± 8300 cells per mL (DP1: 2600 ± 1100, DP2: 9700 ± 13 000 and DP3: 5800 ± 4500 cells per mL) and the contribution of cells from the DWDS pipe biofilm was an average of 75% ± 18 (64% ± 20, 81% ± 16 and 80% ± 14 at DP1, DP2 and DP3, respectively), reaching 98% at DP2 when the water temperature was elevated (Fig. S3†). While comparisons were limited, there was no difference in the number of cells entering the water, during the transition phase (sampling points 3 to 4; 4600 ± 4600 cells per mL; eqn (1)) compared to the later sampling times (sampling points 5 to 6; 2600 ± 1600 cells per mL) ($P > 0.05$, Welch *t*-test).

Observations of absolute counts of HNA cells (Fig. S4A†) and intact cells (Fig. S4B†) were similar to that of the TCC (Fig. 1B). From March 2017 to June 2018 the mean % HNA in the FW was 47% ± 10, and increased with distribution (65% ± 9, 71% ± 8 and 60% ± 6 in water from DP1, DP2 and DP3 respectively; Fig. S5A†). While the % HNA always increased at the DPs, the % ICC difference changed with water temperature (Fig. S5B†): % ICC difference decreased at the DPs from March 2017 to June/July 2017 and then increased, compared to the FW, until March 2018.

3.2 The pipe biofilm and water communities

The bacterial communities in water and biofilm were investigated with 16S rRNA gene amplicon sequencing. The number of observed biofilm ASVs were 20 ± 3.4, 19 ± 2.3, 42 ± 7.0 and 41 ± 7.8 at BF1, BF2, BF3 and BF4, respectively (Fig. S6†). Principal coordinates analysis (PCoA), based on Bray Curtis-dissimilarity, showed that communities at BF3 and BF4 were more similar than those at BF1 and BF2 (Fig. S7A†). The ASVs from the same pipe section (BF1, BF2, BF3), changed with distance from the treatment plant (Fig. 2B). The relative abundance of *Nitrosomonadaceae* decreased between BF1 to BF3, whereas that of *Nitrospira* increased with distance (Fig. 2 and S8†) which was also observed with

Table 1 Selected water quality parameters (mean value ± standard deviation) of the distribution points (DP1, DP2 and DP3), before and after UF start. See Fig. S16 and S17† for other conventional water quality and NOM analyses

	DOC (ppb-C)	CDOC (ppb-C)	COD-Mn (mg O_2 per L)	Absorbance 254 nm (A.U)	Color 410 nm (mg Pt per L)
Before (n = 9)	2500 ± 170	2400 ± 130	2.2 ± 0.12	0.41 ± 0.032	12 ± 1.6
After (n = 24)	1800 ± 170	1700 ± 120	1.3 ± 0.11	0.19 ± 0.048	0.38 ± 1.7

differential abundance analysis (Fig. S9†). At BF1, ASVs classified as *Nitrosomonadaceae*, *Hyphomicrobium* and *Sphingomonas* dominated in relative abundance; at 64% ± 10, 23% ± 10 and 10% ± 12, respectively (Fig. 2A). The community at BF2 was also dominated by *Nitrosomonadaceae,* at 42% ± 6, while the ASV classified as *Nitrospira* increased to 31% ± 14, and relative abundances of *Hyphomicrobium* and *Sphingomonas* were comparable to those at BF1, at 17% ± 12 and 6% ± 2, respectively. Biofilms at BF3 and BF4 were dominated by the ASV classified as *Nitrospira,* at 78% ± 5 (BF3) and 75% ± 12 (BF4), relative abundance of *Hyphomicrobium* was less, at 5% ± 3 (BF3) and 6% ± 3 (BF4), and, relative abundance of *Sphingomonas* was similar to that at BF1 and BF2, at 6% ± 2 (BF3) and 6% ± 2 (BF4).

Observed ASVs in water from the DWTP were 79 ± 13, and 94 ± 13 at the DPs before UF start, decreasing to 45 ± 17 after UF start (Fig. S6†). Before UF start, ASVs in the water at the DPs were similar to the DWTP (Fig. S7B† and 2B), and distinct from those in biofilm. Following UF start, ASVs in the distributed water resembled those in the biofilm, including *Nitrosomonadaceae*, *Nitrospira*, *Hyphomicrobium* and *Sphingomonas* (Fig. 2B). Before UF start, the raw water contributed 86% ± 8 of the bacterial community at DPs (Fig. 3) while following UF start, this decreased to 4% ± 4 and the water community largely consisted of bacteria originating from biofilm (60% ± 20), estimated by SourceTracker. The taxa with highest assignment probability in the DPs within the biofilm source after UF start were *Nitrosomonadaceae*, *Nitrospira*, *Hyphomicrobium* and *Sphingomonas* (data not shown).

Mycobacterium_142, was present in 20/36 samples from BF3 and BF4 (Fig. S10†), ranging from 0.43% to 31%, while *Mycobacterium_144* was present in the RW, feed and FW and water from the DPs before UF start. Following UF start, *Mycobacterium_143* was observed in the water from DP1 and DP2. One ASV classified as the order *Legionellales* (*Legionellales_174*) was present in 47/68 biofilm samples (Fig. S11†), at 0.019% to 1.4% relative abundance, and was also present in 9/12 water samples from DPs after UF start (relative abundance 0.31% to 3.8%) (Fig. 2B). A second ASV classified to genus level as *Legionella_175* was present in four samples from BF1.

The core biofilm community contained six ASVs present at all four BFs, regardless of sampling occasion: two ASVs classified as *Sphingomonas,* two ASVs classified as

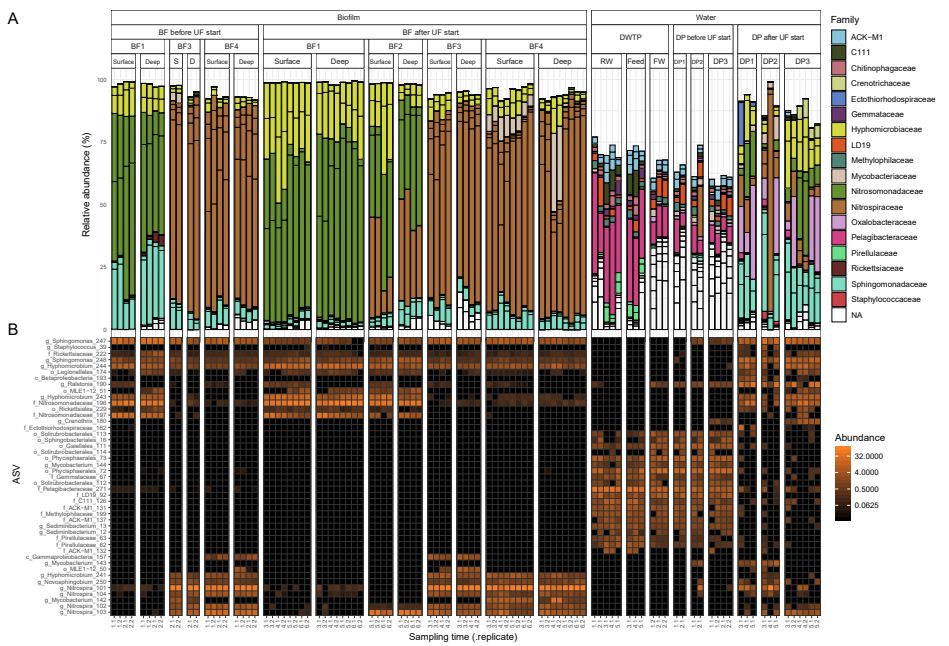

Fig. 2 Bacterial community composition in biofilm and water. Samples are ordered in rows and grouped together based on sample type. ASVs present at >3% in one sample, representing 45 ASVs, are shown in both panels. Each column is one biological replicate. (A) Bar plot showing relative abundance at family level where each ASV is a bar separated by a black line. (B) Heatmap of ASVs with the most specified taxonomy when available, g = genus, f = family, o = order and c = class. Abbreviations; S: surface and D: deep. Sampling time indicates the date of sampling (Fig. 1B).

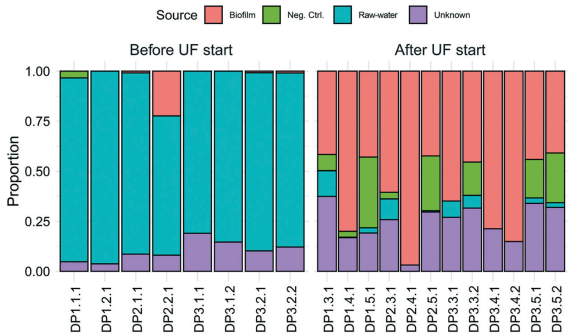

Fig. 3 Identification of the origin of bacteria in the DPs using SourceTracker. Colored bars show the estimated proportion of bacteria from biofilm, negative control (neg. ctrl), raw-water or unknown sources. Samples are ordered in rows and named by their DP number, followed by sampling time and replicate. Each bar is one biological replicate.

Hyphomicrobium, one ASV classified as *Nitrosomonadaceae* and one ASV classified as *Rickettsiaceae* (Fig. 4 and Table S1†). The biofilm communities at BF3 and BF4 shared the most ASVs, at 30.

3.3 Dynamics in pipe biofilm community in response to UF start

Dynamics in the biofilm community as a response to UF start were examined over time, and between surface and deep locations in the biofilm. Only BF1 and BF4 were sampled sufficiently often for statistically robust comparison. In deep biofilm at BF1 and BF4, observed ASVs decreased with time (Fig. 5, $P < 0.05$ and $P = 0.0504$, paired *t*-test), reaching numbers similar to those in their surface biofilm by the end of the study. The number of observed ASVs in the surface biofilm was similar over time at both locations ($P > 0.7$, paired *t*-test) while Shannon and Evenness indices decreased with time in surface and deep biofilm at both locations ($P < 0.05$, paired *t*-test). The biofilm communities at BF1 and BF4 responded in a similar way to UF start: changing from their original composition before UF start (Fig. S12†); moving through a transitional community shortly after UF start, to cluster together in a distinct post-UF community.

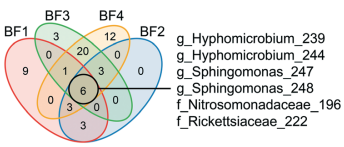

Fig. 4 Identification of the core biofilm community. ASVs shared among the biofilm communities at different sampling points are shown in the different sections of the Venn diagram. ASV core communities for each biofilm represent ASVs >0.1% relative abundance in a minimum of 4 samples. The six ASVs shared by all four biofilms are shown with the most specified taxonomy available, g = genus and f = family. See ESI† Table S1 for all other shared ASVs. BF1: $n = 24$, BF2: $n = 8$, BF3: $n = 12$ and BF4: $n = 24$.

Changes in relative abundance of ASVs over time (Fig. 6), and in surface and deep biofilm, defined the biofilm communities before UF (sampling time 1 and 2), during transition (sampling time 3 and 4), and after UF start (sampling time 5 and 6). At BF1, after UF start, *Nitrosomonadaceae_196* increased in relative abundance, from 41% ± 8.5 to 65% ± 5.6 (surface and deep grouped together, $P < 0.001$, one-way ANOVA), whereas *Nitrosomonadaceae_197* decreased in relative abundance from 17% ± 7.0 to 3.4% ± 1.8 ($P < 0.05$, one-way ANOVA). *Hyphomicrobium_244* and *Hyphomicrobium_243* both increased after UF start (7.0% ± 2.9 to 12% ± 2.4 and 4.4% ± 1.2 to 14% ± 3.7 ($P < 0.05$ and $P < 0.05$, one-way ANOVA), before and after UF start respectively) while *Sphingomonas_247* decreased from a relative abundance of 26% ± 7.7 to 0.46% ± 0.33. *Sphingomonas_248* had a relative abundance of 1.9% ± 0.97 before UF and decreased to 0.64 ± 0.23% in the transition state, before returning to 1.8% ± 0.81 relative abundance after UF start.

At BF4, and after UF start, *Nitrospira_101* increased from 50% ± 6.4 to 76% ± 4.3 ($P < 0.001$, one way ANOVA), whereas three other ASVs in this genera decreased (*Nitrospira_103* from 20% ± 6.4 to 2.3% ± 1.6; *Nitrospira_102* from 5.6% ± 1.3 to 1.6% ± 0.87; and, *Nitrospira_104* from 4.4% ± 1.1 to 1.0% ± 0.60; all $P < 0.001$, one-way ANOVA). *Mycobacterium_142* increased from 0% to 3.3% ± 2.7, following UF start, reaching a maximum relative abundance of 31% ± 1.0 in the deep biofilm during transition (sampling time 4) with ASV *Mycobacterium 141* showing a similar trend. As at BF1, *Hyphomicrobium_244* increased in relative abundance at BF4 after UF start, from 1.4% ± 0.54 to 2.8% ± 1.4 ($P < 0.05$, one-way ANOVA). These observations were comparable to those obtained with differential abundance analysis (Fig. S15†).

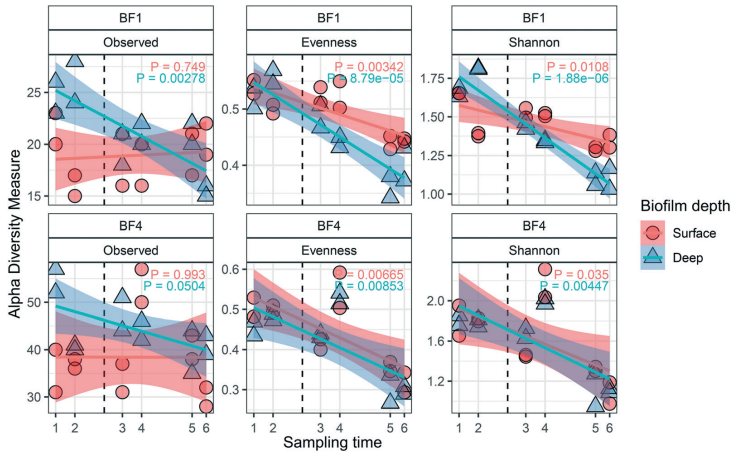

Fig. 5 Diversity metrics describing the impact of UF start on the biofilm community structure for surface (n = 2 at each sampling time) and deep (n = 2 at each sampling time) biofilm. Changes were observed in alpha diversity metrics (observed ASVs, Evenness and Shannon) over time, and for BF1 and BF4. The vertical dashed line indicates the UF start. The transparent areas show the 95% confidence interval for each linear regression. P value shows paired t-test.

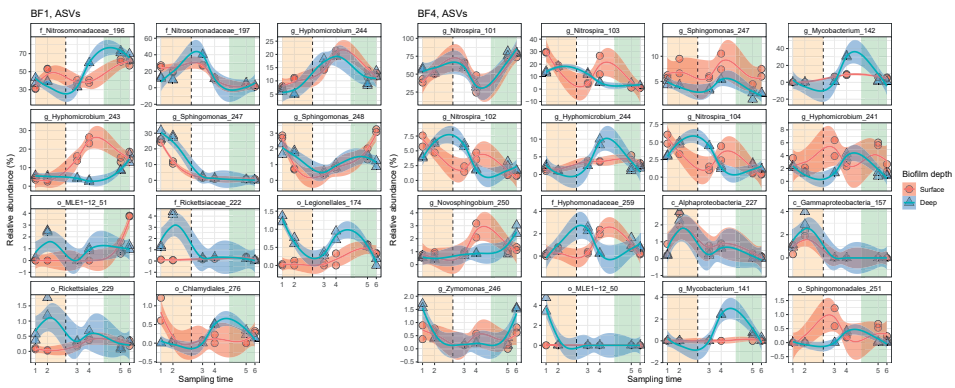

Fig. 6 Dynamics of the predominant relative abundant ASVs (>1.2% in one sample) in surface (n = 2 at each sampling time) and deep (n = 2 at each sampling time) biofilm over time. The change in relative abundance for individual ASVs from BF1 and BF4 are ordered from greatest relative abundance in top left panel, decreasing to bottom right. The vertical dashed line indicates the UF start. Shade areas in orange, white and green represent time periods defined as before UF (sampling time 1 and 2), transition (sampling time 3 and 4) and after UF (sampling time 5 and 6), respectively. ASVs are shown with the most specific taxonomy when available, g = genus, f = family, o = order and c = class. Blue and red lines show locally weighted least squares (loess) regression for each biofilm depth and the transparent areas are 95% confidence intervals for each loess regression. See ESI† Fig. S13 and S14 for full data sets.

3.4 Nitrification in the DWDS

UF status did not impact concentrations of nitrogen species at different locations (Fig. 7) and therefore was not influenced by the number of cells in the distributed water. Ammonium nitrogen in the water decreased between the DWTP and the DPs by an average concentration of 0.025 ± 0.0045 mg L^{-1} before, and 0.021 ± 0.003 mg L^{-1} after UF start (P = 0.17, Welch t-test) with nitrite nitrogen showing an opposite trend and increasing as water passed through the DWDS, by 0.014 ± 0.0023 mg L^{-1} before, and 0.014 ± 0.0012 mg L^{-1} after the UF start (P = 0.87, Welch t-test). Nitrate

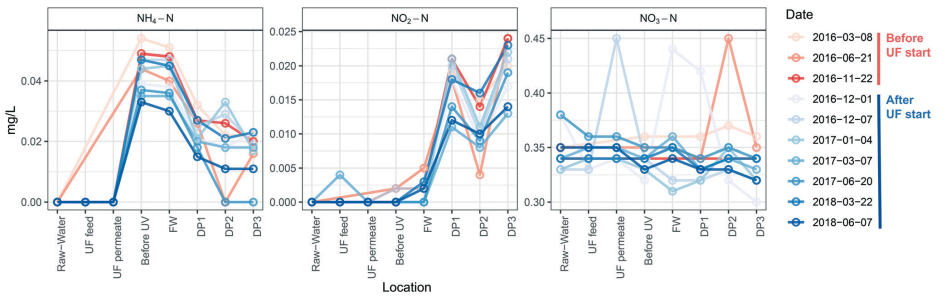

Fig. 7 Concentrations of nitrogen compounds in water were unchanged by installation of UF. Concentrations of ammonia-nitrogen, nitrite-nitrogen and nitrate-nitrogen at the different sampling points and dates, are shown for water samples taken at the different DPS, before (red) and after (blue) UF start. The limits of quantification of ammonium nitrogen and nitrite-nitrogen were 0.01 mg L^{-1} and 0.002 mg L^{-1}, respectively and are depicted as 0 in the figure. n = 1 for each sampling time and location.

nitrogen did not change during distribution of water before UF start (0.017 ± 0.017 mg L^{-1}, $P > 0.37$, Welch t-test), and decreased only slightly after UF start (0.019 ± 0.017 mg L^{-1} ($P < 0.05$, Welch t-test). Ammonium nitrogen and nitrite nitrogen were below the detection limit for DPs further away from the DWTP than DP3 (data not shown).

4. Discussion

This study describes the dynamics of the bacterial community in pipe biofilm and the associated drinking water over a 27 month period in a full scale DWDS. During this time the DWTP was upgraded to combine coagulation with UF treatment, and led to an immediate change in water quality, significantly altering the bacteria and NOM in the DWDS. By sampling multiple pipe sections, and with many fewer cells in the distributed water, the connection between these changes in water quality on the resident biofilm community over this period could be directly assessed and attributed to contact with the pipe biofilm, in both the immediate weeks following the UF start,[11] and over the extended time period in the current study.

4.1 Interaction of the biofilm with the distributed water

No large disturbance or sudden changes in the number of bacteria released from the biofilm were observed following UF start. The numbers of bacteria at the DPs were low, and changed mainly with season, echoing results in other studies of this DWDS[21] with SourceTracker analysis confirming that the majority of these cells originated from the pipe biofilm, and not the DWTP. Significant impacts have been observed when the "balance of forces" required to maintain stability in the quality of distributed water have been altered by, for example, a change of source water, or physical flow characteristics.[41] In the present study, while a great number of cells were removed from the water, with some impact on organic matter, other operational parameters such as chlorination[41] were not changed: and hence the nature of the disturbance can explain why dramatic changes observed in other DWDS during transition were not observed.

The identity of bacteria in the DPs was consistent with those released from biofilm directly after UF start,[11] including more cells defined as HNA at the DPs than in the FW. While some cells may have increased in number during distribution due to growth, including growth of cells released from the biofilm, the doubling time of planktonic bacteria in oligotrophic drinking water has been estimated as 2.31 days (ref. 42) and together with the greatly reduced number of cells (which can also serve as a source of nutrition[43] and the water temperature during the study period, the increase in cell number as the water was distributed can be largely attributed to those entering from the biofilm. The water community in both this and the previous study included abundant *Nitrospira* and *Sphingomonadaceae* and this agrees with the observation that these have previously been identified as HNA bacteria (>0.4 μm)[44] as well as identification of these taxa as abundant members of the biofilms in this study. A previous description of this DWDS (also following UF start) noted a shift to LNA bacteria in the water during distribution, although this study examined water with significantly longer retention times (up to ~170 h).[21] As water is distributed, monochloramine is depleted, other chemical changes occur and there is increasing numbers of bacteria in this system released from the pipe biofilm in proportion to distance, suggesting that at more distal locations, the community in the biofilm is not similar to that observed in this study.

4.2 Changes in the biofilm community driven by nitrification

While pipe material and age in the branch of the DWDS where BF1–BF3 originated were identical, the observations in the biofilm community suggest that water residence time and changed water chemistry (due to upstream biofilm metabolism, see below) began to shift the community after 400 m, with a complete community change after 1300 m. Influence of

hydraulic parameters on the community was also evident when comparing BF3 and BF4. Biofilms formed in contact with drinking water under lower flow rates have higher biomass, DNA concentration and total number of cells,[45] suggesting that water flowing at a reduced rate at BF4 may have had contact with a similar amount of biomass, and subsequent nitrification, as that at BF3, and supporting similar communities at these locations. The pipe section with BF4 serves fewer consumers and thus while equally distant as BF1 from the DWTP, the water at BF4 likely had contact with the biofilm similar to that at BF3, and supported by the higher TCC in the water at DP2 than DP3. That flow is an influencing factor on the community at BF4 is further supported by observations that both nitrate concentration and the presence of *Mycobacterium* have been inversely correlated to flow.[10]

As the presence of NOM facilitates decomposition of monochloramine into ammonia and nitrate;[46] and increased concentrations of bacteria would remove monochloramine,[47] UF start would increase the relative concentration of monochloramine in contact with the biofilm. In contrast, analysis of the nitrogen compounds showed no change at the different DPs following UF start, and nitrification was unaffected by removal of the cells in the water phase, strongly suggesting that nitrification takes place exclusively in the biofilm of this system. A significant role for the pipe biofilm in nitrogen transformation is supported by the observation that nitrifiers *Nitrosomonadaceae* and *Nitrospira*, together with *Hyphomicrobium* and *Sphingomonas*, accounted for 5–78% of the mean relative abundance in the biofilm. The role for chemoautotrophic nitrifiers is well established, metagenomics evidence has described participation of *Sphingomonas* in nitrogen cycling in drinking water.[19] The core community here across all locations was comprised of only genera *Hyphomicrobium* and *Sphingomonas* and families *Nitrosomonadaceae* and *Rickettsiaceae* and coupled with the high relative abundance of *Nitrosomonadaceae* and *Nitrospira,* suggests that the biofilm in this study survives largely *via* ammonia and nitrite oxidation. The relative abundance of family *Nitrosomonadaceae* was higher in BF1, compared to BF3 in the same pipe section, and genus *Nitrospira* gradually predominated as distance, and water residence time, increased from the treatment plant, at sampling locations BF3 and BF4. As nitrification is the conversion of ammonium to nitrite by AOB (*Nitrosomonadaceae*), continued by nitrite to nitrate conversion by NOB (*Nitrospira*), it seems the biofilm converted the majority of the ammonium to nitrite in the distance from BF1 to BF3, and supported by high nitrite concentrations at DP3. Longer water residence time, such as that at BF4, would slow inflow of fresh ammonia, permitting complete nitrification to a greater extent at a shorter distance, and supporting the high relative abundance of *Nitrospira* at BF4. Only the biofilm at BF2 showed a mix of both AOB and NOB, showing that certain locations may support balanced mutualistic symbiosis[48] and; communities at different locations will be determined by the delivery of nitrogen compounds in the flowing water, although the presence of commomox *Nitrospira* within the *Nitrospira* ASVs identified here cannot be ruled out.[49] The water at DP2 downstream from BF4 showed lower nitrite concentrations than at DP3, preceeding the abundant *Nitrospira* at BF3, and ammonia and nitrite were below the detection limit in DPs with longer residence times (data not shown), further supporting that conversion of nitrite to nitrate relies on abundant *Nitrospira* in the biofilm.

Changes in the relative abundance and spatial distribution of ASVs for nitrifiers following UF start indicate that the biofilm community may buffer changes in relative ammonium and nitrate concentrations by changing the abundance of its members: after 1.5 years the changes in the community were apparent in ASVs, but not at family level (Fig. 2). This indicates that the biofilm maintained functionality[50] while adapting to the new water quality.[8,14] The communities at BF1 and BF4, and those in the water following UF start, decreased in evenness and Shannon diversity with time, indicating selection of bacteria (ASVs) for the new environment, and possibly reflecting the relative increase in monochloramine concentration as lower diversity has been proposed to correlate with higher disinfectant concentration.[13] ASVs capable of oxidizing ammonia (*Nitrosomonadaceae* 197, BF1) decreased in relative abundance following UF start, however, other *Nitrosomonadaceae* taxa (196) increased at the same sampling location, reflecting adaptation, and demonstrating functional redundancy for conversion of ammonia to nitrite. Relative abundance of *Nitrospira* also responded to UF start, with decreases in *Nitrospira* ASVs 102 103 and 104 at sampling point BF4, and increase in *Nitrospira* ASV 101, with no change in nitrate concentrations. In a study using batch reactors, ammonia concentrations only decreased in the reactor containing particulate matter obtained from filtration of drinking water, while all reactors maintained similar TCC in the bulk water phase, supporting that nitrification may require cells attached to surfaces.[51] Large populations of nitrifiers were identified in tropical chloraminated pipe biofilms, and nitrification activity in biofilm corresponded to identified taxa;[13] and, nitrogen biotransformation in chloraminated DWDS and reservoirs has been linked to diverse populations including nitrifiers and heterotrophic bacteria.[19,52] This suggests that to maintain monochloramine residual, drinking water producers need to consider nitrification occurring in the biofilm and that, regardless of biological content in the distributed water, disinfection concentration will continue to be determined by location within the DWDS.[17]

Sphingomonas and *Hyphomicrobium* have been observed in high relative abundances in pipe biofilm from real and model DWDS pipe materials exposed to a variety of residual disinfection types[1,10,14,53] and have recently been linked to heterotrophic metabolism of nitrogen species.[19] In the current study, relative abundance of *Sphingomonas* ASV 247 was most affected by UF start at BF1, where a decreased NOM content, together with higher flow than at BF4, may

have pushed past the limits of oligotrophy tolerable for *Sphingomonas*. An increasing abundance of *Sphingomonas* has been associated with decreased disinfectant residual[19] so this could also reflect a relative increase in monochloramine after UF start, and abundance of *Sphingomonas* in the water downstream of BF1 at DP3, and after UF start, suggests shedding of this ASV from BF1, due to the new environment. The changes in relative abundance of *Sphinogomonas* at BF1 may also be linked to the shift in ASV identity of the *Nitrosomonas* representative at BF1, as a metabolic link between these taxa, with *Nitrosomonas* producing tyrosine to be degraded by *Sphingomonas,* has been proposed.[19] Depending on the metabolism of individual ASVs, changes in identity and relative abundance of *Sphingomonas* and *Nitrosomonas* at BF1 may also explain why ASVs for *Hyphomicrobium* increased following UF start, due to a lack of competition from *Sphingomonas,* and altered availability of C1 compounds and nitrite. The flexibility of *Hyphomicrobium* species to utilize C1-compounds likely gives them an advantage in oligotrophic environments like pipes, particularly those distributing ultrafiltered water, as well as *via* denitrification in monochloraminated DWDS.[53]

4.3 Impact of treatment change on taxa associated with opportunistic pathogens

ASVs classified as *Mycobacterium* and *Legionellales* were detected in biofilm and water, and family *Rickettsiaceae* was identified as a member of the core community. Individual species within these classifications (and others, including *Sphingomonas*) may harbor opportunistic pathogens. While this supports previous suggestions that biofilm could be a reservoir for these bacteria,[6] it is important to consider that the approach used in this study is neither able to determine which bacteria are alive or dead, nor represent absolute quantification of any taxa resolved to species identity. *Mycobacterium* has been observed in chloraminated DWDS biofilms[54,55] and bulk water in chlorinated and chloraminated DWDSs[56] although risk of infection has not been associated with chloraminated DWDS.[57] *Mycobacterium* is known to be resistant to many disinfection methods,[58] including ultraviolet (UV) disinfection,[59] which the DWTP in this study is using. *Legionella* has been detected in pipe biofilms[60] and also in bulk water both in chlorinated and chloraminated DWDSs,[56] due in part to their ability to live within protozoa.[61] Dynamics in *Mycobacterium* and *Legionellales* showed elevated relative abundances during summer (Fig. 6) likely due to increased temperatures. At BF1, the relative abundance of ASV *Legionellales* 174 was higher in the deep biofilm compared to the surface, but following UF start, the relative abundance of this ASV was similar in both surface and deep biofilm, and in lower abundance (relative to the deep biofilm). This was also observed at BF1, although this ASV was overall, less abundant (Fig. S14†). *Rickettsiales* (ASV 229) also decreased in relative abundance in the deep biofilm. This suggests that introduction of UF treatment may cause some members of these taxa to either disappear from the surface biofilm, or relocate from the deep to the surface and detection of these same ASVs in the water following UF start suggests they are released into the drinking water. While the same was not observed for *Mycobacterium,* these changes in location may not be specific to taxa including opportunistic pathogens, but may be part of a general remodeling of the deep biofilm following UF start. Overall, the number of observed ASVs decreased with time in the deep biofilm, reaching the same levels of abundance as in the surface biofilm, in both BF1 and BF4 (Fig. 4).

5. Future outlook and conclusions

While biostability is currently defined as maintaining a defined microbial water quality until the drinking water reaches consumers,[62] and "biologically stable water does not promote the growth of microorganisms during its distribution",[63] the current study, and others, suggest that this definition must be reconsidered. The concept of biostability could be revised to reflect natural dynamics in the microbial community which do not compromise public health.[64] This new definition may be especially appropriate when there are few cells in the water and a diverse pipe biofilm, influenced by a number of operational parameters, governs the microbial water quality throughout the DWDS. This definition is needed in the context of DWTP with advanced treatment chains, such as observed in the present study, as well as in the context of water re-use, where produced water can be virtually cell-free. This will require significant efforts to understand how to monitor microbial dynamics with moving baselines influenced by season, residence times and other variables, while ensuring no impact on consumer satisfaction and safety.

In addition, this study showed:

- UF with coagulation decreased the total cell concentration in the DWDS bulk water and altered the bacterial community composition in the pipe biofilm, but this change did not result in any significant biofilm detachment.
- Disinfection using monochloramine supports a high relative abundance of nitrification bacteria in this pipe biofilm, including *Nitrosomonadaceae* and *Nitrospira.* These taxa adapted to the change instigated by UF start, while retaining function, demonstrating functional redundancy *in situ* by a diverse nitrifier community.
- The majority of nitrification in this DWDS was performed by the pipe biofilm both before and after installation of UF.
- Taxa that include possible opportunistic pathogens were detected in the pipe biofilm and their location and prevalence in the biofilm may be influenced by change to distribution of ultrafiltered water, however additional quantitative investigations are required to assess any changes in risk to the consumer.

Conflicts of interest

There are no conflicts of interest to declare.

Acknowledgements

The authors want to thank Jennie Lindgren and Moshe Habagil for assistance in sampling, Emelie Salomonsson for assistance with sequencing, and Marcel Ollila who designed and made the biofilm scraper. The study was funded by Sweden Water Research AB, DRICKS center for drinking water research, Swedish Water and Wastewater Association (SVU), public joint-stock utility Vatten & Miljö i Väst AB (VIVAB).

References

1 G. Liu, G. L. Bakker, S. Li, J. H. G. Vreeburg, J. Q. J. C. Verberk, G. J. Medema, W. T. Liu and J. C. Van Dijk, Pyrosequencing reveals bacterial communities in unchlorinated drinking water distribution system: An integral study of bulk water, suspended solids, loose deposits, and pipe wall biofilm, *Environ. Sci. Technol.*, 2014, **48**, 5467–5476.

2 H. C. Flemming, S. L. Percival and J. T. Walker, Contamination potential of biofilms in water distribution systems, *Water Sci. Technol.: Water Supply*, 2002, **2**, 271–280.

3 C. R. Proctor and F. Hammes, Drinking water microbiology — from measurement to management, *Curr. Opin. Biotechnol.*, 2015, **33**, 87–94.

4 K. Fish, A. M. Osborn and J. B. Boxall, Biofilm structures (EPS and bacterial communities) in drinking water distribution systems are conditioned by hydraulics and influence discolouration, *Sci. Total Environ.*, 2017, **593–594**, 571–580.

5 B. A. Carrico, F. A. Digiano, N. G. Love, P. Vikesland, K. Chandran, M. Fiss and A. Zaklikowski, Effectiveness of switching disinfectants for nitrification control, *J. - Am. Water Works Assoc.*, 2014, **100**(10), 104–115.

6 J. Wingender and H. C. Flemming, Biofilms in drinking water and their role as reservoir for pathogens, *Int. J. Hyg. Environ. Health*, 2011, **214**, 417–423.

7 N. Kip and J. A. van Veen, The dual role of microbes in corrosion, *ISME J.*, 2015, **9**, 542–551.

8 K. Lührig, B. Canbäck, C. J. Paul, T. Johansson, K. M. Persson and P. Rådström, Bacterial Community Analysis of Drinking Water Biofilms in Southern Sweden, *Microbes Environ.*, 2015, **30**, 99–107.

9 P. Deines, R. Sekar, P. S. Husband, J. B. Boxall, A. M. Osborn and C. A. Biggs, A new coupon design for simultaneous analysis of in situ microbial biofilm formation and community structure in drinking water distribution systems, *Appl. Microbiol. Biotechnol.*, 2010, **87**, 749–756.

10 I. Douterelo, M. Jackson, C. Solomon and J. Boxall, Spatial and temporal analogies in microbial communities in natural drinking water biofilms, *Sci. Total Environ.*, 2017, **581–582**, 277–288.

11 S. Chan, K. Pullerits, A. Keucken, K. M. Persson, C. J. Paul and P. Rådström, Bacterial release from pipe biofilm in a full-scale drinking water distribution system, *npj Biofilms Microbiomes*, 2019, **5**, 9.

12 I. Douterelo, B. E. Dutilh, K. Arkhipova, C. Calero and S. Husband, Microbial diversity, ecological networks and functional traits associated to materials used in drinking water distribution systems, *Water Res.*, 2020, **173**, 115586.

13 M. C. Cruz, Y. Woo, H. C. Flemming and S. Wuertz, Nitrifying niche differentiation in biofilms from full-scale chloraminated drinking water distribution system, *Water Res.*, 2020, **176**, 115738.

14 M. Waak, R. M. Hozalski, C. Hallé and T. M. Lapara, Comparison of the microbiomes of two drinking water distribution systems - With and without residual chloramine disinfection, *Microbiome*, 2019, **7**(1), 1–14.

15 G. Liu, Y. Zhang, X. Liu, F. Hammes, W. Liu, G. Medema and P. Wessels, 360-Degree Distribution of Bio fi lm Quantity and Community in an Operational Unchlorinated Drinking Water Distribution Pipe, *Environ. Sci. Technol.*, 2020, **54**(9), 5619–5628.

16 T. H. Chiao, T. M. Clancy, A. Pinto, C. Xi and L. Raskin, Differential resistance of drinking water bacterial populations to monochloramine disinfection, *Environ. Sci. Technol.*, 2014, **48**, 4038–4047.

17 R. A. Li, J. A. McDonald, A. Sathasivan and S. J. Khan, Disinfectant residual stability leading to disinfectant decay and by-product formation in drinking water distribution systems: A systematic review, *Water Res.*, 2019, **153**, 335–348.

18 J. M. Regan, G. W. Harrington, H. Baribeau, R. De Leon and D. R. Noguera, Diversity of nitrifying bacteria in full-scale chloraminated distribution systems, *Water Res.*, 2003, **37**, 197–205.

19 S. C. Potgieter, Z. Dai, S. N. Venter, M. Sigudu and A. J. Pinto, Microbial Nitrogen Metabolism in Chloraminated Drinking Water Reservoirs, *mSphere*, 2020, **5**(2), DOI: 10.1128/mSphere.00274-20.

20 A. Keucken, G. Heinicke, K. M. Persson and S. J. Köhler, Combined coagulation and ultrafiltration process to counteract increasing NOM in brown surface water, *Water*, 2017, **9**(9), 697.

21 C. Schleich, S. Chan, K. Pullerits, M. D. Besmer, C. J. Paul, P. Rådström and A. Keucken, Mapping Dynamics of Bacterial Communities in a Full-Scale Drinking Water Distribution System Using Flow Cytometry, *Water*, 2019, **11**, 2137.

22 L. Neu, C. R. Proctor, J. C. Walser and F. Hammes, Small-scale heterogeneity in drinking water biofilms, *Front. Microbiol.*, 2019, **10**, 1–14.

23 E. I. Prest, F. Hammes, S. Kötzsch, M. C. M. van Loosdrecht and J. S. Vrouwenvelder, Monitoring microbiological changes in drinking water systems using a fast and reproducible flow cytometric method, *Water Res.*, 2013, **47**, 7131–7142.

24 E. Gatza, F. Hammes and E. Prest, Assessing Water Quality with the BD Accuri™ C6 Flow Cytometer White Paper, *BD Biosciences*, 2013.

25 A. Klindworth, E. Pruesse, T. Schweer, J. Peplies, C. Quast, M. Horn and F. O. Glockner, Evaluation of general 16S ribosomal RNA gene PCR primers for classical and next-generation sequencing-based diversity studies, *Nucleic Acids Res.*, 2013, **41**, e1.

26 G. Renaud, U. Stenzel, T. Maricic, V. Wiebe and J. Kelso, deML: robust demultiplexing of Illumina sequences using a likelihood-based approach, *Bioinformatics*, 2015, **31**, 770–772.
27 E. Bolyen, J. R. Rideout, M. R. Dillon, N. A. Bokulich, C. C. Abnet, G. A. Al-Ghalith, H. Alexander, E. J. Alm, M. Arumugam, F. Asnicar, Y. Bai, J. E. Bisanz, K. Bittinger, A. Brejnrod, C. J. Brislawn, C. T. Brown, B. J. Callahan, A. M. Caraballo-Rodríguez, J. Chase, E. K. Cope, R. Da Silva, C. Diener, P. C. Dorrestein, G. M. Douglas, D. M. Durall, C. Duvallet, C. F. Edwardson, M. Ernst, M. Estaki, J. Fouquier, J. M. Gauglitz, S. M. Gibbons, D. L. Gibson, A. Gonzalez, K. Gorlick, J. Guo, B. Hillmann, S. Holmes, H. Holste, C. Huttenhower, G. A. Huttley, S. Janssen, A. K. Jarmusch, L. Jiang, B. D. Kaehler, K. Bin Kang, C. R. Keefe, P. Keim, S. T. Kelley, D. Knights, I. Koester, T. Kosciolek, J. Kreps, M. G. I. Langille, J. Lee, R. Ley, Y.-X. Liu, E. Loftfield, C. Lozupone, M. Maher, C. Marotz, B. D. Martin, D. McDonald, L. J. McIver, A. V. Melnik, J. L. Metcalf, S. C. Morgan, J. T. Morton, A. T. Naimey, J. A. Navas-Molina, L. F. Nothias, S. B. Orchanian, T. Pearson, S. L. Peoples, D. Petras, M. L. Preuss, E. Pruesse, L. B. Rasmussen, A. Rivers, M. S. Robeson, P. Rosenthal, N. Segata, M. Shaffer, A. Shiffer, R. Sinha, S. J. Song, J. R. Spear, A. D. Swafford, L. R. Thompson, P. J. Torres, P. Trinh, A. Tripathi, P. J. Turnbaugh, S. Ul-Hasan, J. J. J. van der Hooft, F. Vargas, Y. Vázquez-Baeza, E. Vogtmann, M. von Hippel, W. Walters, Y. Wan, M. Wang, J. Warren, K. C. Weber, C. H. D. Williamson, A. D. Willis, Z. Z. Xu, J. R. Zaneveld, Y. Zhang, Q. Zhu, R. Knight and J. G. Caporaso, Reproducible, interactive, scalable and extensible microbiome data science using QIIME 2, *Nat. Biotechnol.*, 2019, **37**, 852–857.
28 T. Z. Desantis, P. Hugenholtz, N. Larsen, M. Rojas, E. L. Brodie, K. Keller, T. Huber, D. Dalevi, P. Hu and G. L. Andersen, Greengenes, a Chimera-Checked 16S rRNA Gene Database and Workbench Compatible with ARB, *Appl. Environ. Microbiol.*, 2006, **72**, 5069–5072.
29 P. J. McMurdie and S. Holmes, phyloseq: An R Package for Reproducible Interactive Analysis and Graphics of Microbiome Census Data, *PLoS One*, 2013, **8**, e61217.
30 *R Core Team*, 2018.
31 N. A. Bokulich, S. Subramanian, J. J. Faith, D. Gevers, J. I. Gordon, R. Knight, D. A. Mills and J. G. Caporaso, Quality-filtering vastly improves diversity estimates from Illumina amplicon sequencing, *Nat. Methods*, 2013, **10**, 57–59.
32 H. Wickham, *ggplot2: Elegant Graphics for Data Analysis*, Springer-Verlag New York, 2016.
33 T. van den Brand, *ggnomics: ggnomics. R package version 0.1.1*, 2019.
34 L. Lahti and S. Shetty, *microbiome R package*, 2019.
35 H. Chen, *VennDiagram: Generate High-Resolution Venn and Euler Plots*, R package version 1.6.20.
36 R. S. Kantor, S. E. Miller and K. L. Nelson, The water microbiome through a pilot scale advanced treatment facility for direct potable reuse, *Front. Microbiol.*, 2019, **10**, 1–15.
37 P. J. McMurdie and S. Holmes, Waste Not, Want Not: Why Rarefying Microbiome Data Is Inadmissible, *PLoS Comput. Biol.*, 2014, **10**, e1003531.
38 M. I. Love, W. Huber and S. Anders, Moderated estimation of fold change and dispersion for RNA-seq data with DESeq2, *Genome Biol.*, 2014, **15**, 550.
39 D. Knights, J. Kuczynski, E. S. Charlson, J. Zaneveld, M. C. Mozer, R. G. Collman, F. D. Bushman, R. Knight and S. T. Kelley, Bayesian community-wide culture-independent microbial source tracking, *Nat. Methods*, 2011, **8**, 761–765.
40 M. Hägglund, S. Bäckman, A. Macellaro, P. Lindgren, E. Borgmästars, K. Jacobsson, R. Dryselius, P. Stenberg, A. Sjödin, M. Forsman and J. Ahlinder, Accounting for Bacterial Overlap Between Raw Water Communities and Contaminating Sources Improves the Accuracy of Signature-Based Microbial Source Tracking, *Front. Microbiol.*, 2018, **9**, 2364.
41 G. Liu, Y. Zhang, W. J. Knibbe, C. Feng, W. Liu, G. Medema and W. van der Meer, Potential impacts of changing supply-water quality on drinking water distribution: A review, *Water Res.*, 2017, **116**, 135–148.
42 R. Boe-Hansen, H. J. Albrechtsen, E. Arvin and C. Jørgensen, Bulk water phase and biofilm growth in drinking water at low nutrient conditions, *Water Res.*, 2002, **36**, 4477–4486.
43 I. Chatzigiannidou, R. Props and N. Boon, Drinking water bacterial communities exhibit specific and selective necrotrophic growth, *npj Clean Water*, 2018, **1**, 22.
44 C. R. Proctor, M. D. Besmer, T. Langenegger, K. Beck, J.-C. Walser, M. Ackermann, H. Bürgmann and F. Hammes, Phylogenetic clustering of small low nucleic acid-content bacteria across diverse freshwater ecosystems, *ISME J.*, 2018, **12**(5), 1344–1359.
45 M. W. Cowle, G. Webster, A. O. Babatunde, B. N. Bockelmann-Evans and A. J. Weightman, Impact of flow hydrodynamics and pipe material properties on biofilm development within drinking water systems, *Environ. Technol.*, 2019, **0**, 1–13.
46 P. J. Vikesland, K. Ozekin and R. L. Valentine, Effect of natural organic matter on monochloramine decomposition: Pathway elucidation through the use of mass and redox balances, *Environ. Sci. Technol.*, 1998, **32**, 1409–1416.
47 A. Wilczak, L. L. Hoover and H. Hubert Lai, Effects of treatment changes on chloramine demand and decay, *J. - Am. Water Works Assoc.*, 2003, **95**, 94–106.
48 H. Daims, S. Lücker and M. Wagner, A New Perspective on Microbes Formerly Known as Nitrite-Oxidizing Bacteria, *Trends Microbiol.*, 2016, **24**, 699–712.
49 Y. Wang, L. Ma, Y. Mao, X. Jiang, Y. Xia, K. Yu, B. Li and T. Zhang, Comammox in drinking water systems, *Water Res.*, 2017, **116**, 332–341.
50 S. D. Allison and J. B. H. Martiny, Resistance, resilience, and redundancy in microbial communities, *In the Light of Evolution*, 2009, vol. 2, pp. 149–166.
51 E. Sawade, P. Monis, D. Cook and M. Drikas, Is nitrification the only cause of microbiologically induced chloramine decay?, *Water Res.*, 2016, **88**, 904–911.
52 S. Potgieter, A. Pinto, M. Sigudu, H. du Preez, E. Ncube and S. Venter, Long-term spatial and temporal microbial

community dynamics in a large-scale drinking water distribution system with multiple disinfectant regimes, *Water Res.*, 2018, **139**, 406–419.
53 R. Liu, J. Zhu, Z. Yu, D. R. Joshi, H. Zhang, W. Lin and M. Yang, Molecular analysis of long-term biofilm formation on PVC and cast iron surfaces in drinking water distribution system, *J. Environ. Sci.*, 2014, **26**, 865–874.
54 M. Waak, T. M. Lapara, C. Hallé and R. M. Hozalski, Nontuberculous Mycobacteria in Two Drinking Water Distribution Systems and the Role of Residual Disinfection, *Environ. Sci. Technol.*, 2019, **53**, 8563–8573.
55 C. K. Gomez-Smith, T. M. Lapara and R. M. Hozalski, Sulfate reducing bacteria and mycobacteria dominate the biofilm communities in a chloraminated drinking water distribution system, *Environ. Sci. Technol.*, 2015, **49**, 8432–8440.
56 M. J. Donohue, S. Vesper, J. Mistry and J. M. Donohue, Impact of Chlorine and Chloramine on the Detection and Quantification of Legionella pneumophila and Mycobacterium Species, *Appl. Environ. Microbiol.*, 2019, **85**, 1–11.
57 N. Kotlarz, L. Raskin, M. Zimbric, J. Errickson, J. J. LiPuma and L. J. Caverly, Retrospective Analysis of Nontuberculous Mycobacterial Infection and Monochloramine Disinfection of Municipal Drinking Water in Michigan, *mSphere*, 2019, **4**, e00160.
58 R. H. Taylor, J. O. Falkinham Iii, C. D. Norton and M. W. Lechevallier, Chlorine, Chloramine, Chlorine Dioxide, and Ozone Susceptibility of Mycobacterium avium, *Appl. Environ. Microbiol.*, 2000, **66**(4), 1702–1705.
59 K. Pullerits, J. Ahlinder, L. Holmer, E. Salomonsson, C. Öhrman, K. Jacobsson, R. Dryselius, M. Forsman, C. J. Paul and P. Rådström, Impact of UV irradiation at full scale on bacterial communities in drinking water, *npj Clean Water*, 5, **3**, 1–10.
60 M. Waak, T. M. LaPara, C. Hallé and R. M. Hozalski, Occurrence of Legionella spp. in Water-Main Biofilms from Two Drinking Water Distribution Systems, *Environ. Sci. Technol.*, 2018, **52**, 7630–7639.
61 M. Steinert, U. Hentschel and J. Hacker, Legionella pneumophila: An aquatic microbe goes astray, *FEMS Microbiol. Rev.*, 2002, **26**, 149–162.
62 E. Prest, F. Hammes, M. C. M. van Loosdrecht and J. S. Vrouwenvelder, *Front. Microbiol.*, 2016, **7**, 45.
63 B. E. Rittmann and V. L. Snoeyink, Achieving biologically stable drinking water, *J. - Am. Water Works Assoc.*, 1984, **76**, 106–114.
64 J. El-Chakhtoura, E. Prest, P. Saikaly, M. Van Loosdrecht, F. Hammes and H. Vrouwenvelder, Dynamics of bacterial communities before and after distribution in a full-scale drinking water network, *Water Res.*, 2015, **74**, 180–190.

Electronic Supplementary Material (ESI) for Environmental Science: Water Research & Technology.

Supplementary information – Figures and Tables

Impact of coagulation-ultrafiltration on long-term pipe biofilm dynamics in a full-scale chloraminated drinking water distribution system

Kristjan Pullerits[a,b], Sandy Chan[a,b,1], Jon Ahlinder[c], Alexander Keucken[d,e], Peter Rådström[a], Catherine J. Paul[*,a,e]

[a]Applied Microbiology, Department of Chemistry, Lund University, P.O. Box 124, SE-221 00 Lund, Sweden

[b]Sweden Water Research AB, Ideon Science Park, Scheelevägen 15, SE-223 70 Lund, Sweden

[c]FOI, Swedish Defence Research Agency, Cementvägen 20, SE-906 21 Umeå, Sweden

[d]Vatten & Miljö i Väst AB, P.O. Box 110, SE-311 22 Falkenberg, Sweden

[e]Water Resources Engineering, Department of Building and Environmental Technology, Lund University, P.O. Box 118, SE-221 00 Lund, Sweden

[*]Corresponding author: catherine.paul@tvrl.lth.se

[1]Present address: Sydvatten AB, Hyllie Stationstorg 21, SE-215 32 Malmö, Sweden

Table of contents

Figure S.1 – DWDS pipe sampling

Figure S.2 – DWDS pipe sampling metal scrape

Figure S.3 – Water temperatures

Figure S.4 – HNA and IC concentrations

Figure S.5 – Change in %HNA and %ICC content against FW

Figure S.6 – Alpha diversity measures

Figure S.7 – Principal coordinates analysis on biofilm and all samples

Figure S.8 - Impact of distance from the DWTP on pipe biofilm taxa at family level

Figure S.9 – DESeq2 analysis of BF1, BF2 and BF3 with distance

Figure S.10 – *Mycobacteriaceae* family ASVs in the samples

Figure S.11 – *Legionellales* order ASVs in the samples

Figure S.12 – Principal coordinates analysis on BF1 and BF4

Figure S.13 – ASVs over time in BF1

Figure S.14 – ASVs over time in BF4

Figure S.15 – DESeq2 analysis of BF1 and BF4, before and after UF start

Figure S.16 – Conventional chemical analyses

Figure S.17 – NOM analyses

Table S.1 – Shared core communities between the biofilm samples

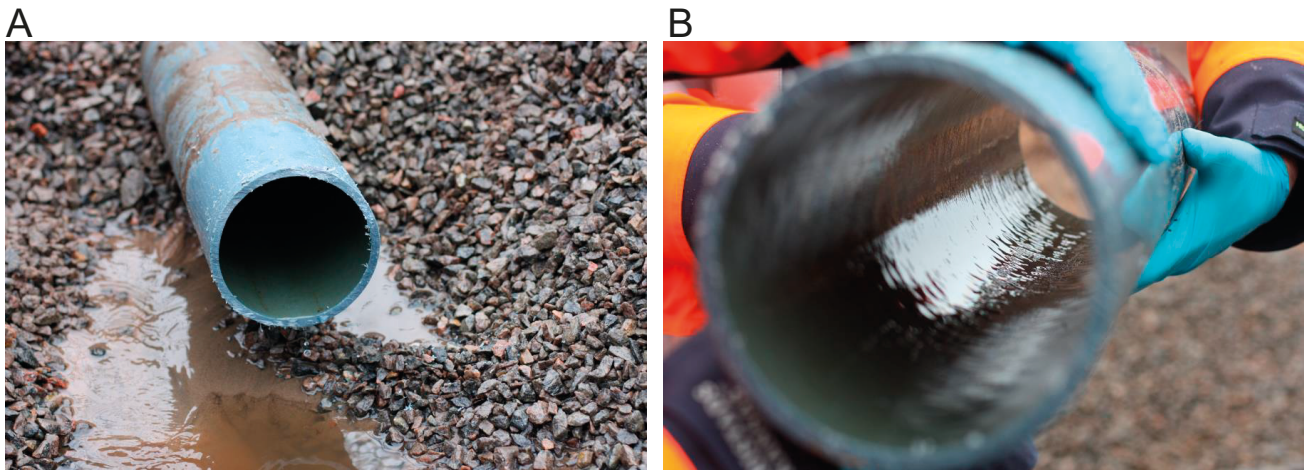

Figure S.1. (A) Cut DWDS pipe. (B) Pipe section brought to the lab.

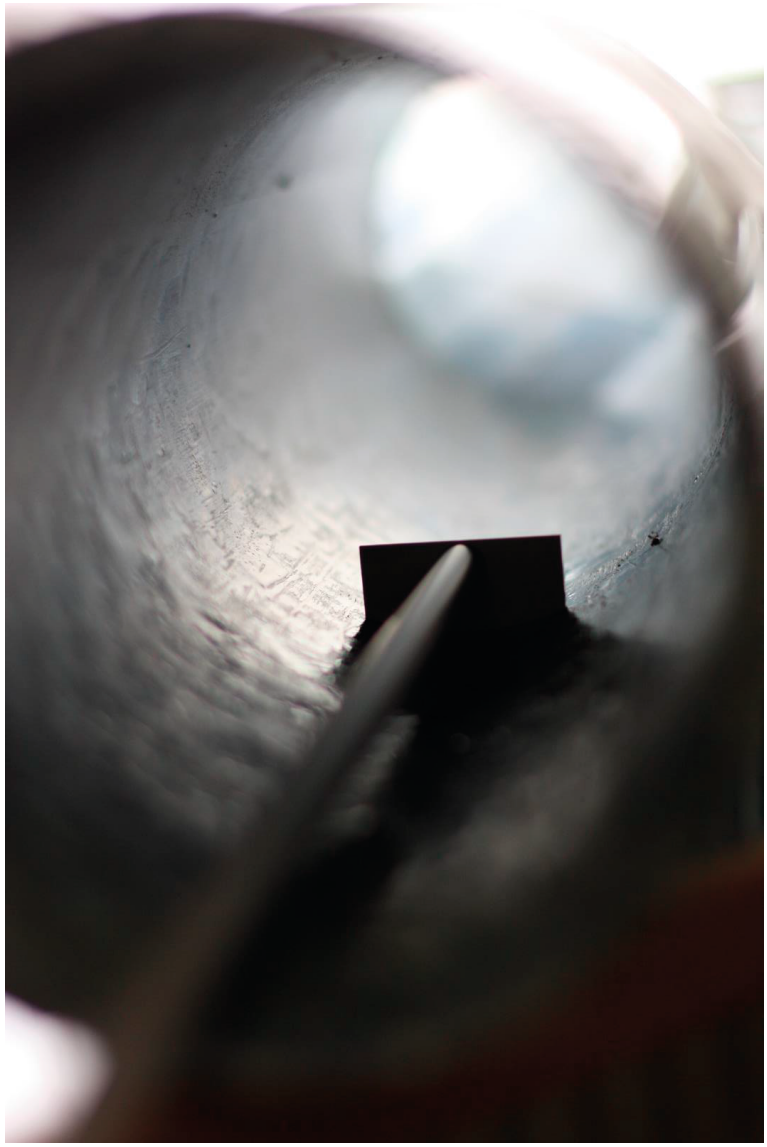

Figure S.2. Custom-made metal scrape used for biofilm collection.

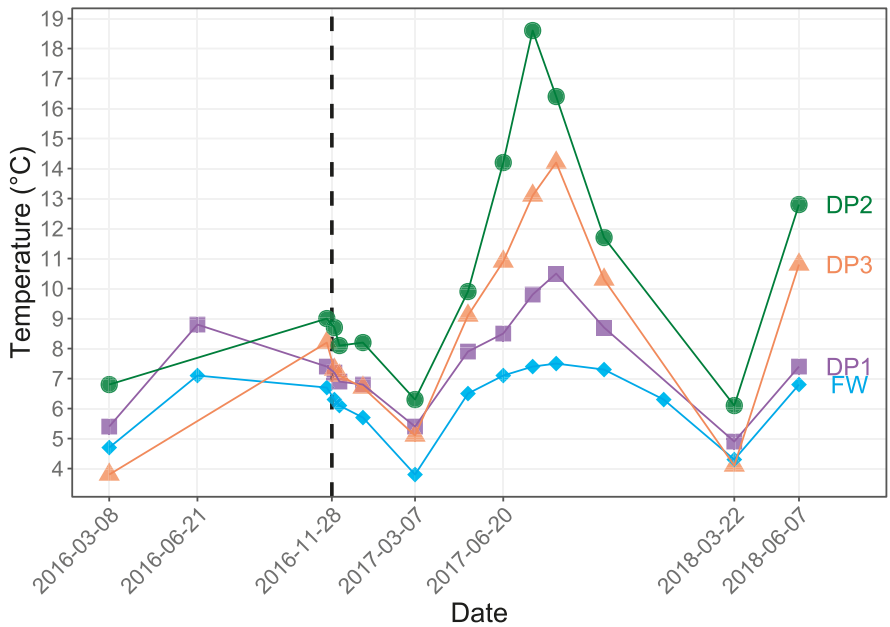

Figure S.3. Water temperatures of the water samples. Dashed vertical line represents the start of the UF, 2016-11-28.

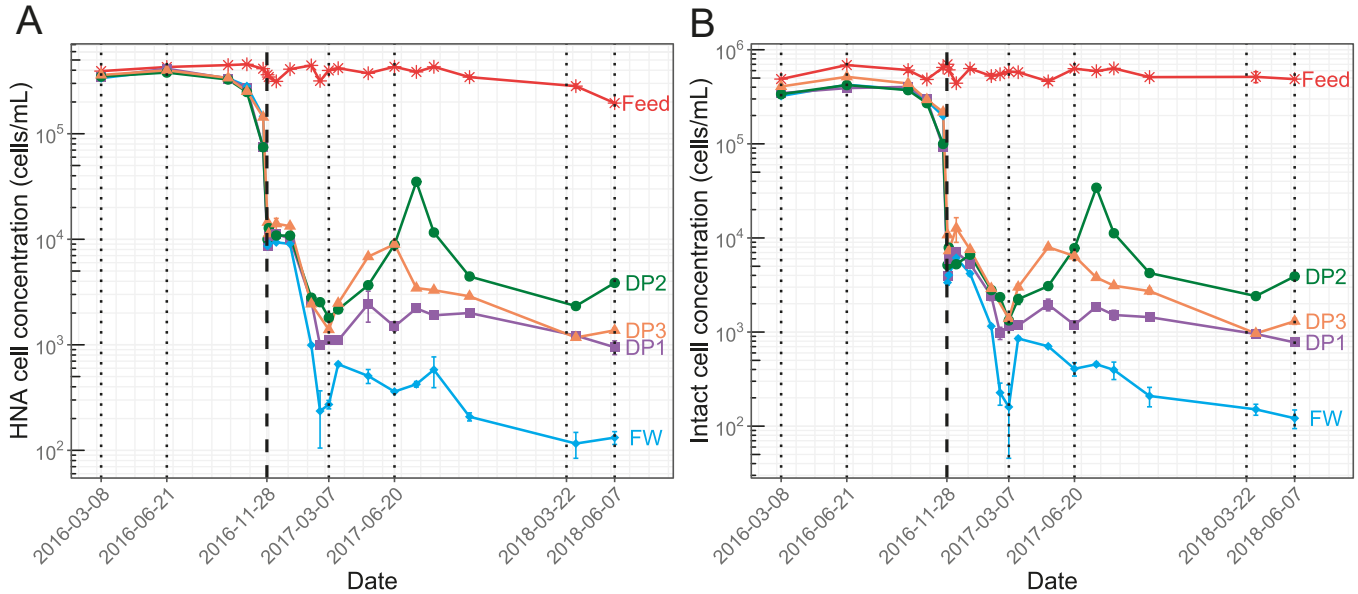

Figure S.4. (A) HNA cell concentration of the water samples. (B) Intact cell concentration of the water samples. (A,B) Error bars show standard deviations in technical triplicates. Dashed vertical line represents the start of the UF, 2016-11-28 and dotted vertical lines represent the biofilm sampling dates.

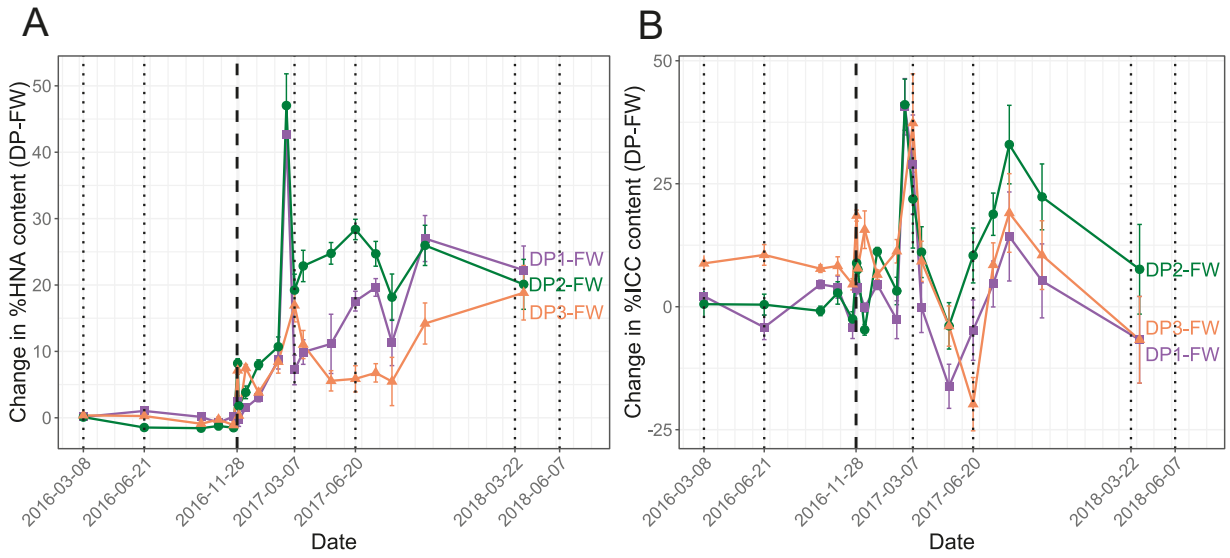

Figure S.5. (A) Change in the %HNA content, taking the %HNA DP and subtracting with the %HNA in FW. (B) Change in the %ICC content, taking the %HNA DP and subtracting with the %HNA in FW. (A,B) Error bars show standard deviations in technical triplicates. Dashed vertical line represents the start of the UF, 2016-11-28 and dotted vertical lines represent the biofilm sampling dates.

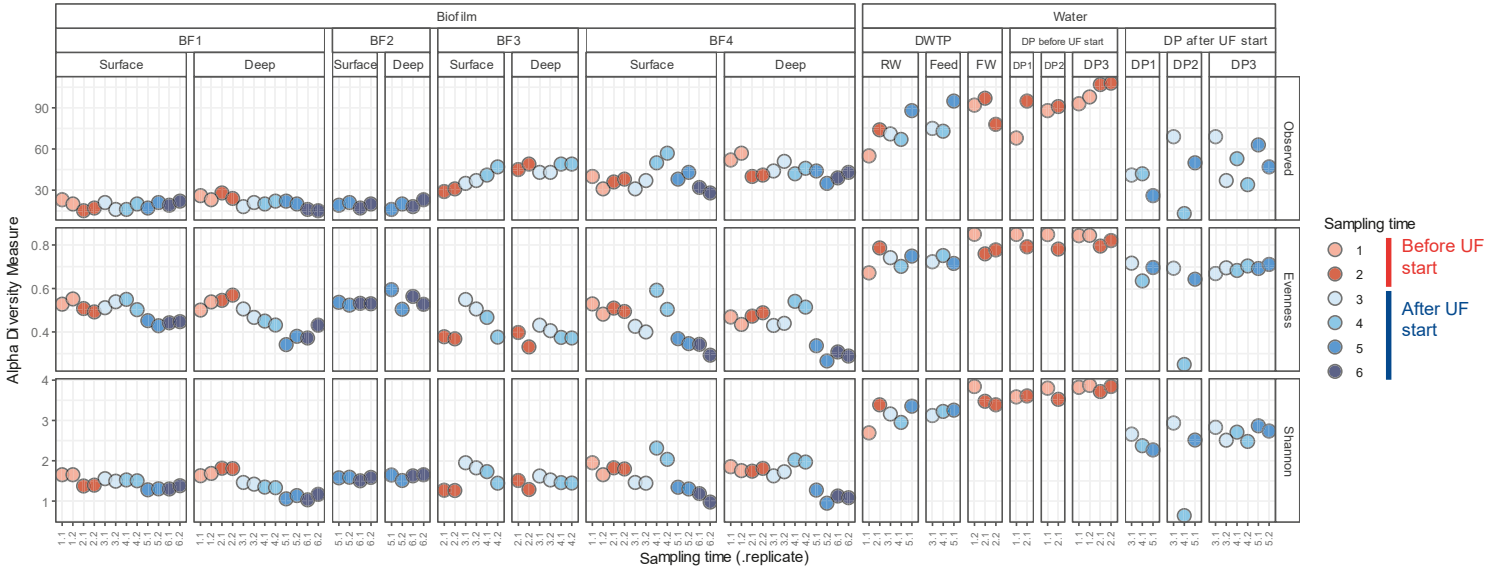

Figure S.6. The alpha diversity measures, observed ASVs, Evenness and Shannon index for the biofilm and water samples. Samples are ordered in rows and grouped together based on sample type. Sampling time indicates the date of sampling (Fig. 1B), samples indicated with red and blue are samples before UF and after UF start, respectively. Each point is one biological replicate.

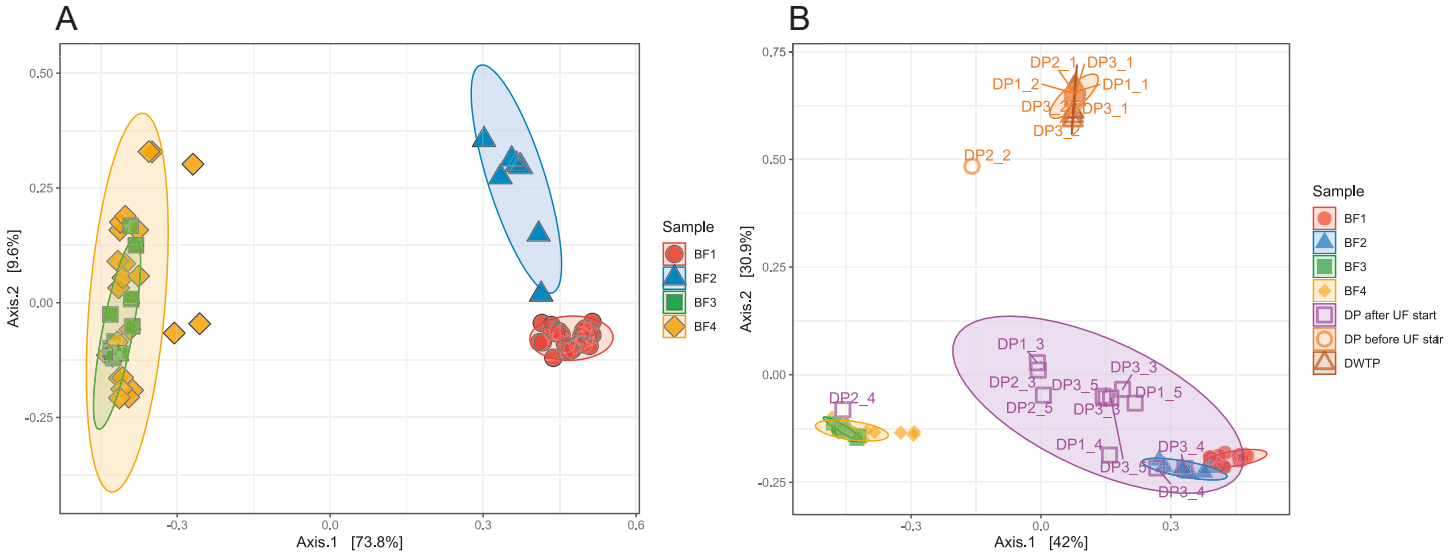

Figure S.7. Principal coordinates analysis (PCoA) plot based on Bray Curtis-dissimilarity of the bacterial communities. (A) Showing only biofilm samples. (B) Showing biofilm and water samples, DPs are indicated with the DP number following underscore and sampling time. (A,B) The transparent areas show the 95% confidence interval of the sample groups. BF1: n = 24, BF2: n = 8, BF3: n = 12, BF4: n = 24, DP after UF start: n = 12, DP before UF start: n = 8 and DWTP: n = 11. Due to uneven dispersion among groups (betadisper > 0.05 in Vegan package), clusters formed could not be confirmed by permutational analyses.

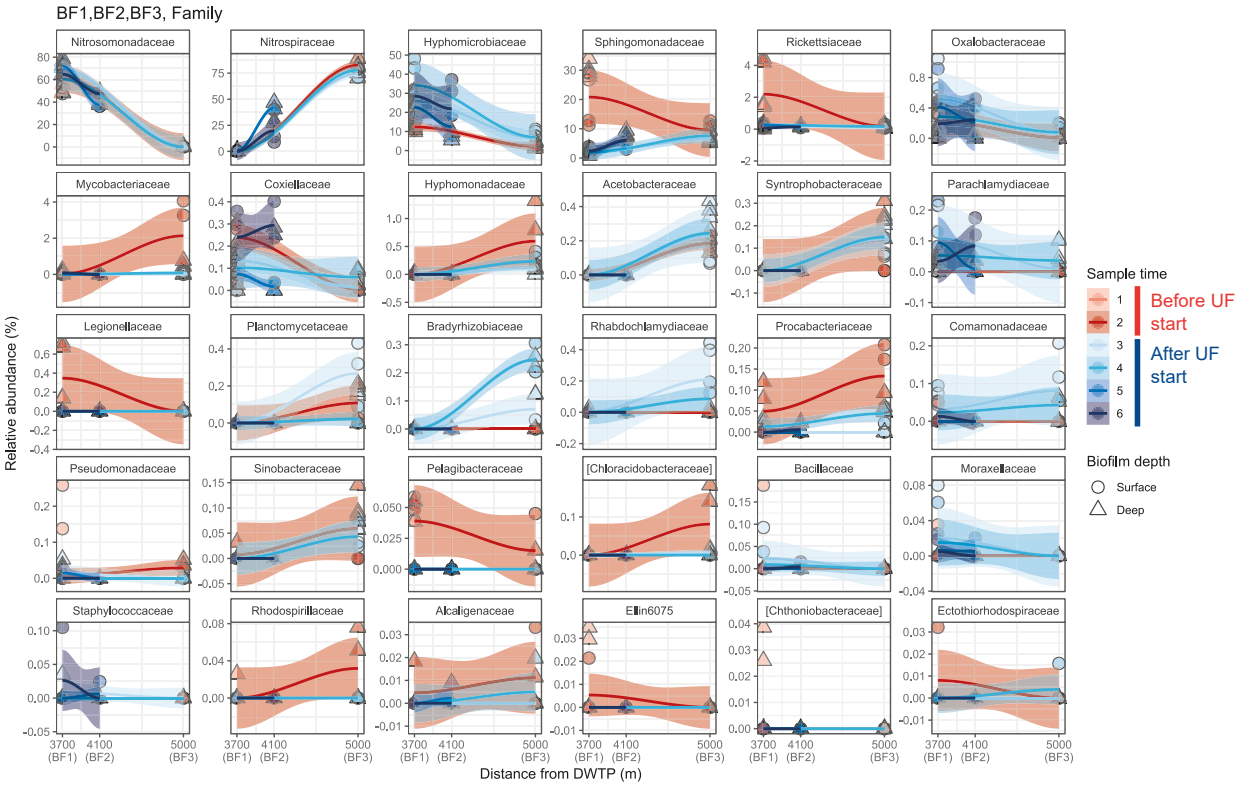

Figure S.8. Impact of distance (BF1, BF2 and BF3) from the DWTP on pipe biofilm taxa at family level. The taxa are ordered with greatest relative abundance in top left panel with subsequent decrease. Sample time 1 and 2 (red) indicate before UF start and 3,4,5 and 6 (blue) indicate after UF start. Blue and red lines show locally weighted least squares (loess) regression for each sample time and the transparent areas show the 95% confidence interval for each loess regression. n = 2 for both surface and deep biofilm at every sampling time.

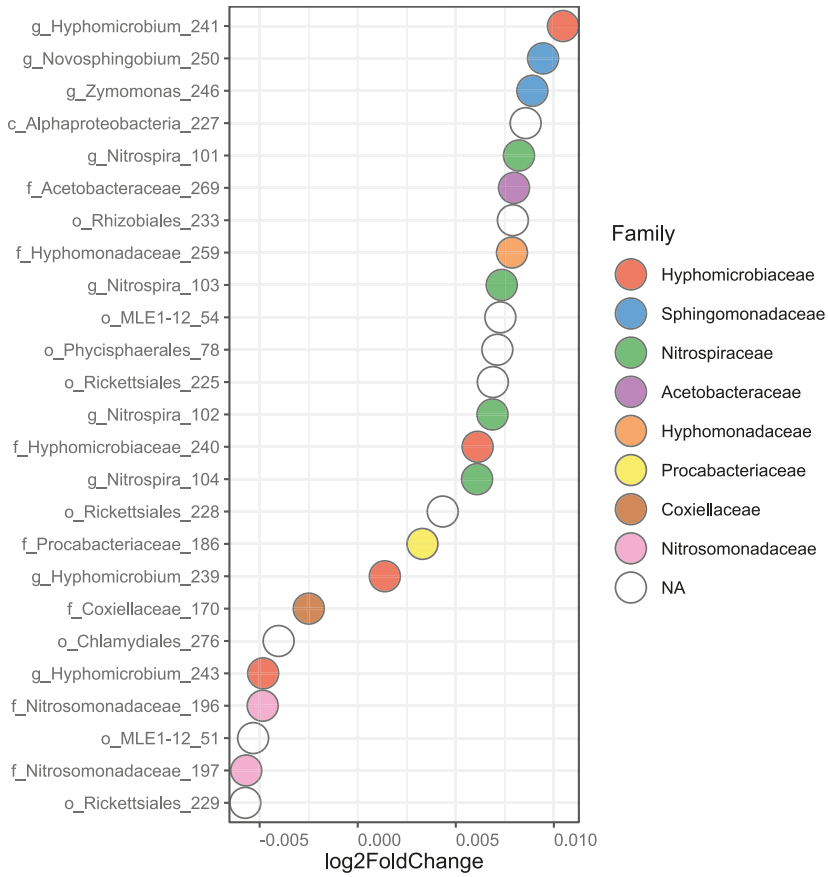

Figure S.9. Differential abundance analysis using DESeq2 ($P_{adjusted} < 0.05$), where BF1 (n = 24, BF2 (n = 8) and BF3 (n = 12) were used and the distance from the DWTP in meters were used as parameter. Positive log2fold change indicate ASV increase with distance.

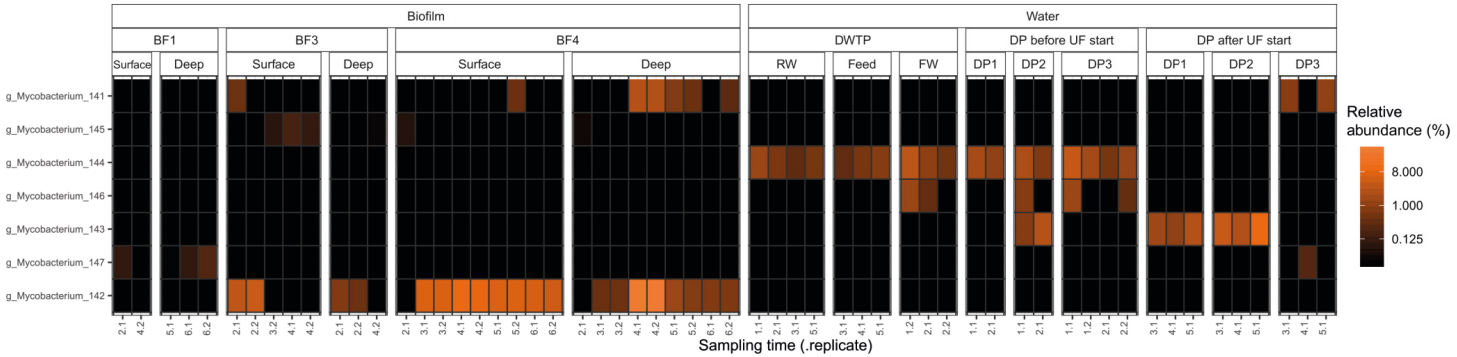

Figure S.10. Heatmap showing only samples with ASVs classified within family *Mycobacteriaceae*. Samples are ordered in rows and grouped together based on sample type. Each column is one biological replicate.

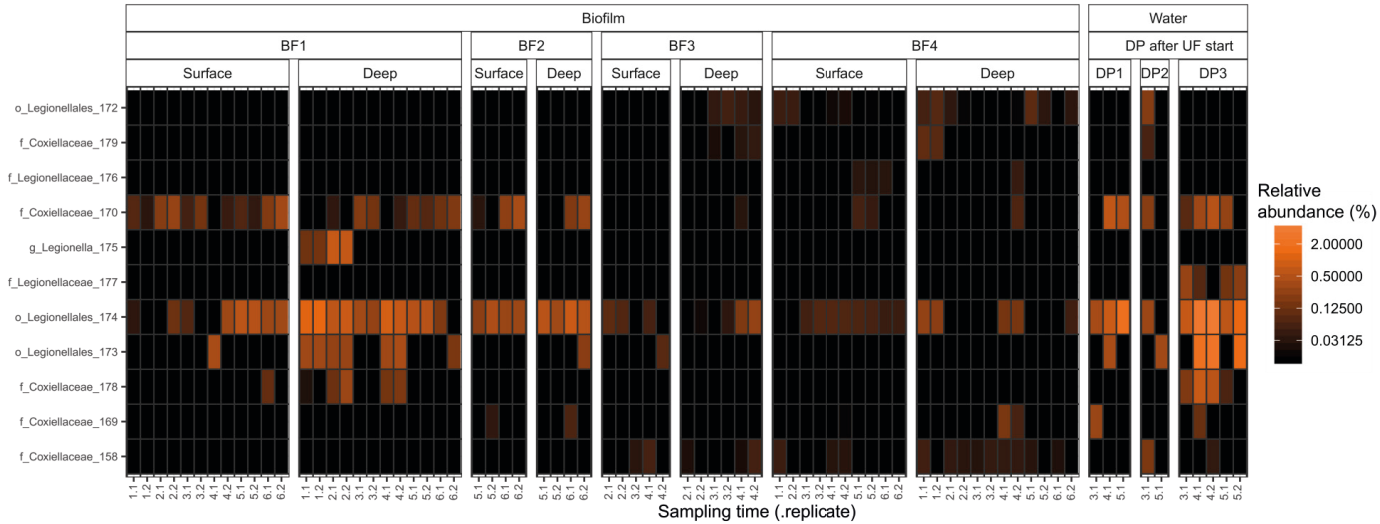

Figure S.11. Heatmap showing only samples with ASVs classified within order *Legionellales*. Samples are ordered in rows and grouped together based on sample type. Each column is one biological replicate.

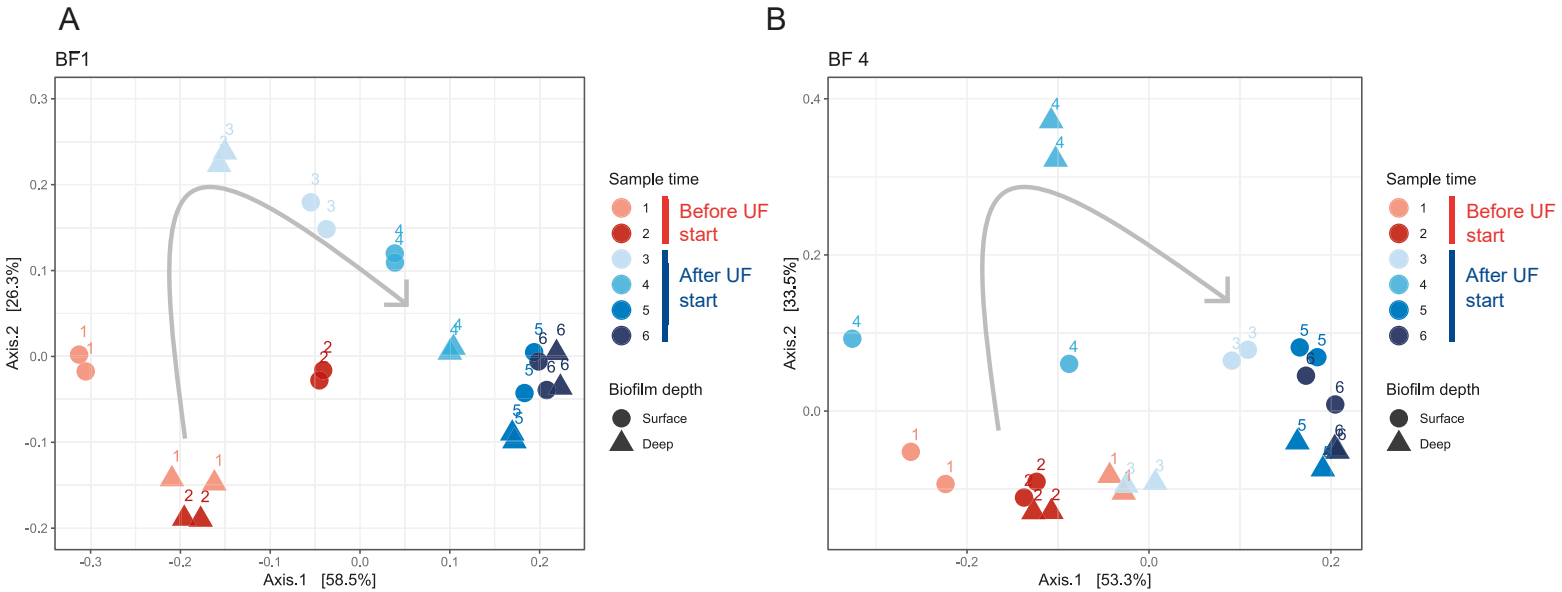

Figure S.12. Principal coordinates analysis (PCoA) plot based on Bray Curtis-dissimilarity of the bacterial communities. (A) Showing only BF1. (B) Showing only BF4. (A,B) The grey arrows indicate the progression of samples over time. Samples indicated with red and blue are samples before UF and after UF start, respectively. n = 2 for both surface and deep biofilm at every sampling time.

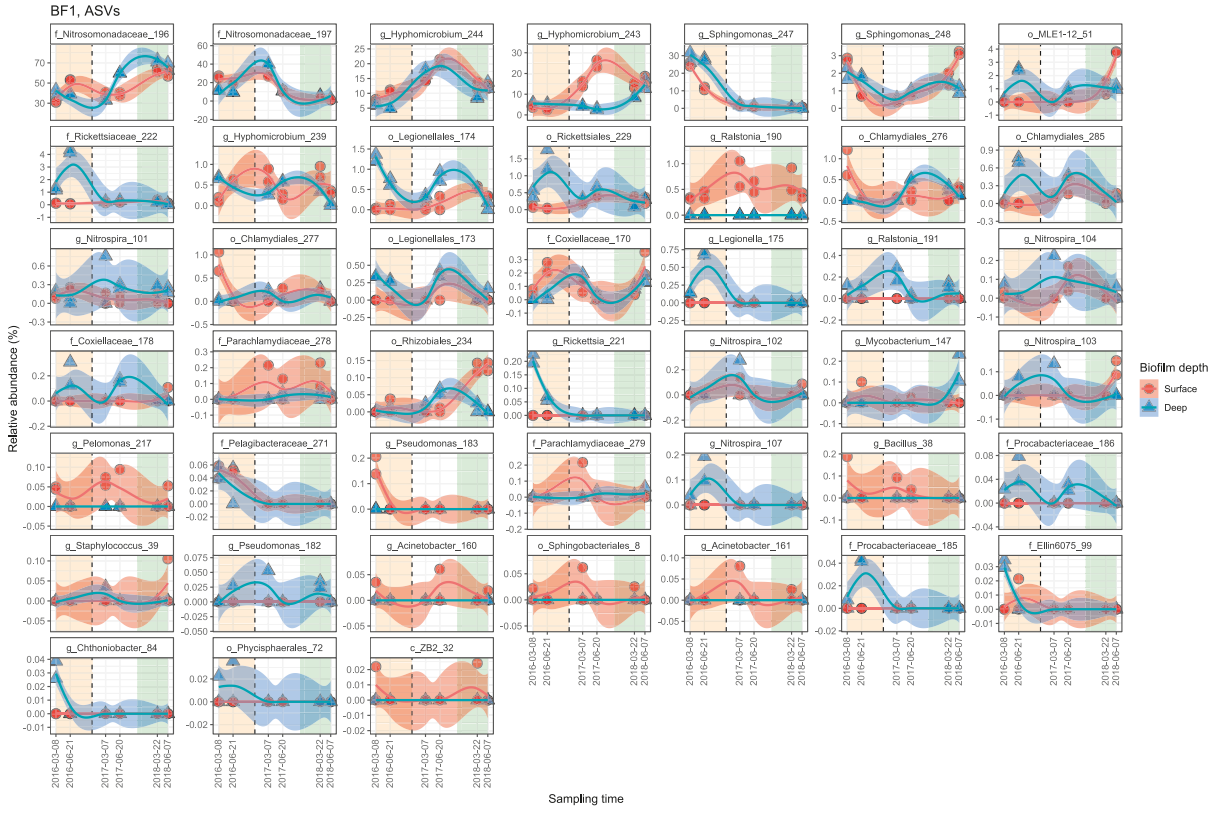

Figure S.13. Dynamics of all ASVs in BF1 over time. The ASVs are ordered with greatest relative abundance in top left panel with subsequent decrease. Vertical dashed line indicates the UF start. Orange, white and green background indicate before UF, transition state and after UF periods, respectively. ASVs are shown with the most specified taxonomy when available, g = genus, f = family, o = order and c = class. Dates indicate the six sampling times. Blue and red lines show locally weighted least squares (loess) regression for each biofilm depth and the transparent areas show the 95% confidence interval for each loess regression. n = 2 for both surface and deep biofilm at every sampling time.

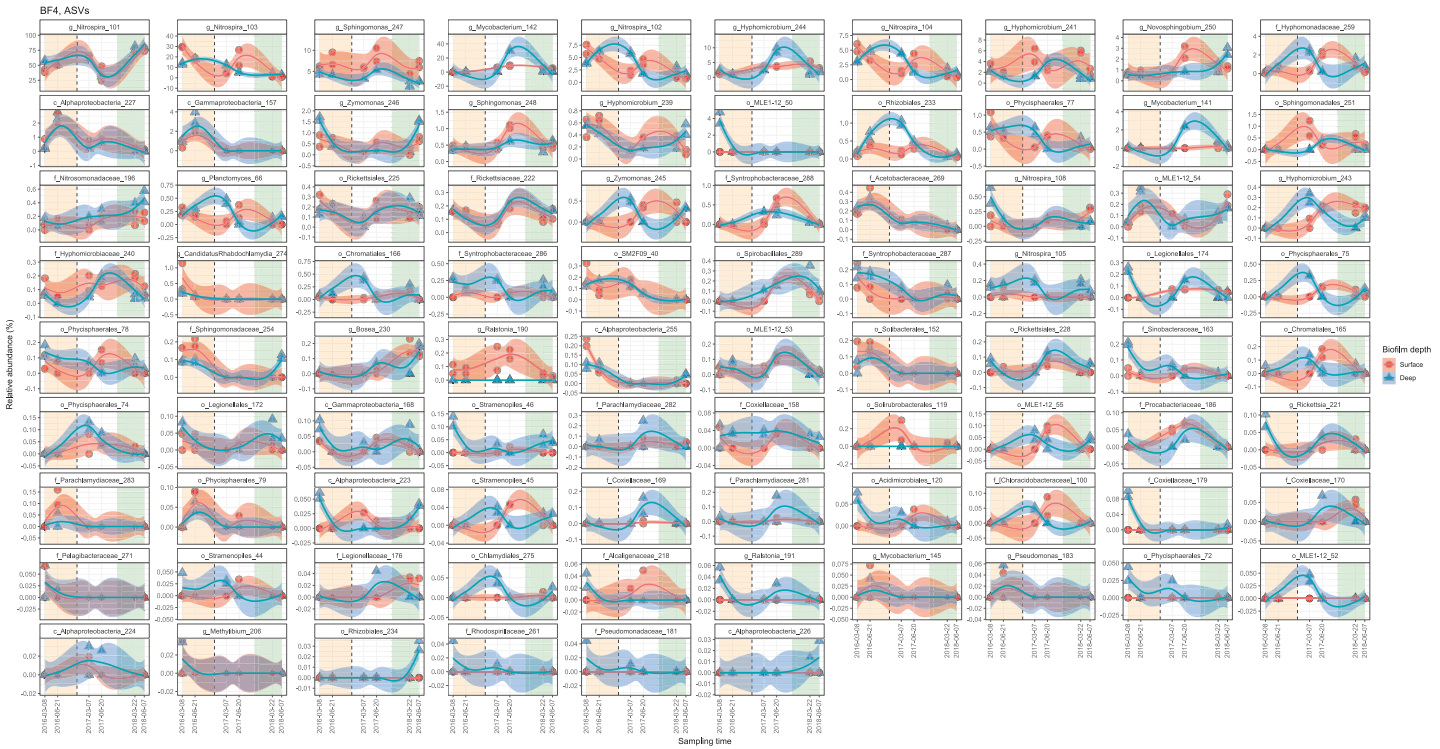

Figure S.14. Dynamics of all ASVs in BF4 over time. The ASVs are ordered with greatest relative abundance in top left panel with subsequent decrease. Vertical dashed line indicates the UF start. Orange, white and green background indicate before UF, transition state and after UF periods, respectively. ASVs are shown with the most specified taxonomy when available, g = genus, f = family, o = order and c = class. Dates indicate the six sampling times. Blue and red lines show locally weighted least squares (loess) regression for each biofilm depth and the transparent areas show the 95% confidence interval for each loess regression. n = 2 for both surface and deep biofilm at every sampling time.

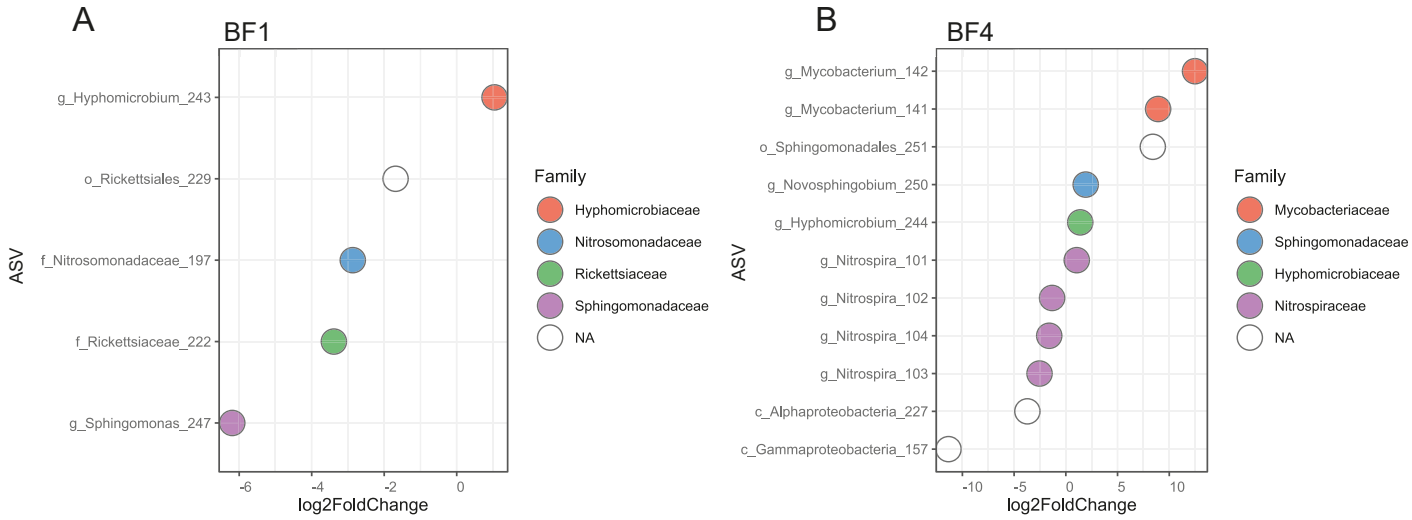

Figure S.15. Differential abundance analysis using DESeq2 ($P_{adjusted} < 0.05$), comparing sampling time 1 and 2 (before UF) to sampling time 5 and 6 (after UF) using only ASVs > 1.2% in one sample, as in figure 5. (A) Log2fold changes of ASVs in BF1. (B) Log2fold changes of ASVs in BF4.

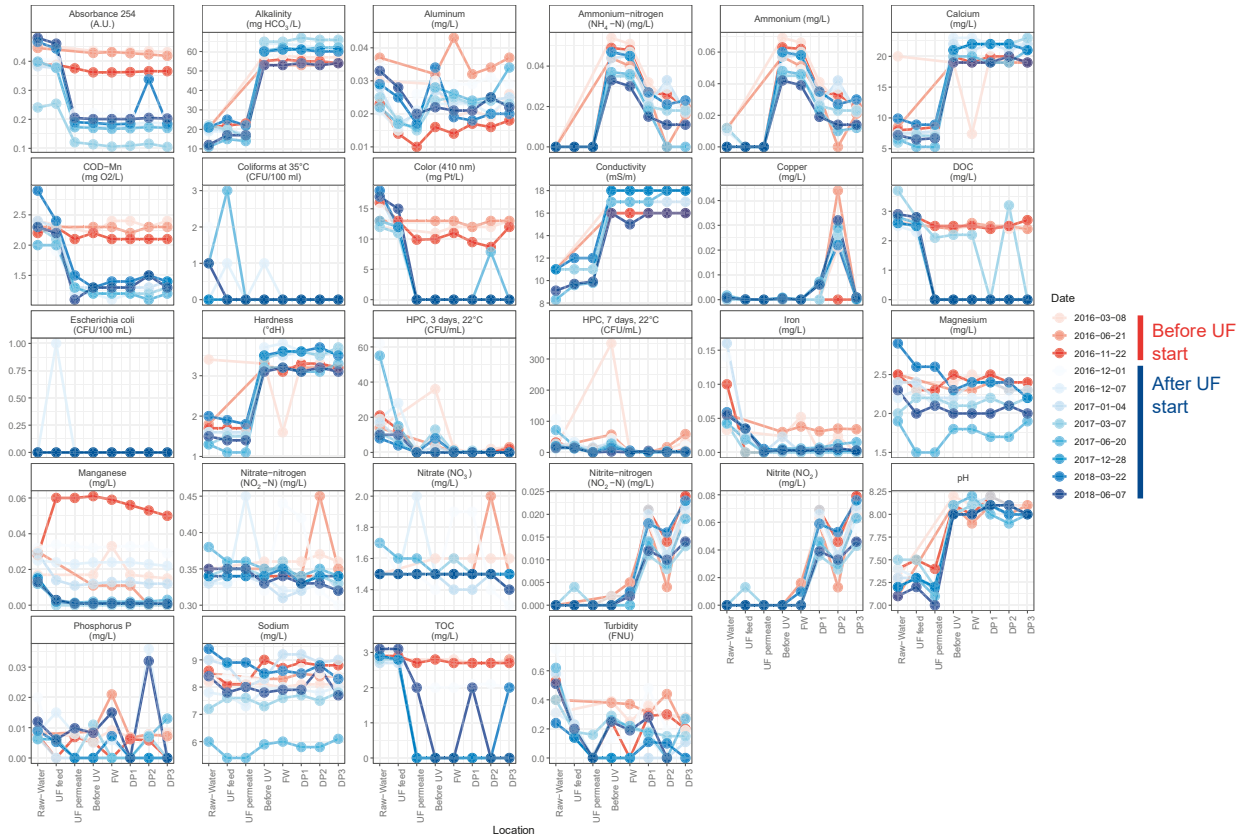

Figure S.16. Conventional chemical analyses on the water samples. Dates indicated with red and blue are samples before UF and after UF start, respectively. Limit of quantification for various analyses was; ammonium-nitrogen: 0.01 mg/L, ammonium: 0.01 mg/L, color: 5.0 mg Pt/L, copper: 0.02 mg/L, DOC: 2.0 mg/L, iron: 0.02 mg/L, manganese: 0.01 mg/L, nitrite-nitrogen: 0.002 mg/L, nitrite: 0.007 mg/L, phosphorus: 0.005 mg/L, TOC: 2.0 mg/L and turbidity: 0.1 FNU, depicted as 0 in the figure. n = 1 for every sampling time.

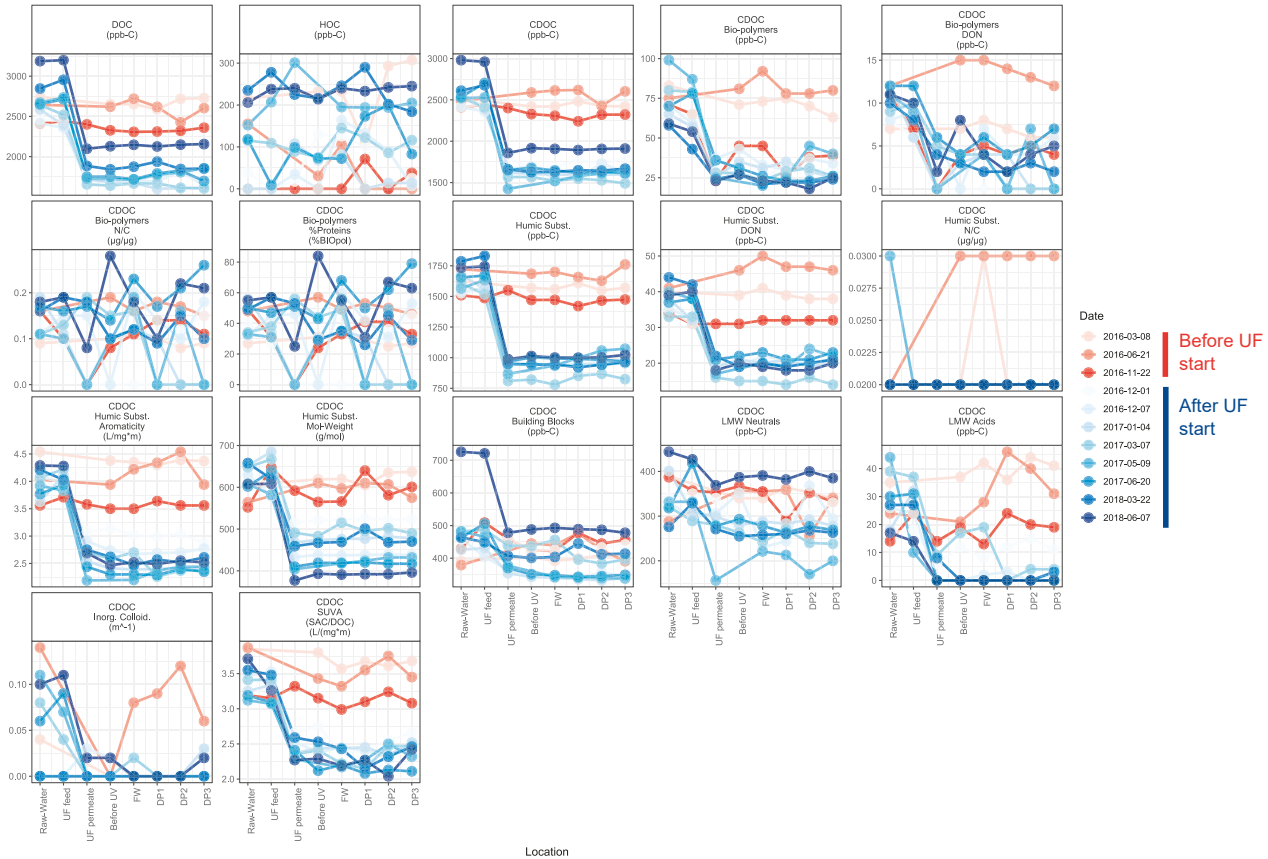

Figure S.17. NOM analyses by LC-OCD-OND on the water samples. Dates indicated with red and blue are samples before UF and after UF start, respectively. Abbreviations; DOC: dissolved organic carbon, HOC: hydrophobic organic carbon, CDOC: chromatographic dissolved organic carbon, DON: dissolved organic nitrogen and SAC: spectral absorption coefficient. 1000 ppb = 1 mg/L. n = 1 for every sampling time.

Table S.1. Shared core communities between the biofilm samples from Fig. 4. Abbreviations; ∩ = intersection, ∪ = union and \ = set subtraction.

BF1∩BF2∩BF3∩BF4	(BF2∩BF3∩BF4)\(BF1)	(BF1∩BF3∩BF4)\(BF2)	(BF3∩BF4)\(BF1∪BF2)	(BF1∩BF2∩BF4)\(BF3)	(BF4)\(BF1∪BF2∪BF3)	(BF3)\(BF1∪BF2∪BF4)	(BF1∩BF2)\(BF3∪BF4)	(BF1)\(BF2∪BF3∪BF4)
f_Nitrosomonadaceae_196	o_MLE1-12_54	g_Nitrospira_101	g_Planctomyces_66	o_Legionellales_174	o_SM2F09_40	o_Stramenopiles_46	o_MLE1-12_51	o_Legionellales_173
f_Rickettsiaceae_222	g_Nitrospira_102		o_Phycisphaerales_78	g_Ralstonia_190	o_Phycisphaerales_75	o_MLE1-12_50	f_Coxiellaceae_170	g_Legionella_175
g_Hyphomicrobium_239	g_Nitrospira_103		g_Nitrospira_104	g_Hyphomicrobium_243	o_Phycisphaerales_77	g_Nitrospira_106	f_Nitrosomonadaceae_197	f_Coxiellaceae_178
g_Hyphomicrobium_244			g_Nitrospira_105		g_Mycobacterium_141			g_Ralstonia_191
g_Sphingomonas_247			g_Nitrospira_108		o_Solibacterales_152			o_Rickettsiales_229
g_Sphingomonas_248			g_Mycobacterium_142		o_Chromatiales_166			o_Rhizobiales_234
			c_Gammaproteobacteria_157		f_Hyphomicrobiaceae_240			o_Chlamydiales_276
			o_Rickettsiales_225		g_Zymomonas_245			o_Chlamydiales_277
			c_Alphaproteobacteria_227		o_Sphingomonadales_251			o_Chlamydiales_285
			g_Bosea_230		f_Syntrophobacteraceae_287			
			o_Rhizobiales_233		f_Syntrophobacteraceae_288			
			g_Hyphomicrobium_241		o_Spirobacillales_289			
			g_Zymomonas_246					
			g_Novosphingobium_250					
			f_Sphingomonadaceae_254					
			c_Alphaproteobacteria_255					
			f_Hyphomonadaceae_259					
			f_Acetobacteraceae_269					
			g_CandidatusRhabdochlamydia_274					
			f_Syntrophobacteraceae_286					

Paper IV

npj | Biofilms and Microbiomes

www.nature.com/npjbiofilms

ARTICLE OPEN

Bacterial release from pipe biofilm in a full-scale drinking water distribution system

Sandy Chan[1,2,3], Kristjan Pullerits[1,2,3], Alexander Keucken[4,5], Kenneth M. Persson[2,3,4], Catherine J. Paul[1,4] and Peter Rådström[1]

Safe drinking water is delivered to the consumer through kilometres of pipes. These pipes are lined with biofilm, which is thought to affect water quality by releasing bacteria into the drinking water. This study describes the number of cells released from this biofilm, their cellular characteristics, and their identity as they shaped a drinking water microbiome. Installation of ultrafiltration (UF) at full scale in Varberg, Sweden reduced the total cell count to $1.5 \times 10^3 \pm 0.5 \times 10^3$ cells mL^{-1} in water leaving the treatment plant. This removed a limitation of both flow cytometry and 16S rRNA amplicon sequencing, which have difficulties in resolving small changes against a high background cell count. Following installation, 58% of the bacteria in the distributed water originated from the pipe biofilm, in contrast to before, when 99.5% of the cells originated from the treatment plant, showing that UF shifts the origin of the drinking water microbiome. The number of bacteria released from the biofilm into the distributed water was $2.1 \times 10^3 \pm 1.3 \times 10^3$ cells mL^{-1} and the percentage of HNA (high nucleic acid) content bacteria and intact cells increased as it moved through the distribution system. DESeq2 analysis of 16S rRNA amplicon reads showed increases in 29 operational taxonomic units (OTUs), including genera identified as *Sphingomonas*, *Nitrospira*, *Mycobacterium*, and *Hyphomicrobium*. This study demonstrated that, due to the installation of UF, the bacteria entering a drinking water microbiome from a pipe biofilm could be both quantitated and described.

npj Biofilms and Microbiomes (2019)5:9 ; https://doi.org/10.1038/s41522-019-0082-9

INTRODUCTION

Drinking water is delivered to the consumer through kilometres of pipes and maintenance of water quality in these drinking water distribution systems (DWDSs) is a prime concern for drinking water providers. These systems contain microorganisms in both the flowing water and in biofilm that lines the interior of the pipes.[1,2] This pipe biofilm may: be a reservoir for pathogens[3,4]; play a role in corrosion[5]; and, impact the aesthetics of the water.[6]

The complex microbial communities of DWDS biofilms[7,8] are distinct from that of the bulk water and differ according to water and location. Bacteria in loose deposits and pipe biofilm were estimated to contain >98% of the bacteria in a DWDS[7] and release of these cells can alter the bulk water.[8] This must always be occurring to some extent,[9] although most studies have focussed on large changes due to season, water pressure or flow in the microbial communities in the biofilm or distributed water.[10–12] Changes in microbial communities in distributed water associated with increasing distance have been attributed to spatial dynamics, including disinfection residuals and pipe connections, and pipe biofilm was suggested as a source of this variation.[13] Liu and colleagues, however, estimated that the majority of bacteria in tap water originated from the treatment plant, with cells from the biofilm contributing only a few percent.[14]

These studies characterized DWDS biofilm material detached by flushing or swabbed from surfaces, and interactions of pipe biofilm with distributed water during normal hydraulic operating conditions have been difficult to observe.[3] This is likely due to the small number of bacteria entering from the biofilm, relative to the number of cells present in the distributed water, which also limits the application of analysis methods for bacterial communities. 16S rRNA gene amplicon sequencing cannot resolve bacteria at very low abundance, against a high abundance background community[15]; and flow cytometry (FCM) cannot detect changes representing <5% of the total cell count.[16]

The drinking water treatment plant (DWTP) in Varberg, Sweden was upgraded to include a full-scale ultrafiltration (UF) facility with two-stage filtration and in-line coagulation at the primary membrane stage.[17] This change created a full-scale DWDS that distributed water containing altered natural organic matter (NOM) and virtually no bacteria. Changes in biofilm likely require extended time frames to respond to a new environment,[18] so the days immediately following UF installation provided a window of opportunity before changes in the water quality would impact the biofilm. With fewer bacterial cells in the distributed water, those originating from the pipe biofilm and released into the water could now be observed. Sampling locations were chosen with short water retention times to ensure that cells detected in the water phase could not be the result of regrowth. The removal of the high background cell count removed the limitations in resolution for FCM and 16S rRNA amplicon sequencing studies and the community of bacteria released from the pipe biofilm in a full-scale DWDS could be quantitated and described, as they shaped the post-UF drinking water microbiome.

[1]Applied Microbiology, Department of Chemistry, Lund University, P.O. Box 124, SE-221 00 Lund, Sweden; [2]Sweden Water Research AB, Ideon Science Park, Scheelevägen 15, SE-223 70 Lund, Sweden; [3]Sydvatten AB, Hyllie Stationstorg 21, SE-215 32 Malmö, Sweden; [4]Water Resources Engineering, Department of Building and Environmental Technology, Lund University, P.O. Box 118, SE-221 00 Lund, Sweden and [5]Vatten & Miljö i Väst AB, P.O. Box 110, SE-311 22 Falkenberg, Sweden
Correspondence: Catherine J. Paul (catherine.paul@tvrl.lth.se)

Received: 8 June 2018 Accepted: 28 January 2019
Published online: 22 February 2019

Published in partnership with Nanyang Technological University

npj nature partner journals

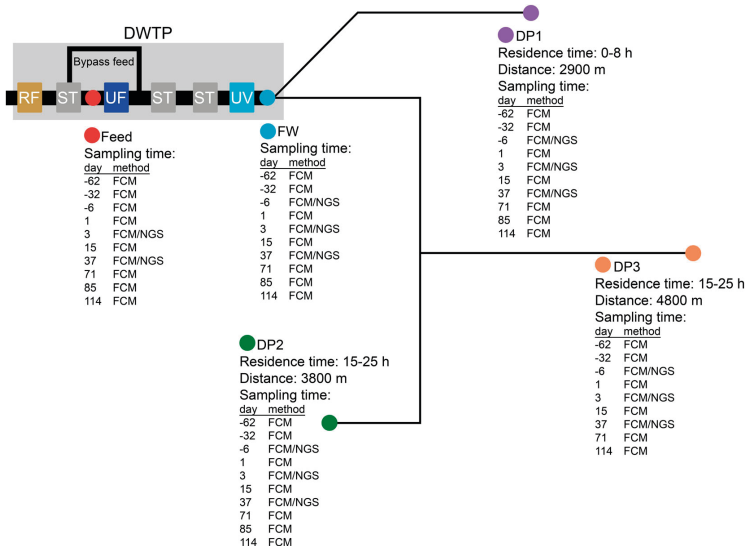

Fig. 1 Schematic illustration of the treatment plant process and sampling points in the distribution network. Locations of DP1, 2 and 3 are not to scale. Distance and time for the water to reach the sampling location from the treatment plant, and types of samples taken on each day, are indicated. In the first 37 days after UF installation, a small fraction of water bypassed the filter, and was used for pH adjustment. After day 37, pH was adjusted using water from UF permeate. *RF* rapid sand filter, *ST* storage tank, *DWTP* drinking water treatment plant

RESULTS

Impact of UF installation

Bacteria in water samples from the DWTP (feed, finished water) and the DWDS (distributed water) were quantified and described by FCM before, and in two distinct time periods after, installation of UF (Fig. 1). From day 0 to day 37, water from the UF feed, and thus containing bacteria, was used for pH regulation, resulting in the addition of approximately $2.2 \times 10^4 \pm 4.5 \times 10^2$ cells mL^{-1} to the UF permeate, whereas after day 37, and until the end of the study period, pH was adjusted using only UF permeate. The permeate had a total cell concentration (TCC) below the quantification limit (data not shown), at around 200 cells mL^{-1},[16] and this was reflected by the instantaneous reduction in TCC at all distribution points (DP), and time points sampled after UF installation (Fig. 2).

In the first 37 days after UF installation, the average TCC of distributed water samples decreased from $4.8 \times 10^5 \pm 1.7 \times 10^5$ cells mL^{-1} ($n = 27$) to $2.7 \times 10^4 \pm 4.3 \times 10^3$ cells mL^{-1} ($n = 36$), a reduction of 93.1 ± 3.3%. This TCC in the distributed water included bacteria released from pipe biofilm and those added during the pH adjustment. Before UF installation, the concentration of cells with high nucleic acid (HNA) content did not change during distribution (48 ± 7.8% finished water; 48 ± 7.5% distributed water). However, in the 37 days after UF installation, the proportion of HNA content bacteria in distributed water increased significantly ($P < 0.01$, one-way analysis of variance (ANOVA)) (Supplementary Figure 1): from 39 ± 2.3% in the finished water to an average of: 40 ± 3.2% at DP1, 44 ± 4.5% at DP2, and 43 ± 3.6% at DP3. During this initial period, intact cell concentration (ICC) in distributed water decreased, from an average of 58 ± 6.0% to 26 ± 6.1% (Supplementary Figure 2) although ICC increased in distributed water compared to finished water, from 19 ± 3.8% to 26 ± 6.1%. This was not observed before the installation of UF (55 ± 3.3% ICC and 58 ± 6.0% ICC, respectively).

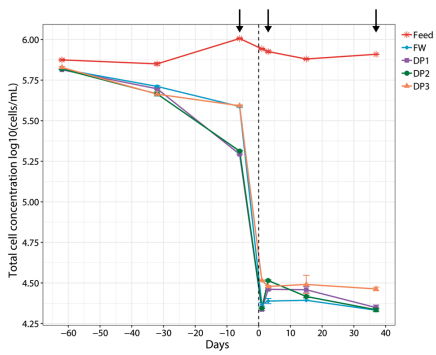

Fig. 2 The number of bacteria in water from the treatment plant and distribution system in the first 37 days following UF installation. TCC were measured in the feed water to the UF (red line, stars); water leaving the treatment plant (finished water FW, blue line, diamonds); and at DP1 (purple line, squares), DP2 (green line, circles) and DP3 (orange line, triangles) in the distribution system, before and after the installation of UF. Day 0 on the *x* axis corresponds to the start of UF (vertical dashed line). The arrows indicate days when water was sampled for sequencing. Error bars represent the variation in technical triplicates

Conventional water quality parameters were measured before, and 3 and 37 days after, installation of UF (Supplementary Table

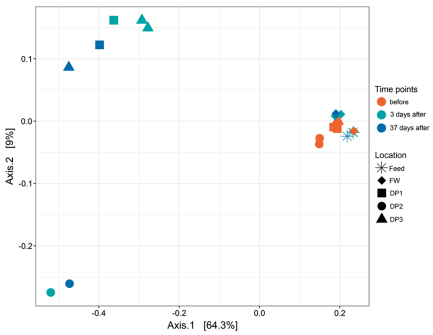

Fig. 3 Comparison of bacterial communities before, and in the first 37 days after, installation of UF using a principal coordinates analysis (PCoA) plot based on Bray–Curtis dissimilarity calculated for bacterial communities from water sampled in the treatment plant: at feed (stars) and finished water (FW, diamonds); and at DP1 (squares), DP2 (circles) and DP3 (triangles). Samples were taken before installation of UF (orange) and at 3 (green) and 37 (blue) days after installation. Communities associated with the distribution system after installation of UF were separated from all other samples

2). Colour, dissolved organic carbon (DOC), turbidity and total organic carbon (TOC) decreased in finished and distributed water after UF installation. Heterotrophic bacteria were only observed after 7 days of incubation and increased slightly in distributed water compared to finished water, regardless of UF treatment. At DP2, water temperature was always highest and took longer to stabilize, nitrite concentrations were lowest and copper concentrations were highest. UF installation also altered NOM (Supplementary Table 3).

Phylogenetic analysis of the bacterial communities

The UF installation did not appear to alter the community composition in the finished water (Fig. 3); however, in the first 37 days, pre-UF water (feed) was used to adjust pH, so this community was in fact a dilution of the feed water community with UF permeate and would have little impact on comparisons based on relative abundance. In contrast, after installation, relative abundance of *Alphaproteobacteria* and *Nitrospira* significantly increased ($P < 0.05$, Mann–Whitney U test) in water from the DWDS (Supplementary Figure 3). The average relative abundance of *Alphaproteobacteria* in distributed water was $20 \pm 1.9\%$ before UF ($n = 6$), with limited variation between DPs, while after installation, *Alphaproteobacteria* increased in relative abundance at DP1 ($42 \pm 5.9\%$, $n = 2$), DP2 ($36 \pm 7.7\%$, $n = 2$) and DP3 ($35 \pm 1.7\%$, $n = 3$). Increased relative abundance of *Nitrospira* was observed at DP1 (from $0.87 \pm 0.061\%$ to $5.9 \pm 0.29\%$) and DP3 (from $0.97 \pm 0.061\%$ to $11 \pm 7.6\%$) with the largest change seen at DP2, from $3.2 \pm 0.44\%$ before UF to the highest observed relative abundance for this class, at $30 \pm 11\%$, after the installation.

Communities at different locations within the DWDS diverged from those in post-UF installation finished water (feed water diluted in permeate) and all of the communities before UF installation (Fig. 3). Communities at DP1 and DP3 were most similar, whereas those at DP2 had a distinct composition. Bacterial communities in the distributed water from before the installation of UF showed highest richness (number of operational taxonomic units (OTUs), sequence similarity cut-off: 97%) and evenness (Pielou's index) and thus the highest diversity (Shannon index, Fig. 4). UF installation did not affect diversity in the finished water, due to the dilution with feed water (Shannon index, 5.1 ± 0.018 vs. 5.1 ± 0.043); however, communities in distributed water had larger variation and significantly lower diversity ($P < 0.05$, one-way ANOVA) after the installation. The community at DP2, 3 days after installation, contained the fewest OTUs (732) and lowest evenness (0.63). All rarefaction curves reached a plateau (Supplementary Figure 4).

Identifying the bacteria released from the biofilm

After installation of UF, sequencing reads originating from finished water were compared to those from distributed water using DESeq2 analysis, with 147 OTUs containing at least 0.1% of the total unrarefied number of sequences as input. Thirty OTUs with a significant change in number of reads ($P < 0.01$) were identified (Supplementary Table 1) with 15 of these classified into 7 genera (Fig. 5). Reads increased >300-fold in distributed water for OTUs classified as *Rhodobacter* (1 OTU), *Nitrospira* (3 OTUs), *Hyphomicrobium* (1 OTU) and *Mycobacterium* (1 OTU) and >150-fold for 2 OTUs classified as *Nitrospira* and *Hyphomicrobium*. OTUs where reads increased >30-fold were classified as *Sphingomonas* (2 OTUs) and *Novosphingobium* (1 OTU). A 30-fold increase was also observed in 14 additional OTUs classified at the family, order and class level (Fig. 5). One OTU could not be classified.

To examine local variations, the abundance of reads within OTUs selected by DESeq2 were compared at each DWDS sampling point, before and after the installation of UF (Fig. 6). This separated DWDS samples collected after the UF installation from all other samples in the study. One OTU classified as *Nitrospira* accounted for 4.5% (5595 of the 24,900 reads) of the total rarefied reads from DP2 sampled 3 days after installation of UF. Communities sampled at DP1 and DP3 after the installation of UF had higher relative abundance for an OTU belonging to the genus *Sphingomonas* (1980 ± 820 reads and 1860 ± 630 reads, respectively) compared to the period before (175 ± 69 reads and 158 ± 59 reads, respectively). A high relative abundance of *Rickettsiales* (2264 reads) and increases in two OTUs belonging to *Nitrospira* were also observed at DP3, on day 37.

Quantifying the bacteria released from the biofilm

After day 37, feed water was replaced with UF permeate for pH adjustment (Supplementary Figure 5), further minimizing the number of cells in the finished water leaving the DWTP. This exposed changes in TCC that could be attributed to release of cells from the biofilm. Finished water now contained an average of $1.5 \times 10^3 \pm 0.5 \times 10^3$ cells mL^{-1} ($n = 9$) from UF permeate (approximately 200 cells mL^{-1}) and contact with biofilms within the treatment plant (Fig. 1). With the average TCC of the distributed water after day 37 of $3.7 \times 10^3 \pm 1.2 \times 10^3$ cells mL^{-1} ($n = 24$, Supplementary Figure 5), the release of bacterial cells from the DWDS biofilm was an average of $2.1 \times 10^3 \pm 1.3 \times 10^3$ cells mL^{-1} or approximately 58% of the TCC in the water. The numbers of cells increased with increasing distance from the treatment plant: with 47% at DP1 ($n = 9$), 60% at DP2 ($n = 9$), and 65% at DP3 ($n = 6$) with similar trends observed in the proportion of cells with HNA (from $38\% \pm 12\%$ to $59\% \pm 6.9\%$) and ICC (from $46\% \pm 18\%$ to $60\% \pm 10\%$). Using the estimate of bacterial release from the pipe biofilm ($2.1 \times 10^3 \pm 1.3 \times 10^3$ cells mL^{-1}) with the average TCC of distributed water *before* the UF installation ($4.8 \times 10^5 \pm 1.7 \times 10^5$ cells mL^{-1}), the percentage of bacteria from the biofilm in the bacterial population of this distributed water was estimated at 0.5%, with 99.5% originating from within the treatment plant. Taken together, this shows that UF installation shifted the bacterial community in the distributed water so that, with increasing distance from the DWTP, it was increasingly comprised of bacteria released from pipe biofilm.

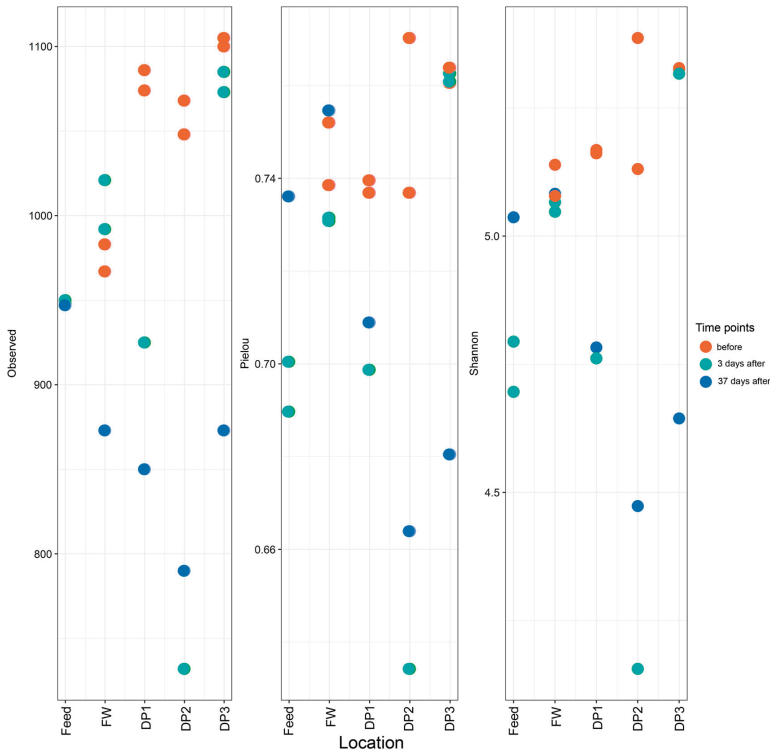

Fig. 4 Installation of UF impacts diversity of bacterial communities in the distributed water. Alpha diversity analysis of bacterial communities in water samples from the treatment plant (feed and finished water (FW)) and distribution system (DP1, 2, 3) were examined before installation of UF (orange) and at 3 (green) and 37 (blue) days after installation. The number of observed OTUs (left), evenness (Pielou's index) (middle) and Shannon index (right) are compared in the different communities

DISCUSSION

Ultrafiltration impacts many aspects of water quality, including changes in the amount and character of both NOM and bacteria.[19] The installation of UF reduced the TCC in the distributed water from $4.8 \times 10^5 \pm 1.7 \times 10^5$ cells mL^{-1} to $3.7 \times 10^3 \pm 1.2 \times 10^3$ cells mL^{-1}, corresponding to a 99% removal of bacteria in the DWDS. This degree of cell removal exposed small relative differences between water sampled at different points within the distribution system, permitting quantification and identification of bacteria from the pipe biofilm that were released into the water as it travelled through the distribution system.

While studies have suggested that the microbiome in distributed drinking water is highly influenced by biofilm on pipe walls,[1,20] others have contradicted this hypothesis[7,21] and suggested that source water[10,22,23] and sand filters[24,25] are more influential. In the current study, after day 37, 58% of the bacteria in the distributed water originated from pipe biofilm. While one explanation for this addition of cells to the water could be regrowth, the DWDS sampling points in this study had short residence times (>25 h), and with a growth rate approximated as 0.30 day^{-1} (or a doubling time of 2.31 days) for distributed water,[26] this is an unlikely explanation for the increases in TCC. Nutrient concentrations (DOC, biopolymers, and humic substances, Supplementary Table 3) were reduced by UF; water temperatures ranged from 5.7 to 9 °C (Supplementary Table 2); and 7-day incubation were required to detect heterotrophs (Supplementary Table 2). Taken together, this evidence strongly suggests that the increase in TCC with distance from the treatment plant was due to release of cells from the pipe biofilm into the water.

The short time frame in this study allowed the contribution of cells from the biofilm to be estimated as 0.5% of the total cells present in the water *before* the change. Applying this estimate for cells released from the biofilm to other systems where the bacterial concentration in the distributed water is high can explain why the contribution from the pipe biofilm to the water microbiome has been difficult to observe. In a year-long sampling campaign by Pinto and colleagues (2014), only water sampled at great distance from the DWTP showed small changes in the water microbiome.[27] Henne and colleagues (2012) compared communities from distributed water and biofilm, and the water had a highly homogeneous bacterial community despite observed diversity in the biofilm communities.[8] We suggest that the community composition in the distributed water will be clearly associated with processes in the treatment plant, such as the use of sand filters[24,25,28] and use of disinfectants[29–31] unless that

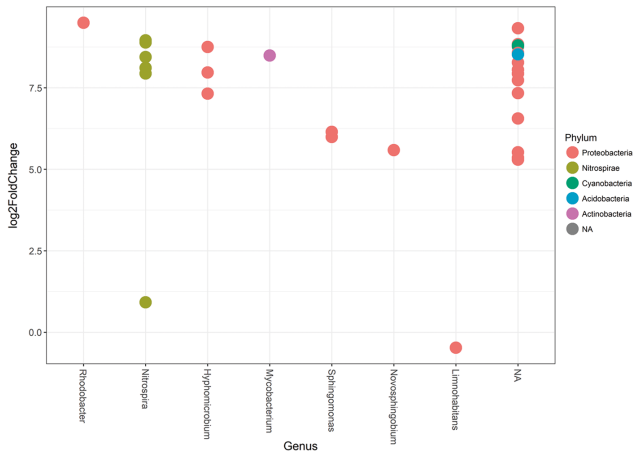

Fig. 5 Operational taxonomic units (OTUs) representing changes in the bacterial community of the distributed water. Log2 fold changes calculated by DESeq2 in R for OTUs describe changes in the bacterial community in the distributed water after the installation of ultrafiltration. Each dot represents an OTU with the classified taxonomic level (genus) shown on the *x* axis, and phylum indicated by colour. A positive value indicates a significant increase of the specific OTU in the distributed water community relative to that of the finished water leaving the treatment plant

treatment (i.e. UF) removes a large percentage of cells. In this case, the bacterial community in the distributed water will contain a majority of cells originating from the pipe biofilm. Given the great diversity in the microbial communities of source water, distributed water and biofilm and other variables governing water quality such as local climate, treatment processes and pipe materials, it is not known if the bacterial community in this study, and the extent to which it was released into the flowing water, reflects what would happen in every DWDS, and additional studies are needed to determine the impact of UF in other systems.

After installation of UF, the percentage of HNA bacteria in the distributed water increased compared to finished water (Supplementary Figure 1). Proctor and colleagues (2018) proposed that HNA bacteria, in contrast to low nucleic acid bacteria, are not as dependent on other bacteria for survival[32] and HNA bacteria may survive in distributed water without the biofilm community. The percentage of intact cells also increased in the water as it travelled through the DWDS, and may be a signature for bacterial release from pipe biofilm. Shifts in HNA[33] and ICC[34] were observed in tap water after overnight stagnation and distributed water, respectively, and may indicate release of biofilm in these contexts.

DNA sequencing studies of bacterial communities in pipe biofilms have shown higher diversity compared to that in the distributed water.[8,35] Henne and colleagues (2012) showed higher diversity with lower richness in the biofilm compared to the water phase and suggested that the biofilm community contains evenly distributed members adapted for this specific environment.[8] This implies that if only some members of the evenly distributed biofilm community are released into the distributed water there will be a shift in the population towards lower evenness. In the current study, lower diversity (due to both decreased richness and lower evenness) was observed for the community in distributed water after UF installation, compared to those in finished water and before UF installation. This altered community structure in the distributed water can be attributed to interaction with the biofilm, with the similarity between the communities in finished water and before UF installation attributed to the use of diluting feed water for pH adjustment in the first 37 days after UF installation. In this period, lower evenness was observed as increasing dominance in the distributed water of a few specific OTUs, such as genera *Nitrospira*, and *Sphingomonas*. Lower diversity in the water microbiome has been observed after flushing, with this uneven detachment of biofilm resulting in a more uneven water community.[12,36]

Installation of UF decreased the richness (lower numbers of OTUs) in the distributed water. A rich bacterial community in the water, with many bacteria at low abundance, can be a seed bank for the biofilm community.[8] Altered environmental conditions initiated by the UF treatment could trigger cells to enter the biofilm, resulting in the observed decrease in richness.[37] This would not appear in the DESeq2 analysis, as this only included OTUs with total read abundance across all the samples >0.1%, and it has been suggested that the rare biosphere represented by OTUs with abundance <0.1% of the community is the dormant microbial seedbank.[37]

Specific OTUs at class level accounted for much of the observed changes in the water microbiome, including *Alphaproteobacteria* and *Nitrospira*, which showed a higher relative abundance in the distributed water after the installation of UF. Higher relative abundance of *Alphaproteobacteria* has been observed in biofilm compared to the distributed water,[8] in water containing biofilm detached by flushing[12] and dominating biofilm communities in DWDS[7] and water meters.[38,39] Observations similar to these seen for *Alphaproteobacteria* have also been observed for *Nitrospira*.[21,35]

Bacteria released from the biofilm were described by 29 OTUs where the absolute read abundance increased in the distributed water compared to the finished water. Two OTUs classified as genus *Sphingomonas* predominated at DP1 and DP3 relative to DP2 and compared to the rest of the OTUs describing the released biofilm community. *Sphingomonas* are often detected in bacterial communities from drinking water, with high abundance in biofilms[10,38] and a relative abundance in DWDS estimated at up to 85%.[7] *Sphingomonas* possess flagella,[40] with this motility perhaps contributing to their release from the biofilm and their

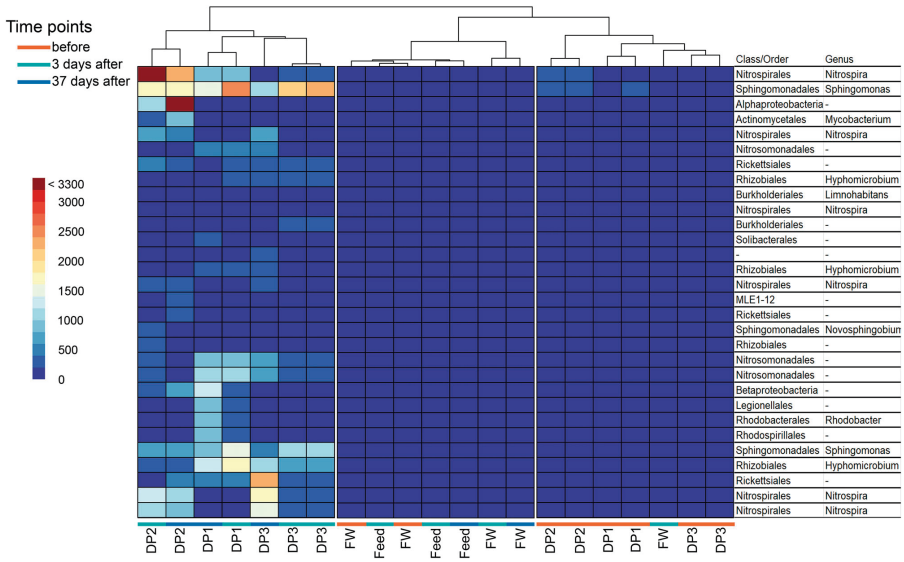

Fig. 6 Changes in read frequencies for specific OTUs at different sampling points in the distribution system. The heatmap shows frequency of reads in the 30 OTUs selected by DESeq2 analysis for feed and finished water (FW) from the treatment plant and DP1, 2 and 3 before installation of ultrafiltration (orange) and at 3 (green) and 37 (blue) days after installation. The classification of the OTUs in class/order and genus are shown to the right of the figure

proposed role as early colonizers DWDS biofilms.[41] *Sphingomonadaceae* are HNA bacteria (as large bacteria >0.4 µm),[32] which supports observed increase of HNA bacteria in distributed water in the current study.

Six of the 29 OTUs released from the biofilm were classified as genus *Nitrospira*, a group of bacteria that has been found in bacterial communities in drinking water, loose deposits and drinking water biofilms.[7,8,21,35] The dominance of this taxa at DP2 might be due to loose deposits containing high amount of biofilm with *Nitrospira* abundance, which can vary between locations in the distribution, although this was not examined in the current study. Members of this genus can use nitrite as an electron donor instead of organic molecules[21,42]: nitrite concentrations at DP2 were lower compared to DP1 and DP3. DP2 was consistently warmer, with higher copper concentrations and low-carbon, chloramine-treated water, which may also favour growth of *Nitrospira*.[43]

While numerous studies have associated *Alphaproteobacteria*, *Sphingomonas*, *Nitrospira* and *Mycobacterium* spp. with drinking water and its biofilms, this study showed that members of these classes and genera also move from the pipe biofilm into the drinking water. It does not appear to be a single mode of motility that is used to escape the biofilm: *Sphingomonas* are almost universally motile via flagella; *Nitrospira* are generally thought to be nonmotile,[44] *Mycobacterium spp.* use sliding motility[45] and *Hyphomicrobium* are motile as swarmer cells with flagella.[46] All modes may be sufficient and, together with random attachment and detachment, account for cell release.[9] This could occur for both live and dead cells leaving the biofilm, and it would be interesting to describe this community in the context of cell viability.

In conclusion, although the UF installation modified the type of organic matter and greatly reduced the number of bacterial cells in the distributed water, destabilization of the biofilm, observed as detachment, sloughing or a sudden increases in the number of total cells in distributed water, was not observed during the 114 days of the study. It can take years for changes to be observed in a microbial community in response to an alteration in the environment,[47] so the observation of consistently low cell counts over the 0.3 year of the current study does not confirm that this will always be the case and it is not known how this biofilm will adapt over the coming years and seasons to the UF installation. Regions in the DWDS with longer retention times may gradually show increasing cell counts in distributed water from prolonged contact with the biofilm or the dynamics of bacterial release may change. Changes in nutrients, such as those described in this study (both NOM and cells), may, over months and years, change the water and biofilm community composition as they adapt to these new conditions.[18] Since this study was conducted during winter, it is also not known to what extent the release of bacterial cells could change with increases in temperature or seasonal changes in water use, which have both been shown to alter the overall numbers of cells in distributed water.[34] The impact of having a higher percentage of bacteria in the water that originates from biofilm is also not known. Given that cells originating from biofilms are more likely to form biofilms themselves,[48] it would be interesting to see whether shifts in the origin of the bacteria in the distributed water can impact formation of biofilms on new DWDS pipes, water meters or household drinking water plumbing systems.

METHODS

Study site and sampling

Water samples were collected from Kvarnagården Waterworks and DWDS operated by VIVAB (Varberg, Sweden). Treatment consisted of pH adjustment, rapid sand filtration, ultraviolet (UV) disinfection and

distributed with a chlorine residual. In November 2016, the DWTP was reconfigured to use rapid sand filtration, coagulation and UF, pH adjustment, UV disinfection and chlorine residual between 0.13 and 0.21 mg L^{-1}. For the first 37 days following UF installation, UF feed water was used for pH adjustment of the finished water, then switched to use UF permeate. Feed water refers to water sampled after rapid filters, after the UF installation. After the addition of chloramine, the water is referred to as finished.

The approximate location, distances and residence times describing the DWDS sampling locations (DP1–3, Fig. 1) were provided by the water company. DP1 is an office building tap at a wastewater treatment plant (VIVAB), DP2 and DP3 are sampling taps at a school and pump station, respectively. Water samples for FCM were collected in sterile 15 mL Falcon tubes, stored on ice or at 4 °C and analysed the following day. Chlorine residuals were quenched by addition of 1% (v/v) sodium thiosulphate (20 g L^{-1}). Water samples for sequencing analysis (1 L for before UF installation, and feed water, 5 L for after UF installation) were collected in sterilized borosilicate bottles, filtered onto 0.22-µm filters (Merck, Germany), stored on ice during travel to the laboratory and at −20 °C until DNA extraction. Conventional water quality sampling and analysis was according to the analysis laboratory Eurofins Scientific (Belgium). NOM was analysed by LC-OCD-OND at DOC-Labor (Germany).

FCM analysis

FCM analysis was performed according to Prest et al.[49] using a BD Accuri C6 flow cytometer (Becton Dickinson, Belgium) equipped with a 50 mW laser, emission wavelength at 488 nm. Briefly, water samples in triplicate were stained with 5 µL mL^{-1} of SYBR Green I at 100× diluted with dimethyl sulphoxide (stock concentration 10,000 ×, Invitrogen AG, Switzerland) at room temperature to a final concentration of 1× SYBR Green I and incubated at 37 °C for 15 min. ICC was determined by including 3 µM propidium iodide (1 mg mL^{-1}, Sigma-Aldrich, Germany). Stained samples (50 µL of the 500 µL) were analysed with a threshold of 500 arbitrary units of green fluorescence. Results were exported as FCS files to FlowJo (Tree Star Inc, USA) and gated identically for all samples with green fluorescence (533 ± 30 nm) and red fluorescence (>670 nm). The number of HNA bacteria were determined using a cut-off for green fluorescence $>2 \times 10^4$ arbitrary units.[49] One-way ANOVA tests were conducted in R.[50]

Microbial community analysis

DNA was extracted using the Fast DNA Spin Kit for Soil according to the manufacturer's instructions from filter papers cut into strips and added directly to tubes containing Lysing Matrix E (MP Biomedicals, USA). Empty filter papers were extracted as a negative control. Extracted DNA was stored at −20 °C until further processing.

Amplicons of the V3–V4 region of 16S rRNA gene were generated using the universal bacterial primers Bact_341F (5′-CCTACGGGNGGCWGCAG-3′) and Bact_785R (5′-GACTACHVGGGTATCTAATCC-3′).[51] PCR reactions (25 µL) containing: 12.2 µL Milli-Q water, 10 µL 5PRIME HotMasterMix (Quantabio, USA), 0.8 µL (10 mg mL^{-1}) bovine serum albumin, 0.5 µL (10 µM) of forward and reverse primers, and 1 µL of template DNA were cycled for 94 °C for 3 min followed by 35 cycles of: 94 °C for 45 s, 50 °C for 1 min, 72 °C for 1.5 min, and a final step of 72 °C for 10 min. Three PCR reactions were performed for each DNA extraction, triplicates were combined and each amplicon was quantified using a Qubit 2.0 dsDNA BR Assay Kit (Thermo Fisher Scientific, USA). Amplicons were inspected by agarose gel electrophoresis, and as sufficient DNA was obtained, no additional measures were required in order to proceed, regardless of the initial volume of water sampled (1 L, 5 L). DNA from each amplicon (50 ng) were then pooled together, purified using the UltraClean PCR Clean-up Kit (Qiagen, Germany) according to the manufacturer's instructions) and quantified again using Qubit. Sequencing was performed on the MiSeq platform using the MiSeq Reagent Kit v3 (600-cycles) (Illumina, USA), according to the manufacturer's instructions, with 10% PhiX added to the sequencing run.

Sequencing data was analysed using Quantitative Insights into Microbial Ecology (QIIME) pipeline.[52] OTUs were clustered with 97% sequence similarity using the open reference OTU-picking method in QIIME. Chimeras were identified using the UCHIME algorithm[53] integrated in the USEARCH[54] pipeline. Taxonomy assignments and sequence alignments with the PyNAST alignment were performed using the GreenGenes database. Analysis using the OTU table (biom format) was performed in R using the phyloseq package,[55] displayed by ggplot2 package.[56] OTUs with total reads across all samples <0.005% were removed and the library rarefied to 24,900 reads per sample. The negative control was removed from further analysis as the number of reads in these samples was lower than the rarefied threshold. Alpha diversity was calculated using Shannon index for diversity by the vegan package[57] and Pielou's index for evenness using the function *evenness* from the microbiome package[58] in R. The Principal Coordinates Analysis (PCoA) plot was created using the Bray–Curtis dissimilarity matrix from the vegan package. Clusters formed in the PCoA plot could not be confirmed by permutational analyses of variance due to uneven dispersion in the data set (tested by the function *betadisp* in R, vegan package).

OTUs with differential read abundance were identified using the DESeq2 package[59] in R. OTUs with total unrarefied reads across all samples >0.1% were used as input with distributed water samples collected after UF as one group compared to the finished water samples after UF. The OTUs selected by DESeq2 analysis were used to construct a heatmap using the pheatmap package[60] in R.

Reporting Summary

Further information on experimental design is available in the Nature Research Reporting Summary linked to this article.

DATA AVAILABILITY

DNA sequences are available at the NCBI Sequence Read Archive, accession number PRJNA494637.

ACKNOWLEDGEMENTS

The authors thank Janine Riechelmann and the employees at VIVAB AB, specifically Jennie Lindgren and Moshe Habagil, for contributions to sampling, and Emelie Salomonsson, Jon Ahlinder, and Moa Hägglund at the Swedish Defense Research Agency for assistance with sequencing and bioinformatics. This study was supported by the Swedish Research Council (Grant 621-2013-587), The Swedish Water and Wastewater Association Development Fund, Sweden Water Research AB and public joint-stock utility Vatten & Miljö i Väst AB (VIVAB).

AUTHOR CONTRIBUTIONS

S.C., A.K., C.J.P. and P.R. planned experiments; S.C. and K.P. conducted experiments and data analysis. S.C., C.J.P. and P.R. drafted the manuscript. All authors contributed to the final manuscript. A.K., K.M.P., C.J.P. and P.R. conceived the study. P.R. is the guarantor.

ADDITIONAL INFORMATION

Supplementary Information accompanies the paper on the *npj Biofilms and Microbiomes* website (https://doi.org/10.1038/s41522-019-0082-9).

Competing interests: The authors declare no competing interests.

Publisher's note: Springer Nature remains neutral with regard to jurisdictional claims in published maps and institutional affiliations.

REFERENCES

1. Flemming, H.-C., Percival, S. L. & Walker, J. T. Contamination potential of biofilms in water distribution systems. *Water Res.* **2**, 271–280 (2002).
2. Wingender, J. & Flemming, H. C. Contamination potential of drinking water distribution network biofilms. *Water Sci. Technol.* **49**, 277–286 (2004).
3. Wingender, J. & Flemming, H.-C. Biofilms in drinking water and their role as reservoir for pathogens. *Int. J. Hyg. Environ. Health* **214**, 417–423 (2011).
4. Berry, D., Xi, C. & Raskin, L. Microbial ecology of drinking water distribution systems. *Curr. Opin. Biotechnol.* **17**, 297–302 (2006).
5. Kip, N. & van Veen, J. A. The dual role of microbes in corrosion. *ISME J.* **9**, 542–551 (2015).
6. Fish, K., Osborn, A. M. & Boxall, J. B. Biofilm structures (EPS and bacterial communities) in drinking water distribution systems are conditioned by hydraulics and influence discolouration. *Sci. Total Environ.* **593-594**, 571–580 (2017).
7. Liu, G. et al. Pyrosequencing reveals bacterial communities in unchlorinated drinking water distribution system: an integral study of bulk water, suspended solids, loose deposits, and pipe wall biofilm. *Environ. Sci. Technol.* **48**, 5467–5476 (2014).

8. Henne, K., Kahlisch, L., Brettar, I. & Hofle, M. G. Analysis of structure and composition of bacterial core communities in mature drinking water biofilms and bulk water of a citywide network in Germany. *Appl. Environ. Microbiol.* **78**, 3530–3538 (2012).
9. Petrova, O. E. & Sauer, K. Escaping the biofilm in more than one way: desorption, detachment or dispersion. *Curr. Opin. Microbiol.* **30**, 67–78 (2016). d.
10. Douterelo, I., Jackson, M., Solomon, C. & Boxall, J. Spatial and temporal analogies in microbial communities in natural drinking water biofilms. *Sci. Total Environ.* **581-582**, 277–288 (2017).
11. Wang, H., Masters, S., Edwards, M. A., Falkinham, J. O. & Pruden, A. Effect of disinfectant, water age, and pipe materials on bacterial and eukaryotic community structure in drinking water biofilm. *Environ. Sci. Technol.* **48**, 1426–1435 (2014).
12. Douterelo, I., Husband, S. & Boxall, J. B. The bacteriological composition of biomass recovered by flushing an operational drinking water distribution system. *Water Res.* **54**, 100–114 (2014).
13. Potgieter, S. et al. Long-term spatial and temporal microbial community dynamics in a large-scale drinking water distribution system with multiple disinfectant regimes. *Water Res.* **139**, 406–419 (2018).
14. Liu, G. et al. Assessing the origin of bacteria in tap water and distribution system in an unchlorinated drinking water system by SourceTracker using microbial community fingerprints. *Water Res.* **138**, 86–96 (2018).
15. Vierheilig, J. et al. Potential applications of next generation DNA sequencing of 16S rRNA gene amplicons in microbial water quality monitoring. *Water Science and Technology* **72**, 1962–1972 (2015).
16. Hammes, F. et al. Flow-cytometric total bacterial cell counts as a descriptive microbiological parameter for drinking water treatment processes. *Water Res.* **42**, 269–277 (2008).
17. Keucken, A., Heinicke, G., Persson, K. & Köhler, S. Combined coagulation and ultrafiltration process to counteract increasing NOM in brown surface water. *Water* **9**, 697 (2017).
18. Liu, G. et al. Potential impacts of changing supply-water quality on drinking water distribution: a review. *Water Res.* **116**, 135–148 (2017).
19. Vickers, J. C., Thompson, M. A. & Kelkar, U. G. The use of membrane filtration in conjunction with coagulation processes for improved NOM removal. *Desalination* **102**, 57–61 (1995).
20. LeChevallier, M. W., Babcock, T. M. & Lee, R. G. Examination and characterization of distribution system biofilms. *Appl. Environ. Microbiol.* **53**, 2714–2724 (1987).
21. Martiny, A. C., Albrechtsen, H. J., Arvin, E. & Molin, S. Identification of bacteria in biofilm and bulk water samples from a nonchlorinated model drinking water distribution system: detection of a large nitrite-oxidizing population associated with Nitrospira spp. *Appl. Environ. Microbiol.* **71**, 8611–8617 (2005).
22. Li, W. et al. Community shift of biofilms developed in a full-scale drinking water distribution system switching from different water sources. *Sci. Total Environ.* **544**, 499–506 (2016).
23. Gomez-Alvarez, V., Humrighouse, B. W., Revetta, R. P. & Santo Domingo, J. W. Bacterial composition in a metropolitan drinking water distribution system utilizing different source waters. *J. Water Health* **13**, 140–151 (2015).
24. Pinto, A. J., Xi, C. & Raskin, L. Bacterial community structure in the drinking water microbiome is governed by filtration processes. *Environ. Sci. Technol.* **46**, 8851–8859 (2012).
25. Lautenschlager, K. et al. Abundance and composition of indigenous bacterial communities in a multi-step biofiltration-based drinking water treatment plant. *Water Res.* **62**, 40–52 (2014).
26. Boe-Hansen, R., Albrechtsen, H.-J., Arvin, E. & Jørgensen, C. Bulk water phase and biofilm growth in drinking water at low nutrient conditions. *Water Res.* **36**, 4477–4486 (2002).
27. Pinto, A. J., Schroeder, J., Lunn, M., Sloan, W. & Raskin, L. Spatial-temporal survey and occupancy-abundance modeling to predict bacterial community dynamics in the drinking water microbiome. *mBio* **5**, e01135–01114 (2014).
28. Chan, S. et al. Monitoring biofilm function in new and matured full-scale slow sand filters using flow cytometric histogram image comparison (CHIC). *Water Res.* **138**, 27–36 (2018).
29. El-Chakhtoura, J. et al. Dynamics of bacterial communities before and after distribution in a full-scale drinking water network. *Water Res.* **74**, 180–190 (2015).
30. Holinger, E. P. et al. Molecular analysis of point-of-use municipal drinking water microbiology. *Water Res.* **49**, 225–235 (2014).
31. Wang, H. et al. Effect of disinfectant, water age, and pipe material on occurrence and persistence of Legionella, mycobacteria, *Pseudomonas aeruginosa*, and two amoebas. *Environ. Sci. Technol.* **46**, 11566–11574 (2012).
32. Proctor, C. R. et al. Phylogenetic clustering of small low nucleic acid-content bacteria across diverse freshwater ecosystems. *ISME J.* **12**, 1344–1359 (2018).
33. Besmer, M. D. et al. The feasibility of automated online flow cytometry for in-situ monitoring of microbial dynamics in aquatic ecosystems. *Front. Microbiol.* **5**, 265 (2014).
34. Prest, E. I., Weissbrodt, D. G., Hammes, F., Loosdrecht, M. C. M. v. & Vrouwenvelder, J. S. Long-term bacterial dynamics in a full-scale drinking water distribution system. *PLoS ONE* **11**, 20 (2016).
35. Martiny, A. C., Jorgensen, T. M., Albrechtsen, H. J., Arvin, E. & Molin, S. Long-term succession of structure and diversity of a biofilm formed in a model drinking water distribution system. *Appl. Environ. Microbiol.* **69**, 6899–6907 (2003).
36. Douterelo, I., Husband, S., Loza, V. & Boxall, J. Dynamics of biofilm regrowth in drinking water distribution systems. *Appl. Environ. Microbiol.* **82**, 4155–4168 (2016).
37. Lynch, M. D. J. & Neufeld, J. D. Ecology and exploration of the rare biosphere. *Nat. Rev. Microbiol.* **13**, 217–229 (2015).
38. Luhrig, K. et al. Bacterial community analysis of drinking water biofilms in southern Sweden. *Microbes Environ.* **30**, 99–107 (2015).
39. Ling, F., Hwang, C., LeChevallier, M. W., Andersen, G. L. & Liu, W. T. Core-satellite populations and seasonality of water meter biofilms in a metropolitan drinking water distribution system. *ISME J.* **10**, 582–595 (2016).
40. Pollock, T. J. & Armentrout, R. W. Planktonic/sessile dimorphism of polysaccharide-encapsulated sphingomonads. *J. Ind. Microbiol. Biotechnol.* **23**, 436 (1999).
41. Bereschenko, L. A., Stams, A. J., Euverink, G. J. & van Loosdrecht, M. C. Biofilm formation on reverse osmosis membranes is initiated and dominated by *Sphingomonas* spp. *Appl. Environ. Microbiol.* **76**, 2623–2632 (2010).
42. Hovanec, T. A., Taylor, L. T., Blakis, A. & Delong, E. F. Nitrospira-like bacteria associated with nitrite oxidation in freshwater aquaria. *Appl. Environ. Microbiol.* **64**, 258–264 (1998).
43. Fowler, J., Dechesne, A., Wagner, F. B., Diwan, V., Albrechtsen, H. J. & Smets, B. F. Niche partitioning within genus Nitrospira is affected by environmental copper concentration. In *ICoN5: 5th International Conference on Nitrification* (2017).
44. Sumbali, G. & Mehrotra, R. S. *Principles of Microbiology* (Tata McGraw-Hill Education, New Delhi, 2009).
45. Martínez, A., Torello, S. & Kolter, R. Sliding motility in mycobacteria. *J. Bacteriol.* **181**, 7331–7338 (1999).
46. Moore, R. L. The biology of Hyphomicrobium and other prosthecate, budding bacteria. *Annu. Rev. Microbiol.* **35**, 567–594 (1981).
47. Allison, S. D. & Martiny, J. B. Colloquium paper: resistance, resilience, and redundancy in microbial communities. *Proc. Natl. Acad. Sci. USA* **105**(Suppl 1), 11512–11519 (2008).
48. Lee, C. K. et al. Multigenerational memory and adaptive adhesion in early bacterial biofilm communities. *Proc. Natl. Acad. Sci.* **115**, 4471–4476 (2018).
49. Prest, E. I., Hammes, F., Kötzsch, S., van Loosdrecht, M. C. & Vrouwenvelder, J. S. Monitoring microbiological changes in drinking water systems using a fast and reproducible flow cytometric method. *Water Res.* **47**, 7131–7142 (2013).
50. R Core Team. *R: A Language and Environment for Statistical Computing* (R Foundation for Statistical Computing, Vienna, 2017).
51. Klindworth, A. et al. Evaluation of general 16S ribosomal RNA gene PCR primers for classical and next-generation sequencing-based diversity studies. *Nucleic Acids Res.* **41**, e1 (2013).
52. Caporaso, J. G. et al. QIIME allows analysis of high-throughput community sequencing data. *Nat Methods* **7**, 335–336 (2010).
53. Edgar, R. C., Haas, B. J., Clemente, J. C., Quince, C. & Knight, R. UCHIME improves sensitivity and speed of chimera detection. *Bioinformatics* **27**, 2194–2200 (2011).
54. Edgar, R. C. Search and clustering orders of magnitude faster than BLAST. *Bioinformatics* **26**, 2460–2461 (2010).
55. McMurdie, P. J. & Holmes, S. phyloseq: an R package for reproducible interactive analysis and graphics of microbiome census data. *PLoS ONE* **8**, e61217 (2013).
56. ggplot2: elegant graphics for data analysis (Springer, New York, 2009).
57. vegan: Community Ecology Package (2017).
58. microbiome R package (2017).
59. Love, M. I., Huber, W. & Anders, S. Moderated estimation of fold change and dispersion for RNA-seq data with DESeq2. *Genome Biol.* **15**, 550 (2014).
60. pheatmap: Pretty Heatmaps (2015).

Supplementary Information - Figures

Bacterial release from pipe biofilm in a full-scale drinking water distribution system

Sandy Chan[a,b,c], Kristjan Pullerits[a,b,c], Alexander Keucken[d,e], Kenneth M. Persson[b,c,d], Catherine J. Paul[a,d*], Peter Rådström[a]

[a]Applied Microbiology, Department of Chemistry, Lund University, P.O. Box 124, SE-221 00 Lund, Sweden

[b]Sweden Water Research AB, Ideon Science Park, Scheelevägen 15, SE-223 70 Lund, Sweden

[c]Sydvatten AB, Hyllie Stationstorg 21, SE-215 32 Malmö, Sweden

[d]Water Resources Engineering, Department of Building and Environmental Technology, Lund University, P.O. Box 118, SE-221 00 Lund, Sweden

[e] Vatten & Miljö i Väst AB, Box 110, 311 22 Falkenberg, Sweden

**corresponding author*

Table of Contents

Supplementary Figure 1 – Changes in high nucleic acid (HNA) content bacteria in DWDS

Supplementary Figure 2 – Intact cell concentrations in the DWTP and DWDS

Supplementary Figure 3 – Relative abundance of bacteria in the different samples at the class level

Supplementary Figure 4 – Rarefraction curves

Supplementary Figure 5 – TCC of the distributed water samples after UF installation

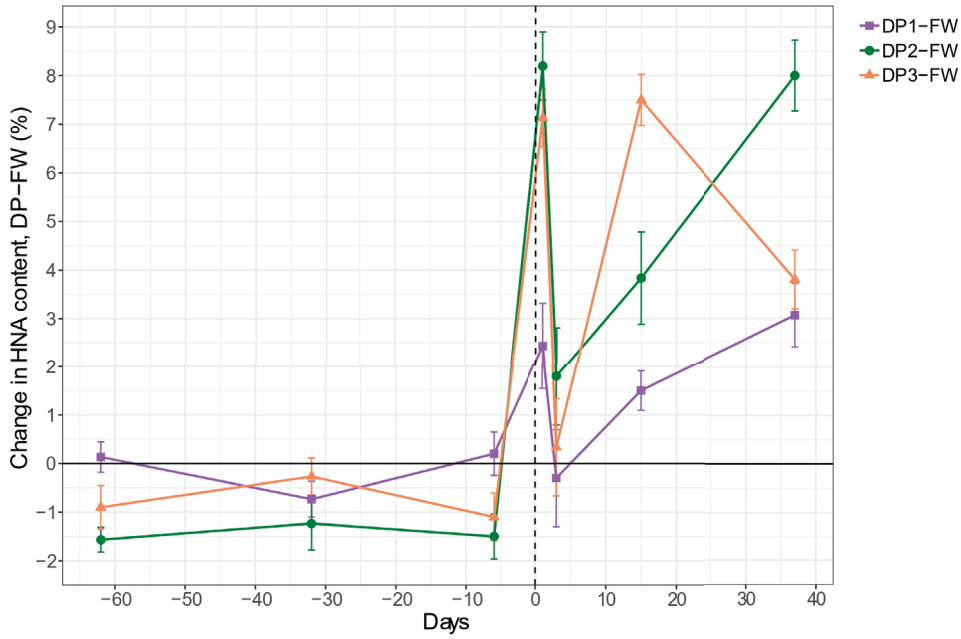

Supplementary Figure 1 – Changes in high nucleic acid (HNA) content bacteria showing an increase in % HNA in distributed water following installation of UF. For each sample, the %HNA in the finished water was subtracted from that measured at DP1 (purple line, squares), DP2 (green line, circles) and DP3 (orange line, triangles) in the distribution system, before and after the installation of UF. Day 0 on the x-axis corresponds to the start of UF (vertical dashed line). Error bars represent the variation in technical triplicates.

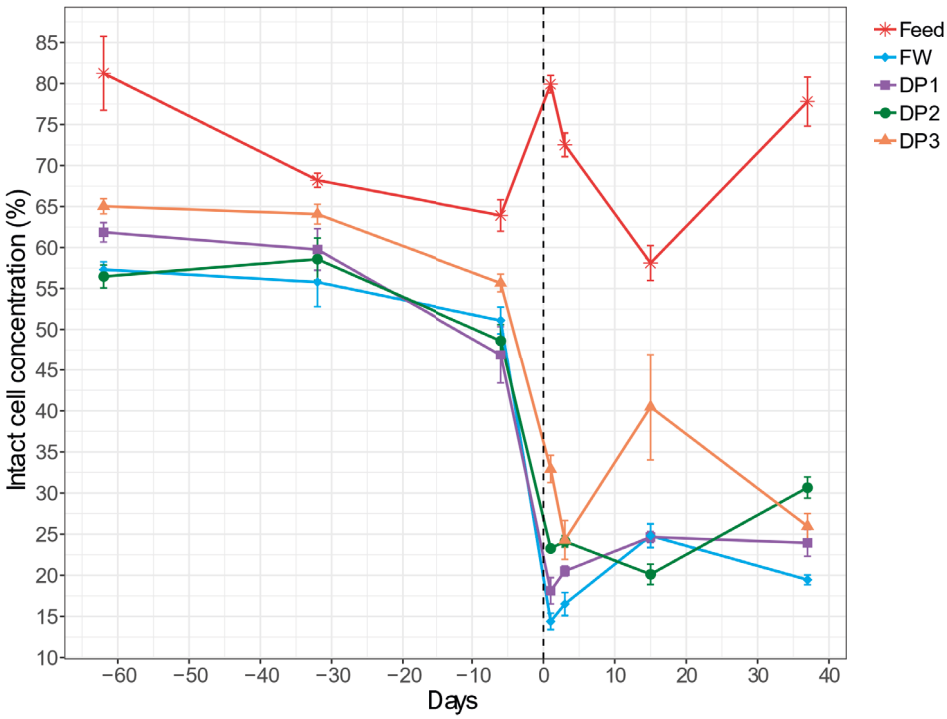

Supplementary Figure 2 – Intact cell concentration measured at the treatment plant for feed water to the UF (red line, stars), finished water (FW, blue line, diamonds), and at DP1 (purple line, squares), DP2 (green line, circles) and DP3 (orange line, triangles) in the distribution system, before and after the installation of UF. The days on the x-axis corresponds to a start of ultrafiltration at day 0 (vertical dashed line). Error bars represent the variation in technical triplicates.

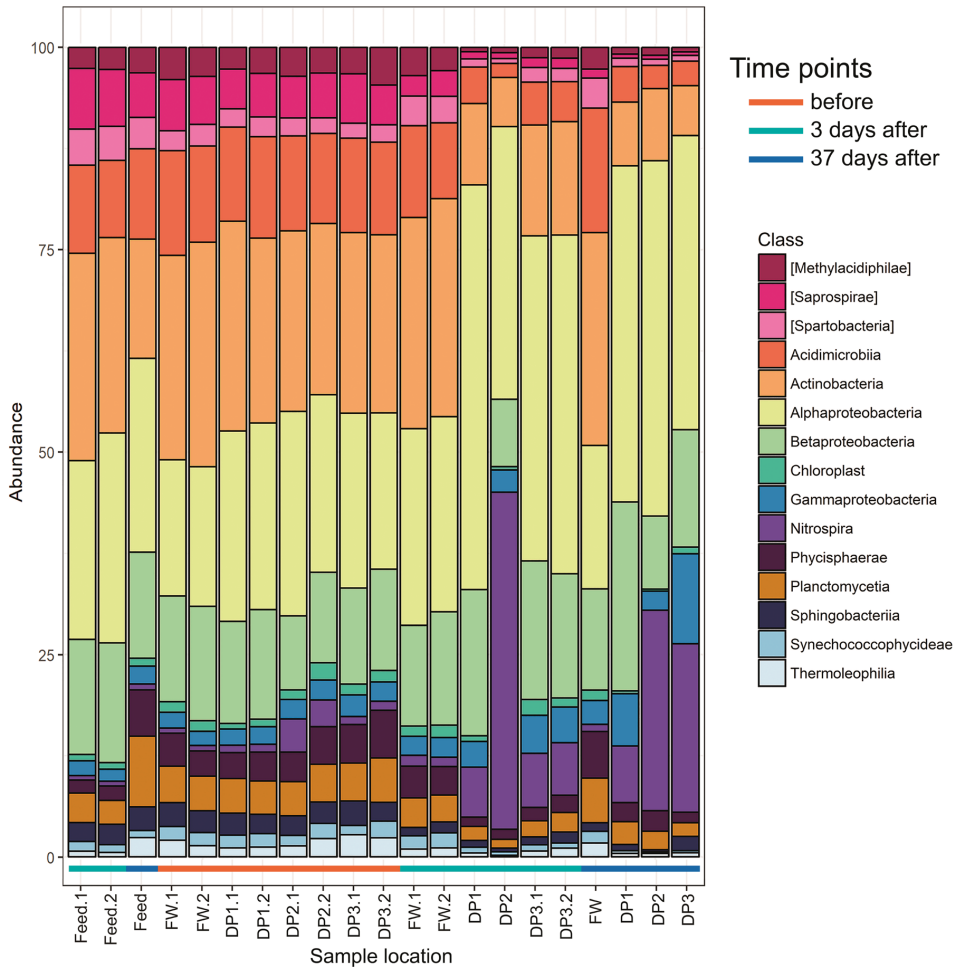

Supplementary Figure 3 – Relative abundance of bacteria in the different samples at the class level. Top 15 most relative abundant classes which contribute to at least 1 % of total reads across all the samples are presented. At each location, one sample was taken before the installation of ultrafiltration (orange line) and two were taken at three and 37 days after the installation (UF1, green line and UF2, blue line). Biological replicates are indicated by a number following the decimal, if included i.e. DP1.1 and DP1.2.

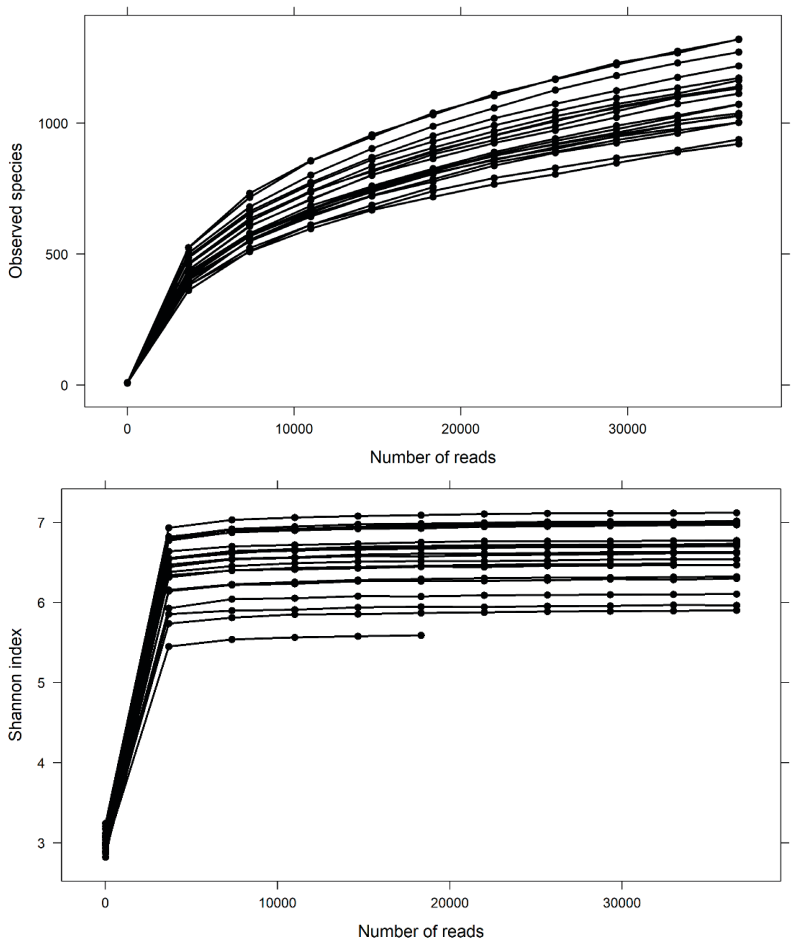

Supplementary Figure 4 – Rarefraction curves based on observed species (number of OTUs) (top) and Shannon index (bottom) for all the 21 samples.

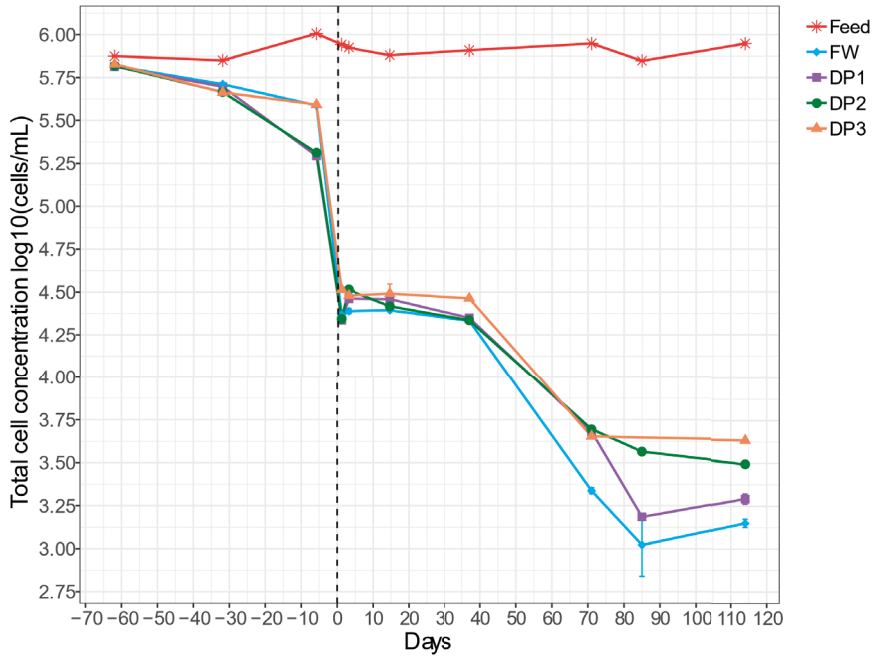

Supplementary Figure 5 – TCC of the distributed water samples before and after UF installation shows an initial drop between days 0 and 37, when feed water was still used for pH regulation, and a final lower plateau, when only UF-treated water was distributed (day 71-114). TCC is shown for feed water to the UF (red line, stars), finished water (FW, blue line, diamonds), and at DP1 (purple line, squares), DP2 (green line, circles) and DP3 (orange line, triangles). Day 0 on the x-axis corresponds to the start of the UF (vertical dashed line). Error bars represent the variation in technical triplicates.

Supplementary Information - Tables

Bacterial release from pipe biofilm in a full-scale drinking water distribution system

Sandy Chan[a,b,c], Kristjan Pullerits[a,b,c], Alexander Keucken[d,e], Kenneth M. Persson[b,c,d], Catherine J. Paul[a,d*], Peter Rådström[a]

[a]Applied Microbiology, Department of Chemistry, Lund University, P.O. Box 124, SE-221 00 Lund, Sweden

[b]Sweden Water Research AB, Ideon Science Park, Scheelevägen 15, SE-223 70 Lund, Sweden

[c]Sydvatten AB, Hyllie Stationstorg 21, SE-215 32 Malmö, Sweden

[d]Water Resources Engineering, Department of Building and Environmental Technology, Lund University, P.O. Box 118, SE-221 00 Lund, Sweden

[e] Vatten & Miljö i Väst AB, Box 110, 311 22 Falkenberg, Sweden

**corresponding author*

Table of Contents

Supplementary Table 1 – Output data from DESeq2 combined with the taxonomic annotation of the different OTUs.

Supplementary Table 2 – Conventional chemical and microbial water quality parameters

Supplementary Table 3 – Natural organic matter content

Supplementary Table 1 – Output data from DESeq2 combined with the taxonomic annotation of the different OTUs.

OTU	baseMean	log2FoldChange	pvalue	padj	Kingdom	Phylum	Class	Order	Family	Genus
807415	433.5328	9.4932781	1.43E-09	5.85E-09	Bacteria	Proteobacteria	Alphaproteobacteria	Rhodobacterales	Rhodobacteraceae	Rhodobacter
New.ReferenceOTU164	2076.0738	9.3259966	2.71E-06	9.38E-06	Bacteria	Proteobacteria	Alphaproteobacteria	*NA*	*NA*	*NA*
328951	1739.4879	8.9535161	2.00E-12	1.13E-11	Bacteria	Nitrospirae	Nitrospira	Nitrospirales	Nitrospiraceae	Nitrospira
264343	975.2421	8.8871578	1.15E-12	6.88E-12	Bacteria	Nitrospirae	Nitrospira	Nitrospirales	Nitrospiraceae	Nitrospira
554981	984.9402	8.8368927	1.32E-13	9.17E-13	Bacteria	Proteobacteria	Betaproteobacteria	*NA*	*NA*	*NA*
1143858	306.662	8.7966979	1.52E-10	7.21E-10	Bacteria	Cyanobacteria	4C0d-2	MLE1-12	*NA*	*NA*
New.ReferenceOTU371	230.3143	8.7659308	2.21E-18	2.49E-17	*NA*	*NA*	*NA*	*NA*	*NA*	*NA*
New.ReferenceOTU202	341.3616	8.7516688	1.17E-30	2.64E-29	Bacteria	Proteobacteria	Alphaproteobacteria	Rhizobiales	Hyphomicrobiaceae	Hyphomicrobium
570344	300.7408	8.5713684	6.28E-16	5.03E-15	Bacteria	Proteobacteria	Alphaproteobacteria	Rickettsiales	*NA*	*NA*
New.CleanUp.ReferenceOTU32754	189.374	8.5244266	2.90E-05	9.66E-05	Bacteria	Acidobacteria	Solibacteres	Solibacterales	*NA*	*NA*
1062748	598.0293	8.4899176	1.20E-10	6.01E-10	Bacteria	Actinobacteria	Actinobacteria	Actinomycetales	Mycobacteriaceae	Mycobacterium
4470200	2036.6014	8.4408388	1.71E-13	1.10E-12	Bacteria	Nitrospirae	Nitrospira	Nitrospirales	Nitrospiraceae	Nitrospira
233724	1664.9664	8.2719846	8.54E-21	1.28E-19	Bacteria	Proteobacteria	Alphaproteobacteria	Rickettsiales	*NA*	*NA*
New.ReferenceOTU24	404.3908	8.1076291	2.86E-11	1.51E-10	Bacteria	Nitrospirae	Nitrospira	Nitrospirales	Nitrospiraceae	Nitrospira
New.ReferenceOTU155	395.014	8.049085	1.68E-08	6.03E-08	Bacteria	Proteobacteria	Gammaproteobacteria	Legionellales	Coxiellaceae	*NA*
134302	1951.4365	7.9683312	6.70E-16	5.03E-15	Bacteria	Proteobacteria	Alphaproteobacteria	Rhizobiales	Hyphomicrobiaceae	Hyphomicrobium
109789	4244.9859	7.9368478	6.56E-10	2.81E-09	Bacteria	Nitrospirae	Nitrospira	Nitrospirales	Nitrospiraceae	Nitrospira
568617	388.9368	7.9347294	1.08E-08	4.05E-08	Bacteria	Proteobacteria	Alphaproteobacteria	Rhodospirillales	Rhodospirillaceae	*NA*
812978	274.1116	7.7282295	2.80E-09	1.09E-08	Bacteria	Proteobacteria	Alphaproteobacteria	Rhizobiales	*NA*	*NA*
New.ReferenceOTU480	163.8361	7.3352637	1.53E-03	4.76E-03	Bacteria	Proteobacteria	Betaproteobacteria	Burkholderiales	Oxalobacteraceae	*NA*
564600	503.6496	7.3197144	1.20E-37	3.59E-36	Bacteria	Proteobacteria	Alphaproteobacteria	Rhizobiales	Hyphomicrobiaceae	Hyphomicrobium
564309	646.4925	6.5569246	1.02E-24	1.83E-23	Bacteria	Proteobacteria	Alphaproteobacteria	Rickettsiales	Rickettsiaceae	*NA*
1108960	4063.7182	6.1449385	1.56E-67	7.00E-66	Bacteria	Proteobacteria	Alphaproteobacteria	Sphingomonadales	Sphingomonadaceae	Sphingomonas
1003206	2011.4925	5.9889776	3.98E-83	3.58E-81	Bacteria	Proteobacteria	Alphaproteobacteria	Sphingomonadales	Sphingomonadaceae	Sphingomonas
37092	261.3607	5.5880807	1.76E-10	7.91E-10	Bacteria	Proteobacteria	Alphaproteobacteria	Sphingomonadales	Sphingomonadaceae	Novosphingobium
692284	1317.3855	5.5199871	2.84E-18	2.84E-17	Bacteria	Proteobacteria	Betaproteobacteria	Nitrosomonadales	Nitrosomonadaceae	*NA*
112204	688.4011	5.3544386	7.60E-18	6.84E-17	Bacteria	Proteobacteria	Betaproteobacteria	Nitrosomonadales	Nitrosomonadaceae	*NA*
New.ReferenceOTU205	1093.1424	5.2954801	1.22E-18	1.57E-17	Bacteria	Proteobacteria	Betaproteobacteria	Nitrosomonadales	Nitrosomonadaceae	*NA*

321513	232.0724	0.9203116	1.32E-03	4.23E-03	Bacteria	Nitrospirae	Nitrospira	Nitrospirales	Nitrospiraceae	Nitrospira
New.ReferenceOTU167	114.5191	-0.471999	1.88E-03	5.63E-03	Bacteria	Proteobacteria	Betaproteobacteria	Burkholderiales	Comamonadaceae	Limnohabitans

Supplementary Table 2 – Conventional chemical and microbial water quality parameters measured before (day -6) and after (day 3 and day 37) the installation of UF. Samples were taken from the different sampling points in the drinking water treatment plant (feed and finished water) and distribution system (DP1, DP2 and DP3).

Sampling day	**-6**					**3**					**37**				
Sampling point	**Feed**	**Finished water**	**DP1**	**DP2**	**DP3**	**Feed**	**Finished water**	**DP1**	**DP2**	**DP3**	**Feed**	**Finished water**	**DP1**	**DP2**	**DP3**
Alkalinity (mg HCO_3/L)	22	56	55	55	54	19	58	61	62	61	20	61	61	61	61
Aluminium (mg/L)	0.014	0.014	0.017	0.016	0.018	0.016	0.029	0.029	0.031	0.029	0.017	0.024	0.023	0.024	0.025
Ammonium (mg/L)	0.005	0.062	0.035	0.033	0.026	0.005	0.049	0.027	0.023	0.03	0.005	0.058	0.027	0.042	0.022
Ammonium-nitrogen (mg/L)	0.005	0.048	0.027	0.026	0.02	0.005	0.038	0.021	0.018	0.023	0.005	0.045	0.021	0.033	0.017
COD-Mn (mg O_2/L)	2.3	2.1	2.1	2.1	2.1	1.9	1.2	1.2	1.3	1.2	2.3	1.3	1.3	1.3	1.4
DOC (mg/L)	2.8	2.5	2.4	2.5	2.7	2.8	1	1	1	1	2.5	1	1	1	1
***Escherichia coli* (CFU/100 mL)**	0.5	0.5	0.5	0.5	0.5	0.5	0.5	0.5	0.5	0.5	0.5	0.5	0.5	0.5	0.5
Phosphorus (mg/L)	0.0025	0.0025	0.0062	0.0058	0.0025	0.0025	0.0025	0.0025	0.0077	0.0025	0.0025	0.0025	0.0025	0.0025	0.0025
Color 410 nm (mg Pt/L)	13	11	9.5	8.7	12	11	2.5	2.5	2.5	2.5	11	2.5	2.5	2.5	2.5
Iron (mg/L)	0.01	0.01	0.01	0.01	0.01	0.029	0.01	0.01	0.01	0.01	0.021	0.01	0.01	0.01	0.01
Calcium (mg/L)	8.2	19	20	20	19	7.5	21	21	21	21	7.6	21	22	21	22
Coliforms (CFU/100 mL)	0.5	0.5	0.5	0.5	0.5	0.5	0.5	0.5	0.5	0.5	0.5	0.5	0.5	0.5	0.5
Conductivity (mS/m)	11	16	16	16	16	11	17	17	17	17	11	17	17	17	17
Copper (mg/L)	0.01	0.01	0.01	0.01	0.01	0.01	0.01	0.01	0.026	0.01	0.01	0.01	0.01	0.026	0.01
Heterotrophic bacteria 7 days (CFU/mL)	17	0.5	0.5	5	6	29	0.5	1	3	22	18	0.5	0.5	3	3
Magnesium (mg/L)	2.3	2.4	2.5	2.4	2.4	2.2	2.2	2.2	2.2	2.1	2.4	2.4	2.4	2.3	2.3
Manganese (mg/L)	0.06	0.059	0.056	0.053	0.05	0.034	0.033	0.033	0.033	0.029	0.014	0.013	0.013	0.012	0.012
Nitrate (mg/L)	1.5				1.5	1.5	1.9	1.9	1.4	1.3	1.5	1.4	1.4	1.5	1.4
Nitrite (mg/L)	0.035	0.0035	0.069	0.046	0.079	0.035	0.0035	0.059	0.03	0.056	0.035	0.0035	0.069	0.036	0.072
Heterotrophic bacteria 3 days (CFU/mL)	13	0.5	0.5	0.5	2	10	0.5	0.5	0.5	0.5	8	0.5	0.5	0.5	0.5
pH	7.5	8	8.2	8.1	8	7.3	8	8.1	8	8	7.3	8.1	8.2	8.1	8
TOC (mg/L)	2.9	2.7	2.7	2.7	2.7	2.8	2	2.1	2.1	2	2.7	1	1	1	1
Hardness (°dH)	1.7	3.1	3.3	3.3	3.2	1.6	3.4	3.5	3.4	3.4	1.6	3.5	3.6	3.5	3.6
Turbidity (FNU)	0.21	0.05	0.29	0.3	0.2	0.22	0.14	0.48	0.19	0.19	0.23	0.05	0.05	0.05	0.11
Temperture (°C)	6.9	6.7	7.4	9	8.2	6.2	6.3	7.2	8.7	7.3	5.7	5.7	6.8	8.2	6.7

Supplementary Table 3 – Natural organic matter content before (day -6) and after (day 3 and day 37) the installation of UF for the different sampling points in the drinking water treatment plant (feed and finished water) and distribution system (DP1, DP2 and DP3).

Sampling day	**-6**					**3**					**37**				
Sampling point	**Feed**	**Finished water**	**DP1**	**DP2**	**DP3**	**Feed**	**Finished water**	**DP1**	**DP2**	**DP3**	**Feed**	**Finished water**	**DP1**	**DP2**	**DP3**
DOC (Dissolved OC) (ppb-C)	2442	2308	2312	2321	2360	2445	1817	1871	1826	1821	2391	1674	1600	1608	1611
HOC (Hydrophobic OC) (ppb-C)	n.q.	n.q.	71	n.q.	38	n.q.	126	101	88	25	n.q.	81	n.q.	14	14
Inorganic colloids (m^{-1})	n.q.	n.q.	n.q.	n.q.	n.q.	n.q.	n.q.	n.q.	n.q.	n.q.	n.q.	n.q.	n.q.	n.q.	0.03
SUVA (L/mg*m)	3.15	2.99	3.1	3.24	3.08	3.29	2.39	2.4	2.55	2.66	3.34	2.44	2.45	2.34	2.52
CDOC (Chromatographic DOC) (ppb-C)	2442	2308	2241	2321	2322	2445	1690	1770	1738	1796	2391	1593	1600	1595	1598
Biopolymers (ppb-C)	65	45	27	38	39	65	24	34	30	30	57	31	35	29	25
Dissolved organic nitrogen (DON) (ppb-N)	7	5	4	5	4	6	n.q.	n.q.	4	5	6	4	4	n.q.	n.q.
N/C ratio (µg/µg)	0.1	0.11	0.14	0.14	0.11	0.09	-	-	0.12	0.15	0.11	0.12	0.1	-	-
% proteins (% of biopolymer)	31	33	41	41	33	27	-	-	36	45	34	35	31	-	-
Humic substances (ppb-C)	1487	1472	1421	1466	1475	1564	957	970	956	983	1562	935	946	942	954
Dissolved organic nitrogen (DON) (ppb-N)	31	32	32	32	32	31	21	22	23	22	32	20	21	19	20
N/C ratio (µg/µg)	0.02	0.02	0.02	0.02	0.02	0.02	0.02	0.02	0.02	0.02	0.02	0.02	0.02	0.02	0.02
Aromaticity (L/mg*m)	3.71	3.5	3.64	3.56	3.56	3.89	3.02	2.99	3.04	2.87	4.11	2.39	2.4	2.42	2.43
Molecular weight (g/mol)	647	566	640	581	601	606	523	525	522	524	685	476	477	482	478
Building blocks (ppb-C)	509	422	478	445	456	448	425	442	433	442	431	340	336	332	340
LMW Neutrals (ppb-C)	509	355	292	352	332	350	276	312	304	330	309	288	283	292	278
LMW Acids (ppb-C)	24	13	24	20	19	18	8	12	15	11	32	0	n.q.	n.q.	0

n.q. = not quantifiable (< 1 ppb;signal to noise ratio)

Paper V

water

MDPI

Article

Mapping Dynamics of Bacterial Communities in a Full-Scale Drinking Water Distribution System Using Flow Cytometry

Caroline Schleich [1], Sandy Chan [2,3,4], Kristjan Pullerits [2,3,4], Michael D. Besmer [5], Catherine J. Paul [2,6], Peter Rådström [2] and Alexander Keucken [1,6,*]

1 Vatten & Miljö i Väst AB, SE-311 22 Falkenberg, Sweden; Caroline.Schleich@vivab.info
2 Applied Microbiology, Department of Chemistry, Lund University, P.O. Box 124, SE-221 00 Lund, Sweden; Sandy.Chan@sydvatten.se (S.C.); kristjan.pullerits@tmb.lth.se (K.P.); catherine.paul@tvrl.lth.se (C.J.P.); peter.radstrom@tmb.lth.se (P.R.)
3 Sweden Water Research AB, Ideon Science Park, Scheelevägen 15, SE-223 70 Lund, Sweden
4 Sydvatten AB, Hyllie Stationstorg 21, SE-215 32 Malmö, Sweden
5 onCyt Microbiology AG, CH-8038 Zürich, Switzerland; michael.besmer@oncyt.com
6 Water Resources Engineering, Department of Building and Environmental Engineering, Faculty of Engineering, Lund University, P.O. Box 118, SE-221 00 Lund, Sweden
* Correspondence: alexander.keucken@vivab.info

Received: 9 September 2019; Accepted: 11 October 2019; Published: 15 October 2019

Abstract: Microbial monitoring of drinking water is required to guarantee high quality water and to mitigate health hazards. Flow cytometry (FCM) is a fast and robust method that determines bacterial concentrations in liquids. In this study, FCM was applied to monitor the dynamics of the bacterial communities over one year in a full-scale drinking water distribution system (DWDS), following implementation of ultrafiltration (UF) combined with coagulation at the drinking water treatment plant (DWTP). Correlations between the environmental conditions in the DWDS and microbial regrowth were observed, including increases in total cell counts with increasing retention time (correlation coefficient $R = 0.89$) and increasing water temperature (up to 5.24-fold increase in cell counts during summer). Temporal and spatial biofilm dynamics affecting the water within the DWDS were also observed, such as changes in the percentage of high nucleic acid bacteria with increasing retention time (correlation coefficient $R = -0.79$). FCM baselines were defined for specific areas in the DWDS to support future management strategies in this DWDS, including a gradual reduction of chloramine.

Keywords: flow cytometry; biofilm; drinking water distribution system; ultrafiltration; coagulation; drinking water management

1. Introduction

Drinking water needs to be safe, esthetically acceptable, and not cause excessive damage to infrastructure. These aspects of water quality are impacted by microorganisms, the majority of which are bacteria that originate from the source water, are shaped by processes in the drinking water treatment plant (DWTP), and are contributed from biofilms in the drinking water distribution system (DWDS) during distribution [1–4]. A high bacterial cell concentration can lead to: Esthetic problems, such as discoloration of the water and/or changes in taste and odor; increased biocorrosion with concomitant high copper and iron concentrations in the water; and thus deterioration of the DWDS [5–7]. Growth of opportunistic pathogens such as *Legionella ssp*. in the drinking water can pose a severe health risk [8,9]. To counter these risks, the DWTP should control bacterial survival

and regrowth in the DWDS, using methods like filtration, which limits the input of nutrients, and disinfection, using UV irradiation and chlorination [4,10,11]. Some bacteria, however, often remain in the drinking water after these and other treatments, and enter the DWDS [12]. The estimated bacterial concentration in most distributed drinking water is between 10^6 to 10^8 cells/L [13,14]. While these high bacterial counts are generally considered to have no direct impact on public health [9], abrupt changes in bacterial concentrations can indicate failure of disinfection or filtration, or pipe breakage, that could indicate occurrences in the treatment process or external contamination in the DWDS that could indirectly impact the consumer [7]. Detecting any sudden changes, however, requires an understanding of which bacterial counts are expected, with this knowledge generated by comprehensive monitoring of the bacterial community in a DWDS.

Conventional bacterial monitoring of process performance is largely based on enumeration of indicator bacteria, such as *Escherichia coli*, coliforms and heterotrophs in grab samples of water [15]. These methods are labor- and resource-intensive and thus expensive. In addition, these methods detect only specific fractions of the bacterial community [16], limiting their resolution for detailed studies of bacterial regrowth in a DWDS [7]. Flow cytometry (FCM) has been proposed as a modern, rapid, standardized, and increasingly used alternative detection method for bacteria in drinking water [13,17]. This laser-based method rapidly, accurately, and reproducibly determines the concentration of bacteria in a water sample [18,19], and can also be used to measure the number of intact cells within the total population to assess the effectiveness of some treatments, such as chlorination [20]. Changes in the type of bacteria within the community are assessed by observing fluctuations in the distribution of DNA within the cells; for example, by comparing the distribution of cells across populations defined by the user (gates), such as high nucleic acid (HNA) bacteria and low nucleic acid (LNA) bacteria [14].

While there is broad consensus regarding typical values from source to tap for FCM-based bacterial concentrations in drinking water, specific baselines and the range of fluctuations around these baselines that are consistent with safe water need to be established for each DWDS individually. This requires large data sets collected from the drinking water treatment and distribution systems of interest. These need to define routine values, to describe proper functioning of the whole system, and identify how, and to what degree, fluctuations in these values reflect abnormalities and can describe the success of corrective actions. Baselines generated by permanent surveillance of routine operations may also be valuable for planning and monitoring changes in the treatment or distribution of water.

In this study, the process of establishing FCM baselines for a drinking water treatment and distribution system is described. Historically, Kvarnagården DWTP in Varberg, Sweden had limited treatment of surface water and very high cell concentrations (7×10^5 cells/mL) of bacteria in the DWDS. In November 2016, the DWTP was upgraded to ultrafiltration (UF) membranes, combined with flocculation, reducing the input of bacterial cells into the DWDS and removing about 50% of natural, especially high molecular weight, organic carbon [2,21]. This upgrade was closely monitored with FCM and showed that bacterial concentrations in treated and distributed water were substantially lowered by the change in treatment processes [2]. With extremely low numbers of bacteria contributed by the treatment plant, the contribution of cells from biofilms in the DWDS to the total bacterial concentrations was observed, and the low bacterial concentrations at several monitoring locations in the DWDS indicated that concerns about an initial massive detachment of biofilm due to the changes in treatment were unwarranted [1,2].

To further monitor the biofilm over a longer time period, and to expand the application of FCM monitoring in this DWDS, additional sampling locations at greater distances and incorporation of different hydrodynamic and material properties in the DWDS were examined. The extensive sampling campaign of the selected sampling points was conducted over 12 months.

The objectives of this study were to:

(1) Confirm that the biofilm did not detach in the long-term.

(2) Assess the impact of seasonal changes on cell concentrations.

(3) Obtain detailed, spatially resolved information throughout the DWDS.

(4) Gather insights on driving environmental and/or technical factors of cell concentrations.

2. Materials and Methods

2.1. Study Site and Sampling

The study location, a DWDS in Varberg, Sweden operated by the utility VIVAB, is comprised of roughly 580 km of pipes, of which the majority are polyvinyl chloride (35%) and polyethylene (20%). This DWDS distributes approximately 5 million m^3 water annually to 60,000 residents, and is produced from surface water by the DWTP Kvarnagården. The treatment process consists of rapid sand filtration, UF combined with a coagulation step, pH adjustment, and disinfection with UV and chloramine (between 0.13 and 0.21 mg/L; Supplementary Materials Figure S1). Eighteen different locations were sampled from April 2018 to April 2019, beginning approximately one and a half years after the installation of the UF membrane at the DWTP in November 2016. This included the UF membrane treatment process (feed water, permeate) and the outgoing water from the DWTP with 15 points located in the DWDS (Supplementary Materials Figure S2). In total, 510 samples were taken and analyzed at two-week sampling intervals, with weekly sampling during July and September and no sampling during August. All water samples were collected in sterile 15 mL Falcon tubes with the addition of 1% (*v*/*v*) sodium thiosulphate (20 g/L) for quenching residual chlorine. The sampling routine included burning off the tap and flushing the line for 10 min before sampling and recording of water temperature. Samples were transported in cooling boxes and analyzed by FCM the same day.

2.2. FCM Analysis

FCM analysis was performed on a BD Accuri C6 Flow Cytometer (BD Biosciences, Belgium) with a 50 mW argon laser, wavelength = 488 nm [22]. Fluorescence from SYBR® Green I (Invitrogen AG, Switzerland) and propidium iodide were read at 533 ± 30 nm = FL1 (green fluorescence) and > 670 nm = FL3 (red fluorescence), respectively. The flow rate was 35 µL/min with a threshold of 500 arbitrary units of green fluorescence. Samples were stained with 5 µL of SYBR Green I at 100× diluted with dimethyl sulphoxide in a total volume of 500 µL corresponding to 1 × SYBR Green I final concentration and incubated in the dark for 15 min at +37 °C. When included, the concentration of propidium iodide was 0.3 mM (Sigma-Aldrich, Germany). Identical gates were applied for both types of staining (intact cell count (ICC) and total cell count (TCC)).

2.3. Other Water Quality Parameters

Total chlorine was analyzed using a SL1000 Portable Parallel Analyzer (Hach, Düsseldorf, Germany). Water temperature was measured with a TD 10 Thermometer (VWR, Radnor, PA, United States). TOCeq was measured online using a s::can (i::scan™; s::can Messtechnik GmbH, Vienna, Austria) with wavelength range 230–350 nm. The online absorbance measurements were calibrated against laboratory TOC analyses from the laboratory to calculate TOCeq.

2.4. Data Analysis

For FCM, manual gating strategies and a pattern analysis approach were applied. FCM fingerprints, including ratios of LNA and HNA bacteria, were compared and analyzed using the single cell analysis software FlowJo (Treestar, Inc., San Carlos, CA, USA). CHIC analysis (CHIC: Cytometric Histogram Image Comparison) was used for pattern analyses using R packages flowCHIC and flowCore [23–25]. FCM scatterplots were converted into 300 × 300 pixel images with 64-channel gray scale resolution for image comparison. The values generated by CHIC describing the differences between water samples were visualized using a non-metric multidimensional scale (NMDS) plot based on Bray–Curtis dissimilarity to capture changes in bacterial community structure [23,24]. To simplify correlations, the *envfit* function for environmental vectors was applied using R software [26].

The contact area between water and biofilm was determined by calculating the ratio between lateral surface and water volume for each pipe segment (Equation (1)).

$$\text{Contact area} = \frac{2\Pi rh}{\Pi r2\ h} \quad (1)$$

Hydraulic modeling using MIKE Urban (DHI) was applied to determine specific retention times for different pressure zones in the DWDS.

3. Results and Discussion

3.1. Long-Term Stability After an Upgrade of the Treatment Process

The implementation of UF combined with coagulation at the DWTP Kvarnagården in Varberg led to a significant change in water quality [2,27]. TCC was reduced by a factor of 10^3 cells/mL and about 50% of natural organic carbon, especially the high molecular weight fraction was removed by direct coagulation over the UF membranes (Figure 1). Before the changes in the treatment process, the number of bacteria in the water was approximately 660,000 ± 7000 cells/mL regardless of sampling site and time. After installation of the new process, TCC diminished to about 27,500 ± 9600 cells/mL at all sampling points, reaching a low of 3400 ± 2000 cells/mL in February 2017. TCC in the outgoing drinking water continued to decrease to about 350 ± 170 cells/mL in March 2018, giving a 1000-fold reduction of TCC in produced drinking water due to installation of UF. TCC determined for an expanded number of DWDS sampling points from April 2018 until April 2019 showed consistent and expected cell counts at all sampling points, subject to seasonal variations, and no large, rapid changes in TCC in the water phase that could indicate detachment of biofilm [20].

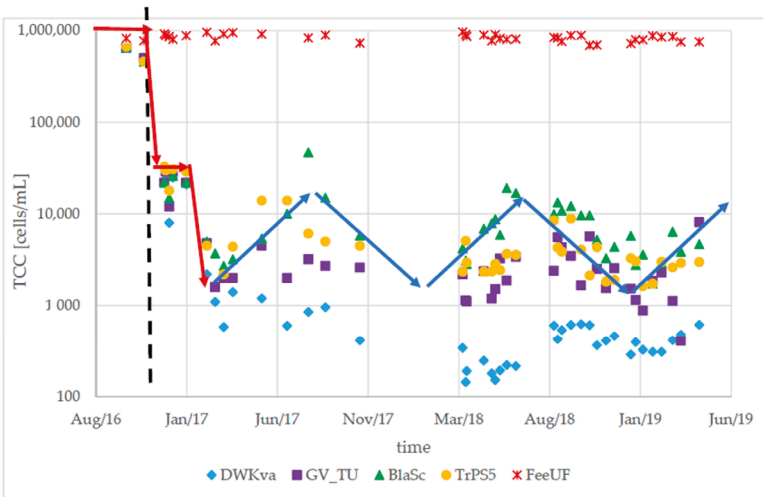

Figure 1. Total cell count (TCC) in water from the drinking water treatment plant (DWTP) and drinking water distribution system (DWDS). TCC was measured in the feed water to the ultrafiltration (UF) membrane (FeeUF, red stars); outgoing drinking water (DWKva, blue diamonds); and distributed water at an office building located at WWTP Getteröverket (GV_TU, purple squares), a public school in Bläshammar (BlaSc, green triangles), and a pump station in Trönningenäs (TrPS5, yellow circles). Measurements were taken before and after the installation of UF, indicated by the vertical dashed line. The red arrows show changes of TCC before, during, and shortly after commissioning of UF; blue arrows indicate seasonal changes in TCC. The graph includes published data (until January 2017, [2]).

3.2. Seasonal Changes in the Bacteral Community

The extended sampling program took place from April 2018 to April 2019 (Supplementary Materials Figure S2). Water temperatures increased at all sampling points during the summer, as expected, from 6.68 ± 1.28 °C in April 2018 to 13.68 ± 2.83 °C in September 2018, an increase of 6.99 ± 2.30 °C (Supplementary Materials Figure S3).

The average TCC during April 2018, considering all DWDS sampling points, was $3.1 \times 10^4 \pm 3.6 \times 10^4$ (range: 3×10^2 to 1.1×10^5 cells/mL). This increased in summer to an average TCC of 1.0×10^5 cells/mL (range: 5×10^2 to 4×10^5 cells/mL), an average 3.35-fold increase (range: 1.51–5.24-fold increase; Supplementary Materials Figure S3). This may be partially explained by regrowth of bacteria due to the elevated water temperatures during summer.

To demonstrate the observed seasonal shifts, values obtained from water collected at sampling point Masar showed TCC fluctuating with changes in water temperature with an increase of TCC during the summer months (Figure 2). The TCC in the outgoing water from the DWTP also increased during this period, from 230 ± 70 cells/mL in April to 540 ± 80 cells/mL in September (temperature increase from 5.8 to 7.5 °C). At Masar, the TCC was 24,400 ± 330 cells/mL in April with a water temperature of 6.3 °C. The water temperature at this sampling point increased to 14.9 °C and TCC increased by 4-fold to 98,300 ± 1200 cells/mL. By April 2019, TCC had returned to 23,350 ± 300 cells/mL with a water temperature of 6.2 °C, showing a clear seasonal trend. The ratio of intact bacteria in the water at Masar also fluctuated seasonally, from 69 ± 1% intact cells in April to 86 ± 2% in September, with an increase in intact cells supporting the observation that increases in TCC during these months are due to bacterial growth.

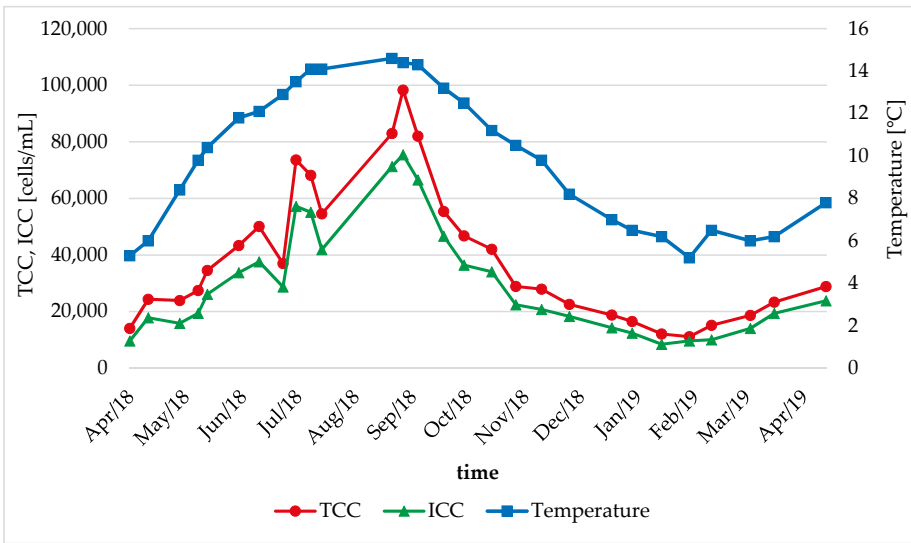

Figure 2. Changes in TCC (red line, circles), intact cell count (ICC) (green line, triangles), and water temperature (blue line; squares) at sampling point Masar. A clear seasonal trend, with increases in TCC and water temperature during the summer period, is shown.

The bacterial community, indicated by nucleic acid content described by FCM, also changed with season. The bacterial population gradually shifted to greater numbers of bacteria described as LNA during the summer months (Figure 3). Analyses from later months indicated a return of the bacterial community to a previous state (both in TCC and community structure, data not shown). A study from 2014 showed equal temporal trends in the microbial community that indicate annual

reproducibility [28]. The histograms shown in Figure 3 represent individual FCM fingerprints of microbial communities. The amount of DNA in a single bacteria cell is described by its position along the x-axis. Cells registering with higher green fluorescence contain increasing amounts of DNA [22].

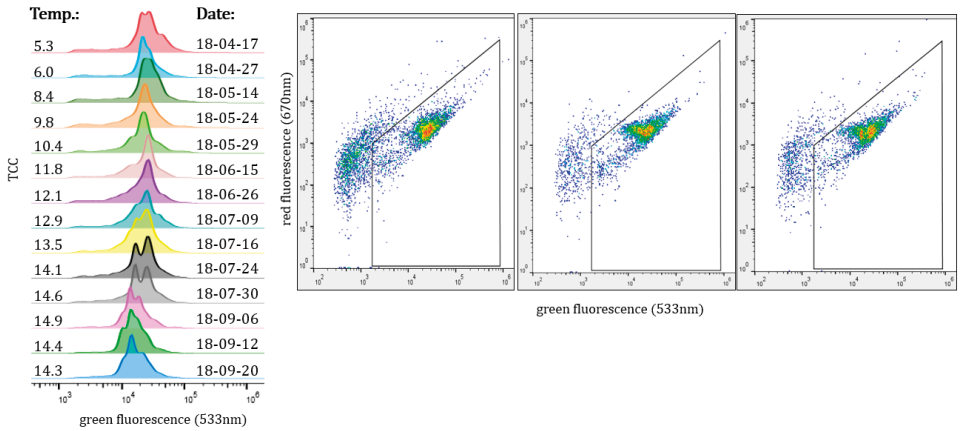

Figure 3. Changes in the bacterial community over season at Masar. FCM fingerprints (left panel) from sampling in April 2018 to September 2018 show a shift to increasing proportions of low nucleic acid (LNA) bacteria, likely due to an increase in water temperature during summer. Scatterplots (right panel) show individual cells within the population, the gate applied, and a gradual increase in intensity corresponding to more cells with LNA (sampling date for left to right: 27/04/18; 16/07/18; 24/07/18).

As expected, more bacterial growth (regrowth) was observed when the temperature in the water rose. Increasing TCC and temperature were also observed at Tofta, Tronn, and BlaSc, with 7000 ± 6200 cells/mL and water temperature: 7.2 ± 1.4 °C during spring, rising to 34,300 ± 28,000 cells/mL and water temperature: 15.5 ± 2.1 °C during summer (5.16 ± 0.89-fold increase in TCC; Supplementary Materials Figure S3). Seasonal changes for bacterial communities in DWDS have been observed in previous studies, and indicate reproducible annual patterns [28–30]. However, in the current study, some sampling points did not show this expected trend. Water from Hunst, Himle, Godst, and Lofta had a high TCC during spring (Supplementary Materials Figures S3 and S5) and an increase in water temperature had only a moderate impact on the TCC. TCC at these points increased from 55,400 ± 14,700 cells/mL (water temperature: 7.2 ± 0.3 °C) during spring to 156,200 ± 38,600 cells/mL (water temperature: 15.8 ± 0.8 °C) during summer, giving only a 2.84 ± 0.13-fold increase associated with the warmer water temperatures. Water from sampling point TrPS5, despite having an increase in water temperature of 7.1 °C (from 5.6 to 12.7 °C), increased TCC by only a factor of 1.79 (from 2900 ± 70 to 5200 ± 100 cells/mL; Supplementary Materials Figure S6). The apparent decoupling between temperature and TCC at this specific sampling location maybe be due to a combination of the low retention time and the short distance between the sampling point and the DWTP, which together would prevent significant accumulation of bacteria, either from regrowth or cells leaving the biofilm, to the water [2].

3.3. Detection of Abnormalities Within the DWDS Using TCC Baselines

Baselines were defined for each water sampling point in the study by grouping months with similar TCC values (standard deviation ≤25%) and then calculating average TCC values for those periods. Warning and alarm limits were determined to describe tailored acceptable TCC values for each sampling point and period. Applications of these defined baselines detected an abnormality within the DWDS in late June 2019. During routine sampling, the TCC at sampling point TrPS5 was 717,000 cells/mL, exceeding the alarm limit of 15,000 cells/mL for this location (Supplementary

Materials Figure S7). Consultations with the personnel responsible for the DWDS revealed that maintenance work had occurred near TrPS5 in March 2019 and further investigation discovered that a valve near this sampling point had been accidentally closed. This resulted in insufficient circulation of the water, and possibly bacterial regrowth due to stagnation, and provided a likely explanation for the increased TCC [14]. The TCC returned to normal after the opening of the valve. While the most likely explanation for the increase in TCC is bacterial growth, additional explanations could include increased detachment of biofilm due to altered fluid dynamics in the pipe [31] or increased contact time of the stagnant water with the biofilm [32].

3.4. Relationship of the Bacterial Population to Contact Time with Biofilm

Possible correlations between TCC, %HNA, %ICC, and characteristics of the DWDS were evaluated using CHIC in combination with the *envfit* function (Figure 4). CHIC analysis compares individual FCM scatterplots describing the bacterial community in water samples. The comparisons are presented as a non-metric multidimensional scale (NMDS) plot, with water samples containing similar bacterial content shown as two dots that are close to each other, and water samples with more dissimilar bacterial content in the water placed further away from each other. This enables a visual determination of changes in the different bacterial communities, with the content of all water samples in one study presented in the same plot. The addition of vector analysis enables visualization of correlations between the bacterial communities, as determined by FCM, and environmental parameters. Longer vectors indicate stronger correlations, and those pointing in opposite directions indicate negative correlations.

Correlations between TCC and retention time, and TCC and the contact area between biofilm and the water, were determined using three data sets for each sampling point (Supplementary Materials Table S1). TCC increased with increasing retention time, as well and increasing contact area (Figure 4A). There was a negative correlation between retention time and %HNA bacteria. The amount of HNA bacteria in the water samples decreased with an increase in retention time. These results were confirmed by a more detailed examination using a subset of samples selected from the range of 0–50 in the NMDS in Figure 4A. This reduced the influence from outliers, such as samples with, for example, a high retention time (Figure 4B). When fewer samples were included in the analysis, the relationship between the correlations of %HNA and retention time shifted slightly (Figure 4B). However, more precise analyses are necessary to confirm these assumptions.

The sampling points are connected to the DWTP by 87.7 km pipes consisting of 6 different pipe materials with a total pipe surface area of 79,900 m^2. Water from sampling points at a greater distance from the DWTP usually had a higher TCC than water sampled closer to the DWTP (Supplementary Materials Figure S3). During April 2018, water leaving the DWTP contained 230 ± 70 cells/mL; water from close to the DWTP (GV_TU, BlaSc) contained 2250 ± 990 cells/mL and a more distant sampling point (Björk) had water containing 113,200 ± 4100 cells/mL. One explanation for the increased cell counts with respect to distance was the increased contact time between the water and the pipe surface biofilm [2]. The contact area between the water and biofilm was then determined by incorporating both pipe lengths and diameters to examine the relationship between TCC and the contact area/mL (Figure 5). This identified a positive correlation between the number of cells in the water and the contact area provided by the pipe biofilm (correlation coefficient $R = 0.75$; $p = 0.0008$).

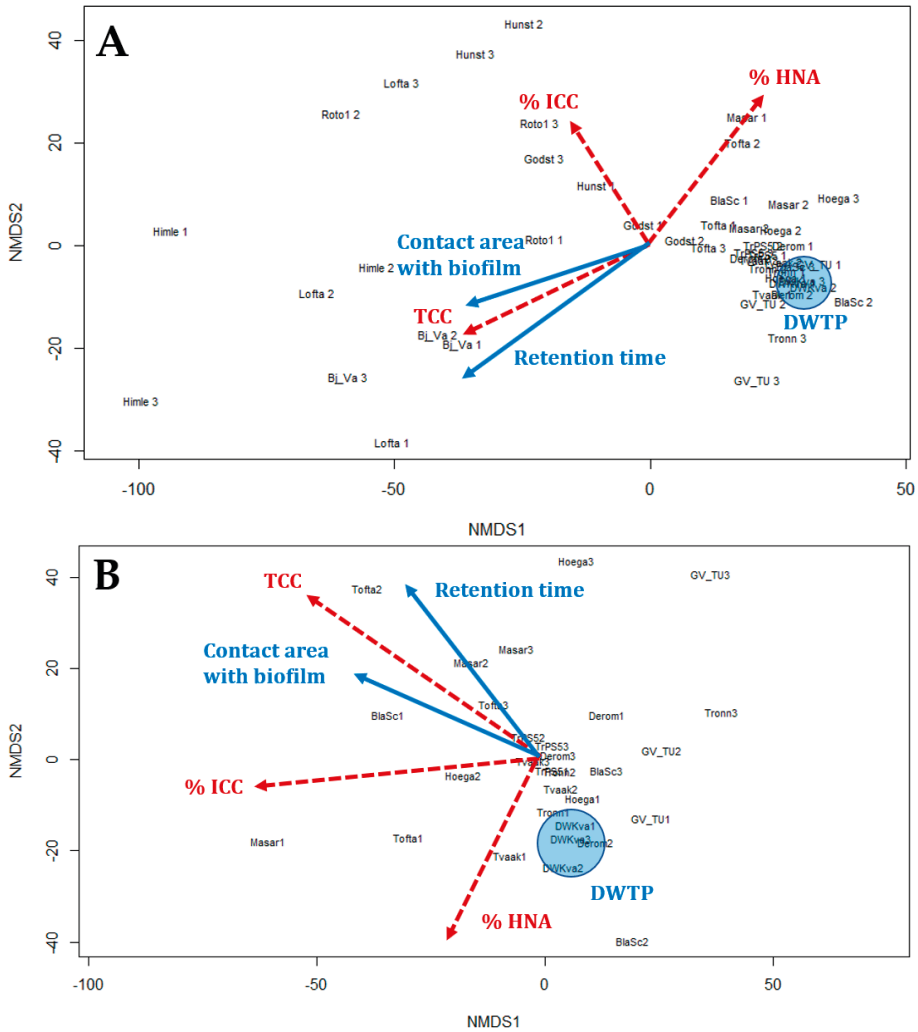

Figure 4. Output from CHIC analysis plot combined with *envfit* showing correlations (red dotted arrows: Bacterial community parameters; blue arrows: Distribution system parameters). Samples that are close to each other in the plot have similar bacterial profiles by FCM; vectors indicate possible correlations. (**A**) Analysis of 16 sampling points (n = 3 for each sampling point) sampled during April and May 2018. (**B**) Analysis of 10 sampling points, selected from the 16 in (**A**) (n = 3 for each sampling point) sampled during April and May 2018. Using the smaller subset of samples permitted a more detailed examination of the correlations shown in panel (**A**) (NMDS1 range = 0–50).

Chlorine residues can influence microbial regrowth, which also changes with retention time and pipe length [29,33]. In this study, water leaving the DWTP contained on average 0.19 ± 0.02 mg/L chloramine; however, as expected, these chloramine concentrations were not present at all points in the distribution system (Supplementary Materials Figure S4). With the exception of a few sampling points close to the DWTP, the total chlorine concentration was below 0.04 mg/L at all other sampling points, and thus below the detection limit. A lack of chlorine can lead to faster regrowth of bacteria [33], and a free chlorine concentration of at least 0.3 mg/L is required to prevent bacterial regrowth in

the distribution system [9]. The only impact that was observed was an inverse correlation between the intact cell concentration and chloramine concentration, with intact cell concentration elevated at sampling points where the total chlorine concentration was below 0.05 mg/L (Supplementary Materials Figure S4).

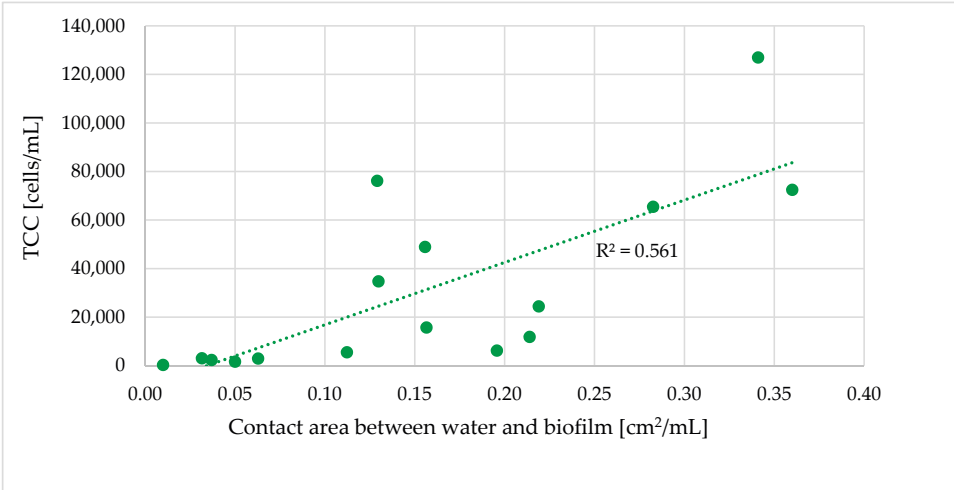

Figure 5. Correlation between the contact area for biofilm and water, and TCC.

This suggests that while changes in chlorine influenced whether the bacteria were intact or not, most of the bacterial dynamics between the water and biofilm observed in the current study as increases in TCC or changed %HNA are not due to loss of chlorine. Instead, a continuous interaction between the water and the biofilm, with the growth and release of bacteria from biofilm, provides a gradually accumulating supply of planktonic bacteria that can be monitored by FCM in the bulk water. A previous study calculated that it takes 2.31 days to double the number of planktonic bacteria in a bioreactor-based model system for DWDS at 13 °C without chlorine [34]. This can be extrapolated to suggest that for growth of the bacteria released from the biofilm, a retention time of at least 55 hours is required to double their number, and at shorter times, changes in the bacterial content of the water must be attributed to addition of cells from biofilm [2]. It should, however, be noted that monitoring of the biofilm by FCM was possible in this current study, and could be applied in other DWDS for inferring biofilm interactions, because the input of cells from the treatment plant is minimal [2]. When the number of cells in the outgoing drinking water is high, due to processes in the DWTP such as biological filtration, the resolution of FCM prevents detailed descriptions of bacteria only entering the water from DWDS biofilm or regrowth.

Prolonged stagnation of water has been associated with significant growth [34], and longer retention times also contribute to increased bacterial growth in the DWDS [9]. In this study, retention time had a significant impact on the bacterial community in the water, impacting both TCC and %HNA bacteria (Figure 6).

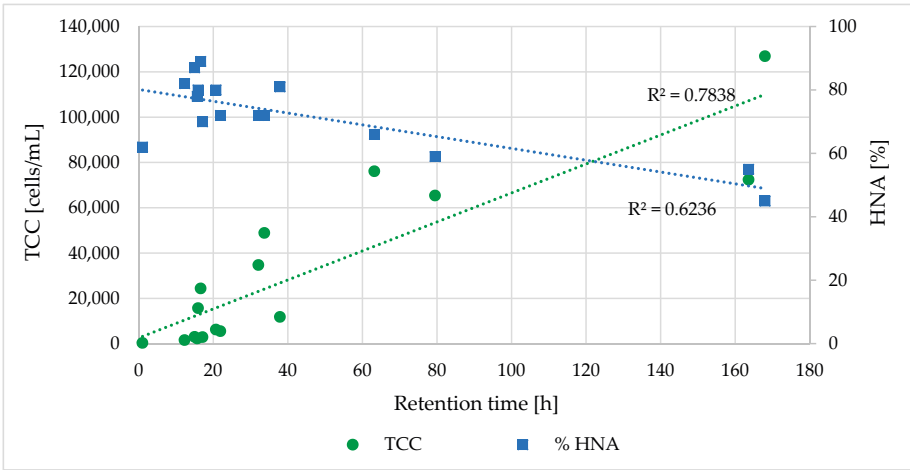

Figure 6. Correlation between retention time and TCC (green dots), as well as %HNA bacteria (blue squares).

An increased contact time between biofilm and water increased the number of bacteria (correlation coefficient $R = 0.89$; $p < 0.0001$). This could be due to an increased time during which the bacteria can detach from the biofilm and accumulate in the water phase, or an increased retention time could also provide bacteria in the water the chance to multiply [35]. Higher retention times were also correlated with a decrease in the %HNA bacteria, from about 80% for water with a retention time below 20 h to 50% when retention time exceeded 160 h (correlation coefficient $R = -0.79$; $p = 0.0003$). Differences in community structures for water samples with disparities in retention time and distance from the DWTP have been observed in previous studies [28]. One recent study showed a predominance of LNA bacteria in branch ends of DWDSs, which indicates similar trends compared to the results of this study [36]. Interestingly, this strong negative correlation between retention time and %HNA bacteria was not observed when %HNA were examined with respect to contact area. Studies show that LNA, as well as HNA, bacteria are able to grow in oligotrophic water [37]. Drinking water is an oligotrophic environment with total organic carbon (TOC) concentrations below 1 mg/L [36], and the DWDS in the current study was no exception: TOCeq measured in the permeate from the UF membrane showed stable and relatively low TOCeq values of about 1.83 ± 0.31 mg/L from April 2018 until April 2019 (Supplementary Materials Figure S8). Those values are comparable with the TOCeq values for the outgoing drinking water. This could explain why, in this DWDS, the %HNA bacteria decreased with retention time. While the specific growth rate of LNA bacteria is lower compared to the specific growth rate of HNA bacteria, suggesting that regrowth of HNA bacteria in the DWDS should be favored [37], LNA bacteria could predominate with increased retention time if the mechanism by which bacteria entering the water is not due to growth. This supports the conclusions made by Chan et al. that it is bacteria entering the water from the biofilm that are the predominant source of bacteria in this distributed water [2]. This is supported by the observation that contact area is only correlated with increasing TCC, and not with any change in %HNA, suggesting that the community of bacteria leaving the biofilm and entering the water has a consistent composition which is not altered by location of the biofilm in the DWDS. Perhaps the water quality in this DWDS selects which bacteria leave the biofilm at different locations, since presumably there are diverse biofilm populations within the DWDS, due to the presence of different pipe materials [38].

4. Conclusions

Using FCM, it was possible to capture the annual dynamics of the biofilm in this DWDS, quantifying changes in TCC, percentage of intact cells, and changes in the community composition, reflected in the amounts of LNA and HNA bacteria. The seasonal changes indicated an annual reproducibility and allowed the determination of baselines for different points in the DWDS.

The major findings of this study are:

1. The bacterial community in the DWDS experienced clear seasonal changes with similar patterns for different areas of the DWDS. An increase in water temperature led to a significant increase in TCC during the summer period (range: 1.51–5.24-fold increase) at some locations.
2. Hydraulic and specific pipe conditions influence the bacterial community in the water. FCM results indicated that an increase in retention time led to a decrease in the %HNA bacteria in the drinking water (correlation coefficient $R = -0.79$).
3. Longer retention times and increased contact between the water and pipe biofilm led to an increase in TCC. Significant differences in the TCC could be seen in different areas of the DWDS depending on distance from the DWTP and retention time.

5. Limitations and Future Perspectives

In this, and other studies, the combination of various water treatments processes in the DWTP, and different conditions even within an individual DWDS, complicates the formulation of general statements regarding the microbiology in the water [1]. This necessitates the examination of each DWDS individually and the determination of baselines in a seasonal context. As changes of the bacteria in the drinking water are influenced by exchange between water and biofilm in the pipes [39] and regrowth due to changes in residual disinfectant concentration or substrate availability [40], determining how each factor contributes at different locations and seasons is difficult. One influence can be favored by different attributes of the heterogeneous features of the DWDS such as pipe dimensions, pipe material, and water path, as well as retention time which varies depending on local water demand [28]. In this context, the current study is limited, only indicating the complexity of the bacterial content in the water, and indirectly the impact of biofilm from the DWDS. Further investigations are needed to advance our understanding of, for example, the impact of nutrients on the biofilm, in order to generate new and detailed insights into the role played by microbiology in environmental engineering.

The main purpose of this study was to compile a comprehensive description of temporal and spatial bacterial dynamics in the drinking water, and indirectly, the biofilm. This resulted in the preliminary definitions of baselines for microbiological water quality in different zones in this DWDS, providing a new and essential strategy for enhanced drinking water management in this system. Future monitoring incorporating these baselines can be used to detect abnormalities and sudden changes in the bacterial content of the water that may occur due to malfunctions, water leakages, or pipe maintenance, as well as ensuring that values return to the baselines to indicate recovery of acceptable water quality in the DWDS. The possibility to rapidly identify changes in the number of bacteria in the water, and any altered pattern of regrowth, becomes even more important with regard to a possible removal of chloramine in this DWDS in the future. The use of FCM to monitor the status of the distributed water can contribute to managing the uncertainty of how the removal of the disinfectant will affect bacterial regrowth in the pipes, as results can be rapidly available and compared to robust baselines for surveillance. However, the lack of disinfectant residual makes proper engineering practices in operation, maintenance, and construction of distribution networks vital in order to protect the drinking water quality [41].

Supplementary Materials: The following are available online at http://www.mdpi.com/2073-4441/11/10/2137/s1: Figure S1: Old and new treatment process at Kvarnagården DWTP in Varberg, Sweden; Figure S2: Water sampling points in the DWDS in Varberg, Sweden; Figure S3: Schematic description of TCC in the DWDS, and increase of TCC and water temperature from spring to summer; Figure S4: Intact cell count in connection with residues of

chloramine in the DWDS in mg/L; Figure S5: Changes in TCC, ICC, and water temperature at sampling point Hunst; Figure S6: Changes in TCC, ICC, and water temperature at sampling point TrPS5; Figure S7: Increase in TCC at sampling point TrPS5 in late June 2019; Figure S8: TOCeq measured in the permeate of the UF membrane from April 2018 to April 2019; Table S1:Flow cytometry results and environmental parameters for different sampling points.

Author Contributions: Conceptualization, All; methodology, All; formal analysis, C.S. and P.R.; investigation, C.S.; writing—original draft preparation, C.S., P.R., M.D.B. and A.K.; writing—review and editing, All; visualization, C.S., K.P. and S.C.; supervision, A.K.; project administration, A.K.; funding acquisition, A.K., P.R. and C.J.P.

Funding: This research received external financial support of the Biofilm study-project (Project no. 17–104) funded by The Swedish Water and Wastewater Association (Swedish Water Development, SVU).

Acknowledgments: The authors acknowledge the financial support from Vatten & Miljö I Väst AB, which funded this long-term study, including monitoring program and analyses.

Conflicts of Interest: The authors declare no conflicts of interest.

References

1. Chan, S. Processes Governing the Drinking Water Microbiome. Ph.D. Thesis, Faculty of Engineering (LTH), Lund, Sweden, 2018.
2. Chan, S.; Pullerits, K.; Keucken, A.; Persson, K.M.; Paul, C.J.; Rådström, P. Bacterial release from pipe biofilm in a full-scale drinking water distribution system. *NPJ Biofilms Microbiomes* **2019**, *5*, 9. [CrossRef] [PubMed]
3. Liu, G.; Zhang, Y.; van der Mark, E.; Magic-Knezev, A.; Pinto, A.; van den Bogert, B.; Liu, W.; van der Meer, W.; Medema, G. Assessing the origin of bacteria in tap water and distribution system in an unchlorinated drinking water system by SourceTracker using microbial community fingerprints. *Water Res.* **2018**, *138*, 86–96. [CrossRef] [PubMed]
4. Waak, M.B.; Hozalski, R.M.; Hallé, C.; Lapara, T.M. Comparison of the microbiomes of two drinking water distribution systems-With and without residual chloramine disinfection. *Microbiome* **2019**, *7*. [CrossRef] [PubMed]
5. Feron, D.; Neumann, E. "Biocorrosion 2012"—From advanced technics towards scientific perspectives. *Bioelectrochemistry* **2014**, *97*, 1. [CrossRef]
6. Piriou, P.; Malleret, L.; Bruchet, A.; Kiéné, L. Trichloroanisole kinetics and musty tastes in drinking water distribution systems. *Water Supply* **2001**, *1*, 11–18. [CrossRef]
7. Van der Kooij, D.; van der Wielen, P.W.J.J. *Microbial Growth in Drinking-Water Supplies: Problems, Causes, Control and Research Needs*, 1st ed.; IWA Publishing: London, UK, 2013; pp. 1–32.
8. Baskerville, A.; Broster, M.; Fitzgeorge, R.B.; Hambleton, P.; Dennis, P.J. Experimental Transmission of Legionnaires' Disease by Exposure to Aerosols of Legionella Pneumophila. *Lancet* **1981**, *318*, 1389–1390. [CrossRef]
9. Bartram, J.; Cotruvo, J.A.; Exner, M.; Fricker, C.; Glasmacher, A. *Heterotrophic Plate Counts and Drinking-Water Safety-The Significance of HPCs for Water Quality and Human Health*, 1st ed.; IWA Publishing: London, UK, 2003; pp. 80–118.
10. Pinto, A.J.; Xi, C.; Raskin, L. Bacterial community structure in the drinking water microbiome is governed by filtration processes. *Environ. Sci. Technol.* **2012**, *46*, 8851–8859. [CrossRef]
11. Hijnen, W.A.M.; Beerendonk, E.F.; Medema, G.J. Inactivation credit of UV radiation for viruses, bacteria and protozoan (oo)cysts in water: A review. *Water Res.* **2006**, *40*, 3–22. [CrossRef]
12. Douterelo, I.; Boxall, J.B.; Deines, P.; Sekar, R.; Fish, K.E.; Biggs, C.A. Methodological approaches for studying the microbial ecology of drinking water distribution systems. *Water Res.* **2014**, *65*, 134–156. [CrossRef]
13. Hammes, F.; Berney, M.; Wang, Y.; Vital, M.; Köster, O.; Egli, T. Flow-cytometric total bacterial cell counts as a descriptive microbiological parameter for drinking water treatment processes. *Water Res.* **2008**, *42*, 269–277. [CrossRef]
14. Lautenschlager, K.; Boon, N.; Wang, Y.; Egli, T.; Hammes, F. Overnight stagnation of drinking water in household taps induces microbial growth and changes in community composition. *Water Res.* **2010**, *44*, 4868–4877. [CrossRef] [PubMed]
15. Payment, P.; Trudel, M.; Plante, R. Elimination of viruses and indicator bacteria at each step of treatment during preparation of drinking water at seven water treatment plants. *Appl. Environ. Microbiol.* **1985**, *49*, 1418–1428. [PubMed]

16. Van Nevel, S.; Buysschaert, B.; De Gusseme, B.; Boon, N. Flow cytometric examination of bacterial growth in a local drinking water network. *Water Environ. J.* **2016**, *30*, 167–176. [CrossRef]
17. Lautenschlager, K.; Hwang, C.; Liu, W.T.; Boon, N.; Köster, O.; Vrouwenvelder, H.; Egli, T.; Hammes, F. A microbiology-based multi-parametric approach towards assessing biological stability in drinking water distribution networks. *Water Res.* **2013**, *47*, 3015–3025. [CrossRef]
18. Van Nevel, S.; Koetzsch, S.; Proctor, C.R.; Besmer, M.D.; Prest, E.I.; Vrouwenvelder, J.S.; Knezev, A.; Boon, N.; Hammes, F. Flow cytometric bacterial cell counts challenge conventional heterotrophic plate counts for routine microbiological drinking water monitoring. *Water Res.* **2017**, *113*, 191–206. [CrossRef]
19. Gatza, E.; Hammes, F.A.; Prest, E.I. White Paper: Assessing Water Quality with the BD Accuri TM C 6 Flow Cytometer. 2013. Available online: https://www.semanticscholar.org/paper/White-Paper-Assessing-Water-Quality-with-the-BD-TM-Gatza-Hammes/8e96101b49bfcb09e28425cf40c0cce2dec1afca (accessed on 18 July 2019).
20. Besmer, M.D.; Sigrist, J.A.; Props, R.; Buysschaert, B.; Mao, G.; Boon, N.; Hammes, F. Laboratory-scale simulation and real-time tracking of a microbial contamination event and subsequent shock-chlorination in drinking water. *Front. Microbiol.* **2017**, *8*, 1900. [CrossRef]
21. Keucken, A.; Heinicke, G.; Persson, K.M.; Köhler, S.J. Combined coagulation and ultrafiltration process to counteract increasing NOM in brown surface water. *Water* **2017**, *9*, 697. [CrossRef]
22. Prest, E.I.; Hammes, F.; Kötzsch, S.; van Loosdrecht, M.C.M.; Vrouwenvelder, J.S. Monitoring microbiological changes in drinking water systems using a fast and reproducible flow cytometric method. *Water Res.* **2013**, *47*, 7131–7142. [CrossRef]
23. Chan, S.; Pullerits, K.; Riechelmann, J.; Persson, K.M.; Rådström, P.; Paul, C.J. Monitoring biofilm function in new and matured full-scale slow sand filters using flow cytometric histogram image comparison (CHIC). *Water Res.* **2018**, *138*, 27–36. [CrossRef]
24. Koch, C.; Fetzer, I.; Harms, H.; Müller, S. CHIC-an automated approach for the detection of dynamic variations in complex microbial communities. *Cytom. Part A* **2013**, *83*, 561–567. [CrossRef]
25. Ellis, B.; Haaland, P.; Hahne, F.; Meur, N.L.; Gopalakrishnan, N.; Spidlen, J.; Jiang, M. FlowCore: Basic Structures for Flow Cytometry Data, Bioconductor R. Package Version 1.40.0. 2016. Available online: https://rdrr.io/bioc/flowCore/ (accessed on 7 August 2019).
26. Oksanen, J.; Blanchet, F.G.; Kindt, R.; Legendre, P.; Minchin, P.; O'Hara, R.B.; Simpson, G.; Solymos, P.; Stevens, M.H.H.; Wagner, H. Vegan: Community Ecology Package. R Package Version 2.2-1. 2015. Available online: http://CRAN.R-project.org/package=vegan (accessed on 14 August 2019).
27. Keucken, A. Climate Change Adaption of Waterworks for Browning Surface Waters: Nano- and Ultrafiltration Membrane Applications for Drinking Water Treatment. Ph.D. Thesis, Faculty of Engineering (LTH), Lund, Sweden, 2017.
28. Pinto, A.J.; Schroeder, J.; Lunn, M.; Sloan, W.; Raskin, L. Spatial-temporal survey and occupancy-abundance modeling to predict bacterial community dynamics in the drinking water microbiome. *mBio* **2014**, *5*. [CrossRef] [PubMed]
29. Liu, S.; Gunawan, C.; Barraud, N.; Rice, S.A.; Harry, E.J.; Amal, R. Understanding, monitoring, and controlling biofilm growth in drinking water distribution systems. *Environ. Sci. Technol.* **2016**, *50*, 8954–8976. [CrossRef] [PubMed]
30. Prest, E.I.; Weissbrodt, D.G.; Hammes, F.; Van Loosdrecht, M.C.M.; Vrouwenvelder, J.S. Long-term bacterial dynamics in a full-scale drinking water distribution system. *PLoS ONE* **2016**, *11*, e0164445. [CrossRef] [PubMed]
31. Douterelo, I.; Sharpe, R.L.; Boxall, J.B. Influence of hydraulic regimes on bacterial community structure and composition in an experimental drinking water distribution system. *Water Res.* **2013**, *47*, 503–516. [CrossRef] [PubMed]
32. Lipphaus, P.; Hammes, F.; Kötzsch, S.; Green, J.; Gillespie, S.; Nocker, A. Microbiological tap water profile of a medium-sized building and effect of water stagnation. *Environ. Technol.* **2014**, *35*, 620–628. [CrossRef] [PubMed]
33. Chiao, T.H.; Clancy, T.M.; Pinto, A.; Xi, C.; Raskin, L. Differential resistance of drinking water bacterial populations to monochloramine disinfection. *Environ. Sci. Technol.* **2014**, *48*, 4038–4047. [CrossRef]
34. Boe-Hansen, R.; Albrechtsen, H.J.; Arvin, E.; Jørgensen, C. Bulk water phase and biofilm growth in drinking water at low nutrient conditions. *Water Res.* **2002**, *36*, 4477–4486. [CrossRef]

35. Universität Göttingen. Available online: https://lp.uni-goettingen.de/get/text/4908 (accessed on 17 June 2019).
36. Liu, J.; Zhao, Z.; Chen, C.; Cao, P.; Wang, Y. In-situ features of LNA and HNA bacteria in branch ends of drinking water distribution systems. *J. Water Supply Res. Technol. AQUA* **2017**, *66*, 300–307. [CrossRef]
37. Wang, Y.; Hammes, F.; Boon, N.; Chami, M.; Egli, T. Isolation and characterization of low nucleic acid (LNA)-content bacteria. *ISME J.* **2009**, *3*, 889–902. [CrossRef]
38. Ren, H.; Wang, W.; Liu, Y.; Liu, S.; Lou, L.; Cheng, D.; He, X.; Zhou, X.; Qiu, S.; Fu, L.; et al. Pyrosequencing analysis of bacterial communities in biofilms from different pipe materials in a city drinking water distribution system of East China. *Appl. Microbiol. Biotechnol.* **2015**, *99*, 10713–10724. [CrossRef]
39. Henne, K.; Kahlisch, L.; Brettar, I.; Höfle, M.G. Analysis of structure and composition of bacterial core communities in mature drinking water biofilms and bulk water of a citywide network in Germany. *Appl. Environ. Microbiol.* **2012**, *78*, 3530–3538. [CrossRef] [PubMed]
40. Srinivasan, S.; Harrington, G.W.; Xagoraraki, I.; Goel, R. Factors affecting bulk to total bacteria ratio in drinking water distribution systems. *Water Res.* **2008**, *42*, 3393–3404. [CrossRef] [PubMed]
41. Medema, G.J.; Smeets, P.W.; Blokker, E.J.; van Lieverloo, J.H. Safe distribution without a disinfectant residual. In *Microbial Growth in Drinking-Water Supplies: Problems, Causes, Control and Research Needs*, 1st ed.; van der Kooij, D., van der Wielen, P.W.J.J., Eds.; IWA Publishing: London, UK, 2013; pp. 95–125.

water

MDPI

Article

Supplementary Materials

Figures

Mapping Dynamics of Bacterial Communities in a Full-Scale Drinking Water Distribution System using Flow Cytometry

Caroline Schleich[1], Sandy Chan[2,3,4], Kristjan Pullerits[2,3,4], Michael D. Besmer[5], Catherine J. Paul[2,6], Peter Rådström[2] and Alexander Keucken[1,6,*]

[1] Vatten & Miljö i Väst AB, SE-311 22, Falkenberg, Sweden; Caroline.Schleich@vivab.info
[2] Applied Microbiology, Department of Chemistry, Lund University, P.O. Box 124, SE-221 00, Lund, Sweden; Sandy.Chan@sydvatten.se (S.C.); kristjan.pullerits@tmb.lth.se (K.P.); catherine.paul@tvrl.lth.se (C.J.P.); peter.radstrom@tmb.lth.se (P.R.)
[3] Sweden Water Research AB, Ideon Science Park, Scheelevägen 15, SE-223 70, Lund, Sweden
[4] Sydvatten AB, Hyllie Stationstorg 21, SE-215 32, Malmö, Sweden
[5] onCyt Microbiology AG, CH-8038, Zürich, Switzerland; michael.besmer@oncyt.com
[6] Water Resources Engineering, Department of Building and Environmental Engineering, Faculty of Engineering, Lund University, P.O. Box 118, SE-221 00, Lund, Sweden
* Correspondence: alexander.keucken@vivab.info

Received: 9 September 2019; Accepted: 11 October 2019; Published: 15 October 2019

Table of Content

Supplementary Figure S1 - Old and new treatment process at Kvarnagården DWTP in Varberg, Sweden
Supplementary Figure S2 - Water sampling points in the DWDS in Varberg, Sweden
Supplementary Figure S3 - Schematic description of TCC in the DWDS, and increase of TCC and water temperature from spring to summer
Supplementary Figure S4 - Intact cell count in connection with residues of chloramine in the DWDS in mg/L^{-}
Supplementary Figure S5 - Changes in TCC, ICC and water temperature at sampling point Hunst
Supplementary Figure S6 - Changes in TCC, ICC and water temperature at sampling point TrPS5
Supplementary Figure S7 - Increase in TCC at sampling point TrPS5 in late June 2019
Supplementary Figure S8 - TOCeq measured in the permeate of the UF membrane from April 2018 to April 2019

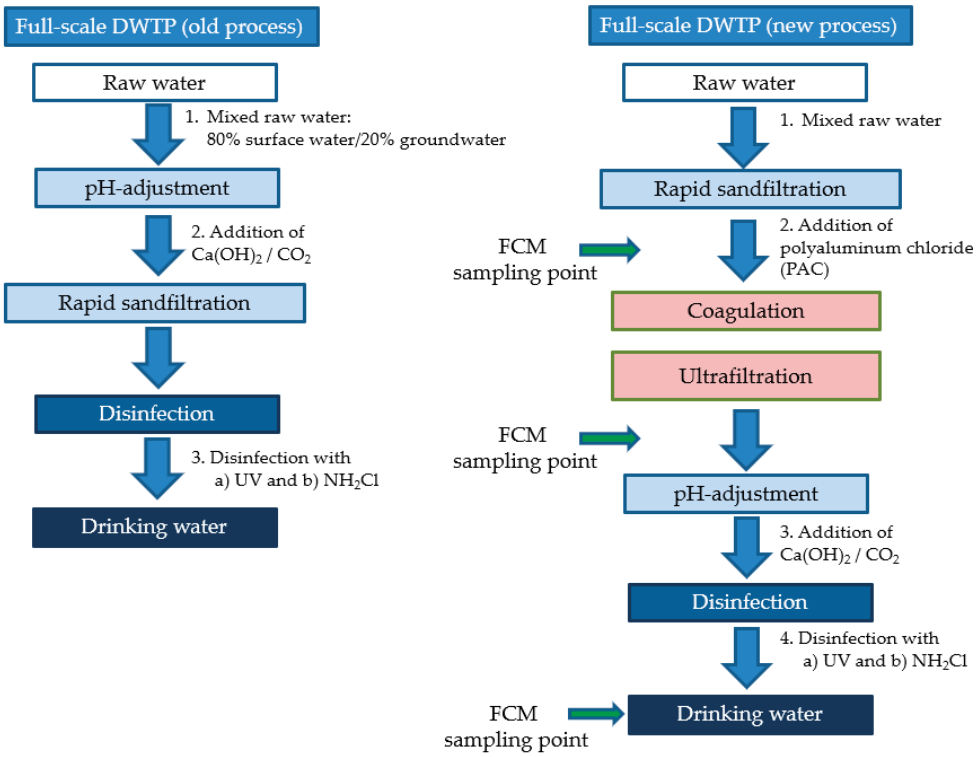

Supplementary Figure S1. Treatment process at Kvarnagården DWTP in Varberg, Sweden before (old) and after (new) implementation of a hybrid membrane process (coagulation combined with UF-membrane filtration).

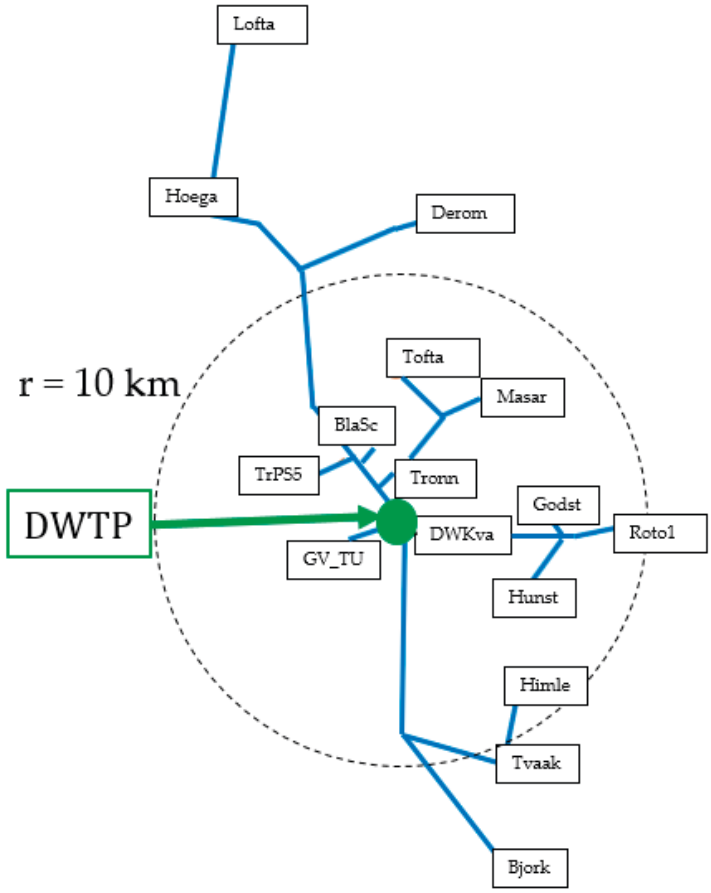

Supplementary Figure S2. Schematic illustration of the DWDS and FCM sampling points in Varberg, Sweden.

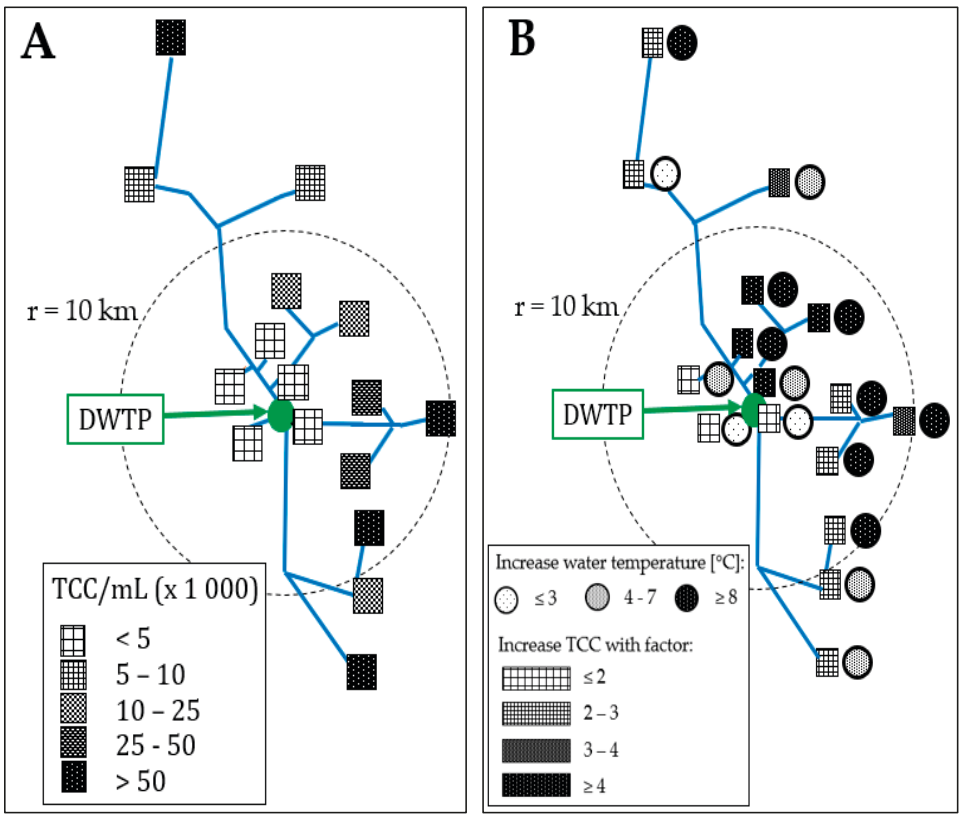

Supplementary Figure S3. Schematic illustration of the DWDS and results for A: The total cell concentrations in April 2018 plotted on their sampling points in the DWDS. The samples close to the WTP show a low total cell concentration whereas sampling points at the end of the DWDS show elevated concentrations. B: Increase of TCC (squares) and water temperature (circles) at all sampling points from April 2018 until September 2018.

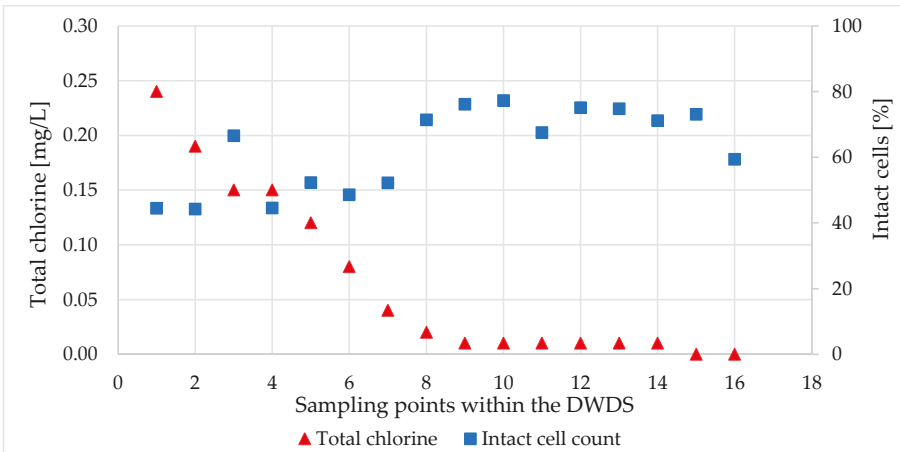

Supplementary Figure S4. Intact cell count in connection with residues of chloramine in the DWDS in mg/L. Sampling points are arranged according to the total chlorine concentration (from highest to lowest).

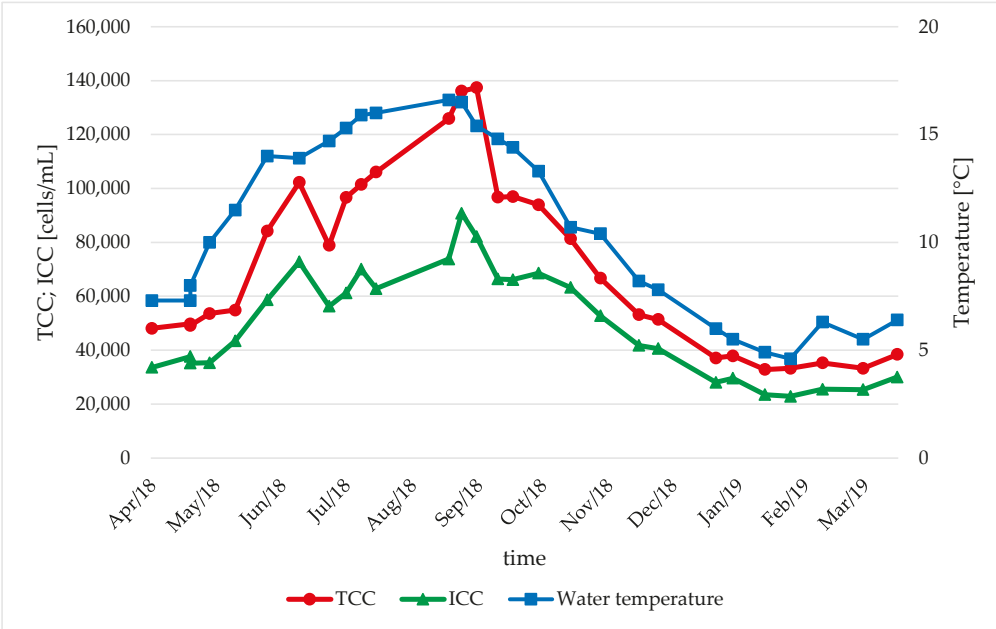

Supplementary Figure S5. Changes in TCC (red line, circles), ICC (green line, triangles) and water temperature (blue line; squares) at sampling point Hunst.

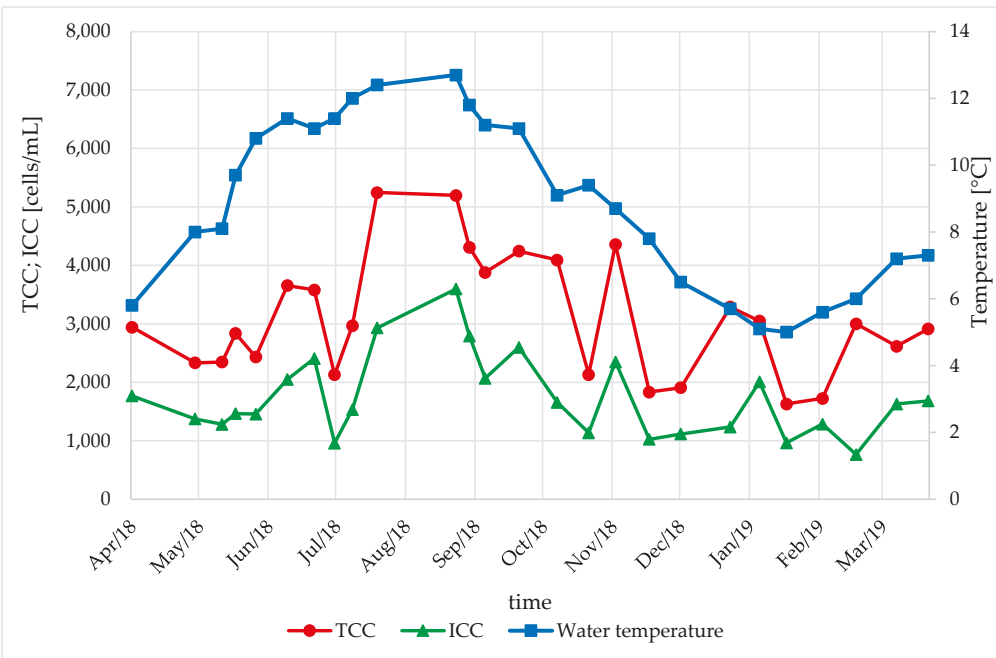

Supplementary Figure S6. Changes in TCC (red line, circles), ICC (green line, triangles) and water temperature (blue line; squares) at sampling point TrPS5.

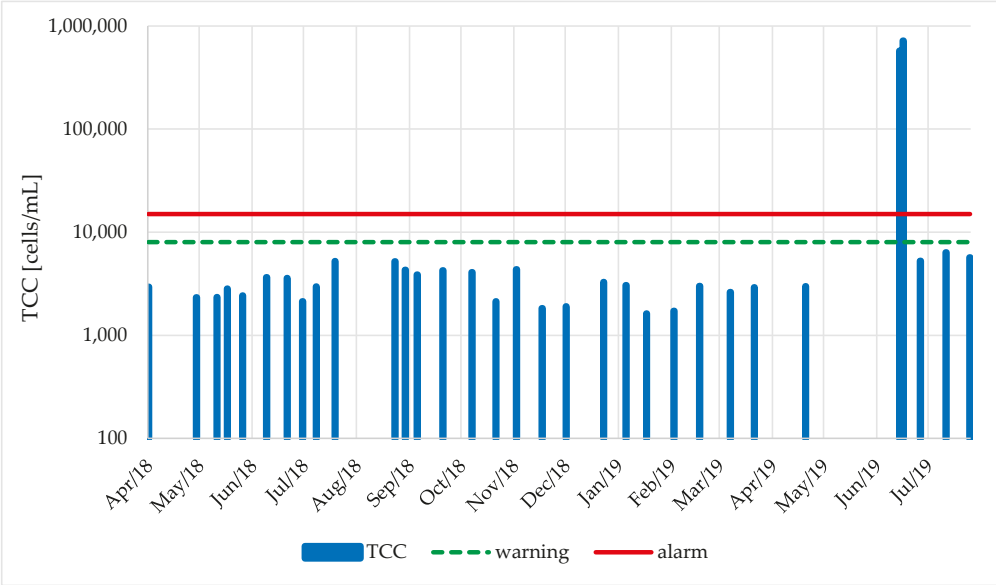

Supplementary Figure S7. Increase in TCC (blue bars) at sampling point TrPS5 in late June 2019 due to a closed valve. The green doted line indicates the warning limit for TCC (9000 cells/mL) and the red line indicates the alarm limit for TCC (15,000 cells/mL).

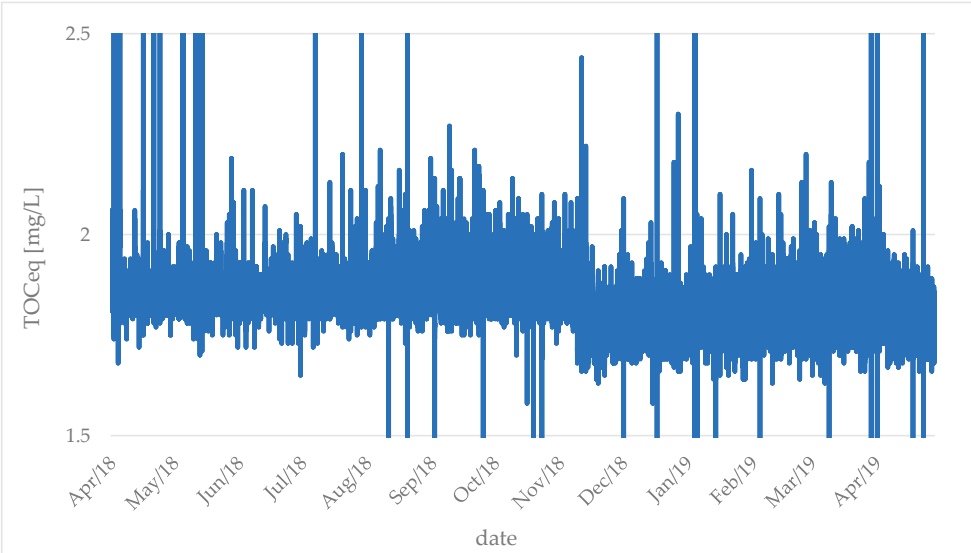

Supplementary Figure S8. TOCeq measured in the permeate of the UF membrane from April 2018 to April 2019.

Tables

Table of content

Supplementary Table S1 - Flow cytometry results and environmental parameters for different sampling points

Supplementary Table S1. Flow cytometry results and environmental parameters for different sampling points (three datasets each).

Sampling point	Retention time [h]	TCC [cells/mL]	pH	HNA [%]	ICC [%]	Contact area with biofilm [cm^2/mL]
Bj_Va 1	168	141 980	7.84	40	71	0.34
Bj_Va 2	168	126 880	8.04	45	70	0.34
Bj_Va 3	168	129 640	7.95	44	72	0.34
BlaSc 1	15	3 580	8.06	83	47	0.03
BlaSc 2	15	1 740	8.25	67	46	0.03
BlaSc 3	15	2 907	8.08	61	34	0.03
Derom 1	20.7	7 320	8.04	71	40	0.2
Derom 2	20.7	6 140	8.31	70	48	0.2
Derom 3	20.7	12 480	8.11	62	38	0.2
DWKva 1	1	324	8.08	74	28	0.01
DWKva 2	1	308	8.11	78	47	0.01
DWKva 3	1	308	8	77	48	0.01
Godst 1	32.1	27 980	8.1	74	64	0.13
Godst 2	32.1	25 300	8.25	75	61	0.13
Godst 3	32.1	26 540	8.13	76	61	0.13
GV_TU 1	12.3	876	8.06	84	43	0.05
GV_TU 2	12.3	1 860	8.34	71	31	0.05
GV_TU 3	12.3	2 308	8.12	54	18	0.05
Himle 1	163.6	71 900	7.95	59	60	0.36
Himle 2	163.6	59 160	8.06	57	53	0.36
Himle 3	163.6	48 880	7.95	59	62	0.36
Hoega 1	21.9	3 810	8.04	81	51	0.11
Hoega 2	21.9	3 670	8.39	77	43	0.11
Hoega 3	21.9	8 270	8.2	70	35	0.11
Hunst 1	33.7	32 840	8.03	73	71	0.16
Hunst 2	33.7	33 240	8.18	73	69	0.16
Hunst 3	33.7	35 280	8.08	72	72	0.16
Lofta 1	79.5	51 360	8.05	55	70	0.28
Lofta 2	79.5	47 500	8.14	57	70	0.28
Lofta 3	79.5	38 160	8.03	65	73	0.28
Masar 1	16.6	12 100	8.11	88	70	0.22
Masar 2	16.6	11 140	8.59	84	87	0.22
Masar 3	16.6	15 140	8.2	87	66	0.22
Roto1 1	63.2	40 520	8.11	65	77	0.13
Roto1 2	63.2	56 520	8.22	62	72	0.13
Roto1 3	63.2	32 800	8.14	67	72	0.13
Tofta 1	15.9	12 440	8.19	76	83	0.16
Tofta 2	15.9	11 420	8.63	77	73	0.16
Tofta 3	15.9	14 760	8.33	82	57	0.16
Tronn 1	15.7	1 700	8.14	77	37	0.04
Tronn 2	15.7	2 647	8.35	79	41	0.04
Tronn 3	15.7	3887	8.18	84	41	0.04
TrPS5 1	17.1	1 628	8.05	75	59	0.06
TrPS5 2	17.1	1 724	8.23	76	74	0.06
TrPS5 3	17.1	3 000	7.98	63	25	0.06
Tvaak 1	37.9	9 820	8.01	80	68	0.21
Tvaak 2	37.9	6 720	8.13	80	70	0.21
Tvaak 3	37.9	8 420	8.08	80	66	0.21

Microorganisms are ubiquitous in nature and live in diverse environments, from hot springs to the human gut. Microorganisms are also major contributors to biogeochemical cycles, meaning that they regulate the elements necessary for life on Earth. The biological activity and metabolic processes of microorganisms have shaped the environment and the chemical speciation of practically all the elements on Earth throughout its 4.5-billion-year history.

In drinking water systems, microorganisms live in the water and on surfaces in communities in a slimy matrix called a biofilm. These biofilms are found on pipe surfaces in drinking water distribution systems and are present on surfaces involved in water treatment. Most microorganisms are harmless to humans, while some are pathogenic, or can be beneficial for the biological treatment of water. Recent technological developments have led to an explosion of molecular data providing insight into microbial life in various environments, improving our understanding of these systems. The work described in this thesis was carried out to investigate how treatment processes and the pipe biofilm in drinking water distribution systems affect the bacterial community and the quality of drinking water. The knowledge gained will contribute to the supply of safe and clean drinking water in the future.

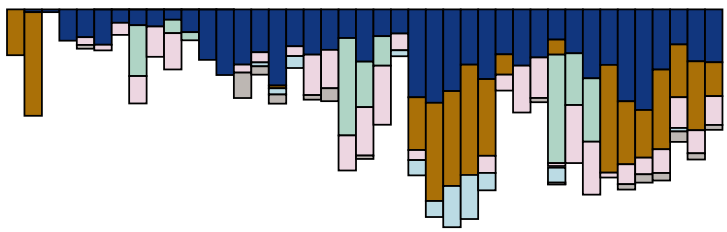

Printed by Media-Tryck, Lund 2020 NORDIC SWAN ECOLABEL 3041 0903

ISBN: 978-91-7422-764-2

Applied Microbiology
Department of Chemistry
Faculty of Engineering
Lund University